

Exploring the Phenomena of Compound Aggregation and Nano-entities for Drug Discovery

By
Fatma Shahout

A thesis submitted for the degree of
Doctor of Philosophy (Ph.D)

Evaluation committee members

President of Jury and Internal Examiner	Dr. Charles Calmettes Armand-Frappier Santé Biotechnologie, INRS
External examiner	Dr. Ewen Lescop Centre national de la recherche scientifique (CNRS)
External examiner	Dr. Steve Bourgault Université du Québec à Montréal (UQAM)
Supervisor	Dr. Steven LaPlante Armand-Frappier Santé Biotechnologie

ACKNOWLEDGEMENTS

I would like to acknowledge and express my appreciation to my supervisor Prof. Steven LaPlante who made my thesis research possible. I deeply thank him for his great supervision, creative discussion, encouragement, guidance and advice. I am very lucky to have such a great and fantastic supervisor for my thesis. I would like also to acknowledge my committee members Prof. Charles Calmettes, Prof. Ewen Lescop, and Prof. Steve Bourgault for reviewing this thesis, comments, suggestions and assistance during this pandemic season.

I would gratefully acknowledge Prof. Patrick Labonte and Prof. Denis Girard for their collaboration, assistance, great advice and help throughout my thesis. I sincerely thank the help of the technician Arnaldo Nakamura for transmission electron microscopy and the technician Jessy Tremblay for confocal microscopy techniques.

I would also like to thank NMX research and solution and all the experts for their help, effort, valuable advice, great comments, fund and expertise throughout all the stages of this work- Simon Woo, Sacha Larda, Luc Farmer, Yann Ayotte, Maria Denk and all NMX experts. I also appreciate and thank the help of all the friends Mustapha Iddir, Richard Boulon, Eleonore Delaire, Hala Elasmy, Tanos Franca, Micheal Maddalena, Valerie Roux and Marwa Dlim.

I would like to give my special thanks to my husband for his continuous support and help in all the stages. My sincere thanks also to my father, mother, brother, sisters, and friends for their support and love.

ABSTRACT

This thesis explores the world of nano-entities. Nano-entities is a name given by our laboratory to describe the natural phenomenon that drugs can self-assemble in a multitude of particle sizes when placed in an aqueous environment. Surprisingly, this phenomenon remains relatively unexplored despite the widespread impact it has throughout the drug discovery and development processes. Given this, I became very interested in nano-entities and launched detailed investigations as described herein. These investigations indeed found that drugs can adopt some amazing free-state behaviors –which have been historically overlooked by the pharmaceutical industry. Perhaps one reason that nano-entities has been overlooked is the widely held assumption that compounds can only exist as lone molecules or as precipitates when placed into aqueous solution. However, recent studies are shedding light onto a non-negligible phenomenon where compounds can naturally adopt into a multi-state equilibrium. The principle states of this equilibrium can be classified as, (1) soluble-lone molecules, (2) soluble nano-entities, and (3) solid precipitates. Here, we focus on the nano-entity state. We and others noticed that many small-molecules can adopt a wide range of aggregate sizes and type, but to date, the size and types of these self-associated particles remain largely unexplored. This is due in part to the fact that each compound has its own fingerprints which are highly dependent on its environment such as, buffer, pH, etc. Also, our limited knowledge of these nano-entities is more complicated by the fact that there are only a few detection techniques to explore the existence of nano-entities and reveal their full range of sizes. As a result, the detection of nano-entities remains elusive.

In my thesis, I wish to welcome you to this small world of drug self-assemblies. I prepared a detailed introduction along with the “hypothesis and objectives” for my investigations. I then provide three chapters which show how we observed these fascinating entities using specialized techniques that include Nuclear Magnetic Resonance (NMR), Transmission Electron Microscopy (TEM), Dynamic Light scattering (DLS) and Confocal Laser Scanning Microscopy (CLSM) assays. I also show that nano-entities can enter and accumulate within cells. The fourth chapter describes my discovery that nano-entities can be recognized by anti-bodies and induce an immune response. This is very interesting because it would be perhaps be first time that we correlate this drug property with drug side-effects. Given that “Knowledge is Power”, these findings may be used as tools to better observe and understand the phenomenon then perhaps identify potential solutions.

Key words Nano-entities, self-assemble, Drugs, equilibrium, Tumbling-molecules, Aggregates

RÉSUMÉ

La thèse explore le monde fascinant des nano-entités, nom donné par notre laboratoire décrivant le phénomène naturel selon lequel les médicaments peuvent réaliser en s'auto-assemblant en une multitude de particules de tailles différentes lorsqu'ils sont placés dans un environnement aqueux. Il est surprenant de constater que ce phénomène reste relativement peu exploré malgré l'impact grandissant qu'il a sur la découverte et le développement des médicaments. C'est pourquoi j'ai commencé à m'intéresser de près aux nanoparticules. Ces recherches ont révélé que les molécules peuvent adopter de surprenants comportements à l'état libre quand elles sont placées en solution. Cela peut être expliqué par cette hypothèse largement répandue, que les composés ne peuvent se solubiliser qu'en solution aqueuse, sous forme de molécules seules ou des précipités. Cependant, des études récentes mettent en lumière un phénomène non négligeable dans lesquels les composés peuvent adopter naturellement un équilibre entre plusieurs états. Ces principaux états sont classés comme suit : (1) des molécules solubles et uniques, (2) des nano-entités auto-assemblées solubles, et (3) des précipités. Ici, nous nous concentrons sur l'état des nano-entités. Nous avons remarqué, avec d'autres laboratoires, que plusieurs médicaments sous formes de petites molécules peuvent s'assembler pour former différents agrégats, dont les tailles et les types restent toujours peu caractérisés. Cela est dû en partie à la singularité de chaque composé dépendant fortement de leur environnement (tampon, pH, température, etc). De plus, les connaissances sur ces nano-entités sont limitées puisqu'il n'existe que quelques techniques de détection, nous permettant de déterminer leur existence, leur type et de caractériser leurs tailles, rendant le suivi des nano-entités insaisissable.

Dans ma thèse, je souhaiterais donc vous inviter à découvrir ce petit monde des médicaments auto-assemblés. J'ai préparé une introduction détaillée suivie d'une partie « hypothèse et objectifs » décrivant mes investigations. Ces parties sont suivies de trois chapitres dans lesquels sont montrés comment mon laboratoire et moi avons observés ces fascinantes entités utilisant des techniques spécialisées incluant la dilution par RMN, la RMN-T2-CPMG, les essais de détergence par RMN, MET, DLS, CLSM. Je montre également que ces nano-entités peuvent pénétrer et s'accumuler dans les cellules. Le quatrième chapitre décrit ma découverte de nano-entités pouvant être reconnues par des anticorps, induisant une réponse immunitaire. Cette découverte nous permettrait alors d'établir une corrélation entre cette propriété des nano-entités et les effets secondaires des médicaments. Sachant que « la connaissance est le pouvoir », ces résultats pourront être utilisés comme outils afin d'observer et comprendre ces phénomènes et peut-être identifier des solutions potentielles.

Mots clefs Nano-entités, auto-assemblage, Médicaments, équilibre, Tumbling-molécules, Agrégats

TABLE OF CONTENTS

ACKNOWLEDGMENTS	III
ABSTRACT	IV
RÉSUMÉ	V
TABLE OF CONTENTS	VI
LIST OF FIGURES	IX
LIST OF TABLES	XI
LIST OF ABBREVIATIONS	XII
1.0 INTRODUCTION	1
2.0 LITERATURE REVIEW	2
2.1 Concept and Definition of Compound Aggregation	2
2.2 Properties of Compound Aggregation	3
2.2.1 Critical Aggregation Concentration (CAC).....	3
2.2.2 Small-molecule Promiscuity and Specificity.....	7
2.2.2.1 Proposed Mechanism of Inhibition and other Properties of Compound Aggregation.....	8
2.2.2.2 Detergent-sensitive enzyme Inhibition Assay.....	9
2.2.3 Aggregation and Cytotoxicity.....	10
2.3 Detection Assays for Aggregation	11
2.3.1 Transmission Electron Microscopy (TEM).....	11
2.3.2 Dynamic Light Scattering (DLS).....	12
2.3.3 Nuclear Magnetic Resonance (1H NMR strategy).....	15
2.3.3.1 Concept of NMR Practical Assay for Monitoring Compound Self-aggregation and Nano-entities.....	15
2.3.3.2 Detection of Compound Aggregation Using 1H NMR Assay as a Function of Compound Serial Dilution.....	16
2.3.3.3 Use of Detergent Assay to Reveal Large Aggregates by NMR.....	19
2.3.3.4 The Correlation between Compound Self-Aggregation and Off-Target Promiscuity <i>in Vitro</i> Pharmacology Using NMR Assay.....	21
2.3.4 T2-CPMG Assay for the Detection of Compound Aggregation.....	24
2.3.5 Advantages and Limitations of TEM, DLS and NMR techniques.....	28

2.4	Aggregation Occurs in Pharmacologically Relevant Media.....	30
2.5	Compound Aggregation as Attractive Nanoparticle Formulations for Targeted Drug Delivery Systems.....	31
3.	HYPOTHESIS AND OBJECTIVES.....	33
4.	Article 1: Revealing dye and dye-drug aggregation into nano-entities using NMR.....	34
4.1	Abstract.....	35
4.2	Introduction.....	36
4.3	Materials and methods.....	37
4.4	Results and discussion.....	39
4.4.1	Detection of aggregation using ¹ H NMR spectra as a function of dye concentration.....	39
4.4.2	NMR assay on structurally different dyes.....	40
4.4.3	NMR assay on structurally similar dyes - Triarymethane class.....	42
4.4.4	NMR assay on structurally similar dyes - Azo dyes with one phenyl and one naphthyl and bis-naphthyl group.....	43
4.4.5	Dye-drug interactions.....	44
4.4.6	Discussion on dyes, solution behavior and properties.....	45
4.5	Conclusion.....	47
4.6	References.....	48
4.7	Appendix A. Supplementary data (Article 1).....	50
5.	Article 2: Revealing Drug Self-Associations into Nano-Entities.....	51
5.1	ABSTRACT.....	52
5.2	INTRODUCTION.....	53
5.3	RESULT AND DISCUSSION.....	54
5.4	CONCLUSIONS.....	61
5.5	EXPERIMENTAL SECTION.....	62
5.6	REFERENCES.....	65
5.7	Supporting Information.....	67
6.	Article 3: Probing the free-state solution behavior of drugs and their tendencies to self-aggregate into nano-entities.....	71
6.1	Abstract.....	72
6.2	Introduction.....	73

6.3 Materials.....	85
6.4 Equipment setup.....	89
6.5 Anticipated results.....	99
6.6 References.....	106
6.7 Extended Data.....	110
6.8 Supplementary Information.....	113
7. Article 4: Drug Self-aggregation Into Nano-entities Can Illicit Immune Responses.....	125
7.1 Abstract.....	126
7.2 Introduction.....	127
7.3 Results and Discussion.....	129
7.3.1 Morphological and Physicochemical Characterization of Colloidal and Non-colloidal Aggregates.....	129
7.3.2 Cellular Uptake and Internalization of Aggregates.....	132
7.3.3 Mapping the Effect of Drugs and Dyes Aggregation on Murine Macrophage RAW 264.7 and Human Neutrophils.....	136
7.4 Experimental Section.....	140
7.5 CONCLUSIONS.....	142
7.6 References.....	144
7.7 Supplementary Information.....	149
8. General Discussion.....	152
8.1 Characterizing and revealing compound aggregation.....	152
8.2 Aggregation illicit immune response.....	155
9. Conclusion.....	157
10. Perspectives.....	160
11. Bibliography.....	162

LIST OF FIGURES

Figure 2.1. Compounds three-phase equilibrium.....	2
Figure 2.2. Critical aggregation concentration (CAC) of the drug nicardipine.....	3
Figure 2.3. Three potential mechanisms of action of non-specific promiscuous small-molecule aggregators.....	9
Figure 2.4. Self-assemblies of phenylalanine into supramolecular fibrils.....	11
Figure 2.5. Shown are TEM images of some compound aggregation.....	12
Figure 2.6. Colloidal aggregation of anticancer drugs measured in cell culture medium by DLS.....	14
Figure 2.7. Light scattering (cSLS) technique on three known aggregator drugs and one non-aggregator drug.....	15
Figure 2.8 NMR features and behaviors of non-aggregating and aggregating compounds as a function of dilution.....	17
Figure 2.9 Examples of NMR assay for several compounds.....	18
Figure 2.10 Example of aggregating drugs and unusual NMR spectral trends.....	19
Figure 2.11 Examples of NMR detergent assay.....	20
Figure 2.12 Centrifugation and detergent NMR assay.....	21
Figure 2.13 Example of ^1H NMR off-target assay of four inhibitors of HIV reverse transcriptase.....	22
Figure 2.14 Example of ^1H NMR off-target assay of four inhibitors of HCV NS5B polymerase.....	23
Figure 2.15 Shown is the principal of T2-CPMG aggregation assay.....	25
Figure 2.16 Shown are examples of T2-CPMG assay for three different compounds.....	26
Figure 2.17 T2-CPMG analysis for the detection of fragment like molecules' aggregates.....	27
Figure 2.18 T2-CPMG assay for revealing aggregation among pools of compounds.....	28
Figure 2.19 The study of aggregation behaviors in pharmacological media.....	31
Figure 2.20 Confocal microscopy represents the cellular uptake Fulvestrant corona.....	32
Figure 4.1 Compounds can adopt a three-phase equilibrium when placed in aqueous media.....	37
Figure 4.2 Detailed procedure for preparing samples for the NMR aggregation assay.....	38
Figure 4.3 Overview of the expected observations of NMR spectra and resonances upon dilution for dyes that aggregate versus those that do not in solution.....	39
Figure 4.4 NMR aggregation assay showing ^1H NMR spectra of three structurally different dyes obtained by dilution from 200 μM to 12 μM . Data displayed for Tartrazine (left), Methylene blue (middle) and Congo red (right).....	41
Figure 4.5 NMR aggregation assay showing ^1H NMR spectra of three structurally different dyes obtained by dilution from 200 μM to 12 μM	41
Figure 4.6 NMR aggregation assay showing ^1H NMR spectra of three structurally similar triarylmethane dyes obtained by dilution from 200 μM to 12 μM	42
Figure 4.7 NMR aggregation assay showing ^1H NMR spectra of three structurally similar azo dyes obtained by dilution from 200 μM to 12 μM	44

Figure 4.8 NMR aggergation assay showing ¹ H NMR spectra of three structurally similar bis-naphthyl azo dyes obtained by dilution from 200 μM to 12 μM.....	44
Figure 4.9 Shown are NMR spectra of the drug Quetiapine and the dye Congo red.....	45
Figure 4.10 Portions of the superimposed ¹ H NMR spectra of three structurally similar azo dyes obtained by dilution from 200 μM to 12 μM.....	47
Figure 5.1 NMR spectra of four compounds.....	56
Figure 5.2 TEM images of four anticancer drugs (Fulvestrant, Sorafenib, Lapatinib, and Gefitinib), and an antileprosy drug (Clofazimine).....	57
Figure 5.3 (a) TEM images of 50 μM Sorafenib, Lapatinib, and Clofazimine incubated for 24 h at 37 °C in DMEM 5% FBS in the absence of 0.025% (v/v) Tween 80, (b) in the presence of 0.025% (v/v) Tween 80.....	58
Figure 5.4 (a) Confocal images of HeLa cells incubated in the presence of 50 μM Lapatinib for 24 h.....	60
Figure 5.5 USEM images of HeLa cells incubated for 24 h in the presence of (a) 50 μM Lapatinib, (b) 50 μM Clofazimine, and (c) 50 μM Light green SF yellowish, (d) represents control cells in the absence of drugs.....	60
Figure. 6.1 Drugs exist in unique multi-phase equilibria in solution.....	73
Figure. 6.2 The presence of large drug colloidal aggregates can be visualized by TEM.....	74
Figure. 6.3 Overview of the protocol to probe drug solution behavior.....	82
Figure. 6.4 NMR dilution assay.....	91
Figure. 6.5 NMR detergent assay.....	93
Figure. 6.6 Probing the solution behavior of valsartan.....	100
Figure. 6.7 Probing the solution behavior of methylene blue.....	101
Figure. 6.8 Probing the solution behavior of candesartan cilexetil.....	102
Figure. 6.9 Probing the solution behavior of lapatinib.....	103
Figure. 6.10 Probing the solution behavior of lapatinib by using orthogonal techniques.....	104
Figure 7.1. Shown are the characterization of aggregates and non-aggregates.....	132
Figure 7.2. Cellular uptake of drug aggregates.....	133
Figure 7.3. Cellular uptake of drug and dye aggregates by human neutrophils.....	135
Figure 7.4. Effects of compound aggregation on the production of cytokine (TNF-α) using the mouse macrophage cells (RAW264).....	138
Figure 7.5. Effect of compound aggregation on the production of cytokines (IL-8) using human neutrophils.....	139
Figure 7.6. Effect of dye aggregation on the production of cytokines (IL-8) using human neutrophil cells.....	140

LIST OF TABLES

Table 2.1. Shown are several aggregator-drugs and their critical aggregation concentrations (CAC).....	4
Table 2.2. Shows the data for HIV inhibitor compounds.....	22
Table 2.3. Shows the data for HIV inhibitor compounds.....	23
Table 2.4. Shows the advantages and dis-advantages of the methods used to detect compound aggregation.....	28
Table 6.1. Comparison of techniques for detecting drug aggregates.....	78
Table 6.2. Troubleshooting.....	98

LIST OF ABBREVIATIONS

HTS	High-throughput screening
NMR	Nuclear magnetic resonance
DLS	Dynamic light scattering
cSLS	Confocal static light scattering
TEM	Transmission electron microscopy
USEM	Ultra section electron microscopy
CLSM	Confocal laser scanning electron microscopy
CAC	Critical aggregation concentration
CMC	Critical micelle concentration
CHO	Chinese hamster ovary
PKU	Phenylketonuria
T2 CPMG	Spin-spin Pur-Cell Meiboom Gill
SGF	Simulated gastric fluid
SNR	Structure nano-entity relationship
FBS	Fetal bovine serum
ELISA	Enzyme-linked immunoassay
TNF-α	Tumor necrosis factor-alpha
IL-8	Interleukin-8
IL-6	Interleukin-6
Lap	Lapatinib
Erlo	Erlotinib
Gef	Gefitinib
Rilu	Riluzole
MB	Methylene blue
Tart	Tartarazine
Neph Y	Nephtol yellow

1 INTRODUCTION

Drug discovery and pharmaceutical efforts often begin with screening libraries of collections of compounds that might serve as drug candidates (Bleicher *et al.*, 2003; Ganesh *et al.*, 2018). Although these high-throughput screening (HTS) assays are widely used to discover new targets related to diseases, they are often associated with false-positive results in enzyme assays and false-negatives in cell-based assays (McGovern *et al.*, 2002a; Owen *et al.*, 2012a; Shoichet, 2006). One of the most common sources of these artifacts in early drug discovery is compound self-aggregation (nano-entities). But to date, little is known about the existence of nano-entities and their full range of sizes, types, etc. This is mainly due to the limitations of detection strategies given that this peculiar phenomenon remained poorly characterized. So, in this context, we are in need to implement sufficient strategies to fully reveal compound nano-entities. In this thesis, we employed practical and valuable techniques to better characterize these nano-entities and their associated properties using NMR, DLS, TEM and CLSM. We further pursued a pilot study to correlate these nano-entities with unknown properties such as the potential to induce an immune response using human neutrophils and murine macrophage cellular models.

In the literature review, I introduced the concept of compound self-aggregation phenomenon giving a brief description of compound solution behaviors and the tri-phasic equilibrium. Afterwards, I highlighted the correlated properties of nano-entities and their impacts on drug discovery pathways. Finally, I introduced and explained the possible strategies used to expose compound aggregation and underline their advantages and limitations. In the first objective of this thesis, practical NMR strategy was introduced to expose the nano-entities of synthetic dyes with the possible detection of their aggregate sizes including smaller nano-entities (first article). We then worked on the second objective of the thesis which was to monitor compound aggregation at the cellular level by confocal microscopy tool and evaluate if aggregating compounds can cross membranes and enter live cells (second article). Following the findings from the first and second publications, we proposed a protocol to enable researchers to monitor the triphasic equilibrium and solution behavior of their drugs/compounds, with a focus on the nano-entities phase (third article). The fourth article deals with the fourth objective of this thesis– to explore the possible correlation of drug and dye nano-entities with immune responses.

2 LITERATURE REVIEW

2.1 Concept and Definition of Compound Aggregation

Compound self-aggregation, also called colloidal aggregation or nano-entities, refers to the tendency for small drug-like molecules to assemble into soluble entities when placed in an aqueous environment. These entities assume a wide range of sizes varying from 50 to 500 nm which form spontaneously in solutions (McGovern *et al.*, 2003). Perhaps one reason that compound self-aggregation has usually been ignored is the well-known held view that molecules will exist either as single molecule or as precipitates when placed in aqueous conditions. This has been commonly validated by the visual observation of either a clear/pure or cloudy/hazy solution. This basic view assumes that small molecule drugs and compounds exist as lone molecules, while insoluble drugs or compounds form amorphous precipitates.

However, there is growing evidence that supports the concept of a triphasic equilibrium as shown in (Figure 2.1), where there is also an unknown intermediate soluble phase called compound aggregates. Perhaps each single compound adopts its unique properties and equilibrium between the three phases which depends on different surrounding conditions, such as pH, concentration, temperature, buffer, media and other environmental conditions (Ayotte *et al.*, 2019; LaPlante *et al.*, 2013a).

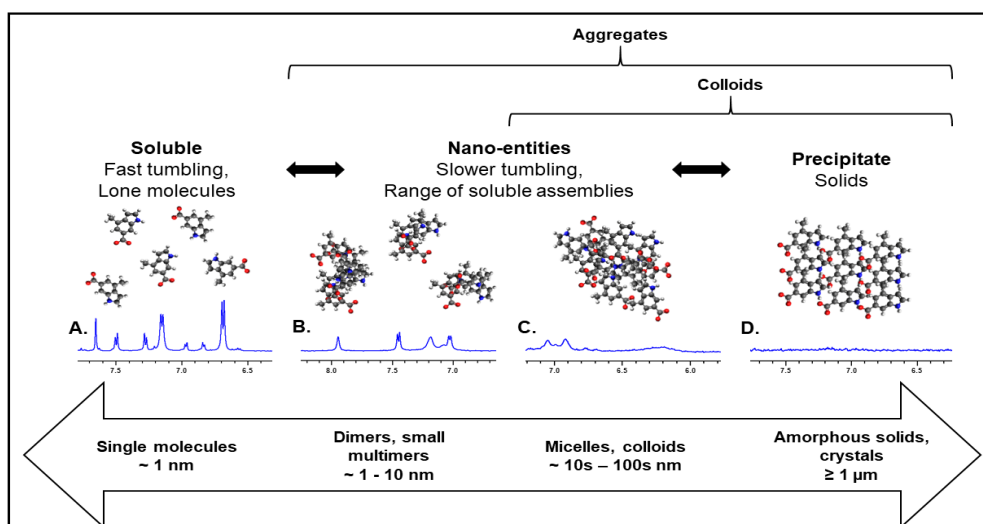


Figure 2.1. Compounds' three-phase equilibrium.

(A-D) are ¹H NMR spectrum for several compounds (A) Light green SF yellowish, (B) Evans blue, (C) acid violet 49, and (D) Pranlukast. All compounds were tested at concentration (300 μM) in 50 mM sodium phosphate, 100 mM NaCl, 10% D₂O, pH 7.4 (Ayotte *et al.*, 2019).

2.2 Properties of Compound Aggregation

Many organic small drug like-molecules can self-assemble into a wide range of sizes at micromolar concentrations. This includes small molecules from library screening hits and fragments, synthetic dyes, and also some FDA approved drugs (McGovern *et al.*, 2002b; McGovern & Shoichet, 2003; Seidler *et al.*, 2003) (Table 2.1). Each of which has its own fingerprints and distinct properties that can influence all drug discovery processes. These properties are briefly characterized below with their implications in drug discovery and developments.

2.2.1 Critical Aggregation Concentration (CAC)

The formation of nano-sized particles is a distinguishing property of colloidal aggregation. The formation of colloidal aggregates typically depends on the concentration of the compound. At lower concentration below the CAC of a particular molecule, the compound is fully solubilized or unaggregated. However, when the concentration reaches the CAC, the compound spontaneously self-aggregates forming unique nanoparticles (Coan & Shoichet, 2008). It should be kept in mind that each compound has its unique attributes that is highly dependent on many conditions such as concentration, pH, buffer (to name a few) (Allen *et al.*, 2020). For example, some approved drugs can aggregate at some conditions at different concentrations as shown in (Figure 2.2) for the drug nifedipine, while others can also display binding and inhibition properties even below the CAC. The tables below describe the CAC of some drugs at different concentrations and conditions (Ganesh *et al.*, 2018).

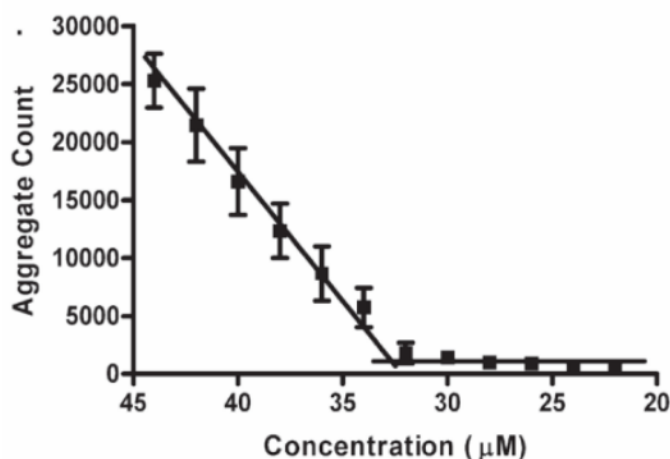
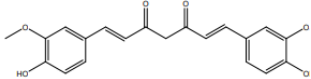
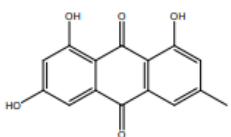
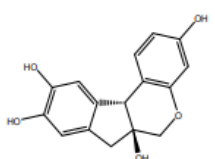
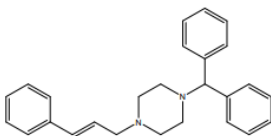
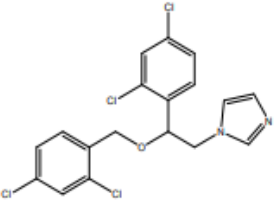
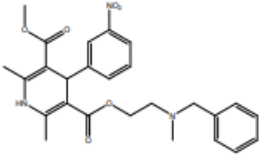
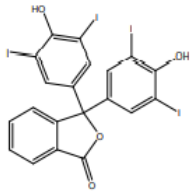
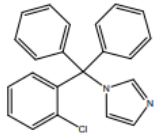
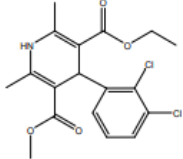
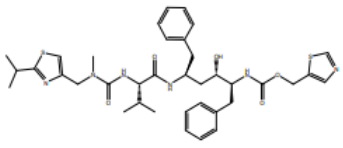
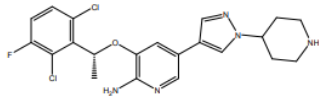
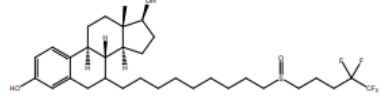
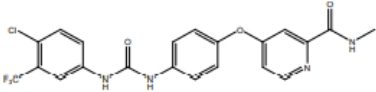
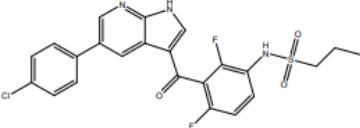
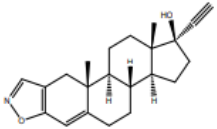
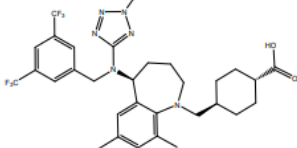


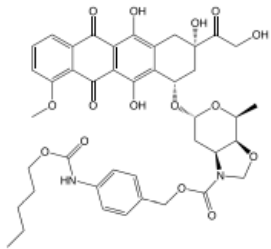
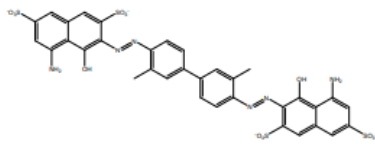
Figure 2.2. Critical aggregation concentration (CAC) of the drug nifedipine (Ganesh *et al.*, 2018).

Table 2.1. Shown are several aggregator drugs, their CAC and several EC₅₀ and IC₅₀ values studied on different targets. Note that not all IC₅₀ and EC₅₀ available in the literature. N/A indicates that no data available.

Compounds	CAC	Representative molecular targets and EC ₅₀ values (μM)	IC ₅₀ (μM) vs	IC ₅₀ (μM) vs
Curcumin (Duan <i>et al.</i> , 2015) 	17 ± 0.44	Ca ²⁺ -ATPase (~3), HER2, HIV-1 (100) and HIV-2 protease (250), cyclooxygenase (52), PkA and PkC	β-lactamase -Detergent (12 μM) +Detergent (>30 μM)	MDH -Detergent (9 μM) +Detergent (>30 μM)
Emodin (Duan <i>et al.</i> , 2015) 	28 ± 2	MMP (12.8-20.1), AMPK (0.5), 11 β HSD1(4.2-7.2), trypsin (50), DYRK1A and CLK1 (4.2 – 6.1)	β-lactamase -Detergent (27 μM) +Detergent (>100 μM)	MDH -Detergent (28 μM) +Detergent (>100 μM)
Brazilin (Duan <i>et al.</i> , 2015) 	57 ± 7	PKC	β-lactamase -Detergent (302 μM) +Detergent (>500 μM)	MDH -Detergent (1.6 μM) +Detergent (84 μM)
Cinnarizine (Coan & Shoichet, 2008) 	7 ± 3	N/A	β-lactamase -Detergent (40 μM)	N/A
Miconazole (Coan & Shoichet, 2008)	3 ± 2	N/A	β-lactamase	N/A

			-Detergent (25 μ M)	
Nicardipine (Coan & Shoichet, 2008) 	32 \pm 3	N/A	β-lactamase -Detergent (66 μ M)	N/A
TIPT (Coan & Shoichet, 2008) 	10 \pm 2	N/A	β-lactamase -Detergent (5 μ M)	N/A
Clotrimazole (Ilevbare & Taylor, 2013) 	15.0 \pm 0.3	N/A	N/A	N/A
Felodipine (Ilevbare & Taylor, 2013) 	26 \pm 1	N/A	N/A	N/A
Ritonavir (Ilevbare & Taylor, 2013) 	26 \pm 0.1	N/A	N/A	N/A
Crizotinib (Owen <i>et al.</i> , 2012a) 	19.3	N/A	Cruzain	N/A

			-Detergent (23.4 μ M) +Detergent (117.8 μ M)	
Fulvestrant (Owen <i>et al.</i> , 2012a) 	0.5	N/A	Cruzain -Detergent (9.1 μ M) +Detergent (>100 μ M)	N/A
Sorafenib (Owen <i>et al.</i> , 2012a) 	3.5	N/A	Cruzain -Detergent (6.8 μ M) +Detergent (>100 μ M)	N/A
Vemurafenib (Owen <i>et al.</i> , 2012a) 	1.2	N/A	Cruzain -Detergent (2.8 μ M) +Detergent (>100 μ M)	N/A
Dansol (Jackson <i>et al.</i> , 2014) 	39	N/A	N/A	N/A
Evacetrapib (Li <i>et al.</i> , 2017) 	0.8	N/A	N/A	N/A
Pentyl-BABC doxazolidine (Ganesh <i>et al.</i> , 2017a)	14	N/A	N/A	N/A

				
<p>Trypan blue</p> 	30	N/A	N/A	N/A

2.2.2 Small-molecule Promiscuity and Specificity

One of the most significant challenges that pharmaceutical industry faces is to ensure desirable safety and stability profiles of a medicine that target specific kind of disease (Cronin, 2004; Price *et al.*, 2009). Although the goal of all industrial drug discovery programs is to design small molecule drugs to target specific receptor pocket of interest, they can also bind to unintended enzymes leading to undesirable adverse off-target/promiscuity or toxicity outcomes. In nature, the origin of *in vivo* toxicology profiles remained not fully understood by drug discovery efforts leading to gaps between *in vitro* and *in vivo* observations. To avoid the toxic outcomes, pharmaceutical efforts are implementing some techniques that can ultimately help to prioritize safe/desirable compounds and deprioritize unsafe/undesirable ones. Although the undesirable toxic effect can result from the presence of some subgroups such as toxicophores, it may also exist as a result of interactions with some proteins other than the intended target or inhibit multiple enzymes, which known here as off-target promiscuity (J Edwards & Sturino, 2011; Kalgutkar *et al.*, 2008).

In industry, promiscuous compounds can be identified as the compounds that inhibit or decrease >50% off-target assays at micromolar nominal concentrations. Moreover, lead discovery efforts have recently recognized that when compounds, e.g lipophilic placed in aqueous solution, it can somehow influence many physiochemical/molecular properties including adverse *in vivo* toxicology (Hughes *et al.*, 2008; Price *et al.*, 2009). However, the principle of this toxicological outcome correlated-molecular properties remains poorly understood. Lipophilic molecules, which is also called “stickier compounds”, have the tendency to be more promiscuous than hydrophilic compounds. This could be due to their higher

attractions to hydrophobic off-target receptors either stoichiometrically or non-stoichiometrically (Bender *et al.*, 2007).

Another cause of off-target promiscuity arises from compound self-aggregation which non-stoichiometrically can lead to off-target inhibition (LaPlante *et al.*, 2013a). This interesting *in vitro* finding implicate the existence of these micelle like-colloids “aggregates” in many unexpected properties including false positive results in many HTS assays or false negative results in cell culture based-assays as mentioned earlier (Seidler *et al.*, 2003; Wang & Matayoshi, 2012). Subsequent studies have argued that the nonstoichiometric protein inhibition by compound aggregation can result by different mechanisms discussed in details below. The three mechanisms can be classified as, (1) partial unfolding, (2) restrained dynamics, or (3) physical sequestration.

2.2.2.1 Proposed Mechanism of Inhibition and other Properties of Compound Aggregation

Colloidal aggregation and nano-entities have unique property to non-specifically inhibit protein targets. It is well-identified that these aggregates can cause false positive results in HTS assays (DeWitte, 2006; Giannetti *et al.*, 2008). Still, the exact mechanism of how these self-assemblies cause the non-specific inhibition remains speculative. However, some efforts have been made to uncover the non-specific inhibition mechanisms caused by aggregated compounds. These efforts focused on understanding the structural changes upon binding of colloidal aggregates and enzymes. McGovern *et al.*, 2003, have proposed three possible mechanisms of non-specific and promiscuous binding inhibition (see Figure 2.3).

In the first mechanism, due to the binding property and surface interactions between aggregates and enzymes, colloidal aggregates can adsorb the protein onto their surface leading to partial unfolding and loss of enzymatic activity. This unique property only specific for proteins that can be adsorbed more strongly to the surface of colloidal aggregates compare to some peptides. For instance, several experiments showed that when full lactamase protein incubated with compound aggregation, a preferential binding of this enzyme to aggregate surfaces and a subsequent inactivation of the enzyme have been demonstrated. Unlike lactamase, the study found that peptide fragments of this protein incubated with colloidal aggregates led to little effect on the protein inhibition (Coan *et al.*, 2009; McGovern *et al.*, 2003).

In the second mechanism, which is called restrained dynamics, aggregation that bind to specific enzymes may have contradictory effect. It may typically restrict the dynamic motion of proteins that required for their catalysis process. Finally, binding of compound aggregates to

enzymes may also cause physical sequestration of a particular enzyme from its substrate, which is the third mechanism of promiscuous inhibition by aggregation as shown in (Figure 2.3) (Coan *et al.*, 2009; McGovern *et al.*, 2003).

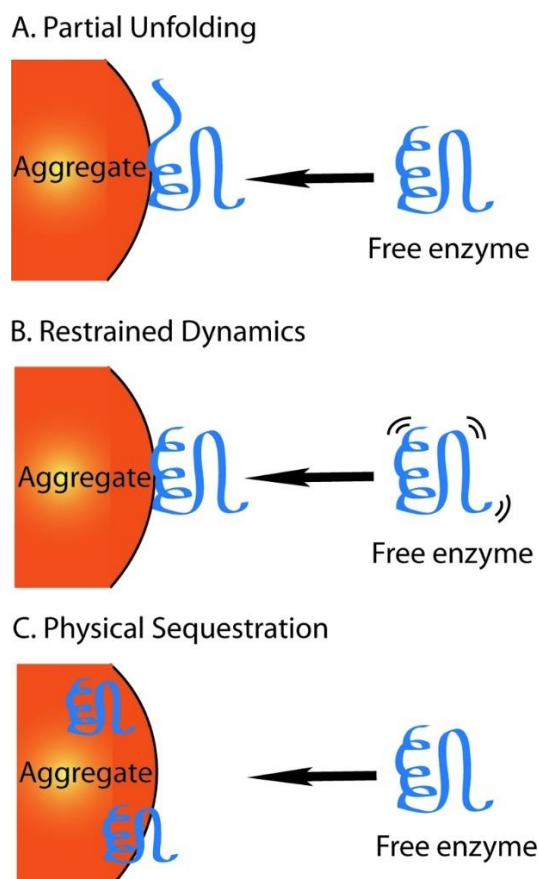


Figure 2.3. Three potential mechanisms of action of non-specific promiscuous small-molecule aggregators.

(A) Shows the binding between aggregates and enzymes that promotes a partial unfolding event (first mechanism), (B) Binding to the aggregate restrict the dynamic motion of proteins and catalytic process (second mechanism), (C) Binding to the aggregates promotes physical sequestration (third mechanism) (Coan *et al.*, 2009).

2.2.2.2 Detergent-sensitive enzyme Inhibition Assay

As a result of false positive hits in HTS campaigns, large libraries of small-molecule aggregators are assayed to discover non-specific inhibition to a variety of proteins as mentioned above. There has been a number of techniques for discovering such this non-specific inhibition caused by compound aggregation. One of these strategies is the detergent-sensitive enzyme-inhibition assay, which is a relatively definitive method and easy way to predict promiscuous aggregate-based inhibition in large-scale screening campaigns. Detergents are used in aggregation assays due to their ability to disrupt colloidal aggregates.

They can be used in many biological applications. In respect to their CMC, detergents such as Tween 80, can have a CMC range between 0.3%-0.35% (Feng *et al.*, 2006). The CMC of sodium dodecyl sulfate (SDS) was also calculated and found to be 0.2 %. All of these concentrations were considered acceptable in HTS assays.

Interestingly, it was documented that enzyme inhibition can be significantly decreased upon the addition of several detergents. For example, some studies found that a greater than two-fold reduction in enzyme inhibition percentage was noticed upon the addition of 0.01% of the detergent (Triton X-100) in most tested aggregators (Feng *et al.*, 2005; McGovern *et al.*, 2003). However, the detergent sensitivity must be considered which is varying from one aggregator to another. For instance, Congo red as a known aggregator dye requires a percentage of around 0.1% of Triton X-100 to exhibit significant reduction in enzyme inhibition assay, while other aggregators may require different percentages. Testing varying concentrations of detergents and small-molecule aggregators are required to address detergent sensitivity and limit the hallmarks of this phenomenon. Still, using enzyme based detergent inhibition assay screening is a unique and fast application to detect promiscuous aggregate-based inhibition (Feng & Shoichet, 2006b).

2.2.3 Aggregation and Cytotoxicity

Drug discovery efforts design medicines to specifically bind to the receptor pocket of the intended target. However, some compounds may unfavorably interact with unintended receptors leading to undesirable *in vivo* toxicological consequences. The origin of this *in vivo* toxicology effects remained poorly understood. It has been reported that compounds are more likely to be toxic if they either cause specific inhibition of biological mechanisms or they interact with receptors other than the specific target of interest (known as off-target promiscuity), that mostly due to compound aggregation as described above (J Edwards & Sturino, 2011; Kalgutkar *et al.*, 2008; LaPlante *et al.*, 2013a). A recent study reported that drug forming self-assemblies are correlated with cytotoxicity outcome such as phenylalanine that forms amyloid-like nanofibrillar aggregate structures at millimolar concentrations (Adler-Abramovich *et al.*, 2012) as shown in (Figure 2.4).

The cytotoxic effect of phenylalanine self-assemblies has been well documented by Adler-Abramovich *et al.*, 2012. It was demonstrated that phenylalanine treated cultured Chinese hamster ovary (CHO) cells and (PC12) cells at elevated concentrations can decrease the viability of those cells up to 80%. Interestingly, the study reported no observable cytotoxicity with alanine, a non-fibrillar assemblies, compare to phenylalanine. Thus, the multi-molecular entities, fibrillar assemblies of phenylalanine might be responsible for this cytotoxicity. Moreover, it was also reported that phenylalanine multi-molecular fibrils can alter the morphological shape of the CHO cells, that shown to be smaller and rounder in comparison

with non-treated cells. Therefore, it might be that the cytotoxic outcome observed with those individuals with phenylketonuria (PKU) disease is the result of phenylalanine fibrillar formation. PKU is a disease in which mutation in the gene that encodes phenylalanine amino acid take place and can result to the accumulation of phenylalanine assemblies in the brain. This amine acid can form fibrils evaluated by TEM, SEM, and confocal microscopy as shown in figure 2.4. It was found that this self-assemblies can cause high level of cytotoxicity *in vitro* and even *in vivo*. The fibrils are kind of self-aggregation, and therefore, this study correlates the presence of self-assemblies to cytotoxicity (Adler-Abramovich *et al.*, 2012).

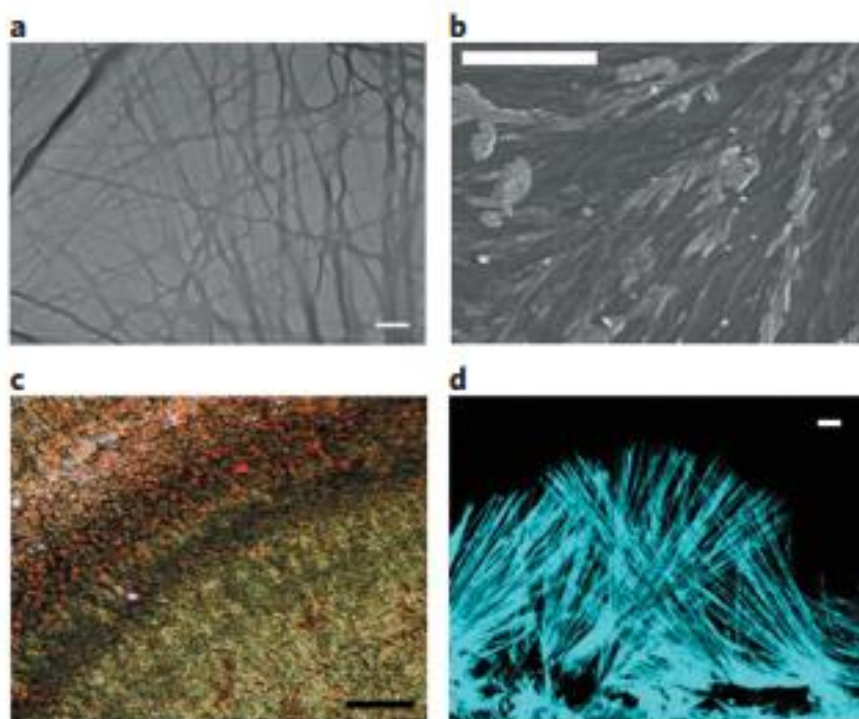


Figure 2.4. Self-assemblies of phenylalanine into supramolecular fibrils.

(a) TEM of phenylalanine assemblies (scale 1 μm), in ddH₂O at 6 mM (b) SEM of phenylalanine assemblies (scale 20 μm), (c) Phenylalanine assemblies stained with Congo red using microscopic examination (scale 500 μm), (d) Confocal microscopy of phenylalanine stained with ThT dye (scale 10 μm) (Adler-Abramovich *et al.*, 2012).

2.3 Detection Assays for Aggregation

2.3.1 Transmission Electron Microscopy (TEM)

Perhaps the most convincing evidence of the existence of compound self-aggregation and nano-entities came from Transmission Electron Micrograph (TEM) technique as shown in (Figure 2.5). This method can directly show that compounds and even drugs can self-assemble

into large micellar like-colloids. At least under stable conditions, TEM can visualize small-drug like molecule aggregates and directly show the amorphous and spherical structure of colloidal aggregates. The characteristic morphological features of those small-molecule aggregates versus can be directly revealed by TEM (McGovern *et al.*, 2002b). In addition, TEM has been widely used to study the phenomena of compound self-aggregation under different physiological conditions including temperature and pH.

Unlike other methods, it is now becoming possible to measure colloidal particle size in diameters using TEM under different conditions e.g media-containing serum 10% conditions (Owen *et al.*, 2012a). However, the particle size of aggregates seems to be quite smaller in diameters by electron microscopy compared to other techniques such as dynamic light scattering (DLS). The reason for this was because of the dehydrated conditions of TEM compare to the hydrated state of DLS. Interestingly, to improve the quality of images and visualization by TEM, most studies use negative stains such as uranyl acetate and ammonium molybdate.

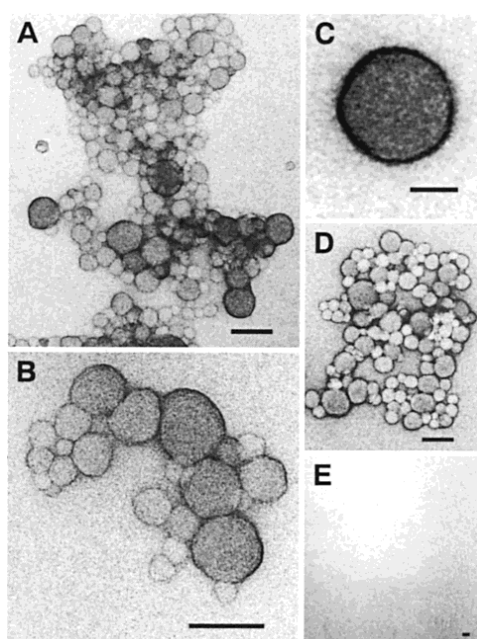


Figure 2.5. Shown are TEM images of some compound colloidal aggregates.

(A to C) 100 μM of compound tetraiodophenolphthalein dissolved in 20 mM of Tris; (D) 50 μM of the dye Congo Red dissolved in 20 mM Tris; and (E) Negative control (no compounds). Bar represents (100 nm) (McGovern *et al.*, 2002b).

2.3.2 Dynamic Light Scattering (DLS)

DLS technique has been widely used to quantitatively measure compound self-aggregation in aqueous solutions (Chan *et al.*, 2009). It has been used to determine the presence of particle size of colloidal aggregates and their distribution in a solution, by monitoring the time-dependent fluctuation of scattering intensities. Upon the formation of nano-entities, a

significant increase in the scattering intensity will be observed, that increases when small molecules reach their CAC.

On the other hand, by the addition of detergents, the scattering intensity can be significantly decreased. However, it must be considered that all detergents form micelles when their concentrations reach the critical micelle concentration (CMC), and therefore, they will have their own scattering intensities that must be taken into account. Moreover, to study the formation of aggregation in physiological conditions e.g in serum-containing media, the background scattering intensities of serum can be disadvantageous and this should be considered in such these assays. A study performed by Owen *et al.*, 2012, shows that colloidal aggregation of some anticancer drugs such as Fulvestrant, Lapatinib and Sorafenib can indeed be detected by DLS. Their aggregation formation can be observed by the scattering intensities compare to controls (e.g buffer or media only). Moreover, in the presence of the detergent (Tween-80), a reduction of the scattering intensities can be observed, indicating the loss of colloidal aggregation (as shown in Figure 2.6) (Owen *et al.*, 2012a).

Although DLS has been extensively used as aggregation detection assay, it has been identified as a low throughput screening assay as well as time-intensive methods in terms of aggregation detection. That said, some measurements observed by DLS are difficult to interpret due to misleading results produced when insoluble (precipitating) small molecules are evaluated, which usually produce large fit of errors. Also, DLS is a limited strategy that can not detect the types of small molecule aggregation (Chan *et al.*, 2009).

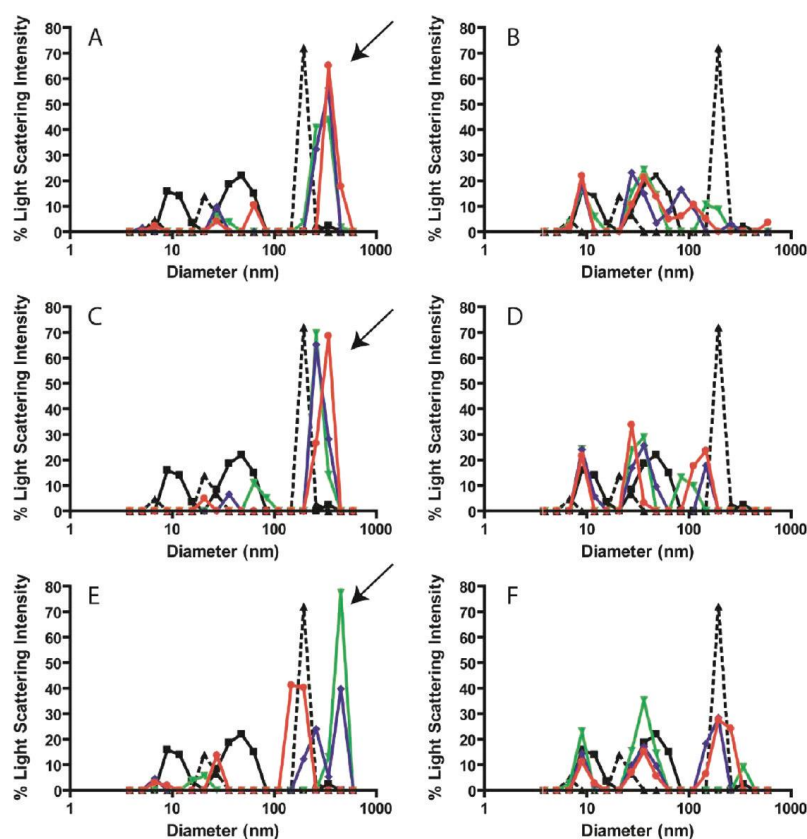


Figure 2.6. Colloidal aggregation of some anticancer drugs measured in cell culture medium by DLS.

(A, B) Fulvestrant, (C, D) Lapatinib, and (E, F) Sorafenib. The left figure (A, C, E) shows the formation of aggregation in the absence of the detergent Tween-80. The right figure (B, D, F) shows drug aggregation in the presence of Tween-80, which shows the break up of the peaks by the addition of the detergent, indicating the loss of drug aggregation (Owen *et al.*, 2012a).

Recently, another practical method that can be run on DLS instruments to detect compound aggregation is called confocal static light scattering (cSLS). It has been identified as a high throughput screening technique due to its ability to determine the monomeric solubility of many small molecules. In a study performed by LaPlante *et al.*, 2013, cSLS was used to assess the CAC of three known small-molecule aggregators and one known non-aggregator as shown in (Figure 2.7). Interestingly, no light scattering intensities were noticed for the known non-aggregator control “Etodolac”. On the other hand, a significant observable increase in the scattering intensities was exposed for the three known aggregator drugs Gefitinib, Pranlukast, and Crizotinib. Interestingly, this notable increase was due to the formation of different sizes of aggregates, more likely larger self-assemblies (LaPlante *et al.*, 2013b). Importantly, in this study using cSLS for the detection of aggregation, the authors observed that some drugs gave scattering intensities of data and unclear baseline that were typically difficult to interpret and understand, thus this method could present some disadvantages.

Light Scattering cSLS and CAC Determinations

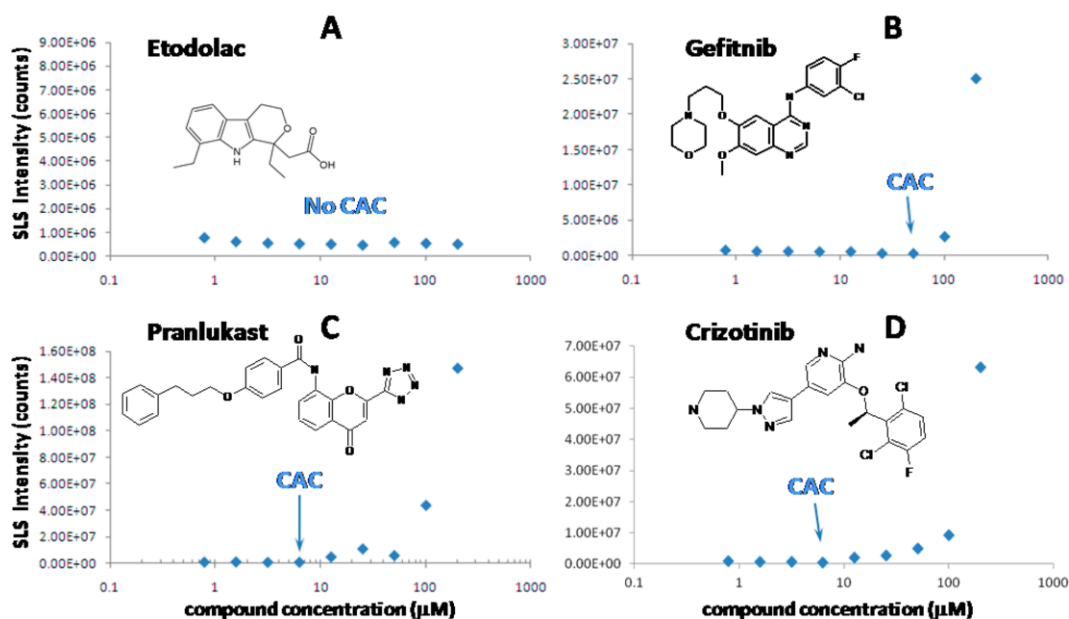


Figure 2.7. cSLS technique on three known aggregator drugs and one non-aggregator control drug.

Etodolac (A) is a non-aggregator drug, and Gefitinib (B), Pranlukast (C), and Crizotinib (D) are the three well-known aggregators. CAC points are determined by cSLS as clear indicators of the formation of aggregation. All compounds were dissolved in the buffer, 50 mM sodium phosphate pH 7.4 in 100% D₂O solvent (LaPlante *et al.*, 2013b).

2.3.3 Nuclear Magnetic Resonance (¹H NMR strategy)

Although methods including DLS and TEM are optimal for revealing compound aggregations and determine their large sizes, characterization of smaller sizes of nano-entities was not possible by these techniques. Recently, a straightforward (1D) ¹H NMR strategy was implemented as a potential and practical assay for monitoring compound self-aggregation and their associated properties in aqueous solution (LaPlante *et al.*, 2013b).

2.3.3.1 Concept of NMR Practical Assay for Monitoring Nano-entities

As described above, when small drug-like molecules are placed in aqueous media, they are expected to equilibrate between three unique phases. These can be classified as 1) soluble single lone molecules, 2) soluble aggregate entities, and 3) insoluble solid-like precipitate forms. The ¹H NMR assay can be used efficiently to distinguish between the three different phases. This could be easily explained by acquiring ¹H NMR spectra. Of note, recent studies have often observed that while some drugs displayed usual features of ¹H NMR spectra, others displayed unusual trends in solution. For instance, it is expected to obtain sharp ¹H NMR resonances for a single lone molecule that tumble so freely and too fast in solution. On the other hand, no resonances at all are expected for solid like-precipitate forms which tumble

too slowly in solution, leading to very broad resonances that are far a way to be detected by NMR solution assay.

However, for the intermediate nano-entity phase, which seems to be quite homogeneous by the naked eye, it is expected to observe unusual broad ^1H NMR resonances revealing the presence of compound soluble self-assemblies. One of the NMR strategies to detect the presence of aggregation is the serial dilution assay using different concentrations e.g. from $12.5\ \mu\text{M}$ - $200\ \mu\text{M}$. The idea of using such a serial dilution assay for aggregate detection originated from that compound self-aggregation are sensitive to concentrations, and such this change in the environment of nano-entities can be clearly stated by the ^1H NMR spectral features. Therefore, ^1H NMR ideally is a practical assay to determine compound behaviour and self-association. If NMR spectra exhibits unusual behaviors as a function of concentration, the compounds then are more likely aggregators (LaPlante *et al.*, 2013b).

2.3.3.2 Detection of Compound Aggregation Using ^1H NMR Assay as a Function of Compound Serial Dilution

The ^1H NMR assay can be used for detecting compound aggregation by monitoring the compound ^1H NMR resonances as a function of serial dilution (concentrations) as shown in (Figure 2.8). Expectedly, for the non-aggregator, the NMR spectra read-out shows that the compound behaves as single lone molecule, tumble so freely in the solution, and not affected by the serial concentrations (Figure 2.8 A). Furthermore, the resonances are sharp at all concentrations and no chemical shifts have been observed. Only changes in the resonance intensities have been noted which is expected due to changes of the concentrations. On the other hand, the NMR spectra read-outs for the aggregator in (Figure 2.8 B), shows that the compound behaves as self-associate at higher concentrations, and tumble more freely and dissociate upon dilution. This unusual attributes in NMR resonance are more likely due to changes in the local environments around the molecule that consistent with the presence of self-aggregation and nano-entities (LaPlante *et al.*, 2013b).

NMR Assay Involves Compound Dilutions

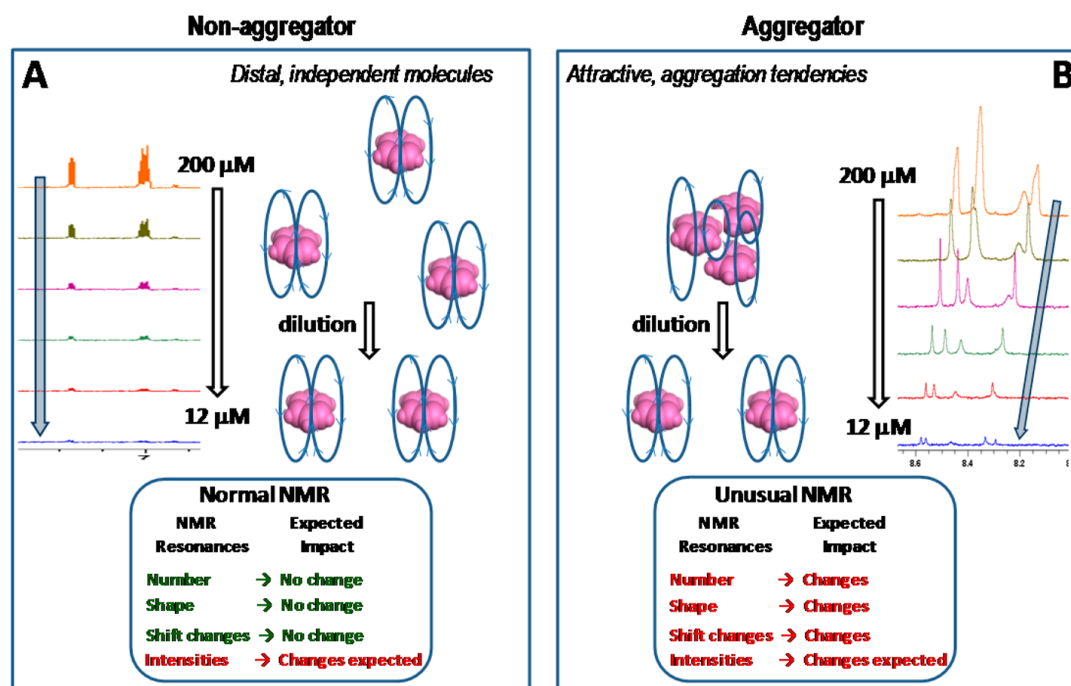


Figure 2.8. NMR features and behaviors of non-aggregating and aggregating compounds as a function of dilution.

(A) shows the non-aggregator compounds (Etodolac) that tumble too freely in a solution at all concentrations; (B) shows the aggregator compounds, unusual NMR features at higher concentrations that tumble freely in a solution upon serial dilution. The solution used in this study was 50 mM sodium phosphate pH 7.4 in 100% D₂O (LaPlante *et al.*, 2013b).

The figure above exemplifies the main parameters of the NMR study for detecting compound aggregation and non-aggregation using serial dilution. These include resonance number, chemical shift, broad/sharp resonances, and intensities. First, resonance number should indicate the existence of all peaks at all concentrations. In the presence of aggregating compounds, changes in the number of peaks is expected upon dilution. Second, the chemical shift that exist as a function of changes in the molecule local environments can also indicate the presence of aggregation. Third, the NMR resonance (sharp or broad) is another indicator of the existence of aggregate or non-aggregate species in relation to tumbling rate and size. If the resonances are broad due to a slower tumbling rate, then larger/multimeric aggregate species are expected. Finally, the NMR resonance intensities usually occur as a result of changes in concentrations, which can be observed in either aggregate or non-aggregate species. In several cases, the resonance intensities are not representative due to the limited solubility or the existence of the compound in equilibria between the two phases (lone molecules and aggregation). Interestingly, employing the use of surfactants such as Tween 80 can differentiate between the two states (as described later) (LaPlante *et al.*, 2013b).

Figure 2.9 exemplifies the solution behavior and NMR observations for aggregator and non-aggregator compounds. In (Figure 2.9 A), the NMR resonance of the well-known non-aggregator compound Riluzole was sharp and well-aligned at all concentrations. No right or left chemical shifts were observed upon dilution, and the resonance intensities were also reduced as a function of serial dilution. All these NMR spectral observations are normal trends for non-aggregating molecules. On the other hand, distinct and unusual NMR spectral trends were observed for the well-known aggregator methylene blue as shown in (Figure 2.9 B). As expected, a chemical shift of the resonances to the left upon dilution was clearly observed, which is an indicator of the presence of aggregation.

In Figure 2.9 C, unusual two sets of NMR resonances (broad and sharp) were reported upon increasing concentrations together with slight shifts to the left. Interestingly, in Figure 2.9 D, the NMR spectra of Pranlukast as an aggregator compound shows very small sharp resonances at all concentrations. This might be due to compound insolubility or the presence of very large aggregate species that are too broad to be detected by NMR dilution assay. A strategy-based addition of surfactants (detergents) was employed to address this issue (described below) (LaPlante *et al.*, 2013b).

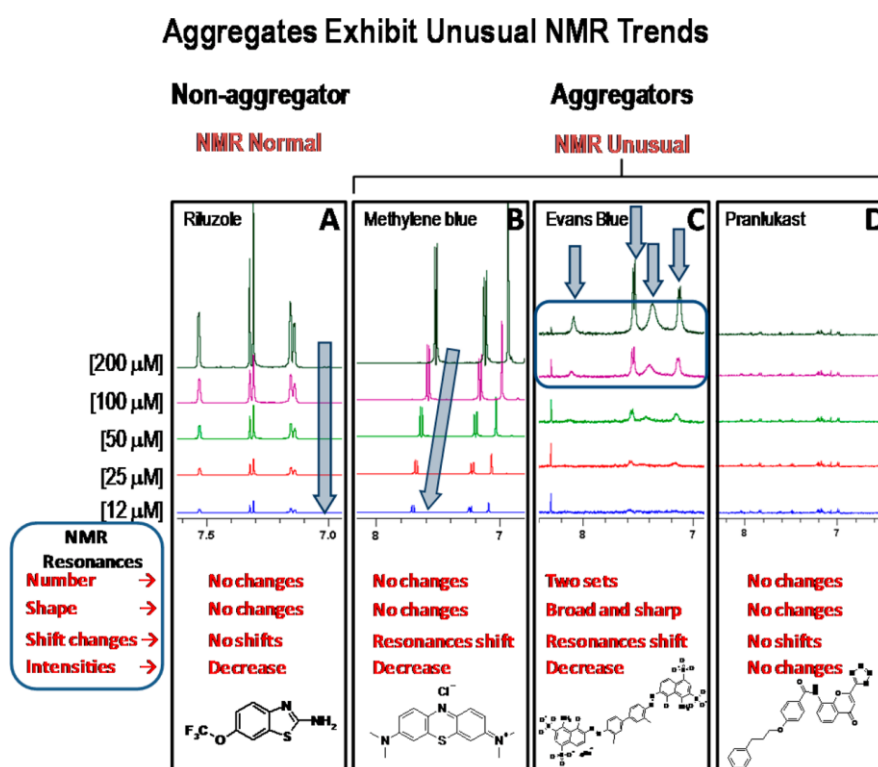


Figure 2.9. Examples of NMR assay for several compounds.

(A) NMR example spectra of a non-aggregator compound, Riluzol. Also, NMR examples of three known aggregators (B) methylene blue, (C) Evans blue, and (D) Pranlukast. The solution used in this study was 50 mM sodium phosphate pH 7.4 in 100% D₂O (LaPlante *et al.*, 2013b).

Another example of NMR assay to detect nano-entities is shown in (Figure 2.10) (LaPlante *et al.*, 2013b). The dilution data obtained from the well-known aggregator benzyl benzoate displays the presence of a new set of resonances at higher concentrations (200 μ M), revealing the existence of nano-entities, which is concentration dependent. This could be compared to the lower concentration spectra that displays usual resonance trends (see Figure 2.10 A). On the other hand, the aggregation tendency of the drug chlorpromazine was less visible when analyzed without zooming in. However, the resonance shifting appeared significant and noticeable when data are viewed by zooming in (see Figure 2.10 B) (LaPlante *et al.*, 2013b). As reported, chlorpromazine is one of the drugs that has been associated with off-target promiscuity on some receptors (Doak *et al.*, 2010).

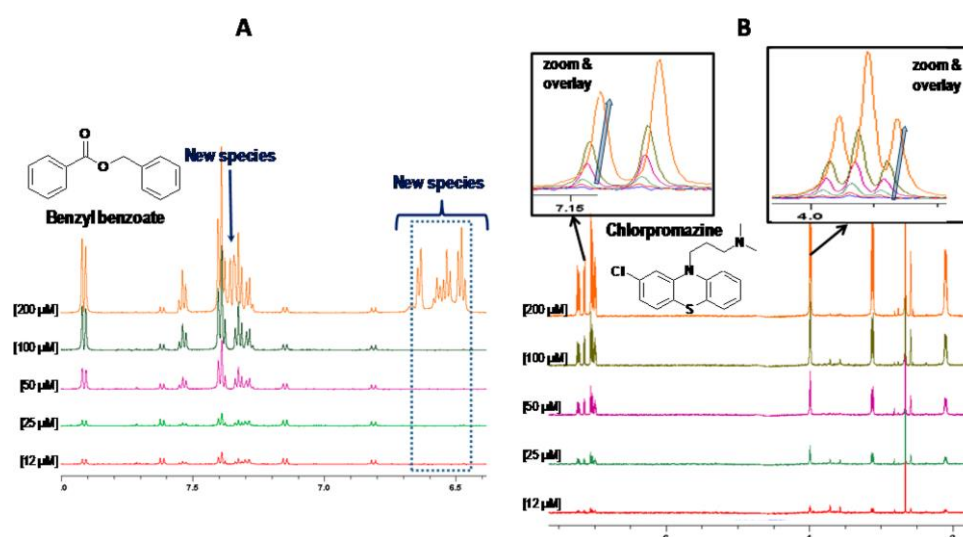


Figure 2.10. Example of aggregating drugs and unusual NMR behaviors.

(A) The ^1H NMR spectra of the known-aggregator benzyl benzoate and (B) The NMR of the known aggregator drug, Chlorpromazine. The buffer used is 50 mM sodium phosphate pH 7.4 in 100% D₂O solvent (LaPlante *et al.*, 2013b).

2.3.3.3 Use of Detergent Assay to Reveal Large Aggregates by NMR

To evaluate the presence of large assemblies, a detergent based-assay by NMR strategy was recently introduced (LaPlante *et al.*, 2013b). Detergents can breakup the aggregate assemblies into smaller entities, which are detectable by NMR resonances. The addition of detergent to larger aggregates was based on Shoichet's studies and co-workers (Feng & Shoichet, 2006a). Detergents such as Triton X-100, which was used in HTS campaigns, eradicated 95% as false positive hits as a result of the nonstoichiometric binding of aggregators. LaPlante *et al.*, 2013, tested the effect of various detergents on compound aggregation including Triton X-100 and Tween 80.

The example of the two aggregator compounds below shows that Tween 80 resulted to the breakup of aggregate assemblies that were observable by NMR spectra. Figure 11A shows that the dilution spectra of Pranlukast had very weak intensities more likely due to low concentrations of the lone molecules. However, upon the addition of Tween 80 to the compound, larger intensities have been emerged due to the presence of smaller entities. Therefore, detergent based-assay by NMR can be a useful strategy for revealing undetectable assemblies. Similar results for Congo Red were also noted as shown in Figure 2.11 B that was also corroborated by electron microscopy (LaPlante *et al.*, 2013b).

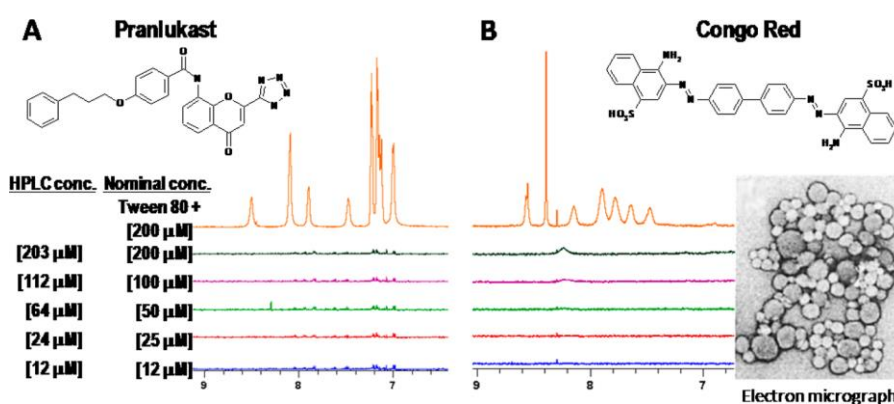


Figure 2.11. Examples of NMR detergent assay.

(A) NMR spectra of Pranlukast in buffer. Additional sample at 200 μM with the addition of detergent (Tween 80). The spectra on the right (B) is NMR spectra of Congo Red with an electron micrograph of Congo Red assemblies. The buffer used is 50 mM sodium phosphate pH 7.4 in 100% D₂O solvent (LaPlante *et al.*, 2013b).

The use of detergents to reveal larger aggregates was also combined with centrifugation. The aggregates were clearly observed in the above example by the detergent Tween 80, which enhanced the solubility of the compounds and resulted to smaller compound entities. However, there are microparticles for several aggregator compounds that are detectable only with electron micrographs. Therefore, mild centrifugation of an NMR sample, and the addition of detergent to the supernatant might help resolve this. More examples of the effect of detergents on breaking up aggregates are described in Figure 2.12 (LaPlante *et al.*, 2013b).

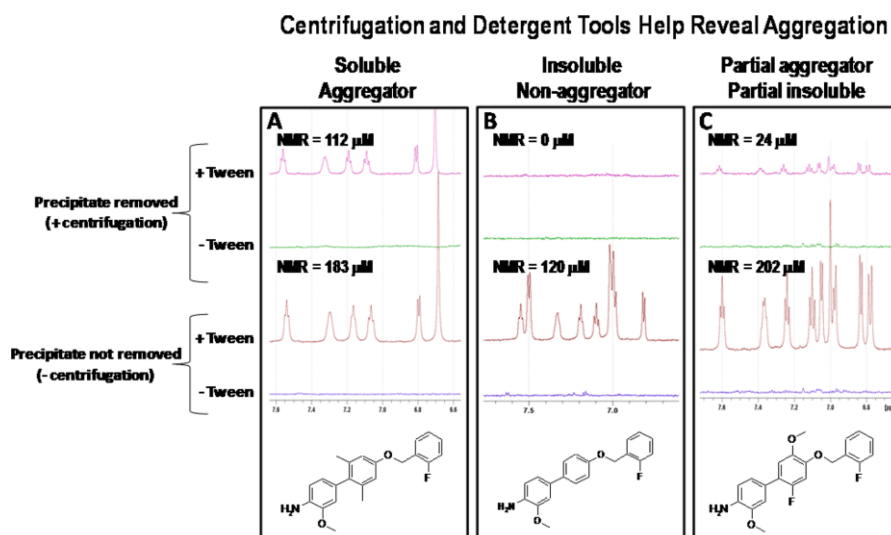


Figure 2.12. Centrifugation and detergent NMR assay.

^1H NMR spectra of three antiviral compounds at $200\ \mu\text{M}$ and were either centrifuged or not, and were exposed to Tween 80 or not. The buffer used is $50\ \text{mM}$ sodium phosphate pH 7.4 in 100% D_2O solvent (LaPlante *et al.*, 2013b)

2.3.3.4 Correlation between Compound Self-Aggregation and Off-Target Promiscuity *in Vitro* Pharmacology Using NMR Assay

Off-target promiscuity assays for multiple compounds have been reported by LaPlante *et al.*, 2013. The series of compounds include targeted HIV reverse transcriptase and HCV NS5B polymerase (see Figure 2.13), which some of them exhibited promiscuous off-target inhibition. The promiscuous hit inhibition was documented when $>50\%$ inhibition noted in the assay. It is well-known from the literature that compound aggregation is a major cause of promiscuous inhibition in HTS assays. LaPlante and co-workers endeavored to find the relation between compound self-assemblies and promiscuity *in vitro* off-target pharmacology assays by ^1H NMR strategy. Interestingly, it was noted that some of those compounds displayed off-target inhibition (promiscuity). The NMR dilution assay for those sets of compounds, targeted HIV reverse transcriptase, displayed unusual NMR spectral features as a result of self-assemblies (Figure 2.13 A and C), compared to clean off-target assay for the compounds shown in (Figure 2.13 B and D). Off-target *in vitro* pharmacology data are described in details in Table 2.2 (LaPlante *et al.*, 2013a).

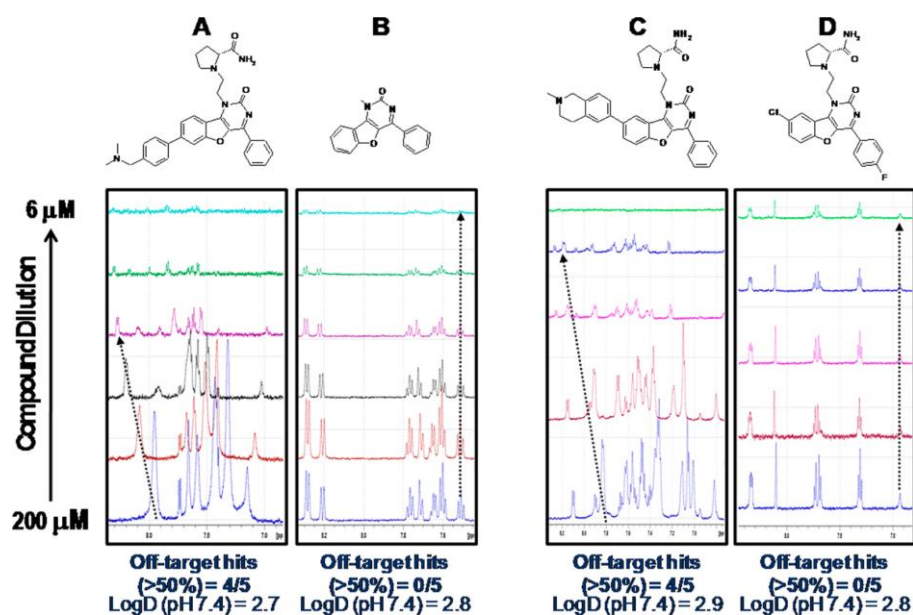


Figure 2.13. Example of ¹H NMR off-target assay of four inhibitors of HIV reverse transcriptase.

Data acquired at various concentrations varying from 200 μM to 6 μM. At the bottom shown are off-target *in vitro* pharmacological assay tested at 10 mM, inhibition (>50%). The buffer used is 50 mM sodium phosphate pH 7.4 in 100% D₂O solvent (LaPlante *et al.*, 2013a).

Table 2.2. Shows are the HIV inhibitor compounds with the same series shown in Figure 2.13. The table explains the aggregation respective properties of these compounds by NMR with the calculation of the parameters that used to measure lipophilicity of compounds including LogD and cLogP (for ionizable and neutral compounds respectively), TPSA parameter that deals with the surface sum over polar atoms of a molecule. These parameters are used to predict the off-target promiscuity (Calc=Calculated). The letters refer to (Y) if the compound probably being promiscuous, (N) if the compound probably being non-promiscuous, and the letter (x) refers to that the calculated values are not applicable for this technique.

The relation of cLogP and TPSA to promiscuity is that; being promiscuous in case if TPSA <75, cLogP>3 and being non-promiscuous if TPSA>75, cLogP<3 (LaPlante *et al.*, 2013a).

Compound	NMR aggre pH 7.4	Off-target hits of five assays >50%	LogD pH 7.4	Calc CLogP	Calc TPSA	Calc Predict promisc
HIV1	+	5	2.4	1.5	105	N
HIV2	+	4	2.9	2.0	98	N
HIV3	+	4	2.7	5.7	138	X
HIV4	+	4	2.3	1.8	98	N
HIV5	+	3	2.2	0.6	114	N
HIV6	-	3	3.7	3.1	76	X
HIV7	-	0	2.8	2.7	93	N

HIV8	-	0	3.2	4.1	73	Y
HIV9	-	0	2.3	3.0	94	N
HIV10	-	0	2.8	3.8	46	Y

Subsequently, another study was conducted on the same series of compounds, and it was apparent that there was a correlation between unusual NMR trends as a result of compound self-assemblies and off-target hits. As shown in (Figure 2.14 A and C), two interesting compounds have the tendencies to form aggregates as displayed in the unusual NMR spectra and off-target promiscuity. The compounds that exhibited abnormal NMR tendencies and promiscuous effect in pharmacological screen are mostly lipophilic with (LogD value=2.2 and 3.7 respectively). Conversely, another two HIV compounds exhibited a clean off-target profile in pharmacological assays with LogD value (=3.3), that was consistent with the usual NMR spectral features and clean self-aggregation, but those were inconsistent with the lipophilicity of the compounds (Figure 2.14 B and D). Therefore, this parameter was not considered practical for predicting promiscuous effect of compounds. The off-target pharmacology data are described in details in Table 2.3 (LaPlante *et al.*, 2013a) (LaPlante *et al.*, 2013a).

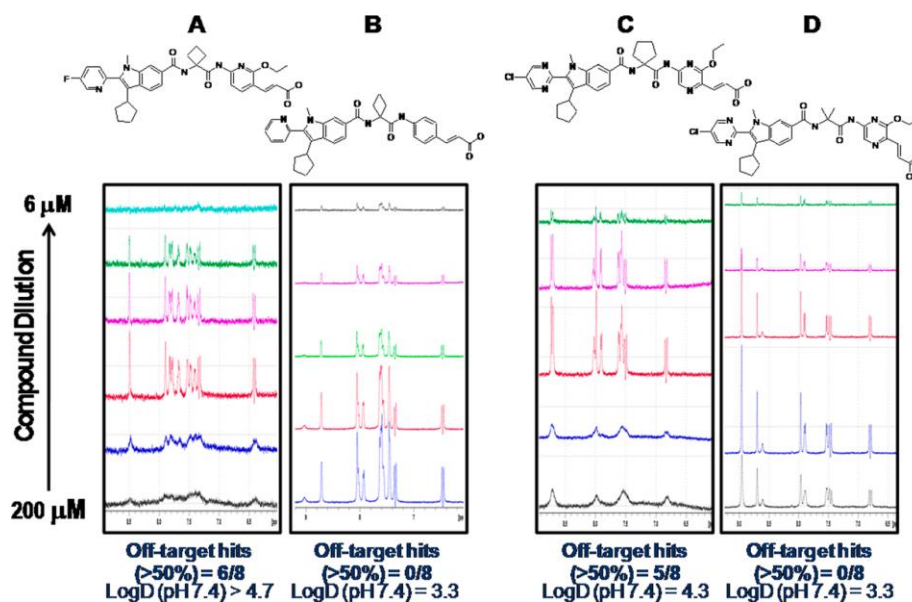


Figure 2.14. Example of ^1H NMR off-target assay of four inhibitors of HCV NS5B polymerase.

Data acquired at various concentrations varying from $200\ \mu\text{M}$ to $6\ \mu\text{M}$. At the bottom shown are off-target in vitro pharmacological assay tested at $10\ \mu\text{M}$, inhibition (>50%). The buffer used is 50 mM sodium phosphate pH 7.4 in 100% D₂O solvent (LaPlante *et al.*, 2013a)

Table 2.3. Shows are HIV inhibitor compounds with the same series shown in Figure 2.14. The table explains the aggregation respective properties of these compounds by NMR with the calculation of the parameters that used to measure lipophilicity of compounds including LogD and cLogP (for ionizable and neutral compounds respectively), TPSA parameter that deals with the surface sum over polar atoms of a molecule. These parameters

are used to predict the off-target promiscuity (Calc=Calculated). The letters refer to (Y) if the compound probably being promiscuous, (N) if the compound probably being non-promiscuous, and the letter (x) refers to that the calculated values are not applicable for this technique (LaPlante *et al.*, 2013a).

Compound	NMR aggre pH 7.4	Off-target hits of five assays >50%	LogD pH 7.4	Calc CLogP	Calc TPSA	Calc Predict promisc
HIV1	+	7	>5.1	5.9	105	X
HIV2	+	6	>4.7	5.1	138	X
HIV3	+	5	>4.8	5.7	138	X
HIV4	+	5	4.3	4.4	164	X
HIV5	+	3	>5.4	5.4	121	X
HIV6	-	3	4.1	5.7	92	X
HIV7	-	2	3.5	4.6	151	X
HIV8	+	1	3.1	4.2	151	X
HIV9	-	1	2.1	4.9	97	X
HIV10	-	0	3.3	3.7	161	X
HIV11	-	0	3.3	5.3	118	X

2.3.4 NMR T2-CPMG Assay for the Detection of Compound Aggregation

The spin-spin Carr-Purcell- Meiboom-Gill (T2-CPMG) relaxation assay has been widely used to monitor protein dynamics and ligand binding interactions (Meiboom & Gill, 1958; Palmer III, 2014). The T2-CPMG assay is a simple and practical method which applies spin echoes (τ - π - τ) and reveals induction decay. One of the applications of T2-CPMG assays was to study mixtures of small molecule drugs and also to study proteins. Therefore, it was rationalized that NMR T2-CPMG assay can be a powerful method for the detection of compound aggregation and nano-entities.

For non-aggregating drug-like molecules, a fast-tumbling lone-molecules is expected to be detected with relatively short correlation time and longer transverse relaxation (T2). In other words, the signal intensities are maintained in the solution across delay times. Conversely, for aggregating small drug-like molecules, a slow-tumbling lone-molecules is expected to be detected with relatively longer correlation time and shorter transverse relaxation (T2). Hence,

the signal intensities are lost across delay times. T2-CPMG was used as a powerful tool for revealing small molecule self-assemblies, which could be detected by preparing an NMR tube of a drug at a desired concentration and acquiring NMR resonances of eight one-dimensional T2-CPMG. In this setting, each experiment exhibits spin-echo pulse with relatively CPMG times (T) with different milliseconds (from 1 to 800 ms) as described in (Figure 2.15).

In this figure, there was a clear minimal loss of signal intensities for the non-aggregating compounds shown in the bottom upon increasing the ms to 800 ms as a function of longer T. This was due to the free tumbling of the non-aggregating compound in the solution. On the other hand, as illustrated in the top of Figure 2.15, there was a significant loss in the signal intensities upon increasing the ms to 800 ms as a function of shorter T, which was due to the slow tumbling rate of aggregating molecules in the solution. By comparing the top and bottom resonance overlays, there are distinct and interesting features that could be used to detect nano-entities in solutions (Ayotte *et al.*, 2019).

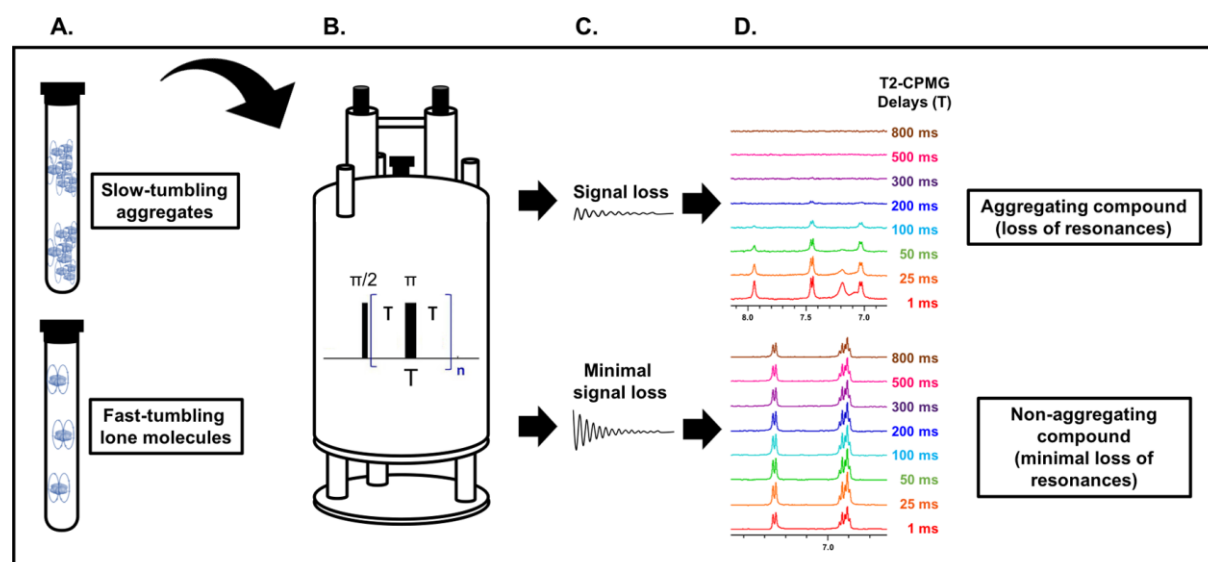


Figure 2.15. Shown is the principal of NMR T2-CPMG aggregation assay.

(A) Aggregating and non-aggregating compounds in NMR tube (top and bottom respectively). (B) 1 H NMR instrument (C) NMR signal decay in case of slow-tumbling aggregates (top) and signal retained in case of fast-tumbling non-aggregates (bottom). (D) Examples of T2-CPMG NMR results. For aggregating compounds, there was a loss in intensity upon increasing to 800ms was observed (top) and in case of non-aggregating compounds, a small and minimal decay of intensity was observed (bottom). Samples are prepared at 200 μ M in 50 mM sodium phosphate buffer, 100 mM NaCl, 10% D2O, pH 7.4 (Ayotte *et al.*, 2019).

Some known aggregators and non-aggregators have been studied by T2-CPMG assay as shown in Figure 2.16 and 2.17. Those compounds including a known non-aggregator drug etodolac, and two known aggregator dyes methylene blue and Evans blue (Ayotte *et al.*, 2019). The behavior of etodolac in aqueous solution has been recently studied by NMR dilution assay as well as DLS (LaPlante *et al.*, 2013b). The spectra of T2 CPMG of etodolac indicates the presence of non-aggregate behavior confirmed by the properties of long T2-CPMG relaxation

times. In addition, upon increasing spin-echo delay times to 800 ms and by comparing the peaks with 1 ms, the signal intensities are maintained and there was no signal decay observed across all delay times (see Figure 2.16 A).

On the other hand, there was a significant difference in the relaxation properties of the two aggregators involved in the study. Unlike etodolac, a signal decay has been observed in the T2 CPMG spectra of both dyes methylene blue and Evans blue upon increasing the delay times to 800 ms (see Figure 2.16 B and C). The sizes of those two dye aggregators are close to 100 nm, which was expected to produce broad resonances by NMR dilution assay. Here, the observed loss of signal intensities and resonance decays as a function of T2-CPMG is therefore an indicative of the presence of larger aggregate species (Ayotte *et al.*, 2019).

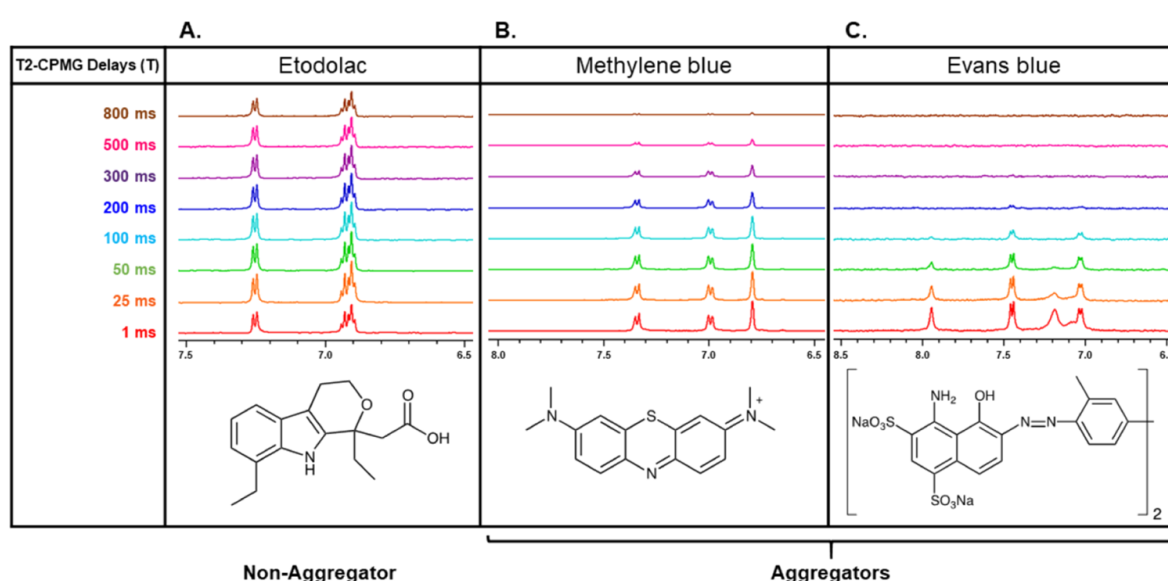


Figure 2.16. Shown are examples of T2-CPMG assay for three different compounds.

All compounds tested at 300 μM (A)–(C), and on the left, shown is the NMR T2-CPMG delay times. Samples are prepared at 200 μM in 50 mM sodium phosphate buffer, 100 mM NaCl, 10% D2O, pH 7.4 (Ayotte *et al.*, 2019).

Lead discovery efforts are using HTS assays to screen their libraries that contain millions of compounds. However, there are a huge number of compounds through the libraries have been mostly associated with promiscuous properties due to the presence of aggregation. For fragment library screening and curation purposes, ^1H NMR has been widely used as a powerful strategy for fast screening purposes. Recently, T2-CPMG strategy was applied to better understand the misbehaving of compounds in aqueous solutions, such as biochemical buffers, for fragment screening optimization. Usually, if there are no NMR resonances or low solubility observed, small-molecules are removed from the screening library.

As illustrated in (Figure 2.17), T2-CPMG NMR assay was applied to demonstrate the behaviors of three structurally related fragment compounds in phosphate buffer. After

increasing spin-echo delay times up to 800 ms, the signal intensities of Nicotinic acid have been maintained (approximately 50% in percentage of the signals) (see Figure 2.17A). On the other hand, the signal intensities for both compounds 5-chloro-2-pyridinecarboxylic acid and 3-methylpyridine-2-carboxylic acid have not been maintained upon increasing to 800 ms and a clear signal decay was observed for both fragments (see Figure 2.17 B and C). For detecting compound nano-entities, T2 CPMG strategy requires only one NMR sample at a desired concentration e.g 200 μ M. This has been considered as an advantage compared to different detection methods. In summary, T2 CPMG NMR assay is a practical method that can offer comprehensive and valuable information on the behaviors of a variety of compounds and even marketed drugs in a solution (Ayotte *et al.*, 2019).

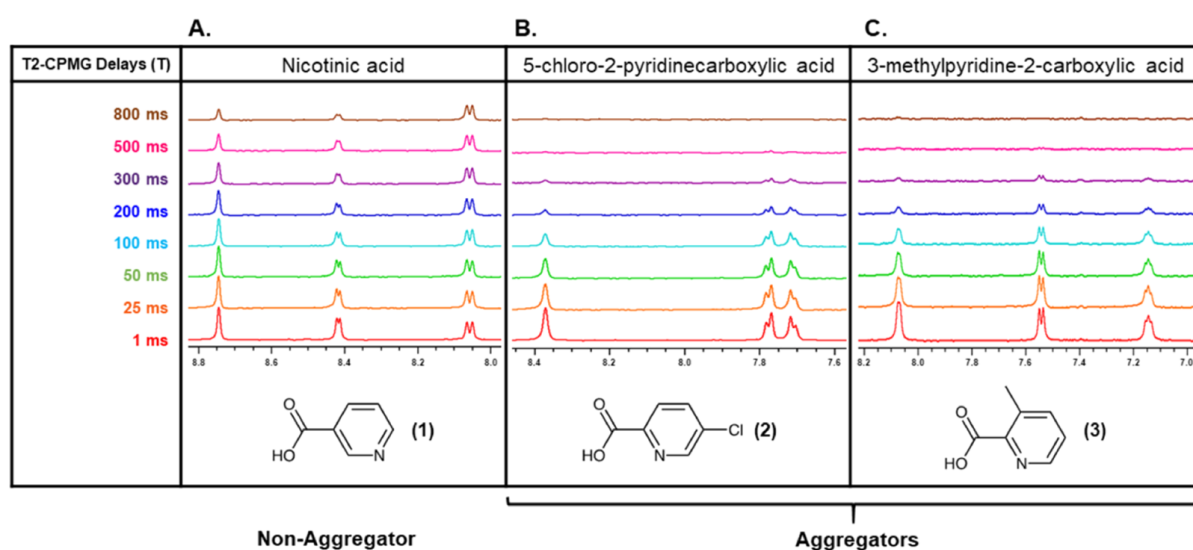


Figure 2.17. T2-CPMG analysis for the detection of aggregation for fragment.

(A-C) and on the left, shown is the T2-CPMG delay times. The buffer used is 50 mM sodium phosphate, 100 mM NaCl, 10% D₂O, pH 7.4 (Ayotte *et al.*, 2019).

Interestingly, T2-CPMG can be used as a tool to monitor solution behaviors of many compounds in pools (mixtures). It can be an efficient tool for screening large chemical library and test the binding of individual compound to its target of interest. T2-CPMG strategy was used to evaluate the aggregation tendencies of several compounds in pools of molecules as shown in (Figure 2.18 A and B). Two compounds named as (1 and 2) were successfully evaluated in mixture. For example, the resonance intensities were maintained for singleton 1 in Figure 2.18 A, which is consistent with the behavior of non-aggregating small-molecules as described above. On the other hand, resonance decays were observable upon increasing the scan to 800 ms for singleton 2 in Figure 2.18 B within the mixture, reporting that compound 2 acts as an aggregator in the fragment pool. In summary, NMR T2-CPMG assay has many

advantages for screening larger libraries which can significantly decrease the cost of materials, NMR sample preparation as well as reduce data acquisition time (Ayotte *et al.*, 2019).

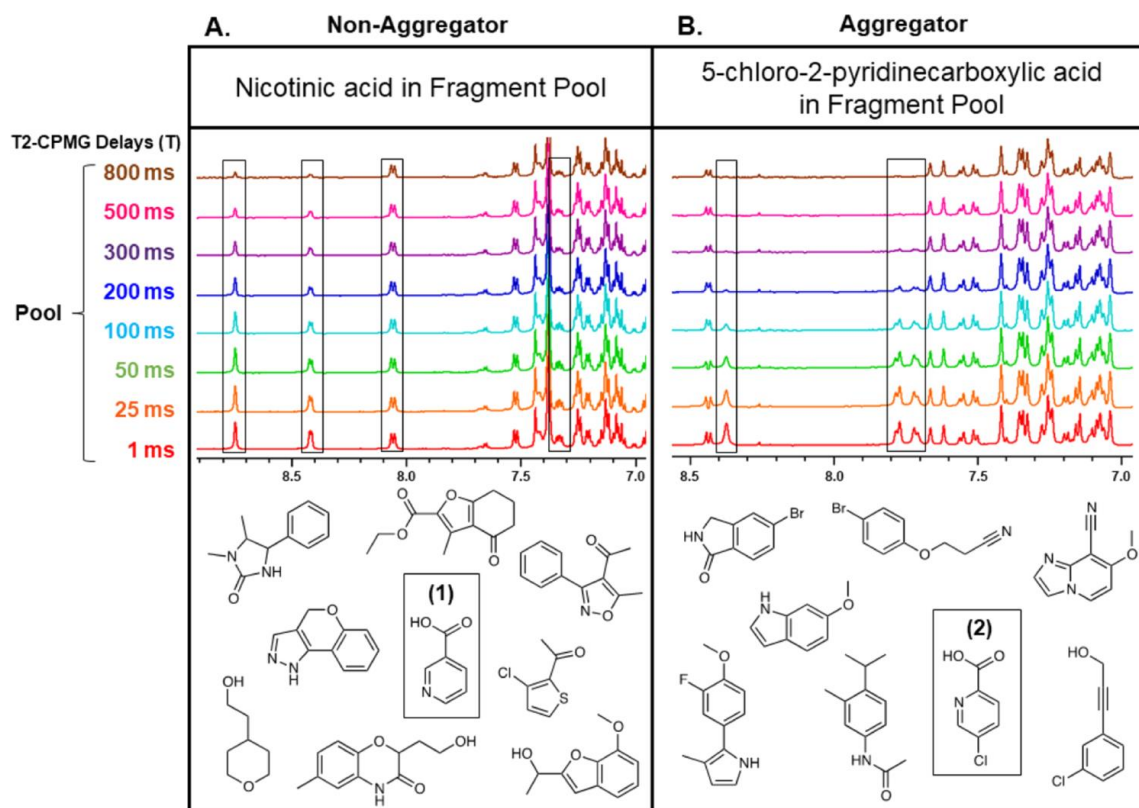


Figure 2.18. T2-CPMG assay for revealing aggregation among pools of compounds. The buffer used is 50 mM sodium phosphate, 100 mM NaCl, 10% D2O, pH 7.4 (Ayotte *et al.*, 2019).

2.3.5 Advantages and Limitations of TEM, DLS and NMR techniques

Table 2.4. Shows the advantages and dis-advantages of the methods used to detect compound aggregation

Techniques	Advantages	Limitations
TEM	<ul style="list-style-type: none"> • Can directly monitor the self-assembly into large nano-entities. • The particle size can be simply detected. • Can directly show the structure of nano-entities (McGovern <i>et al.</i>, 2002b). • Can be used to detect nano-entities under different 	<ul style="list-style-type: none"> • Can not obtain nor improve the quality of images without a negative stain agents e.g uranyl acetate • Smaller sizes of nano-entities cannot be detected. • Some size of nano-entities may not be accurate as a result of dehydrated conditions of TEM.

	<p>conditions including temperature and pH.</p> <ul style="list-style-type: none"> • Can measure the particle size in diameters under different conditions and different medias e.g media+FBS serum 10% (Owen <i>et al.</i>, 2012a). 	
DLS	<ul style="list-style-type: none"> • The aggregation formation and nano-entities can be easily observed by scattering intensities compare to controls (Owen <i>et al.</i>, 2012a). • Can measure very larger nano-entities. • Detergents can be used to reveal larger nano-entities. • Can also be used to detect CAC 	<ul style="list-style-type: none"> • Time-intensive assay in terms of monitoring nano-entities. • Some measurements are difficult to interpret due to the presence of artifacts • DLS is a limited strategy that cannot fully detect all the types of small molecule nano-entities (Chan <i>et al.</i>, 2009) • Difficult or impossible to detect smaller nano-entities • Is not compatible to monitor some compounds with mixtures of nano-entities • Detection of nano-entities in different conditions and solutions such as cell culture media is not possible.
NMR	<ul style="list-style-type: none"> • Simple and high-throughput • Provides details of all small molecule compounds at the atomic level • Can be used efficiently to distinguish between the three phases of compound solution behavior • Non-aggregator compounds can be easily exposed and 	<ul style="list-style-type: none"> • Larger sized of nano-entities can be only revealed indirectly by using detergent based assay to breakup the aggregates. • Requires high concentrations for analysis. • Requires many samples to expose nano-entities by dilution based assay

	<p>monitored by NMR resonances.</p> <ul style="list-style-type: none"> • Can be directly used to detect smaller sizes of nano-entities • Mixtures of multi-nano-entities can be also detected by NMR method • Detergent based assay can be used to effectively reveal larger sizes of nano-entities by NMR (LaPlante <i>et al.</i>, 2013b) • Can detect nano-entities under many different environmental conditions and different buffers/medias. • Can reveal CAC of compounds 	<p>(LaPlante <i>et al.</i>, 2013b).</p>
--	--	---

2.4 Aggregation Occurs in Pharmacologically Relevant Media

The behaviors of compound aggregation have also been studied in pharmacologically relevant media (Doak *et al.*, 2010; Owen *et al.*, 2012b). As shown in Figure 2.19, LaPlante and co-workers studied two interesting compounds in different pharmacological media conditions, and their NMR resonances have been investigated. Interestingly, there were notable differences in the aromatic resonances of the two compounds as demonstrated by the shape and intensities. For example, in human serum and human plasma, the sharpness of compound resonances would be affected as a result of protein binding. In simulated gastric fluid (SGF) media, the compound shown in Figure 2.19 B, seems to be quite insoluble as demonstrated by the lower resonance intensities, that might finally have an effect on the drug efficacy. Conversely, the drug in Figure 2.19 A is more soluble in SGF media. Also, in the taurocholic acid formulation at (pH 7.4), the two compounds exist at high concentrations. However, their aggregation state is different according to the NMR signal intensities (LaPlante *et al.*, 2013a). Indeed, such this evaluation could be valuable for investigating the pH effects and studying more formulations for drug delivery systems.

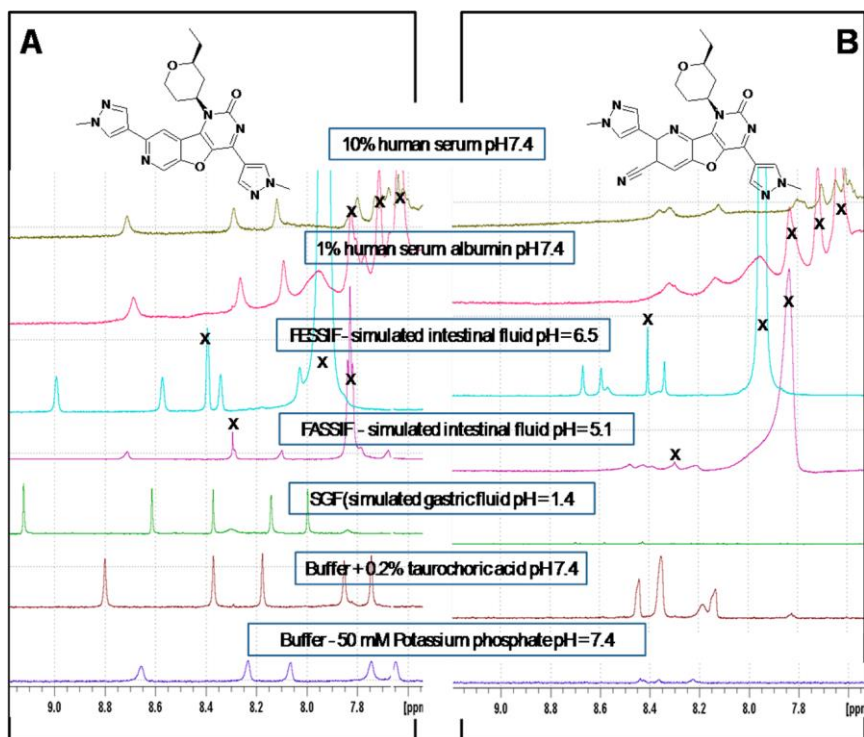


Figure 2.19. The study of aggregation behaviors in pharmacological media.

The NMR spectra of the two HIV reverse transcriptase compounds (A and B) in different pharmacological medias. The two compounds tested at 200 μM . “X” indicates the NMR peaks that arise from the pharmacological media (LaPlante *et al.*, 2013a).

2.5 Compound Aggregation as Attractive Nanoparticle Formulations for Targeted Drug Delivery Systems

As mentioned, compound self-aggregation has long been linked with artifacts since their discovery (McGovern *et al.*, 2002b). Different classes of compounds including organic molecules such as anticancer drugs have been reported to form colloidal aggregates (Owen *et al.*, 2012a). Interestingly, while compound self-aggregations are not desirable in HTS assays, their formulations into nanoparticles could be attractive and promising. Those aggregation and nanoparticles are entirely composed of drug molecules. Therefore, they can overcome the loading issues associated with different nanoparticle and drug delivery systems (Kim *et al.*, 2010; Park, 2013).

To overcome drug loading issues associated with several drug classes, chemical modifications have been made for several compounds to enhance their self-assembly into nano entities. However, other drug classes can be exploited to form self-assemblies and nano-entities without the need of any further chemical modifications (D'Addio & Prud'homme, 2011; Gaudin *et al.*, 2014). Colloidal aggregates can be formed in different environments including biochemical buffers, biological cell culture mediums, various pharmacological medias and simulated gastrointestinal fluids as mentioned previously (Doak *et al.*, 2010; Frenkel *et al.*,

2005). Several drugs form aggregates at micromolar concentrations such as the anticancer drug Fulvestrant (Trastuzumab). However, most of them are polydisperse and precipitate in aqueous solution after hours of formation.

To increase the stability of these aggregates, excipients such as polymers and other colloidal small drug like-molecules have been widely used. In addition, proteins can strongly interact with the surfaces of drug colloids, and therefore, they can be also used as excipients to enhance the stability of colloidal drug aggregates and control their size. Also, since the colloidal formulations were stable in the serum containing media, the cellular uptake of colloidal aggregate formulation by the target cells has been investigated (Figure 2.20). Interestingly, Fulvestrant colloidal aggregate based-antibody formulations have been selectively internalized by human ovarian cancer cell line (SKOV-3) (see Figure 2.20 A). On the other hand, no uptake has been observed by the cells when treated with IgG-stabilized colloids, used as control (Figure 2.20 B). Moreover, the drug Fulvestrant alone and IgG-stabilized colloids in HER2 low-expressing triple negative breast cancer (TNBC) cell line (MDA-MB-231) also showed no cellular uptake (Figure 2.20 C and D). In this study, it was interesting that the drug forming-aggregates can act as a vehicle together with their activities as agents. Therefore, they may address the poor drug loading issues associated with many drugs and improve their efficacy and targeted drug delivery systems (Ganesh *et al.*, 2017b).

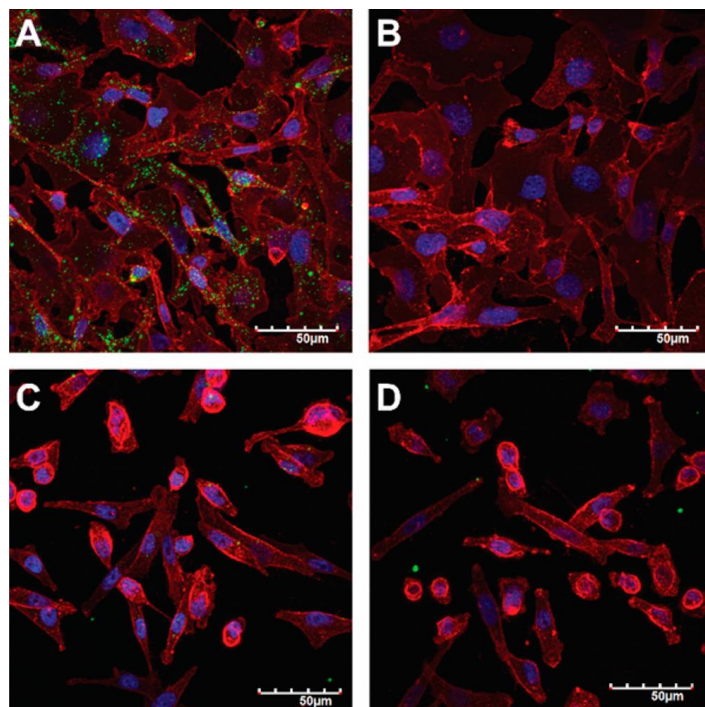


Figure 2.20. Confocal microscopy represents the cellular uptake Fulvestrant corona.

(A) Fulvestran colloidal aggregates shown as green fluorescence internalized in the cytoplasm of the high expressing HER2 receptor cells (SKOV-3) which was co-formulated with a BODIPY dye. **(B)** The control IgG-modified colloidal aggregates. **(C)** No internalization of Fulvestrant-modified (control) or **(D)** No internalization of IgG-modified aggregates by low expressing HER2 receptor cells (MDA-MB-231) (Ganesh *et al.*, 2017b).

3 HYPOTHESIS AND OBJECTIVES

As mentioned, compound aggregation “nano-entities” can have significant impacts at all drug discovery and development stages. With the detection strategies launched in our lab, nano-entities and their full range of sizes and types could be explored. Nano-entities also have properties which the pharmaceutical industry is becoming aware about including false positive/negative hits, off-target promiscuity, toxicity, etc. Many other properties of nano-entities must exist but have yet to be discovered. Revealing them will require new and robust detection strategies. With the pilot study we performed in my thesis, one could speculate that nano-entities could be recognized by antibodies and induce an immune response. Thus, the major objective of this thesis is to explore these nano-entities and correlate their properties.

Specific objectives:

- I. To monitor nano-entities of dyes and better understand their associated properties using NMR aggregation strategy (Article 1).
- II. To monitor nano-entities at the cellular level by confocal microscopy and evaluate if aggregating compounds can cross membranes and enter live cells (Article 2).
- III. To develop a protocol that will enable researchers to monitor the triphasic equilibrium of compounds, with the focus on nano-entities phase (Article 3).
- IV. Explore the possible correlation of drug and dye nano-entities with immune responses (Article 4).

4 ARTICLE 1:

Revealing dye and dye-drug aggregation into nano-entities using NMR

Authors: Jayadeepa R. Murugesan ^a, **Fatma Shahout** ^a, Marwa Dlim ^a, M. Michele Langella ^b, Ernesto Cuadra-Foy ^b, Pat Forgione ^{b,*,*}, Steven R. LaPlante ^{a,*}

^(a) Université du Québec, INRS-Institut Armand-Frappier, 531, Boulevard des Prairies, Laval, Québec H7V 1B7, Canada

^(b) Concordia University, Department of Chemistry and Biochemistry, 7141 rue Sherbrooke O., Montreal, Québec H4B 1R6, Canada

Title of Journal: Dyes and Pigments

153 (2018) 300–306 | Received 11 August 2017; Received in revised form 11 February 2018; Accepted 16 February 2018

Published online: 21 February 2018

DOI <https://doi.org/10.1016/j.dyepig.2018.02.026>

Contribution of the author:

I, Prof. Steven LaPlante, confirm that Fatma Shahout contributed as a primary author of this publication.

F.S was involved in the NMR data analysis and interpretation. **F.S** also did the TEM experiments and involved in reviewing & editing the manuscript.

4.1 Abstract

It is becoming increasingly apparent that small molecules can self-assemble into a wide-range of nano-entities in solution that have intriguing properties. The recently introduced NMR aggregation assay is playing an important role in revealing these nano-entities. Here, we employ the NMR aggregation assay to expose the self-aggregation tendencies of dyes in solution. This dilution-based assay demonstrates that some dyes can exist as single-molecule entities whereas others can adopt aggregates of distinct sizes. Interestingly, dyes with highly related chemical structures can adopt largely different sized aggregates - demonstrating the existence of structure-nanoentity relationships (SNR) – which suggests that they can assume and/or be designed to have distinct properties. One property was evaluated where the drug Quetiapine (Seroquel) was added to the dye Congo red which resulted in the absorption of the drug into the dye nano-entity. This showed a direct drug-dye interaction, and it demonstrated that dye aggregates can have influences on drug solution behaviors. The NMR method described in this study provides a practical and valuable tool to monitor dye aggregates and to better understand their associated properties (e.g. toxicity, off-target activity) and potential utility (e.g. drug encapsulation, drug delivery systems).

4.2 Introduction

Small molecules can assume a wide range of behaviors in solution that can be considered within the context of a tri-phasic equilibrium [1,2]. That is, when a compound is placed in aqueous solution it can equilibrate between at least three states (Fig. 4.1). Some of the molecules can exist as soluble, fast-tumbling lone molecules that are completely diffuse, whereas others can form solid precipitate(s), and others can self-associate and adopt intermediate soluble aggregates or nano-entities. Notably, each compound likely has its own unique equilibrium signature and relative population among these states, and there is a critical dependence on many other factors such as buffer, co-solutes, etc.

The detection and quantification of a compound's signature equilibrium remains elusive to this day [2]. Whereas the solid precipitate phase is detected visually (or via a microscopy for fibrils), the distinctions between the soluble lone-molecules and aggregate phases are not apparent. This is in part due to the limited detection methods available such as dynamic light scattering (DLS) [3]. DLS is a practical technique that can reveal the existence of large, micelle-like aggregates that are homogeneous. However, we recently introduced an NMR aggregation assay that exposed a wide range of nano-entity sizes that can exist [1,2] especially small multimers, which are often undetectable by DLS. Fig. 4.1 shows how NMR is sensitive to compound tumbling rates and behavior for all three phases. That is, fast tumbling molecules exhibit sharp resonances (Fig. 4.1A), and solid precipitates result in extremely broad and unobservable resonances by solution NMR (Fig. 4.1D). Aggregates give rise to intermediate resonance attributes such as broad resonances and/ or unusual features such as those shown in Fig. 4.1B and C. Thus, we chose to employ NMR in this study to explore the behavior of dyes in solution, which could then be a valuable tool to begin correlating with their properties. Here, we demonstrate that the NMR aggregation assay is a feasible method to explore the behavior of dyes in solution, which can then be a practical tool for correlating nano-entity properties.

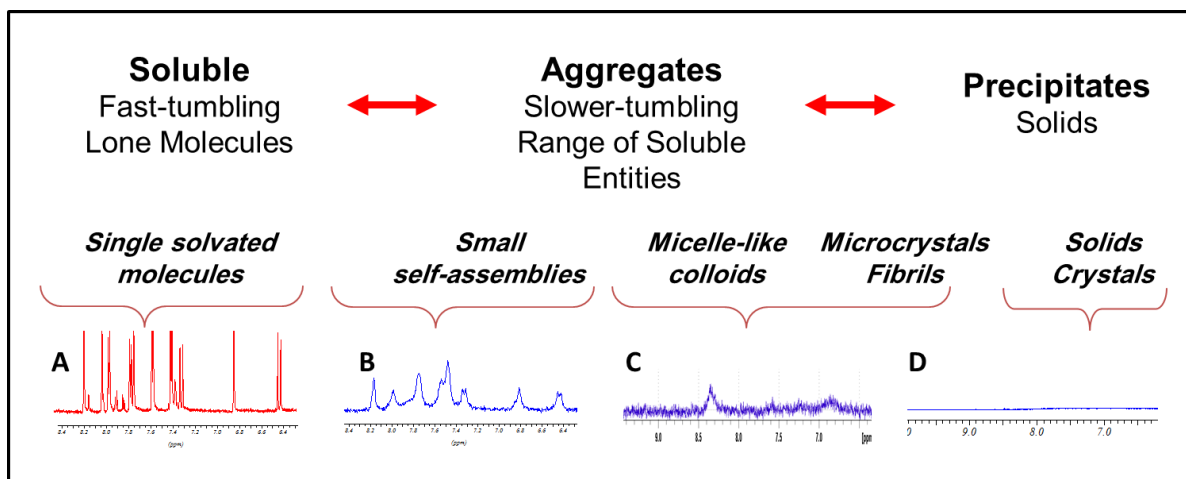


Figure 4.1. Compounds can adopt a three-phase equilibrium when placed in aqueous media.

On the bottom are ^1H NMR spectra (600 MHz) of various compounds in buffer (50 mM sodium phosphate pH 7.4) at nominal concentrations of 200 μM .

4.3 Materials and methods

4.3.1 Compounds – dyes

The dyes and drug used in this study were all obtained from commercial vendors. The dyes and their CAS numbers are as follows: Azo Rubine (3567-69-9), Acid Blue 9 (3844-45-9), Erythrosin B (16423-68-0), Allura Red (25956-17-6), Fast Green (2353-45-9), Eryochrome Blue Black B (3564-14-5), Naphthol Yellow (846-70-8), Sudan II (3118-97-6), Acid Violet (1694-09-3), Indigo carmine (860-22-0), Methylene blue (61-73-4), Tartrazine (1934-21-0), Solvent Orange 2 (2646-17-5), 4,4'-(9-Fluorenylidene) dianiline (15499-84-0), 4-((4-hydroxy-1-naphthalenyl)azo)benzenesulfonic acid, monosodium salt (523-44-4), Fast Green (2353-45-9), Quetiapine fumarate (111974-72-2). All were purchased from TCI whereas Acid Green (3087-16-9) and Patent Blue (3536-49-0) were purchased from Chem-Imp.

4.3.2 NMR sample preparation

Powder dyes were weighed and appropriate amounts placed in Eppendorf tubes followed by the addition of deuterated DMSO to form 20 mM dye stock solutions, as described in Fig. 4.2. The buffer used for preparing the NMR samples was 50 mM sodium phosphate pH 7.4 in 100% D₂O. Tween 80 stock (10% vol/vol in above buffer) was added to samples as defined in the procedure provided below. Further details on how samples were prepared are provided in Fig. 4.2.

Sample Preparation for NMR Aggregation Assay

Required Supplies:

- Aggregation Buffer:
 - 50 mM sodium phosphate pH 7.4 in 100% D₂O
- Tween 80 stock (10 % vol/vol in above buffer)
- 7 Eppendorf tubes
- 2 Pipettes: 2 – 20 µL and 200 – 1000 µL

Calculation for 20 mM compound stock solution:

- X = exact mass weighed in mg (0.3 – 0.6 mg)
- Y = MW of your compound
- Z = volume of DMSO-d₆ to be calculated / added

$$\frac{X \text{ mg}}{Y \text{ mg/mmol}} = Z \text{ mL} \quad \left\{ \begin{array}{l} \text{Volume should work} \\ \text{out to 20 – 200 } \mu\text{L} \end{array} \right.$$

A- Prepare 20 mM compound stock solution (as above)

B- Portion out aggregation buffer

- 1500 µL in tube 5
- 500 µL in each of tubes 1-4

C- Add/mix 15 µL of above 20 mM compound stock to tube 5

- This tube now becomes the 200 µM stock solution
- If precipitate forms, take note and proceed

D- Transfer 500 µL of the 200 µM stock solution to tube 6.

E- Take 500 µL of the 200 µM stock and add to tube 4

- Mix with the 500 µL buffer already present
- This becomes first 2x dilution
- Transfer 500 µL from tube 4 to tube 3. Mix.
- Repeat dilution and mixing for tube 2 then 1.

F- Lightly centrifuge tube 6 (2,000 rpm 10 minutes).

Transfer precipitate-free supernatant to a spare tube

G- Add/Mix 8 µL of Tween 80 stock solution to a spare tube

H- Transfer solution from tubes 1-5 and spare tube to separate NMR tubes

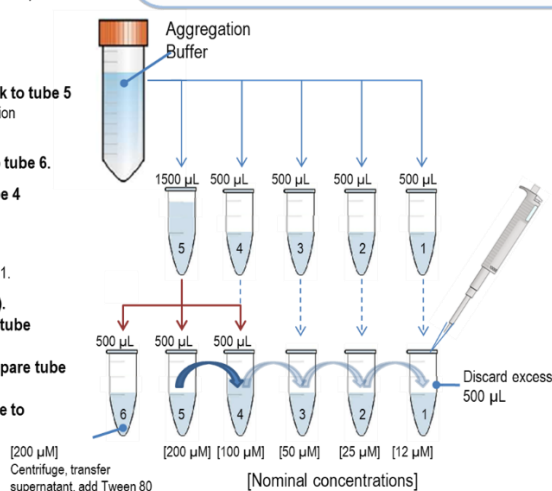


Figure 4.2. Detailed procedure for preparing samples for the NMR aggregation assay [1,2].

4.3.3 NMR experiments

The pulse programs for the NMR aggregation assay are the standard one-dimensional ¹H NMR experiments available on all commercial spectrometers. There are several optional parameters that can be modified if desired. Given that the buffer consists of 100% D₂O, one can choose to use standard ¹H NMR pulse program or one that includes solvent suppression. The latter may be desirable if large H₂O resonance peaks exist due to the hygroscopic property of deuterium oxide. The experiments shown here were run on a 600 MHz Bruker AV III NMR equipped with a sample changer. The number of scans was typically 256 scans, with a relaxation delay plus acquisition time of 2s, which ensured that all samples for each compound could be, acquired overnight using a sample changer. Data visualization and interpretation are also simple. For the work described here, Bruker's TOPSPIN software allows for the facile superposition of 1D NMR spectra along with zooming capabilities. Other software from ACD and other vendors also allow for spectral superpositions. Instant JChem for Office Version 18.3.0 was used for chemical structure handling, data analyzing, visualizing and reporting capabilities within the Microsoft Office environment Chemaxon (<https://www.chemaxon.com>) [4].

4.3.4 Electron microscopy

Congo red was diluted in DMSO with 50 mM sodium phosphate pH 7.4 in 100% D₂O, and was prepared at 600 µM. Briefly, 100 µL of the sample was transferred into a 240 µL Airfuge tube. A carbon coated copper grid was inserted into the bottom of Airfuge tube with

fine tweezers and centrifuged for 5 min at 20 psi. With tweezers, the carbon grid was gently removed and washed with distilled water for 1 min. The carbon grid was then negatively stained with 3% of phosphotungstic acid (PTA-3) for 1 min. The grid was then removed and blotted to dry with a bibulous paper and examined with a transmission electron microscope (Hitachi H-7100). The photographs were processed with the digital camera AMT version 600.147.

4.4 Results and discussion

4.4.1 Detection of aggregation using ^1H NMR spectra as a function of dye concentration

The NMR aggregation assay involves the acquisition and monitoring of ^1H NMR spectra as a function of compound concentration. For single molecules that do not aggregate, each dye molecule is distal to one another, tumbles freely and is not affected by dilution. Sharp resonances are expected at all concentrations and do not shift left or right. Also, there should be no changes in the number and shape of the resonances (Fig. 4.3). The only changes expected are the resonance intensities as a function of concentration. For dyes that aggregate the molecules self-associate at higher concentrations, upon dilution they become more distal and tumble more freely. As a result, unusual NMR features and changes are expected due to changes in local environments (Fig. 4.3).

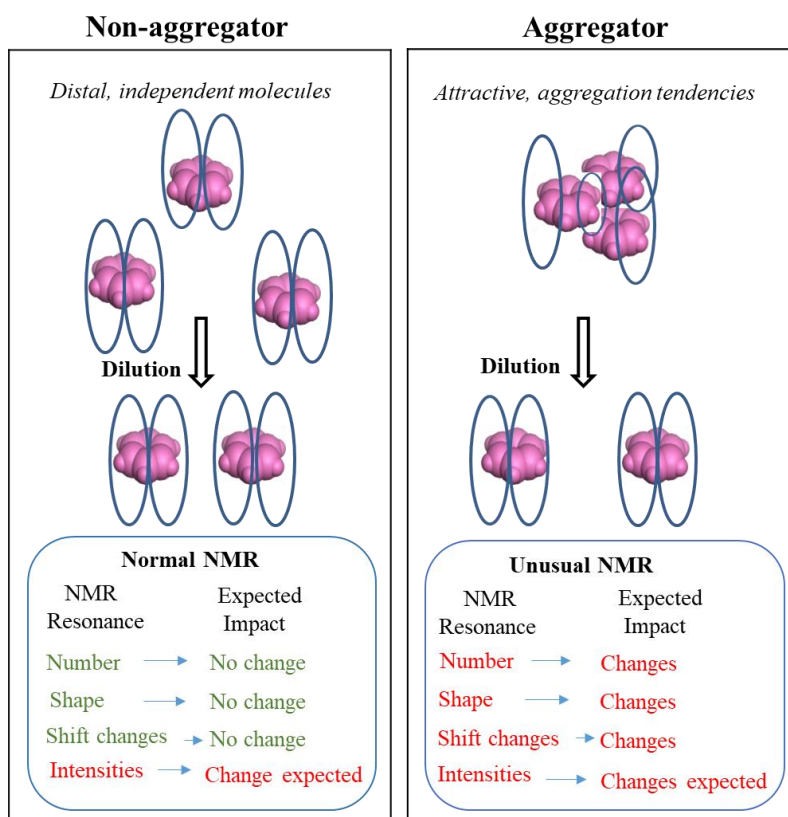


Figure 4.3. Overview of the expected observations of NMR spectra and resonances upon dilution for dyes that aggregate versus those that do not in solution.

4.4.2 NMR assay on structurally different dyes

Fig. 4.4 displays the ^1H NMR spectra as a function of concentration for Tartrazine, Methylene blue and Congo red. An overview of the spectra for Tartrazine suggests that the data is consistent with the predominance of the non-aggregating phase consisting of lone-molecules tumbling rapidly in solution. A single set of resonances exist which are sharp at all concentrations and are well-aligned (no shift left nor right). Furthermore, the addition of Tween 80 had no effect on the resonances intensities, which is expected in the absence of large, micellular aggregates. Electron microscopy also shows no signs of aggregates (Fig. 4.4).

Alternatively, Methylene blue and Congo red exhibit unusual spectral trends that are consistent with the observation of aggregates. Upon increasing the concentration of Methylene blue, the resonances shift significantly indicating changes in local environments upon self-association. These nano-entities are relatively small given the fact that resonances are observed, likely multimeric forms. This is in stark contrast to the observations made for Congo red. No sharp resonances are readily observed at all concentrations, despite exhibiting full solubility (clear solution, precipitate-free). Thus, Congo red self-assembles into very large nano-entities that result in extremely broad, unobservable resonances. A closer look at the 200 μM concentration shows very broad peaks (*vide infra*), which become much sharper but nonetheless relatively broad upon addition of Tween-80. This latter observation suggests that Tween 80 partially breaks apart the Congo red aggregates into smaller entities that are finally observable as shown in Fig. 4.4. Congo red was also reported [5–7] to form large aggregates and here we show this by scanning electron microscopy (see electron micrograph on the top right of Fig. 4.4).

The scope of the current study was expanded to other classes of dyes, naphthol yellow S hydrate, Erythrosine B and 4, 4'-(9-fluor-enylidene) dianiline (Fig. 4.5). Naphthol yellow S (hydrate) exhibited sharp resonances with no shift changes upon increasing the concentration, which is consistent with this dye behaving predominantly as a non-aggregator. For Erythrosine B and 4,4'-(9-fluorenylidene) dianiline, unusual features were observed in ^1H spectra of the NMR assay that were consistent with self-assemblies. ^1H NMR signals shifted right at higher concentrations of Erythrosine B, and resonances of 4,4'-(9- fluorenylidene)dianiline were only notable upon addition of Tween 80.

Other types of dyes were also evaluated (see Supporting Information, Figs. S1–S2). For example, Fig. S1 shows that Acid blue 9, Evans blue, and Indigo carmine also form distinct types of nano-entities. In the spectra of Acid blue 9, the ^1H NMR signals appear as expected for a non-aggregator, except that additional small resonances appear at higher concentrations.

More apparent and unusual features are noted in the spectra of Evans blue and Indigo carmine.

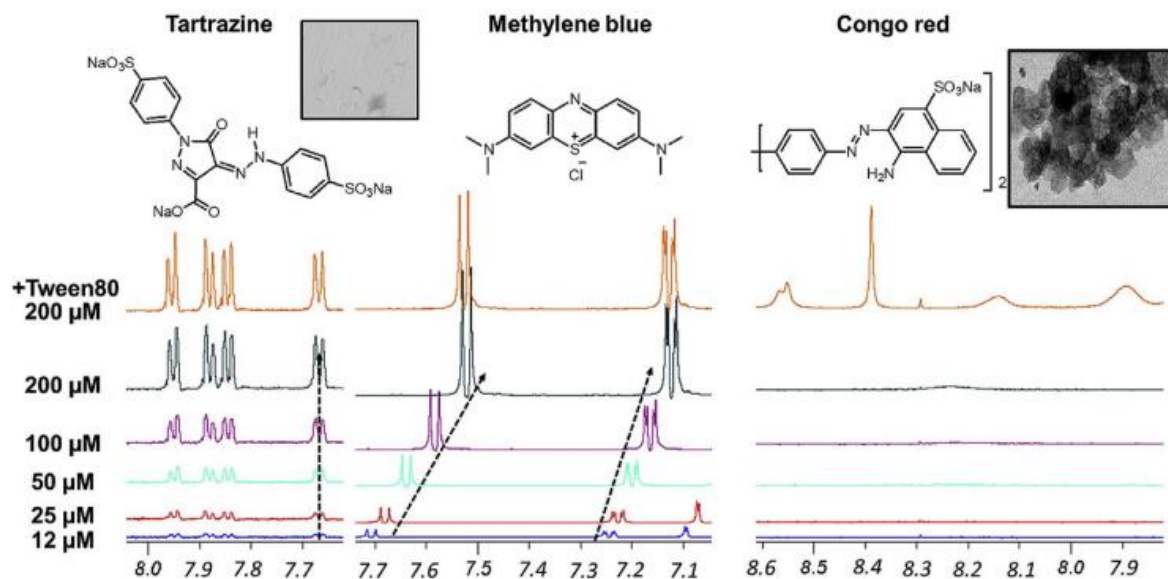


Figure 4.4. NMR aggregation assay showing ^1H NMR spectra of three structurally different dyes obtained by dilution from $200\ \mu\text{M}$ to $12\ \mu\text{M}$. Data displayed for Tartrazine (left), Methylene blue (middle) and Congo red (right).

The insets on the top-right and left are electron micrographs of Congo red and Tartrazine in solution, respectively. (For interpretation of the references to color in this figure legend, the reader is referred to the Web version of this article.)

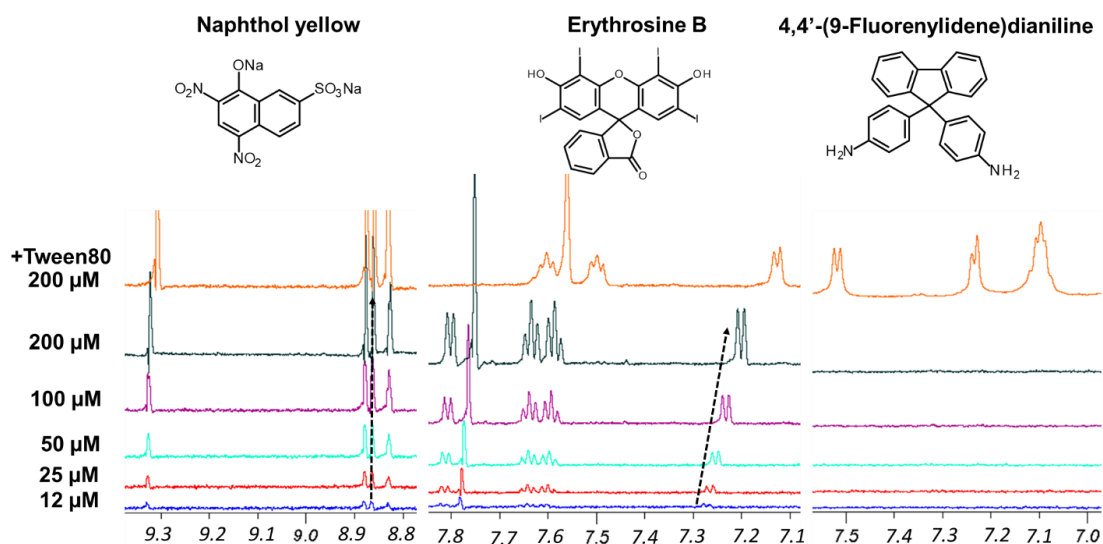


Figure 4.5. NMR aggregation assay showing ^1H NMR spectra of three structurally different dyes obtained by dilution from $200\ \mu\text{M}$ to $12\ \mu\text{M}$.

Data displayed for Naphthol yellow (left), Erythrosine B (middle) and 4,4'-(9-fluorenylidene)dianiline (right). (For interpretation of the references to color in this figure legend, the reader is referred to the Web version of this article.)

4.4.3 NMR assay on structurally similar dyes - Triarylmethane class

We next explored the aggregation tendencies of a series of similar compounds. Overall, it was noted that dyes of the same class with subtle structural differences can show completely different aggregation tendencies. This is exemplified in Fig. 6 for three triarylmethane dyes (Patent blue, Light green SF yellowish and Acid violet 49). On one hand, the spectra of the Patent blue appears such that no aggregation is observed since no changes in the resonance number, shape and chemical shift occurs at the various concentrations. However, the spectra of Light green SF yellowish and Acid violet 49 display notable unusual trends. The resonances of Light green SF Yellowish exhibit shifts and the presence of two sets of peaks, which is indicative of the presence of more than one type of aggregate species. Broad resonances are observed for Acid Violet 49. These findings are consistent with the literature of cyanine dyes that are reported to adopt J and the H aggregates (bathochromic shift and hypsochromic shift in the absorption spectra, respectively) [8].

Perhaps the latter two dyes tend to aggregate as a result of π - π stacking interactions of the planar solvophobic aromatic rings [9], whereas Patent blue has the tetrahedral sulfonate groups in both the ortho and para positions of a phenyl ring that could prevent such π - π interactions. For Light green SF yellowish and Acid violet 49, the substituents are far away from the aromatic system (para) which may minimize steric influences and allow self-assembly.

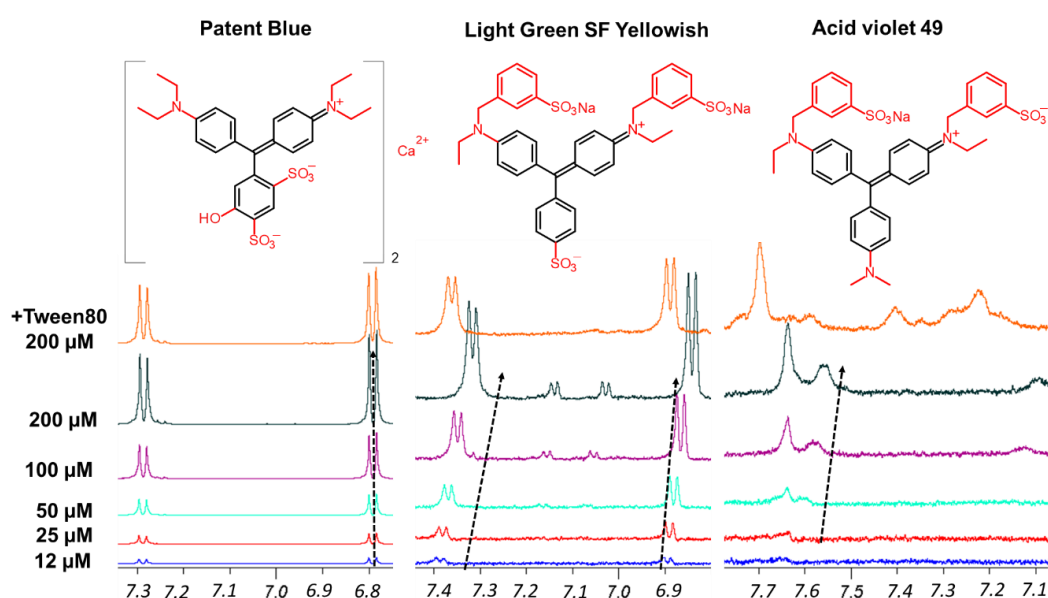


Figure 4.6. NMR aggregation assay showing ^1H NMR spectra of three structurally similar triarylmethane dyes obtained by dilution from $200\ \mu\text{M}$ to $12\ \mu\text{M}$.

Patent blue (left), Light green SF yellowish (middle) and Acid violet 49 (right). (For interpretation of the references to color in this figure legend, the reader is referred to the Web version of this article.)

4.4.4 NMR assay on structurally similar dyes - Azo dyes with one phenyl and one naphthyl and bis-naphthyl group

The aggregation tendencies of another series of structurally related dyes was explored to see if the above observations were specific to one series or general. Fig. 4.7 displays the NMR data for three structurally related azo dyes (Sunset yellow, Allura red and Orange II). In this case, all three compounds have unusual ^1H NMR spectral tendencies. The resonances of Sunset yellow are sharp but shift as a function of higher concentration – which is consistent with the existence of small nano-entities and literature reports using other spectroscopic studies [10–12]. For Allura red, the spectra contains both sharp and broad resonances indicating the presence of a mix of multiple aggregate types. On the other hand, the spectra for Orange II are consistent with the presence of very large nano-entities given that resonances only become apparent upon the addition of detergent. Clearly, these results suggest that structure-aggregate relationships exist and that the sulfonate anions play a more complex role beyond the simple expectation of enhancement of solubility [13].

The structure-aggregation relationships exposed above was then expanded to the structurally similar bis-naphthyl azo dyes that also have a different number of sulfonate anions. Fig. 4.8 reports the ^1H NMR spectra of Acid red 18, Amaranth and Eriochrome blue black B. A single set of resonances of Acid red 18 are observed and sharp throughout the concentration range, although there are some notable resonance shifts at higher concentrations. More dramatic shifts are found for Amaranth that is a regioisomer of Acid red 18. Perhaps the less pronounced aggregate behavior is notable for Acid red 18 due to a suppression of π - π stacking interactions given the proximity of the sulfonate groups to both naphthyl rings, as compared to Amaranth where the sulfonate anions lie at the periphery of the rings. The spectra of Eriochrome blue black B have truly unusual features with many sharp resonances that are inconsistent with a single species.

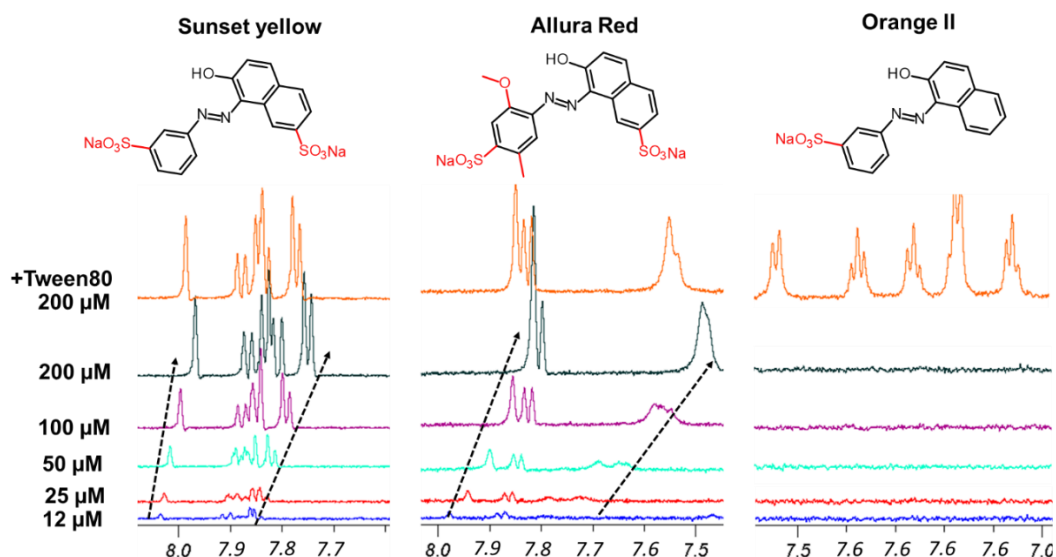


Figure 4.7. NMR aggregation assay showing ^1H NMR spectra of three structurally similar azo dyes obtained by dilution from $200\ \mu\text{M}$ to $12\ \mu\text{M}$.

Sunset yellow (left), Allura red (middle) and Orange II (right). (For interpretation of the references to color in this figure legend, the reader is referred to the Web version of this article.)

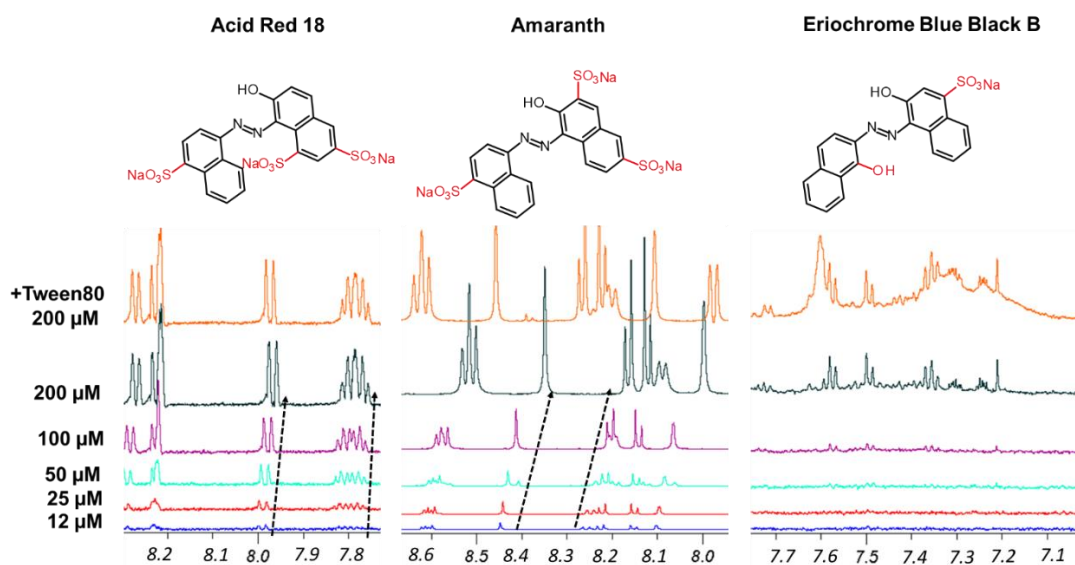


Figure 4.8. NMR aggregation assay showing ^1H NMR spectra of three structurally similar bis-naphthyl azo dyes obtained by dilution from $200\ \mu\text{M}$ to $12\ \mu\text{M}$.

Acid red 18 (left), Amaranth (middle), and Eriochrome blue black B (right). (For interpretation of the references to color in this figure legend, the reader is referred to the Web version of this article.)

4.4.5 Dye-drug interactions

Dyes are used in a wide range of applications, including foods, drinks, cosmetics, tooth paste, medications. etc., Thus, a question worth addressing is whether dyes can interact directly with medical drugs that are also highly prescribed in our society. If so, there may be a

potential that dyes can compromise the intended medical use of certain drugs. Unfortunately, there have been few reports on drugs and other chemicals interacting with dyes to produce undesired effects [14], and as a result a detailed molecular view is lacking.

To illustrate how potential interactions can be studied using NMR, Congo red was added to Quetiapine and the NMR spectrum observed. Quetiapine is an antipsychotic drug used for the treatment of schizophrenia and bipolar disorder. The NMR spectrum of Quetiapine alone in Fig. 4.9 shows sharp resonances that are consistent with a non-aggregator behavior in solution. Congo red, which was used in the cellulose industry before it was banned for toxicity reasons, exhibits very broad resonances in Fig. 4.9 that is consistent with a behavior as an aggregator in solution. When mixed together, the broad resonances of Congo red remain whereas the resonances of Quetiapine become significantly broad. Based on this, it is apparent that Quetiapine interacts with Congo red and adopts its slow tumbling behavior as an aggregate. It also shows the potential impact that aggregates can have on other small molecules. Moreover, this provides a new tool for studying drug-dye or drug-drug interactions.

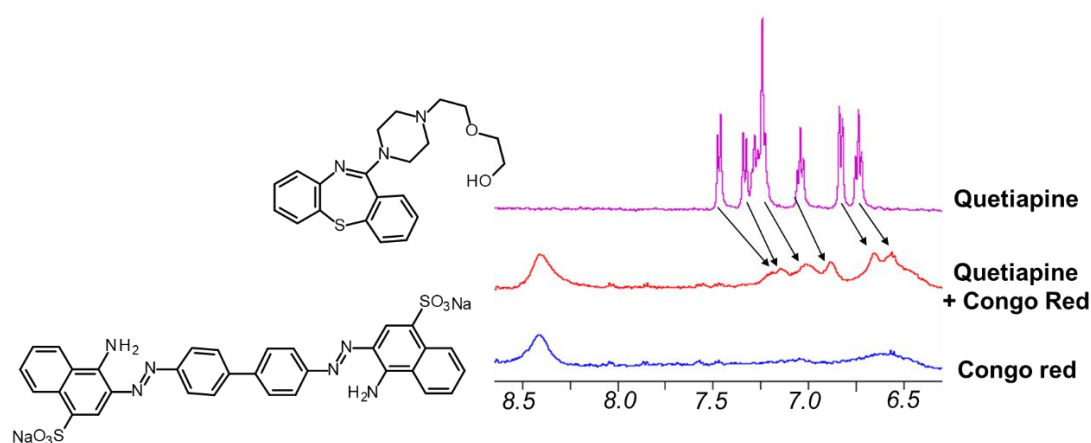


Figure 4.9. Shown are NMR spectra of the drug Quetiapine and the dye Congo red.

1H NMR spectrum of Quetiapine alone (purple above) at 200 μ M. 1 H NMR spectrum of 50/50 mixture of Quetiapine and Congo red at 200 μ M each (red spectrum, middle) and 1 H NMR of Congo red alone at 200 μ M (Blue, bottom spectrum). Note that the broad peaks observed here for free Congo red are less notable in the spectrum of free Congo red in Fig. 3 because the vertical scale is much lower. Samples were prepared in 50 mM sodium phosphate buffer pH 7.4 in 100% D₂O solvent. (For interpretation of the references to color in this figure legend, the reader is referred to the Web version of this article.)

4.4.6 Discussion on dyes, solution behavior and properties

Dyes play an important role in our society, and are used in many products. They are produced in extremely large quantities world-wide for applications in various industries. For example, the clothing industry employs dyes to enhance marketability of their products. Also, the food industry employs color to enhance the attractiveness of their products. As a result,

consumers are heavily exposed to small-molecule dyes that are worn and ingested, despite the fact that relatively little is known about their in vivo behavior, properties and toxicity. The impact on the environment is also significant. Effluents from the dye industry are eventually discharged into the environment as pollutants. Some can be readily degraded, but others, such as azo dyes are persistent as a result of their lipophilic nature. When the latter is degraded, azo dyes are well known to be susceptible to anaerobic reduction, releasing amines and hydrazine that can be carcinogenic [15]. Thus, dyes are highly prevalent in our society and their properties need to be investigated with appropriate tools.

Here, we introduce an NMR aggregation assay and found that some dyes tend to behave as lone single molecules in solution whereas others adopt nano-entity features. It is interesting that we also demonstrated that minor chemical changes can result in major differences in solution behavior. Our previous work [2], suggested that these solution behaviors can have a serious impact on properties (e.g. toxicity) so it is reasonable that dyes having different behaviors can also have distinct properties. This NMR assay now provides a new tool for monitoring the behavior of dyes in solution, and can begin to explore potential correlations with relevant properties.

Correlating nano-entities to specific dye properties will certainly prove to be difficult or even impossible. However, it is tempting to hypothesize that aggregate-property relationships can exist. For example, the aggregation property of an HIV drug has been directly attributed to its high and favorable oral bioavailability [16]. Also, aggregates have been associated with affecting the efficacy of cancer drugs [17,18]. In a 2007 conference in Southampton UK, the use of six dyes (Tartrazine, Sunset Yellow, Allura Red, Acid Red 18, Azorubine and Quinoline Yellow WS) was questioned because they were suspected of causing food intolerance and exasperating attention deficit hyperactivity disorder (ADHD) in children [19]. Interestingly, this study showed that four of the six dyes exhibit nano-entity properties. For example, Azorubine clearly aggregates in our assay as shown in Fig. 4.10. Other potential properties of dyes are beginning to become evident. For example, some artificial coloring agents appear to aggravate attention deficit hyperactivity disorder (ADHD), and it has been established that erythrosine-based food coloring can cause thyroid tumors in rats. Although little is known about the precise mechanism of toxicity of some dyes, many have been banned (e.g. 42 benzidine and 70 azo dyes) [20].

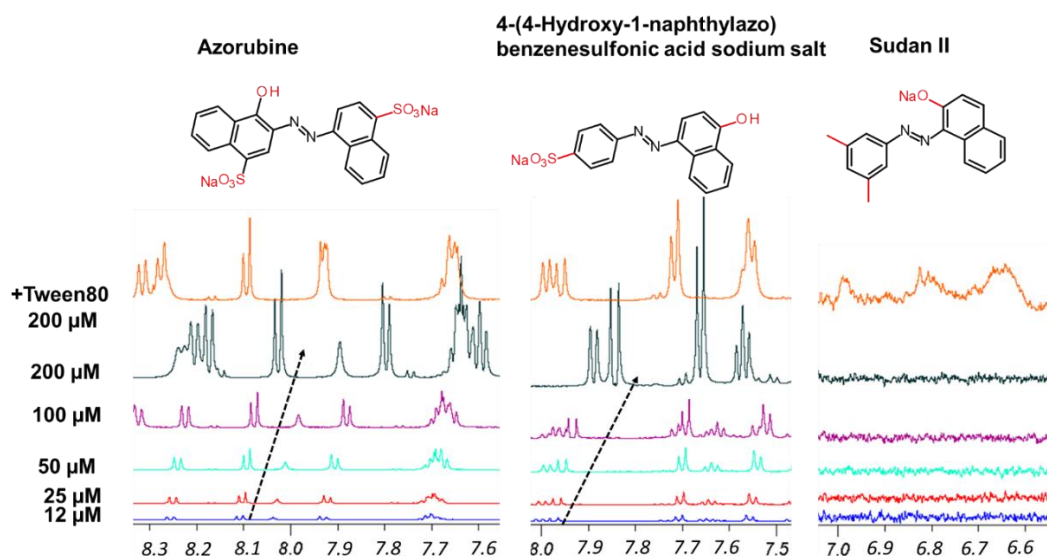


Figure 4.10. Portions of the superimposed ^1H NMR spectra of three structurally similar azo dyes obtained by dilution from $200\ \mu\text{M}$ to $12\ \mu\text{M}$.

Azorubine (left), 4-(4-hydroxy-1-naphthylazo)benzenesulfonic acid sodium salt (middle) and Sudan II (right), 1-(2,4-dimethylphenylazo)-2-naphthol. Broken arrows indicate changes in chemical shift (δ ppm) with concentration. NMR samples were prepared in $50\ \text{mM}$ sodium phosphate buffer pH 7.4 in 100% D_2O .

4.5 Conclusion

Here we introduced the NMR aggregation assay as a new tool for monitoring the behavior of dyes in solution. One potential utility of this tool is to explore potential correlations with relevant properties. On one hand, we know that dyes have a variety of properties where some are benign and others are toxic and have been banned from human consumption. On the other hand, we also now know that some dyes can have a variety of aggregate behaviors, and aggregates have been shown to exhibit promiscuous properties and even toxicity. Although focused studies will be needed to properly establish behavior-property correlations, the NMR methods shown here may be a good method to provide new insights.

Funding

The authors declare no competing financial interest.

Acknowledgments

The authors wish to acknowledge Anne-Laure Larroque and Sanjoy Kumar-Das of the McGill University Health Centre (MUHC) for kindly providing 600 MHz NMR time. They also thank Norman Aubry and Rebekah Carson for helpful discussions and insight. Technical support was provided by Sagar Saran and Paul Oguadinma.

Appendix A. Supplementary data. Supplementary data related to this article can be found at <http://dx.doi.org/10.1016/j.dyepig.2018.02.026>

4.6 REFERENCES

- [1] LaPlante SR, Aubry N, Bolger G, Bonneau P, Carson R, Coulombe R, et al. Monitoring drug self-aggregation and potential for promiscuity in off-target in vitro pharmacology screens by a practical nmr strategy. *J Med Chem* 2013;56:7073–83. <http://dx.doi.org/10.1021/jm4008714>.
- [2] LaPlante SR, Carson R, Gillard J, Aubry N, Coulombe R, Bordeleau S, et al. Compound aggregation in drug discovery: implementing a practical NMR assay for medicinal chemists. *J Med Chem* 2013;56:5142–50. <http://dx.doi.org/10.1021/jm400535b>.
- [3] Coan KED, Shoichet BK. Stoichiometry and physical chemistry of promiscuous aggregate-based inhibitors. *J Am Chem Soc* 2008;130:9606–12. <http://dx.doi.org/10.1021/ja802977h>.
- [4] <https://chemaxon.com/>.
- [5] McGovern SL, Caselli E, Grigorieff N, Shoichet BK. A common mechanism underlying promiscuous inhibitors from virtual and high-throughput screening. *J Med Chem* 2002;45:1712–22. <http://dx.doi.org/10.1021/jm010533y>.
- [6] Heger D, Jirkovský J, Klán P. Aggregation of methylene blue in frozen aqueous solutions studied by absorption spectroscopy. *J Phys Chem A* 2005;109:6702–9. <http://dx.doi.org/10.1021/jp050439j>.
- [7] Al-Thabaiti SA, Aazam ES, Khan Z, Bashir O. Aggregation of Congo red with surfactants and Ag-nanoparticles in an aqueous solution. *Spectrochim Acta Part A Mol Biomol Spectrosc* 2016;156:28–35. <http://dx.doi.org/10.1016/j.saa.2015.11.015>.
- [8] Zhang Y, Xiang J, Tang Y, Xu G, Yan W. Aggregation behaviour of two thiocarbocyanine dyes in aqueous solution. *Dyes Pigments* 2008;76:88–93.
- [9] Zhegalova NG, He S, Zhou H, Kim DM, Berezin MY. Minimization of self-quenching fluorescence on dyes conjugated to biomolecules with multiple labeling sites via asymmetrically charged NIR fluorophores. *Contrast Media Mol Imaging* 2014;9:355–62. <http://dx.doi.org/10.1002/cmml.1585>.
- [10] Horowitz VR, Janowitz LA, Modic AL, Heiney PA, Collings PJ. Aggregation behavior and chromonic liquid crystal properties of an anionic monoazo dye. *Phys Rev E - Stat Nonlinear Soft Matter Phys* 2005;72. <http://dx.doi.org/10.1103/PhysRevE.72.041710>.
- [11] Edwards DJ, Jones JW, Lozman O, Ormerod AP, Sinyureva M, Tiddy GJT. Chromonic liquid crystal formation by edicol sunset yellow. *J Phys Chem B* 2008;112:14628–36. <http://dx.doi.org/10.1021/jp802758m>.

- [12] Chami F, Wilson MR. Molecular order in a chromonic liquid crystal: a molecular simulation study of the anionic azo dye sunset yellow. *J Am Chem Soc* 2010;132:7794–802. <http://dx.doi.org/10.1021/ja102468g>.
- [13] Ishiyama M, Shiga M, Sasamoto K, Mizoguchi M, He P. A new sulfonated tetrazolium salt that produces a highly water-soluble formazan dye. *Chem Pharm Bull (Tokyo)* 1993;41:1118–22. <http://dx.doi.org/10.1248/cpb.41.1118>.
- [14] Swerlick RA, Campbell CF. Medication dyes as a source of drug allergy. *J Drugs Dermatol* 2013;12:99–102.
- [15] <https://www.epa.gov/assessing-and-managing-chemicals-under-tsca/pigmentviolet-29-anthra219-def6510-defdiisoquinoline-0>.
- [16] Boutajangout AM, Sigurdsson EK, Krishnamurthy P. Tau as a therapeutic target for Alzheimer's disease. *Curr Alzheimer Res* 2011;8:666–77. <http://dx.doi.org/10.2174/156720511796717195>.
- [17] Frenkel YV, Clark AD, Das K, Wang YH, Lewi PJ, Janssen PAJ, et al. Concentration and pH dependent aggregation of hydrophobic drug molecules and relevance to oral bioavailability. *J Med Chem* 2005;48:1974–83. <http://dx.doi.org/10.1021/jm049439i>.
- [18] Owen SC, Doak AK, Wassam P, Shoichet MS, Shoichet BK. Colloidal aggregation affects the efficacy of anticancer drugs in cell culture. *ACS Chem Biol* 2012;7:1429–35. <http://dx.doi.org/10.1021/cb300189b>.
- [19] <https://www.food.gov.uk/science/additives/foodcolours>.
- [20] <https://www.ncbi.nlm.nih.gov/books/NBK304402/>.

4.7 APPENDIX A. SUPPLEMENTARY DATA (ARTICLE1)

The NMR aggregation was employed to other dyes and the displays of the NMR data are shown below as Figures S1 and S2.

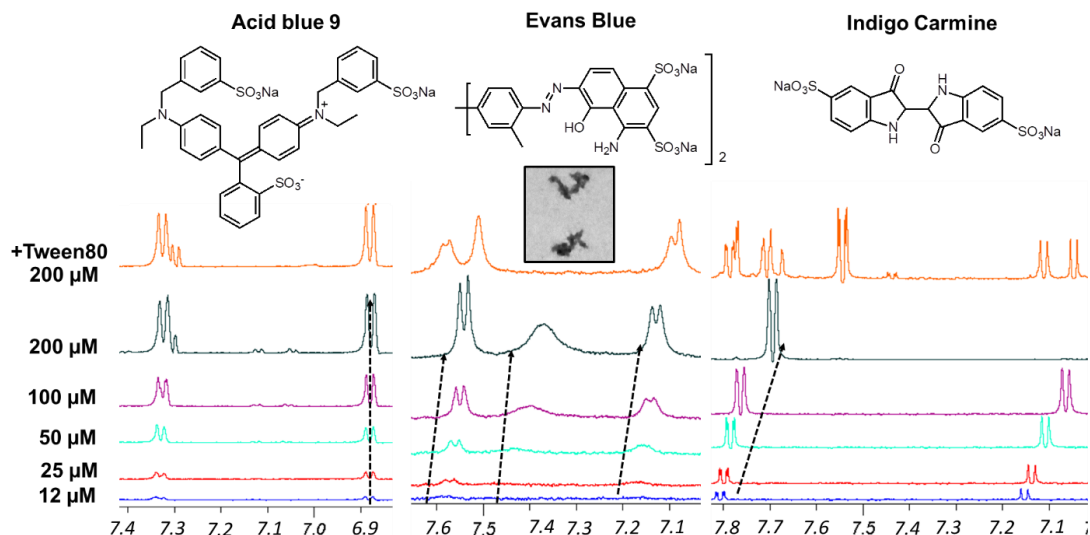


Figure S1. Portions of the superimposed ¹H NMR spectra of three structurally different dyes obtained by dilution from 200 μM to 12 μM. Acid blue 9 (left), Evans blue (middle), both medium-sized and Indigo carmine (right). Broken arrows indicate changes in chemical shift (δ ppm) with concentration. NMR samples were prepared in 50 mM sodium phosphate buffer pH 7.4 in 100% D₂O solvent.

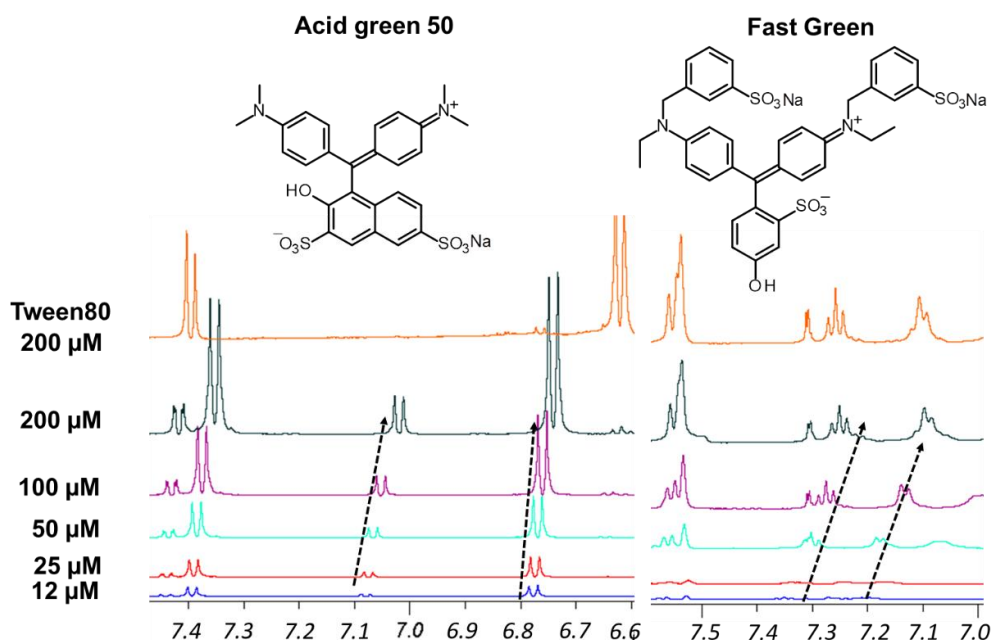


Figure S2. Portions of the superimposed ¹H NMR spectra of Acid Green 50 (left) and Fast Green (right) dyes obtained by dilution from 200 μM to 12 μM. Broken arrows indicate changes in chemical shift (δ ppm) with concentration. NMR samples were prepared in 50 mM sodium phosphate buffer pH 7.4 in 100% D₂O solvent.

5 ARTICLE 2 :

Revealing Drug Self-Associations into Nano-Entities

Marwa M. Dlim [†], **Fatma S. Shahout** [†], Marwa K. Khabir, Patrick P. Labonte, and Steven R. LaPlante

INRS, Institut Armand-Frappier, Université du Québec, 531, boul. des Prairies, Laval, Quebec H7V 1B7, Canada

Title of Journal: ACS Omega

Volume: 4, 8919–8925, Received: March 10, 2019 Accepted: May 7, 2019

Published online: May 23, 2019

DOI: 10.1021/acsomega.9b00667

Author Contributions [†] M.M.D. and [†] F.S.S. contributed equally to this work and should both be considered as first authors.

Contribution of the authors:

I, Prof. Steven LaPlante, confirm that Fatma Shahout contributed equally as a primary author of this publication.

F.S did nuclear magnetic resonance, dynamics light scattering, electron microscopy (including sample preparation in buffer and media and data acquisition), confocal microscopy and ultra-thin section experiments (including cell seeding and compound preparation). Cell thawing, seeding, passaging were done by **F.S**. Proliferation assay was implemented by **F.S**. Detergent based-assay by TEM was implemented by **F.S**. Figures are generated by **F.S**. **F.S** was involved in interpreting and analyzing the data. Also was involved in the writing, editing and reviewing of the manuscript.

5.1 ABSTCT

The aqueous properties of the drugs Sorafenib, Lapatinib, Gefitinib, Fulvestrant, and Clofazimine were explored to monitor their tendency to self-associate. A combination of nuclear magnetic resonance, dynamics light scattering, and electron and confocal microscopies found that they tended to form large nano-entities having distinct types and sizes and were capable of entering cells. The combination of strategies employed serves to detect and reveal nano-entities along with their three-state equilibria and behaviors in buffers, media, and cells.

5.2 INTRODUCTION

The drug discovery community has recognized that the physicochemical attributes of compounds can somehow predispose them to many properties,¹⁻⁹ so pharma workflows focus on prioritizing compound candidates that exhibit favorable properties and deprioritizing those that have undesirable properties. For this, extensive characterization efforts are undertaken.

For many reasons, these characterization efforts are executed and interpreted within the context that compounds in aqueous solvent behave predominantly as either single-molecules in solution or as a solid form such as precipitates. However, it is becoming more apparent that each compound exists in a unique three-phase equilibrium in solution between single lone-tumbling molecules, self-associated aggregates (nano-entities), and solid forms. Although this revised view recognizes the existence of this intermediate aggregate phase, it is becoming clear that drugs can form a wider range of self-assembled nano-entities than previously expected.^{10,12}

To date, little is known about the full range of types and sizes of self-assemblies that drugs can adopt. There have been reports that some can form colloidal aggregates, whereas others can form much smaller multimers.¹⁰ One of the main issues for properly characterizing these nano-entities is insufficient detection strategies, which explains our poor knowledge of this phenomenon and the resultant properties.¹¹⁻¹⁴ No single technology can detect the full range of nano-entities that can exist, but each technology has its advantages and limitations. For example, dynamics light scattering (DLS) and transmission electron microscopy (TEM) are sensitive to large colloidal assemblies (e.g., nanometer size) but are less optimal for small entities and mixtures. nuclear magnetic resonance (NMR) spectroscopy, on the other hand, is highly sensitive to small- to medium-sized aggregates (Ångstrom to subnanometer sizes). This technology can also be used to monitor large aggregates although it requires breaking the aggregates into smaller entities using detergents for detection purposes. Also, confocal laser scanning microscopy (CLSM) can be employed to monitor drugs in cells, but the compounds must be fluorescent and form sufficiently large assemblies. Other potential detection methods can also be used such as nephelometry, SPR, MST, DOSY NMR, and CPMG NMR.

Establishing appropriate detection strategies will be central for thoroughly correlating nano-entities with their respective properties. Impressive examples have already begun to emerge that demonstrate serious impact on drug discovery efforts. Compound and drug aggregates have been attributed to the observation of promiscuity and high incidences of false positives in high-throughput screens for lead discovery.^{13,14} They have also been implicated in affecting the efficacy of drugs in cell culture assays because of lack of cell membrane permeability.¹⁵ This has helped to explain the “bell-shaped” concentration response curves for

formulated drugs.¹⁶ Furthermore, they have been responsible for giving rise to promiscuity in vitro, off-target pharmacology assays and toxicity alerts.¹⁰ Interestingly, aggregates have also been associated with beneficial attributes such as enhancing exceptional drug oral bioavailability.¹⁷ One can also envisage drug nano-entities as potential drug carriers or even delivery systems.

Here, we use several anticancer drugs (Sorafenib, Lapatinib, Gefitinib, and Fulvestrant) and an anti-leprosy drug (Clofazimine) as model systems to explore various techniques for monitoring their physicochemical solution behavior. We evaluate data from NMR, DLS, TEM, and CLSM to characterize the nano-entities formed and to probe the strengths and limitations of the methods. It should be kept in mind that the present study focuses on compounds that form the large colloidal aggregates. Studies involving the smaller nano-forms are referred to an early report and to forthcoming disclosures.^{10,12}

5.3 RESULT AND DISCUSSION

A typical workflow practiced in the pharmaceutical industry is one where medicinal chemists synthesize new compounds based on design concepts intended to capture a range of intended favorable properties, for example, binding and specificity for a target protein, bioavailability, stability, and safety.

Medicinal chemists almost exclusively characterize their candidate drugs in organic solvents, then lyophilize, and expedite the powders or stock solutions to multiple other laboratories for a broad range of pharmaceutical tests where the compounds are dissolved in or diluted with aqueous media. However, drugs behave much differently in organic solvents as compared to aqueous media, and thus the above workflow introduces an important and uncharacterized disconnect. That is, no one along the workflow is responsible for monitoring a compound's aqueous behavior in solution for the aggregate phase, thus, the three-phase equilibrium systematically goes largely unexplored.

This is unfortunate because a simple and quick perusal of the ¹H NMR spectrum of a compound in buffer can easily begin to expose features of its three-state equilibrium.¹² This is illustrated in (Figure 5.1) for the four compounds (Sorafenib, Lapatinib, Clofazimine, and Gefitinib). From 20 mM stock solutions in DMSO-d₆, compounds were diluted in DMSO-d₆ solvent to 200 μM concentration where it was noted that they dissolved well-clear solutions were observed with no precipitate. The 200 μM was only used in NMR assay (no cells) to clearly observe the NMR resonance. ¹H NMR spectra of the later samples (200 μM) were then acquired, respectively, and shown in Figure 5.1a. This atomic view of hydrogen nuclei shows that all resonances are observable and sharp, as expected for compounds that behave as single lone-tumbling molecules in solution.

Samples of these compounds at 200 μM in aqueous buffer were then prepared by placing aliquots of DMSO- d_6 stock solutions into aqueous buffer followed by gentle agitation. Some cloudiness or solid precipitate was noted, and so the samples were subjected to light centrifugation. The supernatant was then placed in NMR tubes and ^1H NMR spectra acquired. Figure 5.1b shows that no NMR resonances were observed. It is possible that the compounds totally existed as a solid-state form and were removed by this latter manipulation. Even if some solid remained as a cloudiness, the resonances of solids are too broad to be observed by solution NMR. Another possible explanation would be that the compounds partitioned between precipitates and very large self-associated and soluble aggregates. The latter would have to tumble too slowly in solution which would also result in resonances that are too broad to be observed by solution NMR. Interestingly, we showed in a previous report that a simple trick of adding a detergent such as Triton or Tween to the samples induced the breakup of the large aggregates, resulting in faster tumbling lone molecules, which then gave rise to observable NMR resonances. To our surprise, the addition of detergent to the Sorafenib sample did not give rise to sharp resonances (see Figure 5.1c), whereas sharp resonances did arise for Lapatinib, Clofazimine, and Gefitinib (see Figure 1c). The latter observations unequivocally report the existence of the large aggregates. However, the lack of resonances for Sorafenib demonstrates our assumptions and limited knowledge of aggregate types and how to manipulate and observe them by NMR.

Interestingly, DLS data acquired on the aqueous samples, after light centrifugation, clearly showed existence of the nanometer-sized aggregates (see Figure 5.1d). The DLS data of these samples after the subsequent addition of detergent report differential changes in aggregate sizes, which demonstrated the potential complementarity of NMR and DLS techniques. TEM also convincingly revealed the presence of very large aggregates in various media such as Dulbecco's modified Eagle's medium (DMEM) with 5% fetal bovine serum (FBS) (see Figure 5.2a), cell culture media (DMEM) without (FBS) (see Figure 5.2b), and aqueous phosphate buffer (see Figure 5.2c). Similar experiments and conditions were also reported by others in which they found that the behaviors of the three anticancer drugs Lapatinib, Fulvestrant, and Sorafenib are consistent with the formation of colloidal aggregates in phosphate buffer and in cell culture media 10% FBS for 24 h at 37 $^\circ\text{C}$.¹⁵

First, it must be kept in mind that our samples were prepared by soaking the compound solutions with a carbon-coated copper grid which is required for TEM observation purposes. Also, it is expected that lone-tumbling single molecules (tumbling radius on the single digit Ångstrom scale) would be invisible by TEM which is sensitive to species that have radii on the double-digit nanometer scale. Keeping these considerations in mind, a number of observations

can nonetheless be made for characterizing these intriguing and large nano-entities observed (see Figure 5.2).

Interestingly, a comparison of the horizontal images along (Figure 5.2c) shows a variety of large aggregates for the drugs in buffer. Some are smaller such as that found for Clofazimine, whereas very large globs are noted for Fulvestrant, Sorafenib, and Lapatinib. A range of sizes are also noted. Gefitinib appears as a solid-like form. Changes in the aggregates are notable when the compounds are soaked in DMEM media compare Figure 5.2a with 5.2b. Likewise, dramatic changes are observed when comparing all three media conditions (see Figure 5.2 a–c). We then studied the effect of adding detergent to large nano-entities. The addition of detergents to samples suspected of forming large aggregates is a widely used strategy in many biochemical assays to reveal false-positive hits in screening campaigns.

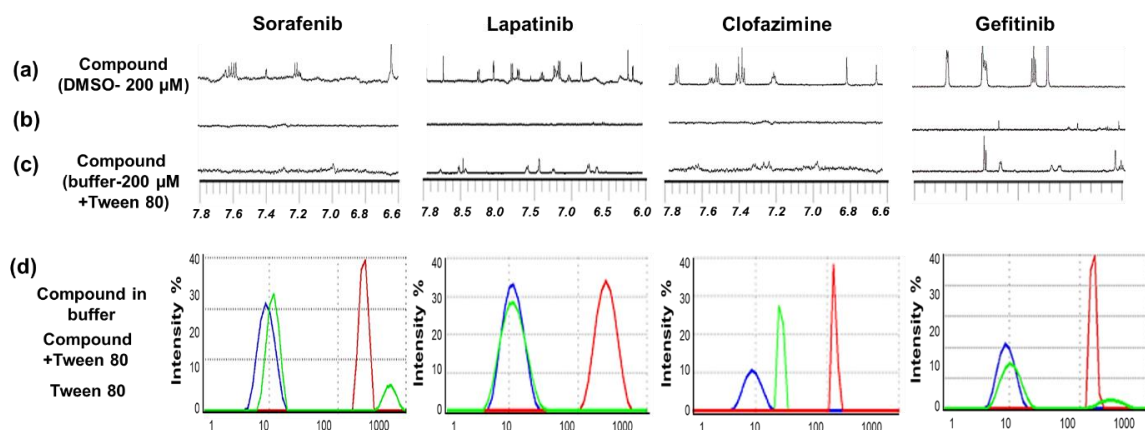


Figure 5.1. NMR spectra of four compounds.

(a) Compounds in DMSO-d₆ at 200 μM, (b) compounds in buffer at 200 μM, (c) compounds in the presence of Tween 80, (d) DLS data for the four compounds. Both techniques involving buffer contained 50 mM sodium phosphate, 100 mM NaCl, 10% D₂O, pH 7.4 in the absence and presence of 0.025% (v/v) Tween 80 for 24 h.

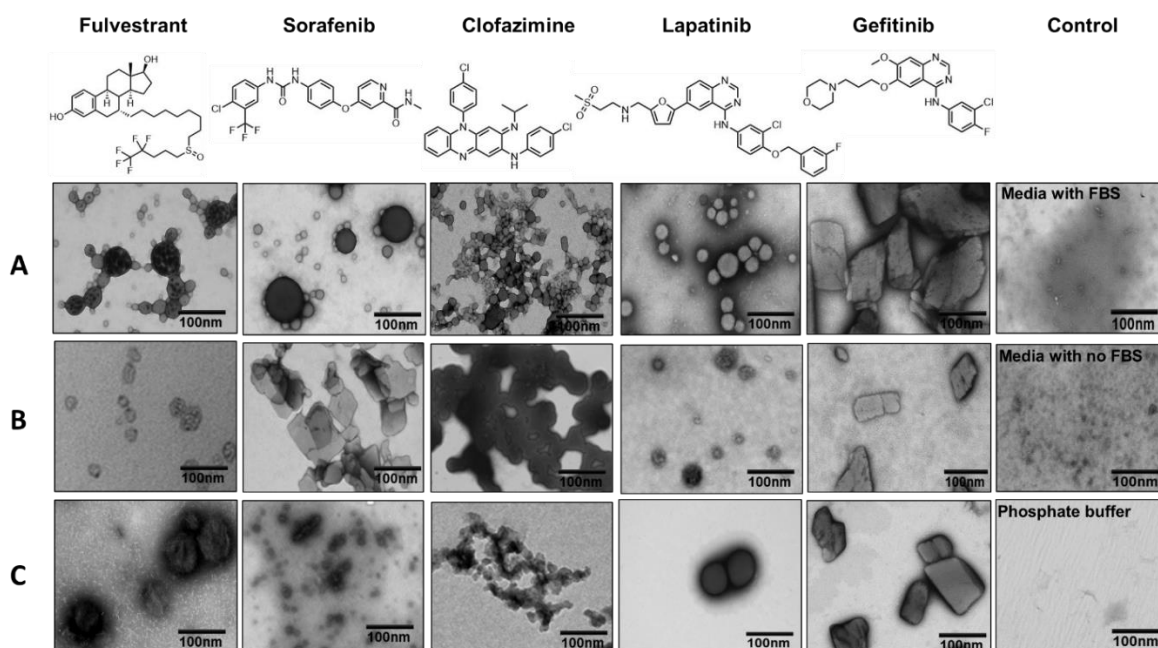


Figure 5.2. TEM images of four anticancer drugs (Fulvestrant, Sorafenib, Lapatinib, and Gefitinib), and an antileprosy drug (Clofazimine)

(a) 50 μM of compounds incubated for 24 h in DMEM 5% FBS, or (b) in DMEM with no FBS, or (c) in phosphate buffer pH 7.4. Bars represent 100 nm.

One typically runs screening campaigns to identify lonetumbling compounds that inhibit a protein, but these assays are frequently contaminated with false-positive hits from compounds which form large aggregates and inhibit via nonstoichiometry and nonspecific means. Running follow-up validation screens typically involves the addition of a detergent, which presumably breaks up drug aggregates, and results in the loss of false-positive inhibition.

We thus explored the effect of the addition of detergents on the aggregates of the drugs studied here (see Figure 5.3a). The TEM images shown in Figure 5.3a for Sorafenib, Lapatinib, and Clofazimine (in the absence of detergent) clearly display large aggregates. Upon addition of 0.025% Tween 80 detergent, the TEM images in Figure 5.3b show that these large aggregates have been seriously altered and disrupted. Taking the ^1H NMR experiments in Figure 5.1 into account, it is clear that addition of detergent breaks the aggregates into very small tumbling entities for Lapatinib and Clofazimine, which is consistent with the TEM changes in Figure 5.3b. However, small entities were not observed for Sorafenib upon addition of detergent, whereas the TEM data clearly shows disruption of the large aggregates. Therefore, the example of Sorafenib demonstrates that solubility is limited, or more likely here, there might be aggregate types that NMR and TEM simply cannot detect. This suggests that each

compound can assume its unique fingerprint of self-assemblies, thus one must remain vigilant regarding assumptions and dogma in this field of study.

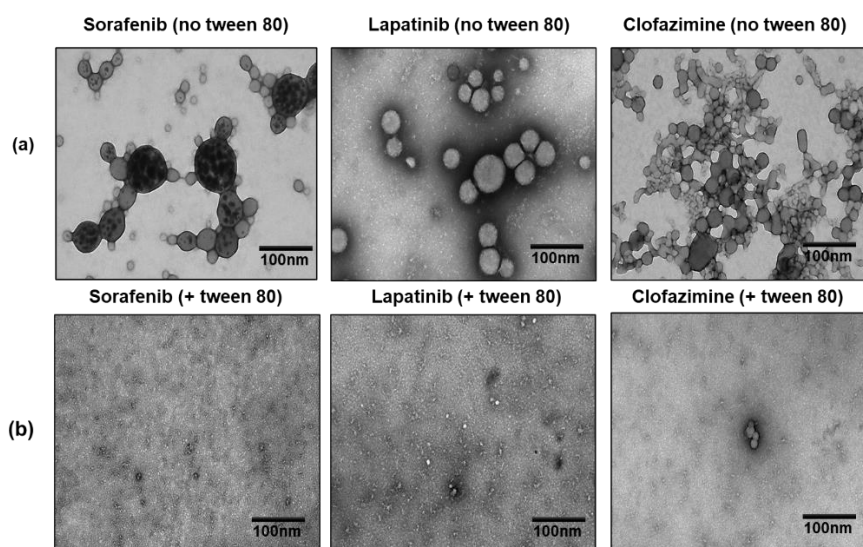


Figure 5.3. (a) TEM images of 50 μM Sorafenib, Lapatinib, and Clofazimine incubated for 24 h at 37 $^{\circ}\text{C}$ in DMEM 5% FBS in the absence of 0.025% (v/v) Tween 80, (b) in the presence of 0.025% (v/v) Tween 80. Bar represent 100 nm.

Note that in our previous work (chapter 2) and the following work (chapter 4), 0.1% of detergents were used in NMR assays (no cells) which was shown to break up some aggregates. Here in this chapter, a percentage of 0.025% was chosen due to its non-toxic effect on the cells as confirmed by us (supporting information) and by others (Owen *et al.*, 2012a). Both percentages are below the CMC. 0.1% has not been tested yet for their toxicity on cells (future work).

Two notable and contentious assumptions are that compound aggregates cannot exist in plasma nor be able to cross membranes to enter cells.¹⁸ The former assumption has often been rationalized, given that many drugs have been found to be highly serum-bound in vivo.¹⁹ Given this, the majority of a compound would be expected to be bound to serum proteins such as albumin, leaving compounds mostly unavailable to self-associate. This assumption is unfounded. In a previous study, involving an NMR aggregation test, it was clearly shown that aggregating compounds remained self-associated in a range of pharmacology buffers, plasma, and blood. This would suggest that there is a significant affinity for self-association for some compounds.¹⁰ It has also recently been reported that Evans Blue forms colloids that adsorb albumin.¹⁵

Regarding these assumptions, we set out here to identify tools that can help determine if aggregating compounds can cross membranes and enter cells. Others assumed that aggregates are too large and cannot diffuse through cell membrane of live cells.¹⁶ For our study, we explored the use of CLSM. First, one must realize and consider that all the methods used here make observations at very distinct resolutions. NMR makes measurements at the

atomic level or Ångstroms, whereas TEM and DLS resolve particles at the nanometer scale, and CLSM at the micrometer level. Thus, CLSM is the most appropriate method for observations at the cellular level. However, to render a compound observable by CLSM, it must have inherent fluorescence, so we were limited in the compounds that could be studied; thus, potential compounds were prescreened by a standard fluorescent microscope.

We began this study by the incubation of HeLa cells in the presence of Lapatinib at 50 μM for 24 h and acquired CLSM views (see Figure 5.4a). Data from a range of other concentrations, conditions, and compounds are provided in the Supporting Information, along with a description of the procedures employed and experimental information. Figure 5.4a shows that the green fluorescence of Lapatinib indeed had entered the cell and appears mostly localized to the cytoplasm. Note that the cell membrane and nuclei can be visualized (see Figure 5.4a) based on the red and blue dyes Alexa Fluor 555 conjugate of WGA and DRAQ5, respectively, which are well-known markers. Interestingly, Lapatinib appears to be well-distributed within the cytoplasm given that green fluorescence is observed for all the cytoplasm. We also measured the antiproliferative activities of aggregate form (no Tween) and monomer forms (+Tween) of Lapatinib on HeLa cells. Our study found that both forms exhibit similar antiproliferative activities suggesting that both forms are capable of entering HeLa cells (see Supporting Information, Figure S6). Note that we and others confirmed that 0.025% of Tween 80 was nontoxic (Supporting Information).¹⁵ In contrast, others found that the monomer form had significantly improved activity versus the aggregate form using MDA-MB-231 cells, suggesting that the monomer form has better capability of entering cells as compared to the aggregate form. Thus, aggregate penetration is likely cell type-dependent.

Further CLSM studies were then focused on another compound Clofazimine, and distinct findings were observed. Clofazimine was incubated with Huh-7 cells for 1 hour (see Figure 5.4b). Although Figure 5.4b shows a well-distributed green fluorescence within the cytoplasm, there are stronger compound signals arising from the nucleus. Note that the nuclei can be visualized (see Figure 5.4b) based on the blue dye DAPI, but the cell membrane cannot be easily distinguishable given that no Alexa Fluor 555 conjugate of WGA dye was added in this experiment because of signal interferences with the drug. In order to verify that the compound aggregates were occurring intra- and not extra-cellularly, care was taken to wash the cells after the incubation step. They were washed twice in phosphate-buffered saline (PBS) to remove any existing extracellular aggregates, and fresh DMEM 5% FBS were added to the cells.²⁰

It is also interesting that Clofazimine is considered as a lipophilic antibiotic which has very long pharmacokinetic half-life of up to 70 days.²⁰ It was noted that Clofazimine aggregates/accumulates in cells (in vitro) over several days, where it formed intracellular

inclusions in the cytoplasm. Perhaps the long half-life is related to sequestering via aggregation. It was also reported that Clofazimine can be toxic as it induces changes to the mitochondria structure and function. Also, Clofazimine has reported to form stable complexes with DNA and transfer RNA, which resulted in spectral red shifts.²¹ In our study, no red shifts were observed and detections were made using the same green emission wavelengths in the nucleus and cytoplasm.

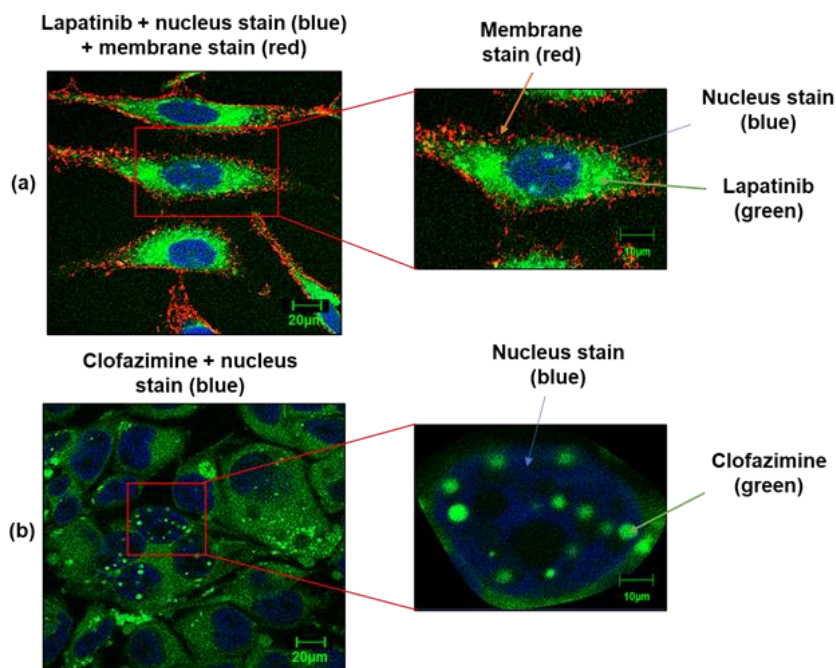


Figure 5.4. (a) Confocal images of HeLa cells incubated in the presence of 50 μM Lapatinib for 24 h.

Alexa fluor WGA 555 was used to stain cell membranes and DRAQ5 to stain the nucleus. (b) Huh-7 cells incubated in the presence of 50 μM Clofazimine for 24 h. DAPI was used to stain the nucleus. Bar represents 20 and 10 μm .

Our study also employed ultrathin section electron microscopy (USEM) to observe aggregates within cells but as a complementary technique with higher resolution at the nanometer scale. Figure 5.5 shows USEM images involving Clofazimine, Lapatinib, and Light green SF yellowish to probe these compounds in cells. Interestingly, distinct dark inclusions were noted in the presence of compounds. These inclusions appeared to resemble the size, number, and distribution to the drug inclusions observed by transmission light microscopy.

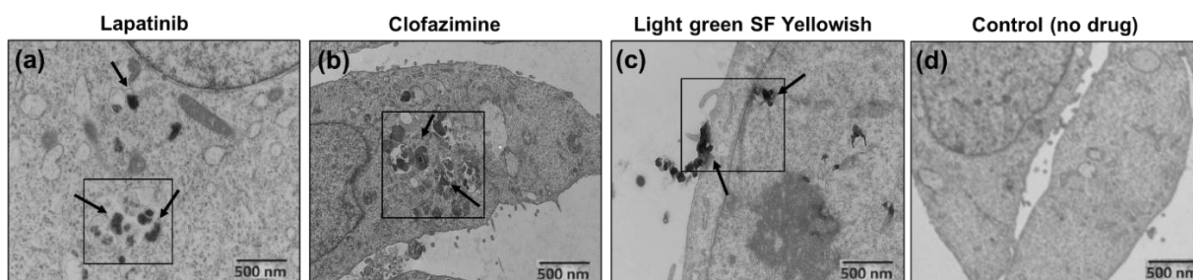


Figure 5.5. USEM images of HeLa cells incubated for 24 h in the presence of (a) 50 μ M Lapatinib, (b) 50 μ M Clofazimine, and (c) 50 μ M Light green SF yellowish, (d) represents control cells in the absence of drugs. Bar represent 500 nm.

5.4 CONCLUSIONS

This work begins the process of evaluating tools for detecting large nano-entities. We found some strengths and weaknesses of a set of techniques, which nonetheless together have allowed us to reveal features of nano-entities from the atomic level to the micrometer scale. It was noted that these large nano-entities can adopt a variety of sizes and types that highly depend on the solution conditions. It was also confirmed that compounds that form nano-entities can indeed enter cells, and will certainly have properties (e.g., see ref 20). However, it is still unclear where nano-entities can enter cells as the monomer form versus aggregate form. Perhaps this is cell and aggregate dependent. Others suggest that colloids do not,^{15,16} whereas we observe compounds that have colloidal forms and can enter cells. The exact mechanism of entry remains unknown.

Another important point is whether the compounds exist in cells as self-associated aggregates or subcellular localized with organelles. Perhaps both occur. The self-association into aggregates certainly helps to augment the observed fluorescence signal either localized with lysosomal compartment or without co-localization (see Figures 4 and S1–S5) as compared to a fluorescent compound Tartrazine that behave as lone-tumbling molecules and have low signal-to-noise (Figure S7). Certainly, colocalization also occurs. Figure S1 suggests that Lapatinib can colocalize with lysosomes. To better address the question of intracellular self-association, further studies are warranted involving the lack and addition of tween. Unfortunately, the toxicity of some compound studies here impeded such experiments.

It is our assessment that the scientific community has only begun to reveal this fascinating drug nano-world. First, a platform of techniques needs to be established, which will allow the scientific community to characterize nano-entities then establish their correlation with salient properties. For example, it has already been established that large-nano-entities can be correlated with compounds high bioavailability, promiscuity, false-positives in screens, and so forth. Perhaps a better understanding of nano-entities can help minimize drug side effects, promote safer compounds to the clinic, or to serve as drug delivery systems. For example, the corresponding author has used the detection of aggregates to deprioritize promiscuous drug candidates and promote selective compounds for the clinic.^{12,22,23}

5.5 EXPERIMENTAL SECTION

Compounds (Drugs and Dyes). Drugs and dyes used in this study were obtained from commercial vendors. CAS numbers are as following: Sorafenib (284461-73-0) from Synchem, Inc.; Fulvestrant (129453-61-8) from Sigma; Lapatinib (388082-78-8) from Larid Road; Clofazimine (2030-63-9) from Sigma; Tartrazine (1934-21-0), and Light green SF yellowish (5141-20-8) from Alfa Aesar. Alexa fluor WGA555 and Prolong Diamond Anti-fade with DAPI was purchased from Thermo Fisher Scientific.

Transmission Electron Microscopy. Compounds were diluted in 50 mM sodium phosphate pH 7.4 and in DMEM 5% FBS. Next, 100 μ L of the samples were transferred into a 240 μ L Airfuge tube. A carbon-coated copper grid was inserted into the bottom of the Airfuge tube with fine tweezers and centrifuged for 5 min at 20 psi. The carbon grid was gently removed with tweezers and washed with distilled water, and the carbon grid was negatively stained with 3% of phosphotungstic acid (PTA-3). The grid was removed, blotted, and dried with a bibulous paper, then examined by transmission electron microscope (Hitachi H-7100). The photographs were processed with the digital camera AMT version 600.147.

Cell Culture. HeLa and Huh-7 cell lines were maintained in DMEM supplemented with 5% of FBS albumin and in 1% penicillin/streptomycin.

Confocal Laser Scanning Microscopy. CLSM was employed to observe the self-aggregation of compounds within the cells. HeLa and Huh-7 cells were grown on glass coverslips in 24 well plates and cultured overnight in DMEM (5% FBS, 1% penicillin/streptomycin) at 37 °C in 5% CO₂. Cell culture media was removed and washed twice with PBS (50 mM sodium phosphate, 100 mM sodium chloride). Compounds at the given concentrations were added to the wells. After 1, 2, 4, 6, and 24 h of incubation, the cells were washed twice with 1 \times PBS (50 mM sodium phosphate, 100 mM sodium chloride) and treated with Alexa Fluor WGA555 for membrane staining. The cells were then fixed in 4% paraformaldehyde solution for 10 minutes and washed twice with PBS 1 \times . Further, the coverslips were mounted on a prolong diamond antifade with DAPI nucleus staining for Clofazimine and Light green SF yellowish and DRAQ-5 for Lapatinib. The cells were imaged by a Zeiss CLSM-780 confocal microscopy (ZEISS, Jena, Germany) on an Olympus FV1000 at 60 \times magnification, using the excitation and emission wavelengths for DAPI, excitation was at 405 nm and emission at 460 nm; for Alexa Fluor WGA555, excitation and emission were at 520 and 550 nm, respectively. Compound excitation and emission information are as follows: Clofazimine excitation (460–495 nm) and emission (515–550 nm), Lapatinib excitation (405 nm) and emission 460 nm), and Light green SF yellowish excitation (405 nm) and emission (460 nm).

Cell Proliferation Assay and in Vitro Cytotoxicity Study (MTT Assay). The cytotoxicity of the panel of compounds and DMSO were evaluated in vitro using MTT assays. HeLa and Huh-7 cells were plated in 96-well plates and cultured overnight in DMEM 5% FBS, in the absence or presence of compounds. After removing the culture medium, various concentrations of the compounds added to the cells, and incubated for 24 h. The medium in each well was then aspirated and discarded. Next, 10 μ L of 5 mg/mL MTT solution 3-(4,5-dimethylthiazol-2,5-diphenyl tetrazolium bromide), was added to each well and incubated for 2 to 4 h. Following incubation, the medium was replaced with 150 μ L DMSO solution. After 15 min, the optical densities at 570 nm were measured by spectrophotometer.

Dynamic Light Scattering. Compounds were measured in DMEM 5% FBS or phosphate buffer, pH 7.4. Measurements were performed by polystyrol/polystyrene 10 \times 10 \times 45 mm cuvettes, utilizing the Zetasizer Nano ZS (Malvern), version 1.7, with a 60 mW laser operating at 830 nm and a detector angle of 158°. All samples were centrifuged before analysis performed in triplicate at 25 °C and the data were acquired using the Dynamics software. Compounds were at 50 μ M.

Nuclear Magnetic Resonance. Compounds were prepared from 20 mM DMSO stock solutions into buffer consisting of 50 mM sodium phosphate pH 7.4 and 10% D₂O. DMSO samples were prepared by diluting the stock samples. NMR data was acquired on a Bruker 600 MHz NMR spectrometer equipped with a helium cryoprobe.^{10,12}

Thin-Section Electron Microscopy. The cells were plated at 1 \times 10⁵ cells/well and incubated in the presence of 50 μ M of all compounds for 24 h. The medium was then aspirated, and the cells washed two times with 1 \times PBS. The cells were then fixed with glutaraldehyde (2.5% in 0.1 M cacodylate buffer or phosphate-buffered saline, overnight) and again washed 2 \times with PBS. Next, the cells were collected and centrifuged at 1000g for 10 min. The fixed-cell pellets were resuspended in a freshly prepared solution 1.3% (w/v) osmium tetroxide in a colliding buffer for 1–2 h and then dehydrated by successive washes with 25, 50, 75, and 95% solutions of acetone in water (15–30 min each). This was followed by two changes of pure acetone incubated for 30 min each. The cell pellets were then resuspended in SPURR acetone (1:1) and incubated for 16– 18 h at room temperature. The cells were cut into small pieces and placed in BEEM capsules to capacity. The capsules were incubated at 600–650 °C for the polymerization reaction to occur. The final stage involved cutting the embedded cells into ultrathin sections and placing the sections on a carbon-covered copper 200-mesh grid. The grids were then stained with 50% ethanol for 20–25 min. Examination of the sections was performed using an electron microscope (Hitachi H-7100), and the photographs were processed using the digital camera AMT, version 600.147.

ASSOCIATED CONTENT

Supporting Information The Supporting Information is available free of charge on the ACS Publications website at DOI: 10.1021/acsomega.9b00667.

Experimental section, additional data, and confocal and electron microscopy images (PDF)

AUTHOR INFORMATION Corresponding Author *E-mail: steven.laplante@iaf.inrs.ca. Phone: +1-514-914-8501.

ORCID

Steven R. LaPlante: 0000-0002-9394-6553

Author Contributions † M.M.D. and † F.S.S. contributed equally to this work and should both be considered as first authors.

Notes

The authors declare no competing financial interest

ACKNOWLEDGMENTS

The authors wish to acknowledge technical support from J. Tremblay (confocal microscopy), Sami Alsabri (assay) and from M. Letarte and A. Nakamura (electron microscopy). This work was supported by NSERC and NMX Research and Solutions Inc.

ABBREVIATIONS

NMR, nuclear magnetic resonance; DLS, dynamic light scattering; TEM, transmission electron microscope; TPSA, total polar surface area; CLSM, confocal laser scanning microscopy; DMEM, Dulbecco's modified Eagle's medium; FBS, fetal bovine serum; BPS, phosphate-buffered saline; USEM, ultra-thin section electron microscopy.

5.6 REFERENCES

- (1) Leeson, P. D.; Springthorpe, B. The influence of drug-like concepts on decision-making in medicinal chemistry. *Nat. Rev. Drug Discovery* 2007, 6, 881.
- (2) Lipinski, C. A.; Lombardo, F.; Dominy, B. W.; Feeney, P. J. Experimental and computational approaches to estimate solubility and permeability in drug discovery and development settings. *Adv. Drug Delivery Rev* 1997, 23, 3.
- (3) Lipinski, C. A. Lead-and drug-like compounds: the rule-of-five revolution. *Drug Discovery Today: Technol.* 2004, 1, 337.
- (4) Vieth, M.; Siegel, M. G.; Higgs, R. E.; Watson, I. A.; Robertson, D. H.; Savin, K. A.; Durst, G. L.; Hipskind, P. A. Characteristic physical properties and structural fragments of marketed oral drugs. *J. Med. Chem.* 2004, 47, 224.
- (5) Proudfoot, J. R. The evolution of synthetic oral drug properties. *Bioorg. Med. Chem. Lett.* 2005, 15, 1087.
- (6) Morphy, R. The influence of target family and functional activity on the physicochemical properties of pre-clinical compounds. *J. Med. Chem.* 2006, 49, 2969.
- (7) Van De Waterbeemd, H.; Smith, D. A.; Beaumont, K.; Walker, D. K. Property-based design: optimization of drug absorption and pharmacokinetics. *J. Med. Chem.* 2001, 44, 1313.
- (8) Cronin, M. D.; Mark, T. The role of hydrophobicity in toxicity prediction. *Curr. Comput.-Aided Drug Des.* 2006, 2, 405.
- (9) Meanwell, N. A. Improving drug candidates by design: a focus on physicochemical properties as a means of improving compound disposition and safety. *Chem. Res. Toxicol.* 2011, 24, 1420.
- (10) LaPlante, S. R.; Aubry, N.; Bolger, G.; Bonneau, P.; Carson, R.; Coulombe, R.; Sturino, C.; Beaulieu, P. L. Monitoring drug selfaggregation and potential for promiscuity in off-target in vitro pharmacology screens by a practical NMR strategy. *J. Med. Chem.* 2013, 56, 7073–7083.
- (11) Hughes, J. D.; Blagg, J.; Price, D. A.; Bailey, S.; DeCrescenzo, G. A.; Devraj, R. V.; Ellsworth, E.; Fobian, Y. M.; Gibbs, M. E.; Gilles, R. W.; Greene, N.; Huang, E.; Krieger-Burke, T.; Loesel, J.; Wager, T.; Whiteley, L.; Zhang, Y. Physicochemical drug properties associated with in vivo toxicological outcomes. *Bioorg. Med. Chem. Lett.* 2008, 18, 4872–4875.
- (12) LaPlante, S. R.; Carson, R.; Gillard, J.; Aubry, N.; Coulombe, R.; Bordeleau, S.; Bonneau, P.; Little, M.; O'Meara, J.; Beaulieu, P. L. Compound aggregation in drug discovery:

implementing a practical NMR assay for medicinal chemists. *J. Med. Chem.* 2013, 56, 5142–5150.

(13) Seidler, J.; McGovern, S. L.; Doman, T. N.; Shoichet, B. K. Identification and prediction of promiscuous aggregating inhibitors among known drugs. *J. Med. Chem.* 2003, 46, 4477–4486.

(14) Feng, B. Y.; Simeonov, A.; Jadhav, A.; Babaoglu, K.; Inglese, J.; Shoichet, B. K.; Austin, C. P. A high-throughput screen for aggregation-based inhibition in a large compound library. *J. Med. Chem.* 2007, 50, 2385–2390.

(15) Owen, S. C.; Doak, A. K.; Wassam, P.; Shoichet, M. S.; Shoichet, B. K. Colloidal Aggregation Affects the Efficacy of Anticancer Drugs in Cell Culture. *ACS Chem. Biol.* 2012, 7, 1429–1435.

(16) Owen, S. C.; Doak, A. K.; Ganesh, A. N.; Nedyalkova, L.; McLaughlin, C. K.; Shoichet, B. K.; Shoichet, M. S. Colloidal Drug Formulations Can Explain “Bell-Shaped” Concentration–Response Curves. *ACS Chem. Biol.* 2014, 9, 777–784.

(17) Frenkel, Y. V.; Clark, A. D.; Das, K.; Wang, Y.-H.; Lewi, P. J.; Janssen, P. A. J.; Arnold, E. Concentration and pH dependent aggregation of hydrophobic drug molecules and relevance to oral bioavailability. *J. Med. Chem.* 2005, 48, 1974.

(18) Ganesh, A. N.; Donders, E. N.; Shoichet, B. K.; Shoichet, M. S. Colloidal aggregation: From screening nuisance to formulation nuance. *Nano Today* 2018, 19, 188–200.

(19) Lu, J.; Owen, S. C.; Shoichet, M. S. Stability of self-assembled polymeric micelles in serum. *Macromolecules* 2011, 44, 6002.

(20) Baik, J.; Rosania, G. R. Molecular imaging of intracellular drug–membrane aggregate formation. *Mol. Pharm.* 2011, 8, 1742.

(21) Morrison, N. E.; Marley, G. M. Clofazimine binding studies with deoxyribonucleic acid. *Int J Lepr Other Mycobact Dis* 1976, 44, 475–481.

(22) Beaulieu, P. L.; Bolger, G.; Deon, D.; Duplessis, M.; Fazal, G.; Gagnon, A.; Garneau, M.; LaPlante, S.; Stammers, T.; Kukolj, G.; Duan, J. Multi-parameter optimization of aza-follow-ups to BI 207524, a thumb pocket 1 HCV NS5B polymerase inhibitor. Part 2: Impact of lipophilicity on promiscuity and in vivo toxicity. *Bioorg. Med. Chem. Lett.* 2015, 25, 1140.

(23) LaPlante, S. R.; Bös, M.; Brochu, C.; Chabot, C.; Coulombe, R.; Gillard, J. R.; Jakalian, A.; Poirier, M.; Rancourt, J.; Stammers, T.; Thavonekham, B.; Beaulieu, P. L.; Kukolj, G.; Tsantrizos, Y. S. Conformation-based restrictions and scaffold replacements in the design of hepatitis C virus polymerase inhibitors: discovery of deleobuvir (BI 207127). *J. Med. Chem.* 2013, 57, 1845

5.7 SUPPORTING INFORMATION

Figure S1. Confocal images of HeLa cells incubated in the presence of 50 μ M of Lapatinib.

Figure S2. Confocal images of HeLa cells incubated in the presence of 50 μ M Light green SF yellowish.

Figure S3. Monitoring the stability of aggregates. Confocal images of HeLa cells incubated in the presence of 50 μ M Light Green SF Yellowish.

Figure S4. Confocal images of Huh-7 cells incubated in the presence of 50 μ M Light Green SF Yellowish.

Figure S5. Confocal images of Huh-7 cells treated with Clofazimine.

Figure S6. Measurement of anti-proliferative activities of aggregate and monomer forms of Lapatinib.

Figure S7. Confocal images of Huh-7 cells incubated in the presence of 50 mM Tartrazine dye incubated for 24 hours at 37°C.

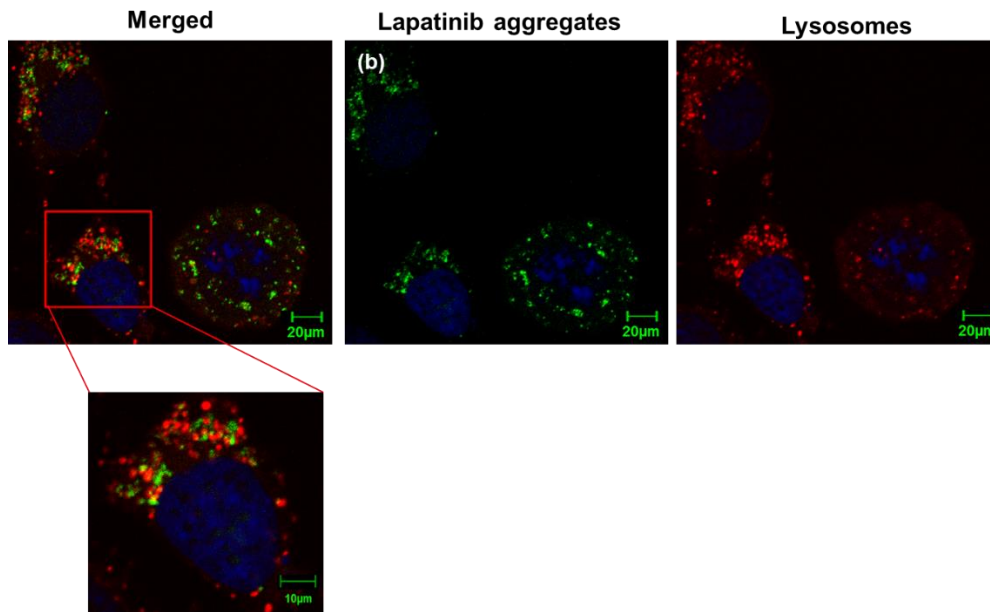


Figure S1. Confocal images of HeLa cells incubated in the presence of 50 μM of Lapatinib.

Intracellular occupancy of drug correlates with the location of the lysosomal compartments. (a) Merged Lapatinib co-localized with the lysosome, (b) Lapatinib (green), (c) lysotracker (red). DRAQ5 was used to stain the nucleus (blue) to monitor lysosome locations. Bars represent 20 μm and 10 μm .

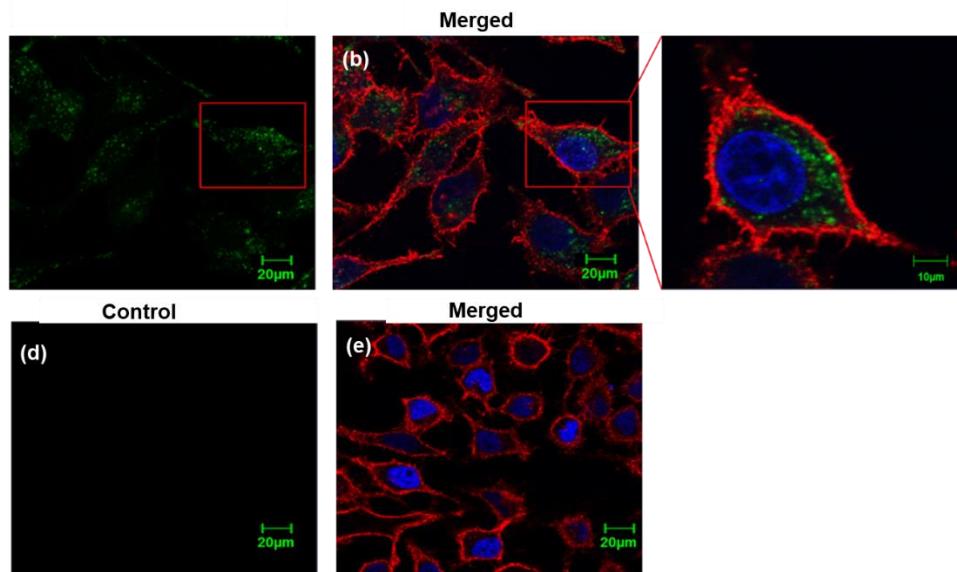


Figure S2. Confocal images of HeLa cells incubated in the presence of 50 μM Light green SF yellowish for 24 hrs (upper row) (a-c), as compared to untreated cells incubated in the absence of Light green SF yellowish (lower row) (d) and (e). Alexa fluor WGA 555 was used to stain the cell membranes, and DAPI was used to stain the nucleus. Bars represent 20 μm .

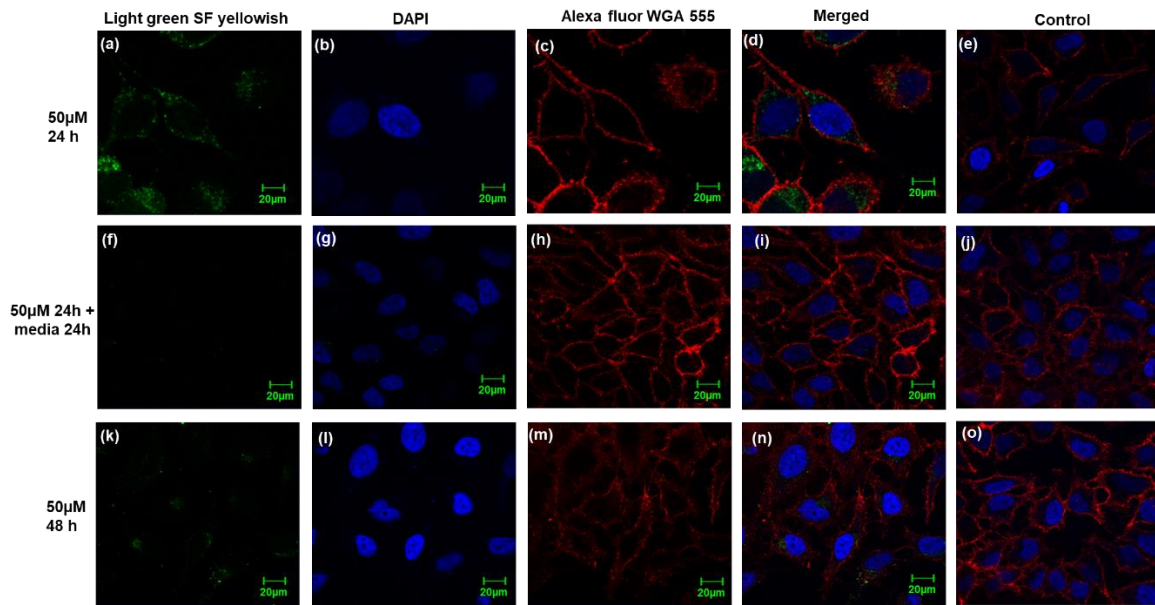


Figure S3. Monitoring the stability of aggregates. Confocal images of HeLa cells incubated in the presence of 50 μM Light Green SF Yellowish for 24 hrs (top row) (a-d), as compared to untreated cells incubated in the absence of compound (e). The media were removed after 24 hrs, refreshed with new media, and then incubated for an additional 24 hrs (middle row) (f-i), as compared to untreated cells (j). HeLa cells incubated in the presence of 50 μM Light Green SF Yellowish for 48 hrs (bottom row) (k-n), as compared to untreated cells (o). Alexa fluor WGA 555 was used to stain the cell membranes, and DAPI was used to stain the nucleus. Bars represent 20 μM .

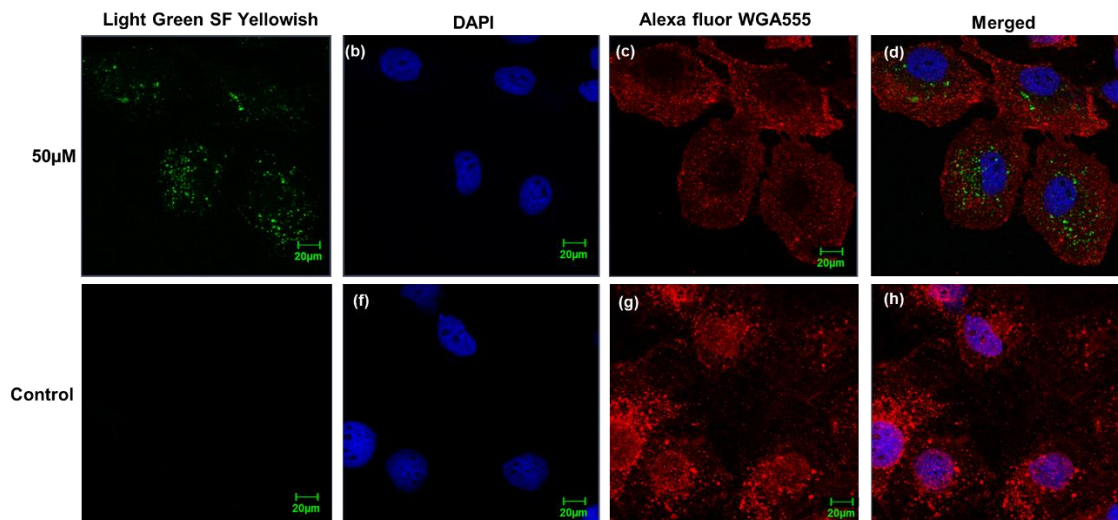


Figure S4. Confocal images of Huh-7 cells incubated in the presence of 50 μM Light Green SF Yellowish for 24 hrs (upper row) (a-d), as compared to untreated cells incubated in the absence of compound (bottom row) (e-h). Alexa fluor WGA 555 was used to stain the cell membranes, and DAPI was used to stain the nucleus. Bars represent 20 μM .

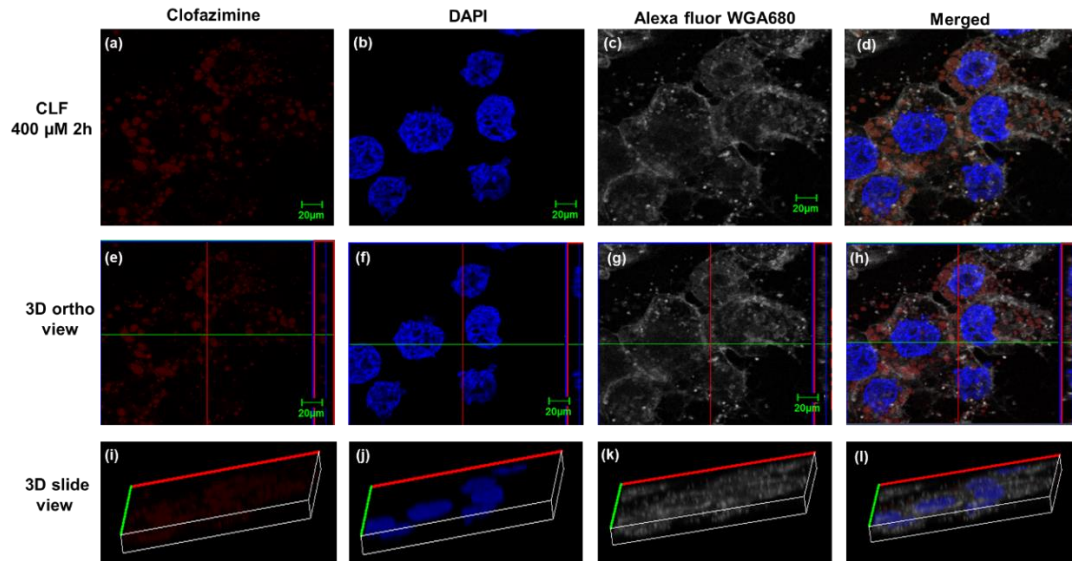


Figure S5. Confocal images of Huh-7 cells treated with Clofazimine at 200 μM for 2 hrs (upper row) (a-d), 3D ortho view (middle row) (e-h), and 3D slide view (bottom row) (i-l). Bars represent 20 μM .

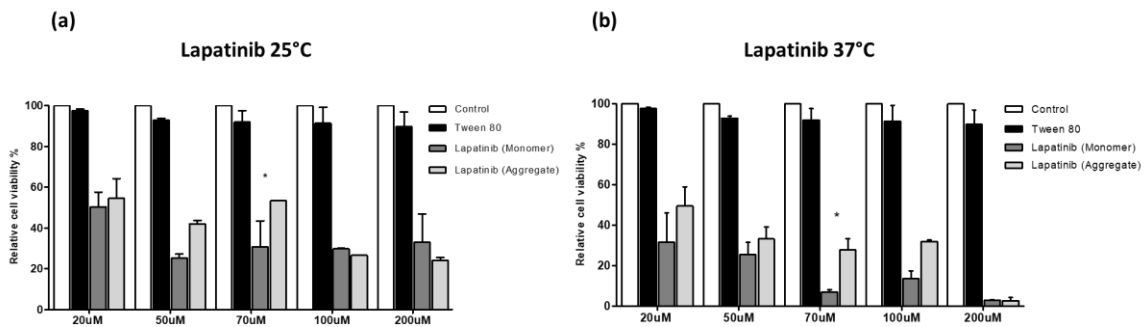


Figure S6. Measurement of anti-proliferative activities of aggregate and monomer forms of Lapatinib (a) at 25°C and (b) at 37°C in HeLa cell line, incubated in the presence and absence of 0.025% (v/v) Tween 80. Graph represents as (Means \pm SEM) (*P < 0.05).

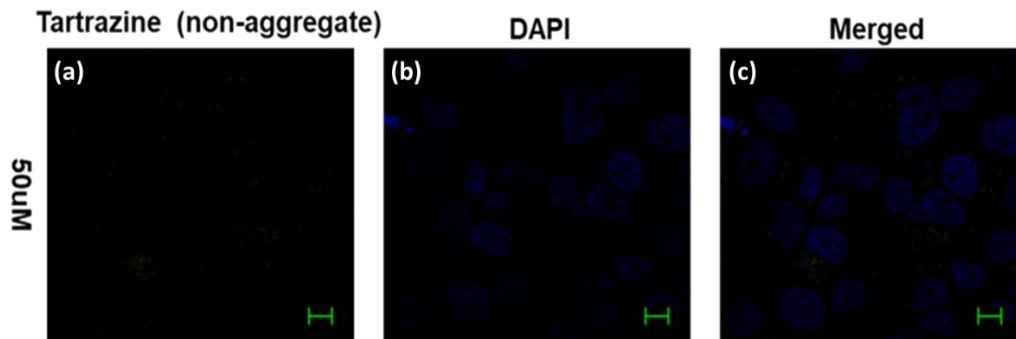


Figure S7. Confocal images of Huh-7 cells incubated in the presence of 50 μM non-aggregate dye (Tartrazine) incubated for 24 hrs at 37°C; (a) tartarazine only, (b) DAPI only for nucleus stain, and (c) merged image of tartarazine and DAPI. Bars represent 20 μM

Probing the free-state solution behavior of drugs and their tendencies to self-aggregate into nano-entities

Steven R. LaPlante^{1,2*}, Valérie Roux¹, **Fatma Shahout**¹, Gabriela Laplante², Simon Woo¹, Y. Ayotte¹, Maria Denk², Patricia Bouchard², Sacha T. Larda²

¹ Université du Québec, INRS-Centre Armand-Frappier Santé Biotechnologie, 531 Boulevard des Prairies, Laval, Québec, H7V 1B7, CANADA

² NMX Research and Solutions, Inc., 500 Boulevard Cartier Ouest, Laval, Québec, H7V 5B7, CANADA

Journal title: NATURE PROTOCOLS

Volume 16 | NOVEMBER 2021 | 5250–5273 | Received: 17 April 2021; Accepted: 9 August 2021

Published online: 27 October 2021

Author contributions

F.S performed the experiments and/or helped with interpretations (transmission electron microscopy, dynamic light scattering, confocal microscopy and NMR aggregation assays) including sample preparations, data acquisition, cell thawing, seeding and compound treatments. **F.S** was involved in data interpretation and analysis, editing and reviewing the manuscript.

6.1 Abstract

The free-state solution behaviors of drugs profoundly affect their properties. Therefore, it is critical to properly evaluate a drug's unique multiphase equilibrium when in an aqueous environment, which can comprise lone molecules, self-associating aggregate states and solid phases. To date, the full-range of nano-entities that drugs can adopt has been a largely unexplored phenomenon. This protocol describes how to monitor the solution behavior of drugs, revealing the nano-entities formed as a result of self-associations. The procedure begins with a simple NMR ^1H assay, and depending on the observations, subsequent NMR dilution, NMR T2-CPMG (Carr-Purcell Meiboom-Gill) and NMR detergent assays are used to distinguish between the existence of fast-tumbling lone drug molecules, small drug aggregates, and slow-tumbling colloids. Three orthogonal techniques (dynamic light scattering, transmission electron microscopy and confocal laser scanning microscopy) are also described that can be used to further characterize any large colloids. The protocol can take a non-specialist between minutes to a few hours, thus libraries of compounds can be evaluated within days.

6.2 Introduction

A clear understanding of the behavior of compounds in aqueous solution is central to the rational design and development of pharmaceutical agents¹⁻⁴. The behavior of compound solutions can be complex and involve mixtures of soluble, aggregate and precipitate forms (Fig. 6.1). Each compound adopts its own fingerprint multi-phase equilibrium in solution that is highly dependent on environmental conditions, such as concentration, buffer, salt, pH, temperature, metals, proteins and the presence of other molecular entities¹⁻⁵. Knowledge of the relative solubility of a compound is therefore important because the relative solubility of a compound can affect its activity in chemical and biological assays as well as in vivo. Unfortunately, a lack of appropriate detection technologies has hindered acquisition of information about a compound's multi-phase equilibrium. As a consequence, the solution behavior of compounds under aqueous conditions remains poorly understood and is largely undetected. The aim of this protocol is to enable expert and non-expert researchers to monitor the solution behaviors of their compounds, with an emphasis on monitoring the aggregate phases. It includes detailed procedures for sample preparation, data acquisition, interpretation and how to use the information obtained in decision-making during the drug-discovery pipeline. The workflow is based on years of experience of the corresponding author in the pharmaceutical industry and involves the judicious use of various equipment and assays that, as an ensemble, present the best potential means for exposing the full range of drug nano-entity types and sizes that can exist. For example, we have previously used the components of this protocol in references^{1,6-9}.

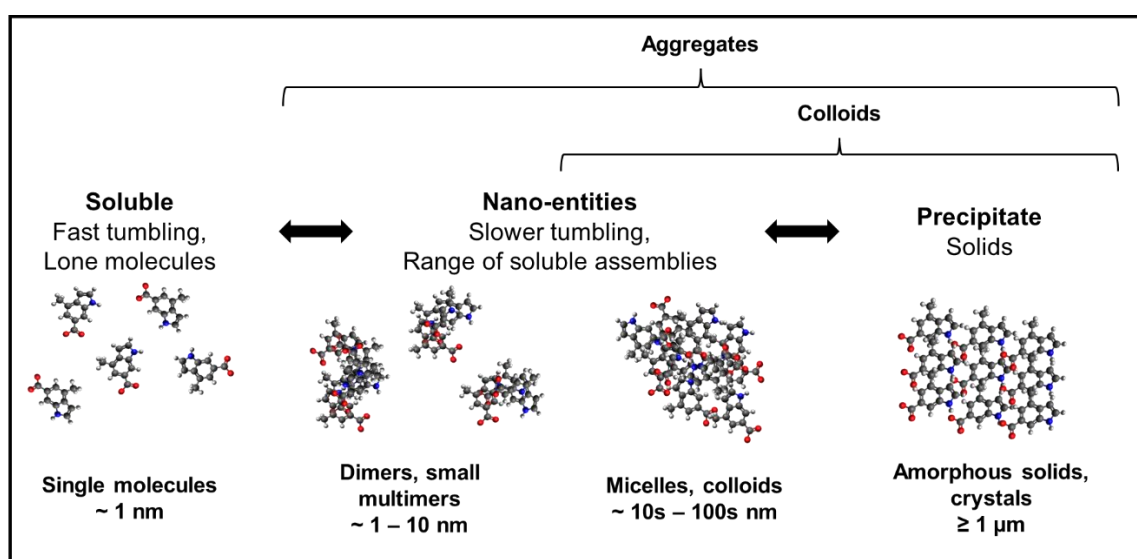


Fig. 6.1 | Drugs exist in unique multi-phase equilibria in solution. They can range from lone molecules (left) to a solid (right), with intermediate states (center) of nano-entities that can exhibit many shapes and sizes

Rationale for the development of the protocol

Existence of compound aggregates (nano-entities)

All compounds naturally adopt a multi-phase equilibrium in solution. From a practical point of view, this property can be categorized as a three-phase equilibrium, ranging from single lone-tumbling molecules to insoluble solid precipitate with an intermediate array of soluble self-associated nano-entities or colloids. This is illustrated in Fig. 6.1, which also shows that distinctions can be made on the basis of molecular sizes. The term colloidal aggregates is often used to describe particles with sizes extending beyond the nanoscale, whereas nano-entities refer to soluble aggregates having sizes between 1 and 1,000 nm. In general, compounds that behave as single lone-tumbling drug molecules fall within a 1-nm range, whereas amorphous solids can be $\geq 1 \mu\text{m}$. Drugs can also adopt self-assembled intermediate nano-entities such as dimers and small multimers sized $\sim 1\text{--}10 \text{ nm}$ (Fig. 6.1). NMR spectroscopy is ideally suited for detection of 1–10-nm entities. In contrast, some nano-entities are much larger and thus visible via transmission electron microscopy (TEM) as shown in Fig. 6.2. For example, the images in Fig. 6.2 show that an anti-leprosy drug (clofazimine), two anti-cancer drugs (lapatinib and sorafenib) and curcumin form self-assemblies ranging from hundreds of nanometers to several micrometers in size. Although the exact molecular architecture and environmental parameters that dictate these equilibria have yet to be deciphered, it is clear that environmental conditions have an impact. For example, changes in colloid features can be observed when different media are used, and smaller aggregates can experience profound equilibrium shifts upon exposure to different buffer conditions^{1,6}.

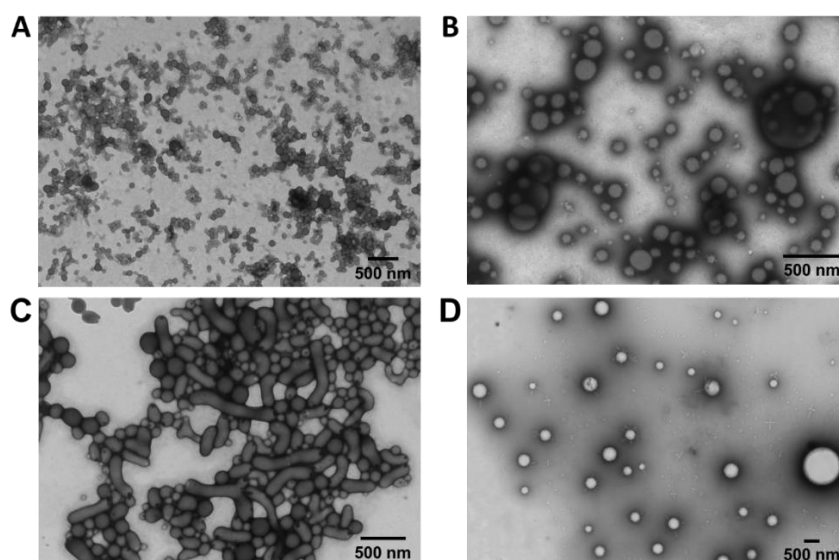


Fig. 6.2 | The presence of large drug colloidal aggregates can be visualized by TEM.

a–d, TEM images show aggregates of clofazimine (a), curcumin (b), sorafenib (c) and lapatinib (d). Compounds were incubated at 100 μM (except for lapatinib, which was tested at 50 μM) in DMEM in the presence of 5% (vol/vol) FBS.

Importance of the characterization of nano-entities for decision making during drug discovery and development

To date, the pharmaceutical industry has undertaken little characterization of multi-phase characteristics of compounds or correlation of these characteristics with function. The initiatives that have been undertaken have demonstrated that these properties have considerable impact at various stages of drug discovery and development. For example, compound aggregates can act as pan-assay interference-like entities and have been implicated in up to 85–95% of artifacts in early highthroughput screens (HTSs)^{2,4}. These hits appear because of the formation of large drug colloids that can bind to and adsorb protein macromolecules in a non-specific manner, leading to changes in dynamics or partial denaturation of the protein. During unpublished industrial research projects, we frequently observed nano-entities when evaluating hits from HTSs and virtual and biophysics screens. These types of hits are often non-stoichiometric and/or non-specific binders.

The impact on decision making at the early lead identification stages of a project when searching for new starting-chemical matter can be profound. When evaluating hits from an HTS, counterscreens can be implemented by adding detergents that break up compound colloids^{1,3}. Significant changes in activity can then be construed as undesirable activity, induced by hits that form colloidal aggregates. Deprioritizing such hits could avoid issues and downstream waste in productivity. Implementing well-designed counter-screens also enables detection of promiscuous hits.

The impact of nano-entities on fragment-based lead discovery can also be profound. Fragment screens usually require high compound concentrations and often involve pools of multiple compounds all at high concentrations. These conditions tend to shift equilibria toward the aggregation and solid phases. Thus, it would be prudent to implement an aggregation assay to first curate libraries of free fragments in buffer⁷. Furthermore, given findings that compound aggregation is also buffer dependent, one should consider running screens and aggregation tests on the free state of compounds in the same buffer used for biological assays. We suggest deprioritizing hits that exhibit aggregation at this stage, given the difficulties in distinguishing between stoichiometric-specific hits and aggregate binding hits. The impacts at the lead optimization stage can also be significant. Colloids have been found to result in false-negative activity in cell-culture assays^{5,10}. In addition, inaccurate results from other biological assays and biophysics affinity measurements are likely, given that it is hard to determine a compound's solubility. Structure-activity relationship conclusions can also be skewed if the influence of aggregation is not taken into account. Distinct variations in aggregation can occur even within a series of closely related compounds⁷. Thus, it is prudent to continuously monitor and evaluate compounds' free-state solution behaviors throughout the lead optimization

stages. When aggregates are observed at such a stage, it would probably be worthwhile to determine if stoichiometric single-molecule binding also exists. Aggregation tendencies can then be monitored as the series progresses, and the information can be incorporated in decision making. For example, we have shown that aggregation behavior can be minimized via minor chemical modifications¹.

Monitoring aggregation tendencies is also recommended for compound series that are approaching selection for clinical studies. Compound aggregation has been implicated in undesirable off-target and promiscuous inhibition⁹, toxicity^{1,6}, altered pharmacokinetics^{11,12} and immune responses (unpublished data). To minimize these undesirable properties, we have successfully used NMR aggregation assays to prioritize non-aggregating compounds for pre-clinical testing¹. Nevertheless, some drug self-assemblies have also been associated with favorable properties such as conferring unusually high drug bioavailability^{13,14}. Thus, the decision to prioritize or deprioritize aggregation will depend on the desired properties required for the drug-discovery program. However, it is likely that the examples of aggregators exhibiting desirable properties might be the exception rather than the rule. Either way, it is becoming clear that the solution behavior of compounds is important; thus, detection technologies are needed to better understand the relationships between these multi-phase solution behaviors and pharmacological properties.

Limitations in free-state detection and monitoring methods

The most widely used methods to detect aggregates in solution are dynamic light scattering (DLS) and electron microscopy^{5,15}. However, both are limited to the detection of large (>10 nm) nanoentities and colloids^{16,17} and are thus unable to detect the full range of self-assemblies that can exist in solution. DLS can also be inadequate in the case of inhomogeneous (polydisperse) samples, whereas electron microscopy usually has relatively limited throughput. Although there is no single scientific instrument that can directly detect the full range of nano-entity sizes and types that exist, NMR is probably the most encompassing option. Fortunately, spectrometers are widely available at most research institutes; thus, NMR is usually the most practical technology available that is also sensitive to the widest range of behaviors of compounds in solution. We introduced several NMR aggregation assays^{1,6-8}, and these are described within this protocol. However, for optimal characterization, interested scientists must first learn and understand the pros and cons of various instruments and techniques, which can be overwhelming because of the challenges in acquiring and interpreting datasets within the context of the peculiarities of nano-entities and colloids.

Comparison of methods: advantages and limitations

Table 1 provides a comparison of the advantages and limitations of the methods used in this protocol. Given this, the protocol described here attempts to establish a pragmatic approach that capitalizes on the advantages and mitigates the limitations of each technique. Perhaps the most versatile and widely encompassing technique described in Table 1 is NMR spectroscopy. The NMR assays best allow one to monitor the solution behavior of compounds and their multi-phase equilibria. Lone molecules, as well as small- and medium-sized aggregates, can be directly monitored, whereas large colloids can be exposed only upon breakup via the addition of detergents. The presence of the latter can also be indirectly inferred through quantification (e.g., by using the electronic reference to access *in vivo* concentrations (ERETIC) method)¹⁸, the acquisition of spectra acquired in dimethyl sulfoxide (DMSO)-*d*₆ solvent or by difference in spin-spin relaxation Carr-Purcell-Meiboom-Gill (T2-CPMG).

Other traditional techniques used in this protocol are limited to the detection of medium to large aggregates and are insensitive to small aggregates and lone molecules. For example, DLS has been used extensively to study colloids^{17,19–21}; thus, it is a great method for detecting large aggregates and for determining sizes and critical aggregation concentrations (CACs). Another added benefit is that DLS is also amenable to high-throughput screening. However, DLS cannot detect small-to-medium-range aggregates and has trouble resolving mixtures of aggregates of roughly equivalent size. Furthermore, it is prone to potential artifacts, which can make detection and analysis difficult or confusing.

TEM can be useful for visualizing large aggregates and for determining sizes^{6,22,23}. It can detect mixtures of large aggregates and could be used to determine CACs. In some cases, it is also amenable to a wide variety of buffers and media. However, it cannot detect small-to-medium-range aggregates, may require high concentrations and is not amenable to high-throughput screening. It is also noteworthy that visualization usually requires the addition of negative stains, which may affect compound multi-phase equilibria. In addition, the size of aggregates can be lower as a result of dehydration. Confocal laser scanning microscopy (CLSM) is an excellent method to visualize large aggregates in cells along with their effects on cells^{6,22}. However, sample preparations are lengthy, analyses are limited to fluorescent compounds and it is less sensitive to small-to-medium-sized aggregates. Moreover, only compounds that are able to cross the cell membrane, either as monomers or as aggregates, will be observed by using this method.

Other techniques that are not detailed in this protocol, such as aggregation-induced emission^{24,25}, nanoparticle tracking analysis (NTA)²⁶, nephelometry²⁷, ultracentrifugation¹¹, small-angle X-ray scattering² and other NMR methods (saturation-transfer difference^{28,29},

diffusion ordered spectroscopy^{7,8} and nuclear Overhauser effect spectroscopy¹) can potentially be used to study solution behaviors of compounds. We chose not to describe the use of these assays because the current scope of these techniques is limited. Aggregation-induced emission relies on the induction of chromophore fluorescence and emission upon the formation of aggregates, which limits its applicability to only large, highly aromatic compounds^{24,25}. NTA has been used in the tracking of colloids²⁶ and to track aggregates; however, we observed that the aggregates seemed to have a tendency to stick to the capillary. Similar to DLS, NTA is sensitive to contaminants²⁶. Nephelometry has been previously used to determine compound solubility²⁷; however, there is no mention in the literature on use to detect drug aggregation. Ultracentrifugation and small-angle X-ray scattering represent interesting approaches, but instrumentation is not always readily available. Many other NMR methods exist, but they are not as straightforward to set up and interpret, can be more time consuming and may not be as sensitive as the methods suggested here. Finally, one can also refer to databases that predict whether compounds have a tendency to aggregate^{30,31}. However, these databases were constructed by using mainly DLS data and thus have inherent limitations.

Besides the technological limitations, there are multiple ‘gaps’ that continue to impede pharmaceutical scientists from effectively pursuing and detecting the existence of drug aggregates. Although some impacts are described here, we have not covered all issues and are therefore currently preparing a more encompassing evaluation in a review article. Perhaps the most daunting gap, and the easiest to overcome, is the lack of appreciation that the phenomenon of drug aggregation can have serious impacts at all stages of drug discovery and development. Another important gap consists of the disconnect in pharmaceutical workflows and the expertise of personnel. For example, medicinal chemists synthesize new compounds and characterize them (at the atomic level by NMR) in organic solvents before delivering the powder form of these compounds (or stocks in organic solvent) to biochemists, who dissolve them in aqueous buffer and perform assays at the macroscopic level. Because no one is responsible for characterizing the compounds in water at the atomic level, important aspects of their solution behaviors can go undetected⁸.

Table 6.1 | Comparison of techniques for detecting drug aggregates.

Methods	Advantages	Limitations
NMR Assays	<ul style="list-style-type: none"> • Provides atomic-level details of compounds • Best methods for direct detection of small- to medium-sized aggregates • Simple methods to implement • Can be used with mixtures of aggregates 	<ul style="list-style-type: none"> • Large aggregates are detected indirectly via T2-CPMG exchange or addition of detergents • Multiple samples required for NMR Dilution Assay • Aggregate sizes can usually only be determined qualitatively

	<ul style="list-style-type: none"> • Both qualitative and quantitative methods • Amenable to a wide variety of buffers/media • Amenable to high-throughput screens • Instruments widely available at institutions • Can detect critical aggregate concentrations (CAC) 	<ul style="list-style-type: none"> • Relatively insensitive technique so requires relatively high concentrations
DLS Assay	<ul style="list-style-type: none"> • Can detect large aggregates and determine sizes • Can detect critical aggregate concentrations (CAC) • Amenable to high-throughput 	<ul style="list-style-type: none"> • Cannot detect small- to medium-sized aggregates • Not compatible with mixtures of aggregates (polydisperse samples). • Not amenable to a wide variety of buffers/media • Many potential artifacts make detection and analyses difficult or confusing
TEM Assay	<ul style="list-style-type: none"> • Can visualize large aggregates and determine sizes • Can detect mixtures of large aggregates • Amenable to a wide variety of buffers/media 	<ul style="list-style-type: none"> • Cannot detect small- to medium-sized aggregates • Can require high concentrations • Visualization usually requires the addition of negative stains • Not amenable for high-throughput • Size of aggregates may be underestimated compared to other techniques due to need to dehydrate
CLSM Assay	<ul style="list-style-type: none"> • Can visualize large aggregates in cells • Possible to observe distribution of aggregates in cells 	<ul style="list-style-type: none"> • Preparation is time-consuming • Limited to fluorescent compounds • Cannot detect small- to medium-sized aggregates • If aggregates/compounds do not cross cell membranes, they will get washed away during the fixation steps • Addition of foetal bovine serum (FBS) may sequester some/all aggregates, leading to no fluorescence being observed inside the cells (false-negatives)

Overview of the procedure

Figure 6.3 provides an overview of the whole protocol. The protocol was designed to allow a scientist to first easily comprehend the solution behavior of a compound (or library of compounds) by using the quick NMR 1 H assay and NMR dilution assay. Depending on the results, other optional assays can then be undertaken to further characterize the multi-phase equilibrium and nano-entities present. The protocol begins with an NMR 1 H assay in which a simple 1 H NMR spectrum of the compound in aqueous buffer at 200 μM nominal concentration

is acquired. In parallel, the sample should be visually inspected to assess solubility (a clear sample suggests adequate solubility, whereas a turbid sample and/or formation of precipitate suggests limited solubility). The top of Fig. 6.3 provides examples of typical results seen for solutions behaving as lone molecules (a), small aggregates (b), large aggregates (c) and precipitate (d). The shape of the ^1H NMR resonances of a compound depends on the tumbling rate of the species present in solution and on exchange between multiple states/entities. In scenario a in Fig. 6.3, visibly sharp resonances are seen as a result of lone molecules that tumble rapidly in solution. In contrast, larger aggregated entities tumble more slowly, resulting in broader resonances (scenario b in Fig. 6.3), or have resonances that are so broad that they appear to not exist (scenarios c and d in Fig. 6.3). If the observed NMR resonances are similar to scenarios a or b, then the concentration in solution can be determined (see Procedure below).

As a control experiment, the acquisition of a ^1H NMR spectrum of the compound at the same 200 μM nominal concentration in DMSO- d_6 solvent is also recommended. This has several purposes. Assuming that most drug-like compounds are more soluble and are expected to aggregate less in DMSO solvent than in buffer, one can compare the observed concentration of a compound between the two solvents by using an external reference¹⁸. This allows the quantitative determination of the total concentration of lone molecules and/or small aggregates. Note that appreciable differences are often observed between nominal and observed concentrations of a compound in spectra from DMSO- d_6 solvent because of powder-weighting issues and solid sample adducts (e.g., salt forms and hydrated powder).

If NMR resonances are observed for the compound in both buffer and DMSO, then the NMR dilution assay^{1,8} can be undertaken along pathways e or f (Fig. 6.3). For this, the acquisition of a ^1H NMR spectrum of the compound at lower concentration (50 μM in buffer) is compared with the 200 μM spectrum in buffer. If abnormal dilution effects are observed, this confirms that small aggregates are present (Fig. 6.3, scenario f), whereas if only normal dilution effects are detected, then it is likely that only lone molecules are present, with no small aggregates (Fig. 6.3, scenario e). However, it is prudent to also run the NMR T2-CPMG assay^{7,32} on the 200 μM spectrum in buffer, given that some nano-entities have been reported to be insensitive to the dilution assay but are sensitive to the T2-CPMG assay. Thus, if significant resonance decay is observed in the NMR T2-CPMG assay, then small and/or large aggregates exist (Fig. 6.3, scenario i), whereas if only minimal decay is noted, then the sample has lone molecules and no small aggregates (Fig. 6.3, scenario j).

If the actual measured concentration of the compound in buffer is significantly less than that in DMSO- d_6 solvent, then it is prudent to test if large NMR-invisible colloidal aggregates also exist. In general, aggregates are sensitive to detergents, such that they show detergent

reversibility^{19,33}. There have been a few assays developed for testing for aggregates on the basis of this property^{3,34}. Running the NMR detergent assay tests for the presence of aggregates. This assay comprises the addition of a series of detergents (examples are given in Supplementary Table 1) to the samples containing the compound. The rationale is that because NMR resonances of large colloids are often very broad or too broad to be visible by NMR, adding detergent can effectively dissociate the colloids into smaller, faster-tumbling pieces. The subsequent observation of any increases in intensity of compound resonances thus confirms the pre-existence of large aggregates, which can be quantified by using the ensemble of NMR data. These colloids are referred to here as 'soft aggregates' (e.g., candesartan; *vide infra*), whereas large colloids that are insensitive to detergents are referred to here as 'hard aggregates' (e.g., lapatinib; *vide infra*).

The NMR detergent assay should be run if no peaks are observed after acquisition of the simple ¹H NMR spectrum for the compound in buffer but resonances are observed for the compound in DMSO-d₆ (Fig. 6.3, scenario G). This assay should also be run if compound resonances begin to appear at the 50- μ M concentration in buffer. The appearance of compound resonances after the addition of detergent suggests the existence of large soft aggregates (Fig. 6.3, scenario K). If compound resonances do not appear (and there was precipitate), it is likely that the compound is insoluble in buffer, and large hard aggregates could be present (Fig. 6.3, scenario L). In contrast, if compound resonances do not appear (and there was no precipitate), then it is possible that the compound exists as a large hard aggregate that is insensitive to the detergents used in the assay (Fig. 6.3, scenario M). Such results should be verified by an orthogonal method such as electron microscopy or DLS.

If no resonances were observed when the compound was placed in DMSO or buffer, this could indicate that the compound is insoluble (Fig. 6.3, scenario H). In this scenario, other solvents should be tested by using the solvent solubility assay. Once a solvent is identified for which the compound is soluble, then the NMR detergent assay should be run for the compound in buffer. However, if the compound is not soluble in any of the solvents tested, then we recommend performing a primary structure verification or abandoning the compound. It is difficult to obtain reproducible results from biological assays that attempt to evaluate insoluble compounds. The final part of the procedure uses orthogonal assays to confirm whether large colloids are present. We describe how to use DLS, TEM and CLSM. However, alternative assays can be used. By combining all the assays that we describe here, a comprehensive analysis of compounds and their behaviors in aqueous solution can be obtained.

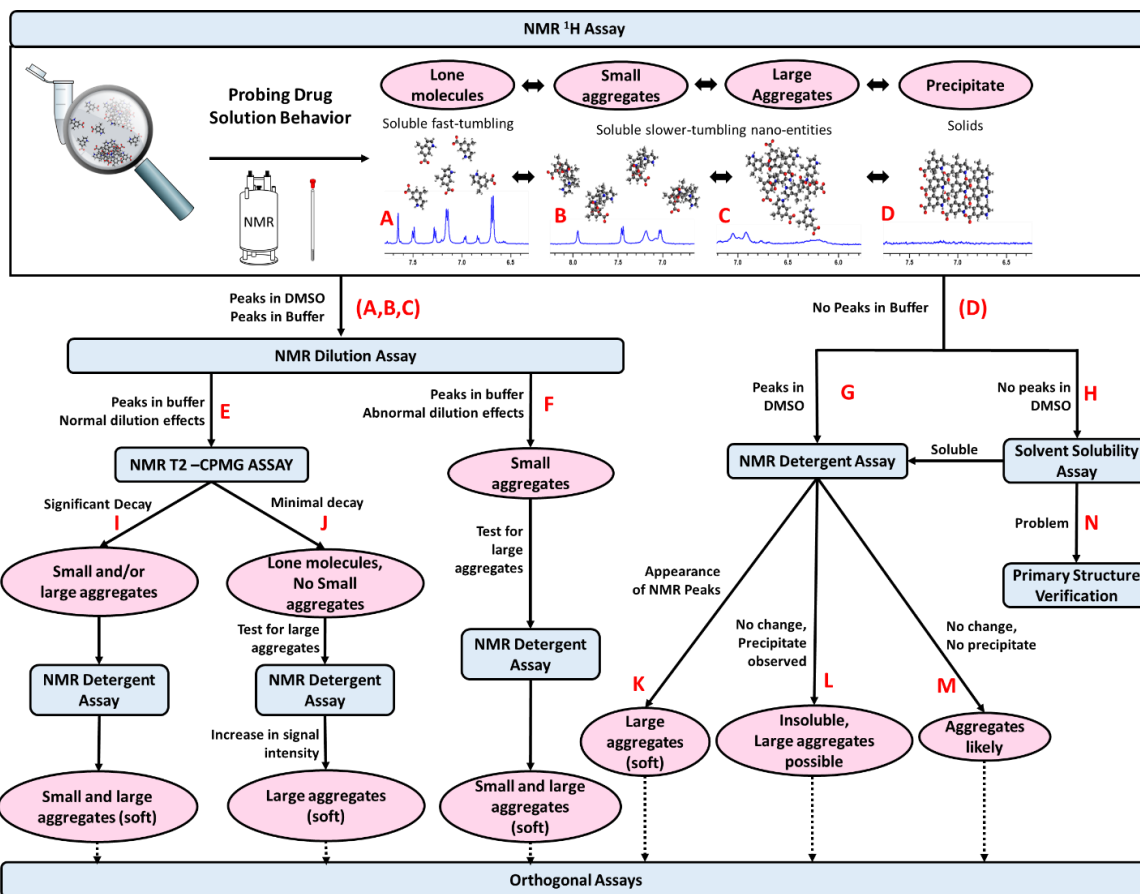


Fig. 6.3 | Overview of the protocol to probe drug solution behavior.

The protocol consists of the following parts to be used depending on each result: NMR 1 H assay, NMR dilution assay, NMR T2-CPMG assay, NMR detergent assay and orthogonal assays. The red lettering indicates possible scenarios along the various stages of the protocol, and further details regarding the interpretation are given in the main text.

Development of the protocol

The initial development of the protocol began in 1996 as a result of a simple observation. The corresponding author had dissolved a drug-like compound in PBS buffer at 200 μM and noted that the sample was clear (no precipitate); he then proceeded to take a 1 H NMR spectrum. To his surprise, there were no observable NMR resonances for the compound as it resembled the spectrum shown in Fig. 6.3d. Given that the subsequent 1 H NMR spectrum of the stock in DMSO- d_6 solvent confirmed the presence of the compound, the only reasonable conclusion was that the compound formed soluble self-associating aggregates that were very large in size in the buffer. Because there were no reports of this phenomenon at that time, further investigations were undertaken. Subsequent 1 H NMR spectra on this series of hepatitis C virus polymerase inhibitors showed diverse spectral observations that resembled the spectra A, B, C and D in Fig. 6.3, demonstrating that this series exhibited a wide range of aggregate types that varied depending on minor differences in primary structure (structure nanoentity

relationships)¹. Thus, in the process of undertaking this study, the first components of this protocol were developed.

Further additions to the procedure were introduced subsequently, and the whole procedure has been successfully applied to industry drug-discovery projects. We explored orthogonal methods routinely used in drug discovery such as DLS, diffusion ordered spectroscopy, nuclear Overhauser effect spectroscopy, etc.³⁵, testing their ability to enable characterization of aggregates. Only an ensemble of strategies was found to reliably detect the full range of nano-entity sizes and types^{7,8}. Concurrent to these efforts, literature reports described large drug colloidal aggregates visualized by using DLS as the main technology^{19,20}. As noted below, DLS has proven to be a valuable technique and is applied here as a useful orthogonal method that uses its advantages while addressing its limitations (*vide infra*). Over time, we developed and published the practical NMR-based methods (NMR 1 H assay, NMR dilution assay and NMR detergent assay)^{1,6,8}, which are amenable for routine use by non-specialists and medicinal chemists. These NMR-based methods also showed the presence of small aggregates for the first time in the context of drug discovery. More recently, we implemented a new aggregation assay based on the observation of relaxation in T2-CPMG experiments⁷, and we have incrementally improved parts of this NMR T2-CPMG assay (e.g., quantification) and exploited orthogonal assays (e.g., TEM, CLSM and DLS)^{3,6,8}.

The ensemble of tools mentioned above is already having an impact and revealing drug aggregates, but until the publication of this protocol, no clear 'best practices protocol' was available to guide scientists monitoring the solution behavior of their compounds. Thus, this protocol attempts to combine the details we and others have learned regarding nano-entities, to provide a protocol for best practice.

Application of the protocol

The procedure described here was designed to provide new users with a series of practical and efficient strategies to address their experimental problems. Users can use the protocol as is, in which case the NMR 1 H assay should be run first to qualitatively assess the predominant state adopted by the compound of interest. On the basis of results obtained, specific subsequent assays and pathways are suggested in Fig. 6.3 that enable more precise conclusions and quantifications to be obtained. The general nature of the protocol renders it amenable to many different applications along the drug-discovery pipeline. The protocol can easily be further adapted to address specific needs for various applications. For example, alternative buffers can be used in place of the phosphate buffer used in the current procedure if these are more relevant to any subsequent biological assays. However, a deviation from

phosphate buffer may require the use of deuterated buffer components for NMR assays. Individual assays can be run in place of the ensemble of assays shown in Fig. 6.3.

As another example, if a higher-throughput assay is required, for library curation or triaging of many hits from high-throughput or virtual screens, each assay can be modified. For the NMR ^1H assay, compounds can be screened in buffer only. Spectra of compounds in DMSO- d_6 can be run later if needed. For the NMR dilution assay, data can be acquired for samples only at 200- and 50- μM concentrations. Follow-up studies can then use the full set of dilution experiments for selected compounds. For the T2-CPMG assay, one could run only the 1- and 800-ms experiments. If relaxation rates are desired for selected compounds, follow-up experiments can use the full set of delays. For the NMR detergent assay, one could use only one detergent as an initial screen (e.g., Tween). Supplementary Table 2 gives guidance on procedure adaptations and timing for sample sets ranging from 1 to >50 compounds.

Other modifications could be made to better address the question at hand. For example, the NMR assays can be run at lower concentrations (e.g., compounds at 10 μM) if such concentrations are more relevant to other experiments (such as cell culture). Moreover, researchers who are working with optimized compounds that have more limited solubility may want to decrease the concentrations if the dilution range yields no signal. For this, an increase in the number of NMR scans would be recommended. Alternatively, higher millimolar concentrations may be used to mimic conditions in the stomach for orally administered drugs or as needed for X-ray crystallography studies. One could also run experiments in other pharmacologically relevant buffers¹, formulations and conditions (e.g., temperatures). One may also want to solely use orthogonal methods. For example, if screening only for the presence of large colloids, a DLS screen may be most appropriate.

Expertise needed to implement the protocol

The protocol described here was designed to enable non-experts to prepare samples, to acquire data and to make their own interpretations. The main focus is on the NMR ^1H assay, the NMR dilution assay, the NMR T2-CPMG assay and the NMR detergent assay, all of which can be easily performed by graduate students and even undergraduate students. NMR spectrometers are readily available in most graduate and undergraduate institutions. No special experimental NMR setup is required to acquire a water-suppressed ^1H spectrum; however, it should be possible to modify some parameters as described in Equipment setup. The T2-CPMG experimental parameters are often configured on most modern NMR spectrometers. If not, they can be easily implemented by an in-house NMR technician or the instrument manufacturer. The ERETIC method can also be implemented for concentration determination. NMR data processing can be done directly on the spectrometer or through

software that can be downloaded from the Bruker BioSpin website (<https://www.bruker.com/en/products-and-solutions/mr/nmr-software/topspin.html>).

Instruments required for the orthogonal assays (DLS, TEM and CLSM) can often be found at most graduate institutions. As with NMR, institutions that have these instruments often also have in-house technicians or users who can help with experimental setup and use.

6.3 Materials

Reagents

- Compounds of interest. We show results from valsartan (BETAPHARMA, cat. no. 56-02004), methylene blue (SIGMA ALDRICH, cat. no. E0516-50MG), candesartan cilexetil (BETAPHARM, cat. no. 56-05418) and lapatinib (Ontario Chemicals Inc, cat. no. L1034) as example data.

Required for the NMR Assays only

- Deuterated NMR solvents, including dimethyl sulfoxide-d₆ (DMSO-d₆) (Cambridge Isotope Laboratories, cat. no. DLM-10-10X1) & acetonitrile-d₃ (ACN-d₃) (CDN isotopes, cat. no. 2206-26-0)

CRITICAL Solvents should be handled under a fume hood

- Deuterium oxide (D₂O) (Cambridge Isotope Laboratories, cat. no. DLM-4-100)
- Tween 80 (Fisher Scientific, cat. no. BP338-500)
- Tween 20 (Fisher Scientific, cat. no. BP337-100)
- Nonidet P-40 (NP-40) (Roche, cat. no. 11754599001)
- Triton X-100 (Sigma-Aldrich, cat. no. 9002-93-1)
- Sodium Dodecyl Sulfate (SDS) (Sigma-Aldrich, cat. no. 151-21-3)
- 3-((3-cholamidopropyl) dimethylammonium)-1 propane sulfonate (CHAPS) detergent (Fisher Scientific, cat. no. PI28299)
- Milli-Q or HPLC grade water
- Sodium phosphate dibasic anhydrous (Fisher Scientific, cat. no. S374-500)
- Sodium phosphate monobasic anhydrous (Fisher Scientific, cat. no. BP329-500)
- Hydrochloric acid (HCl) (Sigma-Aldrich, cat. no. 7647-01-0)

CRITICAL Concentrated HCl should be handled under a fume hood

- Sodium hydroxide (NaOH) (Supelco, cat. no. 1310-73-2)
- Sodium Chloride (NaCl) (Wisent Bioproducts, cat. no. 600-082-WG)

Required for the TEM (SEM) Assay only

- Phosphotungstic acid (PTA) (MECALAB, cat. No. 4098)
- Milli-Q or HPLC grade water

- Sodium hydroxide solution (NaOH) 1N (Fischer Scientific, cat. No. SS2661)

Required for the CLSM Assay only

- DRAQ-5™ (Biostatus, cat. no. DR50200)
- Wheat Germ Agglutinin conjugate (WGA-555) (Invitrogen, cat. no. W32464)
- Glycerol (Wisent Bioproducts, cat. no. 800-040-LL)
- Paraformaldehyde (PFA) at 16% w/v (Fischer Scientific, cat. no. AA433689L)

CRITICAL PFA should be handled under a fume hood or in a well-ventilated area

- Media required to culture cells (we use DMEM (Dulbecco's Modified Eagle Medium) to culture RAW 264.7) (Gibco, cat. no. 11039-021)

CRITICAL The presence of serum in the medium may sequester aggregates in the medium, resulting in less fluorescence observed inside the cells.

- Cells of interest. We have used RAW 264.7 cells (macrophages) (Sigma Cat. no. 91062702, ECACC Cat# 91062702, RRID:CVCL_0493; https://scicrunch.org/resolver/RRID:CVCL_0493) but other cells could be used
CAUTION The cell lines used in your research should be regularly checked to ensure they are authentic and are not infected with mycoplasma.
- Phosphate Buffered Saline (PBS) (HyClone, GE Healthcare, cat. no. SH30256.01)
- Trypsin (Gibco, cat. no. 25200-056)

Equipment

Standard equipment required for all assays

- Recommended protective equipment: Lab coat, gloves and safety glasses

Required for the NMR Assays only

- 400 MHz NMR spectrometer or higher field (e.g. 600 MHz Bruker AV III NMR)
- Magnetic stir bar
- Beaker (500 mL or larger)
- Microcentrifuge tubes
- Laboratory micro-centrifuge
- NMR tubes (3 or 5 mm sizes)
- Pasteur pipettes
- Bulbs
- pH meter
- Magnetic stir plate

Required for the TEM Assay only

- Beaker (250 mL)
- Pasteur pipette
- Bulbs
- Magnetic stir plate
- TEM (a Hitachi H-7100 was used here)
- Parafilm
- Copper grid (200 mesh)

Required for the CLSM Assay only

- Confocal microscope (a Zeiss CLSM-780 confocal microscope was used here)
- 250 mL beaker
- Glass stirring rod
- Biological safety cabinet
- Cell culture flasks (e.g. 25cm²)
- Cell culture plate (24 wells)
- Microscope coverslips (Fisher Scientific, cat. no. 12-565-88)
- Microscope slide (Fisher Scientific, cat. no. 12-552)
- Vacuum
- 50 mL conical centrifuge tubes (Fisher Scientific, cat. no. 14-432-22)
- Task wipers
- Lab curved tweezer
- CO₂ incubator (Sanyo)

Required for the DLS Assay only

- Zetasizer Nano (or another instrument in the Zetasizer range) (Malvern Panalytical)
- Cuvettes (Fisherbrand)
- 0.22 µm filter (Millipore, cat. no. GSWP14250), 0.22 µm bottle-top filter 0.22 µm (Millipore, cat. no. SCGPS01RE) or 0.22 µm syringe filter (Fisher Scientific, cat. no. 09-719G)

Software

- NMR data processing software (e.g. Bruker's Topspin or MestReNova)
- DLS analysis software (e.g. Zetasizer Nano)
- Confocal analysis software (e.g. ZEN)
- TEM analysis software (e.g. AMT)

Reagent setup –

Preparation of sodium phosphate buffer (500 mL)

The sodium phosphate buffer is prepared as 50 mM phosphate and 100 mM NaCl at pH 7.4.

1. Place 400 mL of Milli-Q or HPLC water in a beaker along with a magnetic stir bar.
2. Add 2.68 g of sodium phosphate dibasic anhydrous, and 0.76 g of sodium phosphate monobasic anhydrous.
3. Add 10 mL of 5 M NaCl solution.
4. Add 50 mL of D₂O (to achieve 10% of D₂O for the total volume).
5. Adjust the pH to 7.4 using hydrochloric acid (HCl) or sodium hydroxide (NaOH) with the aid of a pH meter.
6. Add water to bring the volume to 500 mL.
7. Filter the solution with a 0.22 µm filter.
8. Store at -20°C for up to 1 month and monitor the pH before use.

CRITICAL Sodium phosphate dibasic heptahydrate and sodium phosphate monobasic monohydrate may be used, but the amounts must be modified to account for the difference in molecular weight.

Preparation of detergent at 10% (w/v) (1 mL)

Examples of detergents we have used are given in Supplementary Table 1.

1. Weigh 0.1 mg of detergent.
2. Add 1 mL of the sodium phosphate buffer made previously.
3. Store at room temperature (15-25°C) for up to 1 month, mix well before use.

Preparation of phosphotungstic acid (PTA) at 3% (w/v) (100 mL)

1. Weigh 3.0 g of phosphotungstic acid and add to a 250 mL beaker equipped with a magnetic stir bar.
2. Add 80 mL of Milli-Q or HPLC grade water.
3. Adjust the pH to 6.0 using a 1N sodium hydroxide (NaOH) solution (roughly 8 mL).
4. Add Milli-Q or HPLC grade water to bring the volume to 100 mL.
5. Store in a fridge (4°C) for up to 6 months.

Preparation of mounting media- Glycerol 70% (v/v) (1 mL)

1. Pipette 700 µL of glycerol in an Eppendorf tube.
2. Add 300 µL of the sodium phosphate buffer.
3. Shake well after closing the cap
4. Store at room temperature for up to a month.

Preparation of paraformaldehyde (PFA) 4 % (w/v) (25 mL)

1. Add 6.25 mL of Paraformaldehyde 16% (w/v) to a 50 mL falcon tube
2. Add 18.75 mL of sodium phosphate buffer to the tube and mix well.
3. Store at 4 °C for up to one month.
4. Before usage, let the 4 % (w/v) PFA solution warm to room temperature for at least 2 hours.

6.4 Equipment setup

NMR Assays

For the NMR ^1H Assay, NMR Dilution Assay and NMR Detergent Assay, NMR experiments can be run on a 400 MHz or higher field instrument. The spectra shown in the figures were run on a 600 MHz Bruker Avance III spectrometer equipped with a helium cryoprobe. A standard Bruker ^1H pulse sequence can be used. Here, we also used a water suppression sequence that employed excitation sculpting (zgesgp)³⁷. Spectra can be acquired with 32 scans for the NMR ^1H Assay and the NMR Detergent Assay, whereas 128 scans per spectrum are recommended for the NMR Dilution Assay. If one wishes to use quantification, then a relaxation delay of 10s should be used to ensure sufficient relaxation of the aromatic spins prior to subsequent scans to allow reasonably accurate measurement of the solution concentration.

For the NMR T2-CPMG Assay, the parameters used here are a modified version of the standard Bruker ^1H sequence with excitation sculpting (zgesgp) and the addition of a CPMG pulse train after the initial 90-deg excitation pulse. For the results shown here, the total duration of each spin echo was fixed to 1 msec whereas the number of echoes in the pulse train was varied according to the total time (T). The number of scans for all spectra was 4.

CRITICAL If one decides to prepare samples with buffer containing 90% H_2O and 10% D_2O , then ^1H experiments should employ water-suppression.

CRITICAL If the NMR spectrometer is equipped with a cooled (5-6°C) SampleJet sample changer, samples in DMSO-d_6 solvent will freeze (melting point for DMSO is $\sim 18^\circ\text{C}$) and the freeze-thaw cycle could have a negative effect on the NMR data obtained. In this case, it is possible to substitute DMSO-d_6 for a 50:50 mixture $\text{DMSO-d}_6:\text{ACN-d}_3$ (50:50) which has a lower freezing point as long as the compound has sufficient solubility in the mixed solvent.

Procedure

Preparation of a stock solution of a compound. Timing 12 min.

CRITICAL This section describes how to prepare compound stock solutions at a concentration of 20 mM in DMSO-d_6 .

1. Weigh between 0.3 and 0.6 mg of the compound and place it in a microcentrifuge tube.
2. Use the following formula to calculate the volume of DMSO-d₆ to be added:

$$DMSO \text{ volume (mL)} = \frac{\text{Exact mass weighed (mg)}}{MW \text{ of compound } \left(\frac{\text{mg}}{\text{mmol}}\right)} \cdot \frac{1 \times 10^6}{20 \text{ (mM)}}$$

3. Dissolve the compound with DMSO-d₆ in the microcentrifuge tube to give a 20 mM solution and mix. We recommend letting the DMSO stock sit at room temperature for at least 1-2 hours to allow better dissolution. If particles are still visible after that time, sonication can be used to improve dissolution.

PAUSE POINT: If compounds are sufficiently stable, DMSO stock can often be left to sit at room temperature in a closed tube for several hours or even a few days. We recommend freezing the stocks if the compounds are not going to be used during several days. If compound stability is limited, fresh stocks should ideally be prepared before each experiments.

NMR ¹H Assay. Timing 3 min (preparation)

CRITICAL: Note that use of differing brands of NMR tubes may require slightly different volumes (due to potential differences in glass thickness). Moreover, different types of NMR probes might require the use of additional volumes. The suggested values here represent a general rule of thumb which should work with most spectrometers. Ensure that the appropriate solution volume is used. In order to have sufficient volume for proper lock and shim we suggest using approximately 200 μL for 3 mm tubes, and 600 μL for 5 mm tubes. In the following protocols, the volumes required for 5 mm NMR tubes are shown in parentheses.

CRITICAL: This section of the procedure is summarized in Extended Data Figure 1.

4. Prepare 200 μM compound solutions in DMSO-d₆ and appropriate buffers as described in options A and B.

A. Assays in DMSO-d₆:

- i. Add 198 μL (594 μL) of DMSO-d₆ in a microcentrifuge tube.
- ii. Add 2 μL (6 μL) of 20 mM stock solution and mix.
- iii. Transfer into an NMR tube with a Pasteur pipette and analyse.

B. Assays in buffer:

- i. Add 198 μL (594 μL) of buffer in a microcentrifuge tube.
- ii. Add 2 μL (6 μL) of 20 mM stock solution and mix.
- iii. Transfer into an NMR tube with a Pasteur pipette and analyse.

TROUBLESHOOTING

NMR Dilution Assay Timing 27 min (preparation).

CRITICAL : If undertaking the fast-track dilution strategy (see the beige highlighted segments in Figure 6.4A), data acquisition is only performed on the 50 μM and 200 μM samples. Thus in place of this section, 50 (150) μL of the 200 μM sample can instead be diluted into 150 (450) μL buffer in order to get the 50 μM concentration point.

CRITICAL: This section of the procedure is summarized in Figure 6.4.

5. Add buffer into microcentrifugation tubes – 396 (1188) μL in a tube labelled #5 and 200 (600) μL in each of tubes labelled #1 to #4.
6. Add 4 (12) μL of the 20 mM stock solution to tube #5. This tube now becomes the 200 μM stock sample in buffer.
7. Prepare the remaining samples by serial dilution by transferring 200 (600) μL of the 200 μM stock sample in buffer to tube #4, and mixing well to produce the 100 μM sample.
8. Continue serial dilutions using 200 (600) μL from the previous sample to get 50, 25, and 12 μM samples.
9. Transfer each of the solutions from tubes #1 to #5 into separate NMR tubes and analyse.

TROUBLESHOOTING

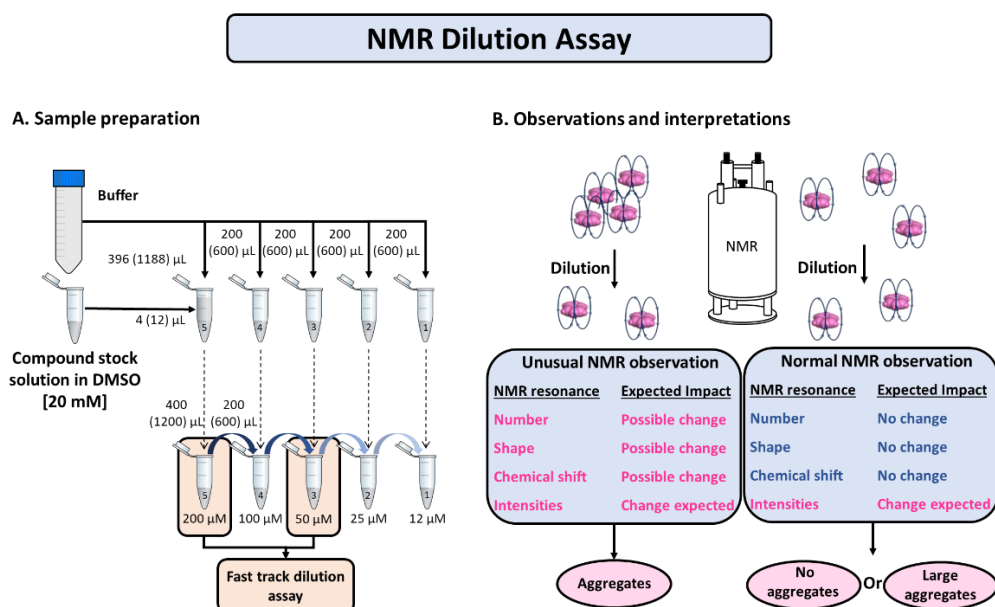


Fig. 6.4 | NMR dilution assay

a, Two options for preparation of the samples: the ensemble of samples for the full dilution assay and the shorter fast track strategy as highlighted in beige boxes. b, Interpretation of the results. Shown are volumes suggested for 3-mm NMR tubes, and volumes for 5-mm tubes are in parentheses.

NMR Detergent Assay Timing 30 min (preparation).

CRITICAL: This section of the procedure is summarized in Figure 6.5.

10. Prepare a stock solution of compound at 200 μM in buffer, allowing for 200 (600) μL for each detergent condition to be tested in addition to a control sample without detergent.
11. Place 200 μL (600 μL) in separate microcentrifuge tubes for each detergent.
12. Centrifuge at 400 g for 10 minutes.
13. Take the supernatant and add 3.2 (9.6) μL of detergent stock solution at 10% in 200 (600) μL of the solution. To the control tube, add 3.2 (9.6) μL of buffer to compensate the slight dilution from the addition of detergent.

CRITICAL STEP Different detergent concentrations can be used in order to cover ranges above and below their critical micelle concentration (CMC). The concentrations stated here serve as a practical starting point.

14. Transfer to NMR tubes and analyse.

TROUBLESHOOTING

CRITICAL STEP: Triton X-100, Nonidet P-40 and CHAPS have resonances in the aromatic region which may overlap with aromatic signals of the compound. If this is the case, one should analyze the signals which are not overlapping and/or change the detergent.

CRITICAL STEP: For aggregating compounds one would expect an increase in intensity or appearance of new peaks. For non-aggregating compounds one would expect no increased intensity or appearance of peaks however, it is possible to see a decrease/broadening of the signal as a result of compound interaction with the detergent.

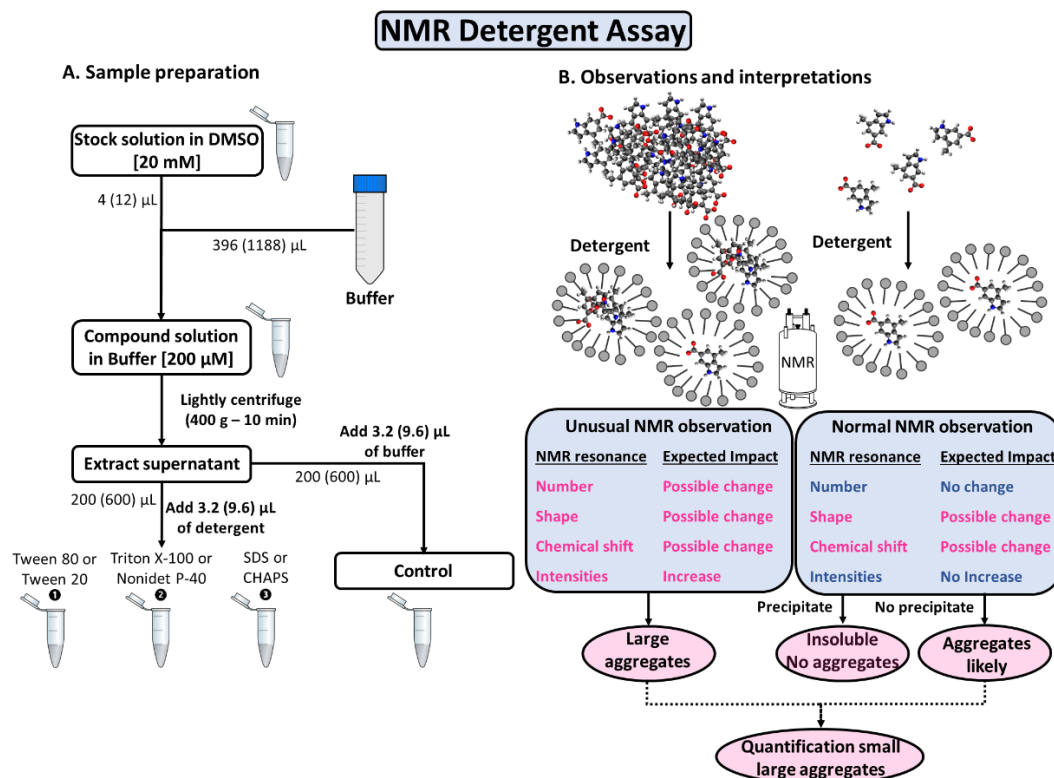


Fig. 6.5 | NMR detergent assay.

a, Preparation of the samples. b, Interpretation of the results. Shown are volumes suggested for 3-mm NMR tubes, and volumes for 5-mm tubes are in parentheses. CHAPS, 3-((3-cholamidopropyl) dimethylammonium)-1 propane sulfonate.

NMR T2-CPMG Assay Timing 15 min (preparation).

CRITICAL: If this experiment follows after the NMR ^1H Assay (step 4B), there is no need to reprepare the 200 μM sample. The 200 μM sample can be reused to run the T2-CPMG experiments. In this scenario, proceed direct to step 17.

CRITICAL: This section of the procedure is summarized in Extended Data Figure 2.

15. Prepare a solution with compound at 200 μM in buffer.
16. Transfer to an NMR tube.
17. Set up separate NMR T2-CPMG experiments with various delay times (1, 25, 50, 100, 200, 300, 500 and 800 ms) or under the fast-track strategy, acquire only two spectra with delay times of 1 and 800 ms.

Solvent Solubility Assay Timing 15-20 min.

CRITICAL: This section of the procedure is summarized in Extended Data Figure 3.

18. Prepare a series of samples of the compound at 200 μM in deuterated solvents (ACN- d_3 , chloroform- d , etc.).

CRITICAL STEP: The same stock of compound from step 3 can be used to prepare 200 μ M samples as described in step 4 instead of preparing a new stock.

CRITICAL: Some solvents may not be compatible with the use of plastic tubes for sample preparation. Glass vials may be more appropriate in such cases.

19. Transfer samples to NMR tubes and visually observe whether the compound appears to be soluble.

TROUBLESHOOTING

20. Acquire a regular 1D ^1H NMR spectrum of each sample.

NMR data analysis by TopSpin. Timing 30 min – 2 hours depending on the number of datasets.

CRITICAL There are many options in TopSpin for data processing. The steps given below constitute a practical workflow however, depending on the dataset, other autophasing algorithm may work better.

21. Load the appropriate data folder containing NMR data in the TopSpin software.
22. Add the first spectrum and process it by typing the following in the command line at the bottom of the graphics interface: lb 1; efp; apk; abs.
23. If the automatic phasing routine did not yield satisfactory results, adjust the spectrum phase as needed to achieve a straight baseline.
24. If the ERETIC method has been implemented on the NMR spectrometer, then use it to calculate the actual concentration of the compound in solvent or in buffer. To this end, integration of peaks in the aromatic region is usually simpler, but well-defined aliphatic resonances can also be used. However, aliphatic protons can exhibit relaxation time that could differ significantly from their aromatic counterparts. Therefore, the relaxation delays might require optimization to allow reliable estimation of concentration based on aliphatic resonances. In doubt, a longer delay can be used at the expense of longer acquisition time. Ensure that peaks chosen for quantitation are outside the chemical shift range affected by water suppression, if used.
25. In Integration mode, left-click on the desired integral to select the ERETIC command and calculate the observed concentration of the compound.

Orthogonal assays

CRITICAL: This section of the procedure is summarized in Extended Data Figure 4.

26. Further analyse compound behavior as appropriate by following options A, B and/or C to analyse by DLS, TEM and/or CLSM respectively.

A. DLS. Timing 30 – 50 min depending of the number of samples to be evaluated.

- i. Prepare a solution of the compound at a concentration of 200 μM in buffer (approximately 1 ml, although smaller volumes of cuvette exist).

CRITICAL STEP: It is recommended to filter the buffer before use with a 0.22 μm filter in order to reduce the contamination risks as small dust particles can significantly skew results. The solvent used to dissolve the compound should also ideally be filtered before use with a solvent compatible 0.02 μm filter. Preparation of samples under a laminar flow cabinet is also strongly suggested.

- ii. Centrifuge the sample tubes (400 g, 10 minutes).
- iii. Transfer the solution supernatant to a cuvette for DLS measurements.

CRITICAL: The use of compressed air duster is recommended to clear cuvettes of possible particles before use.

- iv. Use the Zetasizer software to perform the measurements, choosing the following parameters: Sample name, temperature, cuvette type and number of measurements (a minimum of 3 experiments is recommended).

TROUBLESHOOTING

- v. Place the cuvette in the Zetasizer Nano (or other DLS equipment employed).
- vi. Use the Zetasizer software (Malvern Analytical) to analyze the data.

CRITICAL STEP: Results can be viewed according to various functions. The Count Rate display allows monitoring of sample quality. The Correlation Function can be useful to identify potential problems with the sample. The default view is Intensity PSD (Particle Size Distribution) which is considered as the best choice for most scenarios. Additional information can be found in the instrument user manual.

B. TEM. Timing 1 – 4 hours depending of the number of samples to be analyzed.

- i. Prepare a sample of the compound with a concentration of 200 μM in buffer or media (as required for the function of the desired experiment).
- ii. Centrifuge at 400 g for 10 minutes at room temperature.
- iii. Deposit 100 μL (1 drop) of the compound supernatant solution on the parafilm.
- iv. Add the copper grid (200 mesh) on the drop and wait 5-10 minutes.

CRITICAL STEP: the shiny side of the grid must be appropriately placed in order to be facing the droplet (not the matte side).

- v. Remove the grid and place it on a drop of 3% PTA for 15 seconds.
- vi. Remove the grid and dry it with an absorbent paper.
- vii. Place the grid in the transmission electron microscope for analysis.

CRITICAL STEP: Higher concentrations of sample might be required to observe self-assemblies by TEM. However, bear in mind that, as discussed in the Introduction, the physical sizes of the aggregates may differ from those seen by DLS, CLSM and NMR so result will need to be interpreted with caution in such cases.

TROUBLESHOOTING

C. CLSM. Timing 2 – 3 days depending of the required incubation time.

CAUTION: Before starting determine whether the compound is fluorescent with a fluorometer or directly on the microscope by using the compound alone. Note the fluorescent wavelength. If compound is not fluorescent, CLSM cannot be used.

CRITICAL If cells are already growing in culture, in place of steps i-ii obtain a suspension of cells.

Cell thawing

- i. If required, remove cell vial (frozen at 1 million cells/vial) from the freezer and thaw cells in a water bath at 37°C. This usually takes less than a minute.

TROUBLESHOOTING

- ii. When the sample is thawed, transfer the cells to a centrifuge tube.
- iii. Centrifuge at 125 g for 7 minutes at room temperature.
- iv. Remove the supernatant.
- v. Add 5 mL of media and resuspend the cell pellet.
- vi. Transfer all of the cells and media to a 25 cm² flask.
- vii. Incubate at 37°C in an incubator with 5% CO₂ for 3 or 4 days, or until cells reach 80% confluency.

CRITICAL STEP, check for cell contamination and occasionally monitor the growth of the cells.

- viii. Make a stock solution with the compound at 20 mM in DMSO, as detailed in steps 1-3.

CRITICAL STEP: Although deuterated DMSO is not required for this assay, the same DMSO-d₆ stocks used for NMR assays can be used (from step 3).

- ix. From the stock solution, make a new 100 µM sample in medium (e.g. DMEM). Ensure sufficient 100 µM sample is made up; at least 500 µl is required for each well of a 24 well plate that requires compound treatment.

CRITICAL STEP: Bear in mind that if DMEM with phenol red is used, fluorescence from the additive may overlap/interfere with any produced by the compound. It is therefore recommended to use DMEM without phenol red.

Cell seeding

- x. When the cells reach 80% confluency, remove the old medium and wash with sterile PBS (use 2 mL if using a 25 cm² flask).
- xi. Remove the PBS solution.
- xii. Add trypsin (use 1 mL if using a 25 cm² flask) and put the flask in an incubator at 37°C with 5% of CO₂ for a duration of 5 to 10 minutes.

CRITICAL STEP, after 5 minutes, check to see if the cells started to detach. If so, proceed to the next step.

- xiii. Centrifuge the cell suspension at 800g for 7 minutes. Discard the supernatant.
- xiv. Add media (use 4 mL if using a 25 cm² flask) and resuspend the cells.
- xv. Count the cells and then dilute them in order to obtain 600,000 cells/well (1.2 million cells/ml) and 500 µL per well.
- xvi. Add one glass coverslip on the bottom of each well to be used in a 24 well plate.
- xvii. Add 500 µL of the cell stock to each well and put these plates in the incubator at 37°C with 5% of CO₂ overnight.

Cell treatment

- xviii. The next day, if the cells are growing well, remove the old medium. CRITICAL STEP Cells can alternatively be left for longer before proceeding with treatment.
- xix. Wash cells with PBS.
- xx. Add 500 µL of the compound solution (at 100 µM in medium).

CRITICAL STEP: Compound concentrations used for other techniques may not directly transpose to CLSM as they can result in higher cell toxicity. Testing a range of concentrations might be required depending on the molecules tested.

- xxi. Put the plate in an incubator for the desired incubation time (e.g. 2, 3, 4 hours or more)

Staining and fixation

- xxii. Remove the old media and wash cells with PBS.
- xxiii. Add 300 µL of membrane stain (WGA 555) at a concentration of 3.33 µg/ml and wait 5 minutes.
- xxiv. Remove the membrane stain solution and wash cells once with PBS.
- xxv. Add 350 µL of the fixative PFA at 4% and wait another 10 minutes.
- xxvi. Remove PFA and wash cells twice with PBS.
- xxvii. Add 300 µL of the nucleus stain (DRAQ-5) and wait 15 minutes.
- xxviii. Remove the staining solution and add 1 ml of PBS.
- xxix. Add one drop of mounting media (glycerol at 70-90%) on the slide.

- xxx. Remove the coverslip from the well and dry it on the absorbent paper.
- xxxi. Put the coverslip on the slide with mounting medium on the appropriate side (cells should be between the slide and coverslip, with the mounting medium).
- xxxii. Let dry for 5-10 minutes under a ventilated hood.
- xxxiii. Visualize under a confocal microscope.

TROUBLESHOOTING

Table 6.2 | Troubleshooting

Step	Problem	Possible reason	Possible solution
4Biii (NMR ¹ H Assay – Sample preparation in buffer)	Precipitate formation	Insolubility of the compound	Use of the supernatant following centrifugation at 400 g for 10 minutes. If this is done, any observable precipitate should be noted
9 (NMR Dilution Assay – NMR spectra)	No signal or weak signals for samples used in the fast-track method	Solubility is too low	Run the NMR Dilution Assay using lower concentrations
14 (NMR Detergent Assay – Addition of detergent to the samples)	Compound forms a suspension	Centrifugation speed too low or duration is not long enough	Increase the time and/or speed of the centrifugation Note any observations
19 (Solvent Solubility Assay - Compound dissolution in solvent)	Precipitate formation	Insolubility of the compound	Centrifugation at 400 g for 10 minutes. If this isn't enough, increase the time and/or speed
26 Avi (DLS Assay)	Failure of measurement	Incompatible sample (color, polydispersity)	Trying a different laser color (if your instrumentation allows it) may help circumvent problems with colored samples. Reducing sample concentration might help reduce polydispersity, although results might not directly

			compare with techniques that used different concentrations.
26Avi (DLS Assay – Data analysis)	Inconclusive results	Inappropriate sample preparation	Wash the cuvette with alcohol and dry with pressurized air canister to remove any contaminants Try using different compound concentrations
26 Bvii (TEM Assay – Micrograph observation)	Nothing observable in TEM micrograph	Low concentration or precipitate	Try different compound concentrations. Some compounds have distinct aggregation behavior that vary with concentration, depending on the type of buffer, temperature, detergents, etc.
26 Cxxxiii (CLSM Assay – Visualisation under the microscope)	No coloration or insufficient fixation	Incubation time with the stains or fixative was too short or too low concentration of the reagents	Increase the incubation time or increase the concentration of the stains
26 Cxxxiii (CLSM Assay – Visualisation under the microscope)	No aggregates observables	Addition of foetal bovine serum (FBS) may sequester some or all aggregates, leading to no fluorescence being observed inside the cells (false-negatives)	Use culture medium without FBS

6.5 Anticipated results

To date, we have used this procedure (in whole or in part) to monitor the solution behavior of thousands of compounds in both confidential projects and some published papers^{1,6-8,11}. Here, we show four examples of results we have obtained that demonstrate the type of data acquired, how it can be displayed and how to interpret the results obtained. We also

include further examples of results we have obtained in Supplementary Figures 1-6. Full details of all compounds used are given in Supplementary Table 3.

In the first example we evaluated the solution behavior of valsartan. Sharp NMR resonances were observed by NMR ^1H Assay for valsartan in the spectra acquired in buffer and DMSO- d_6 at 200 μM nominal concentration (Fig 6.6A). Also, all samples were clear with no precipitate upon visual inspection, confirming that valsartan is soluble in both solvents.

Furthermore, upon dilution in buffer from 200 μM to 12 μM , normal trends were seen (i.e. Fig. 6.6A - decreases in intensity with no changes peak shapes or chemical shifts). These observations were consistent with the behavior of lone tumbling molecules with no self-association tendencies. These conclusions were corroborated by data from the NMR T2-CPMG Assay (Fig. 6.6B) where the resonance intensities were minimally affected upon comparison of the resonances of the spectra employing 1 ms versus 800 ms (small resonance intensity decay < 50%). Furthermore, no significant increases in resonance intensities or appearance of new peaks were noted upon addition of detergents in the NMR Detergent Assay (Fig. 6.6C), supporting the conclusion that no large aggregates exist.

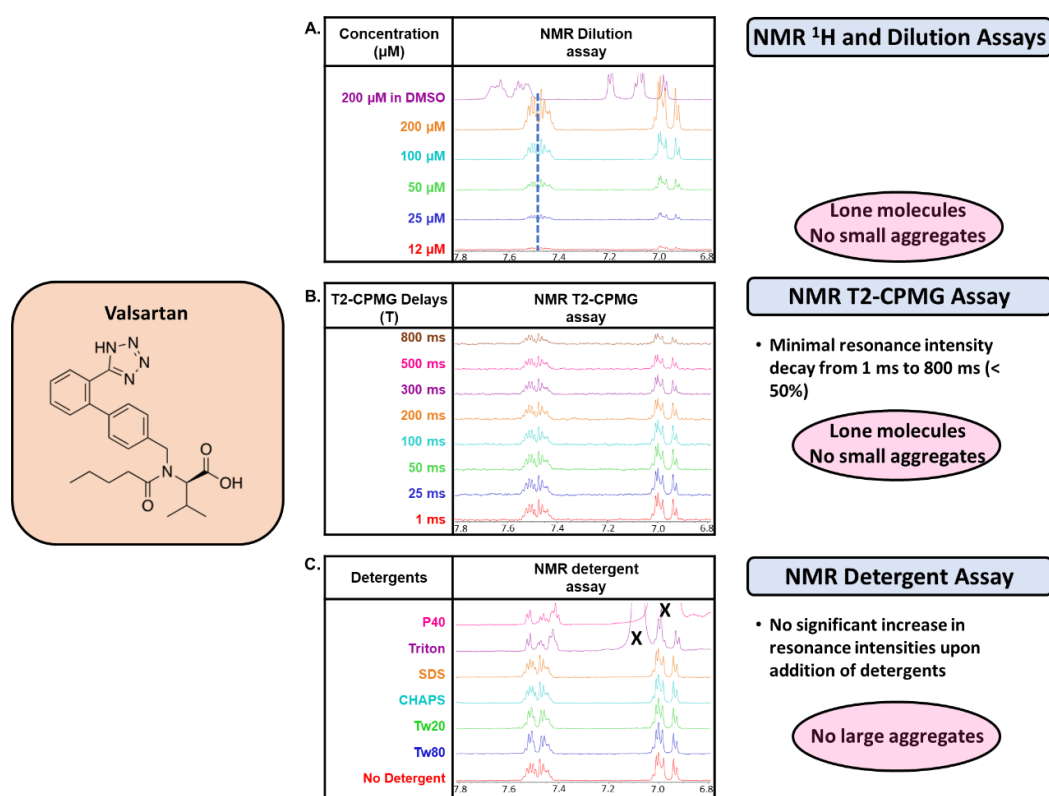


Fig. 6.6 | Probing the solution behavior of valsartan.

a–c, Shown are NMR data from the NMR ^1H and dilution assays (a), the T2-CPMG assay (b) and the NMR detergent assay (c). The chemical structure is shown on the left. The 'X's in c denote resonances that arise from the detergent and not from the compound. Tw20, Tween 20; Tw80, Tween 80.

In the second example we evaluated the solution behavior of methylene blue. NMR resonances are observed for methylene blue in both buffer and DMSO- d_6 by NMR 1H Assay (Fig. 6.7A). Also, the samples were blue and clear with no precipitate upon visual inspection, confirming that methylene blue was soluble in both conditions. However, upon dilution in buffer from 200 μM to 12 μM , abnormal trends were seen. Indeed, concentration-dependent changes in chemical shifts are observable, consistent with the behavior of self-association into small aggregates. These conclusions were corroborated by data from the NMR T2-CPMG Assay (Fig. 6.7B) where the resonance intensities were appreciably different between the resonances of the spectra employing 1 ms versus 800 ms delays (major resonance intensity decay > 75%). Interestingly, no significant increases in resonance intensities were noted upon addition of detergents in the NMR Detergent Assay (Fig. 6.7C) suggesting that no large aggregates exist. Thus, methylene blue likely self-associates into small aggregates and not into large aggregates.

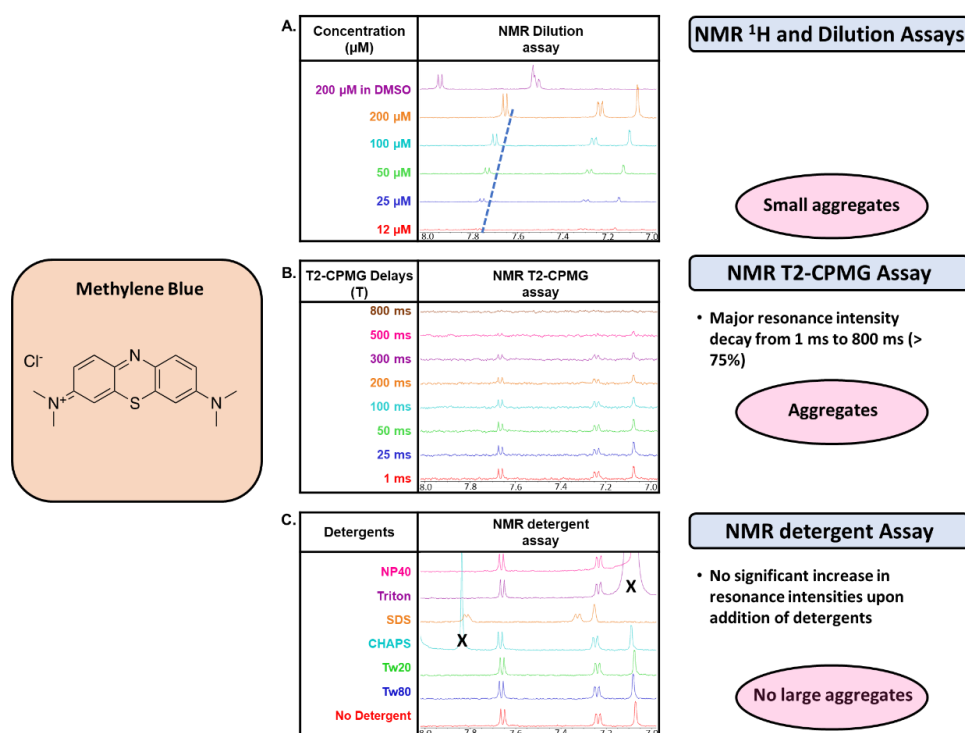


Fig. 6.7 | Probing the solution behavior of methylene blue.

a–c, Shown are NMR data from the NMR 1H and dilution assays (a), the T2-CPMG assay (b) and the NMR detergent assay (c). The chemical structure is shown on the left. The 'X's in c denote resonances that arise from the detergent and not from the compound.

In the third example we evaluated candesartan cilexetil (referred to here as candesartan). NMR resonances are present for the DMSO- d_6 sample, but non-existent in buffer by NMR 1H Assay (Fig. 6.8A). Also, the samples were clear and neither turbid nor had

precipitate upon visual inspection, which confirms that candesartan is soluble in both conditions. Furthermore, upon dilution in buffer from 200 μM to 12 μM , no resonances were noted (Fig. 6.8A) and no cloudiness nor precipitate were notable. The absence of resonances obviously lead to no resonances being observed in the NMR T2-CPMG Assay (Fig. 6.8B). Taken together, these observations were consistent with the lack of lone tumbling molecules and small aggregates, and suggestive of the presence of large aggregates. Interestingly, significant increases in resonance intensities were noted upon addition of detergents in the NMR Detergent Assay (Fig. 6.8C) demonstrating that candesartan exists as large soft-aggregates in buffer that can be disrupted by the addition of detergents.

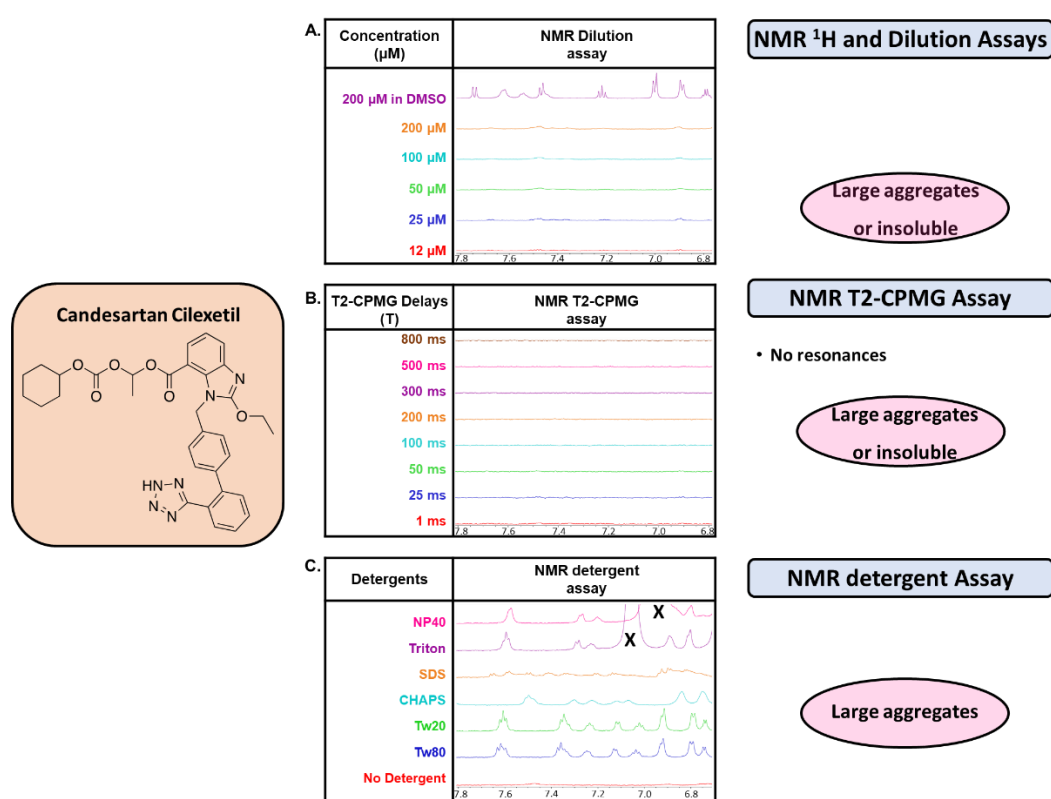


Fig. 6.8 | Probing the solution behavior of candesartan cilexetil.

a–c, Shown are NMR data from the NMR ^1H and dilution assays (a), the T2-CPMG assay (b) and the NMR detergent assay (c). The chemical structure is shown on the left. The 'X's in c denote resonances that arise from the detergent and not from the compound.

In the fourth example we evaluated the solution behavior of lapatinib, showing unexpected trends. NMR resonances were observed for lapatinib in DMSO- d_6 at 200 μM nominal concentration but not in buffer by NMR ^1H Assay (Fig. 6.9A). The buffer samples were slightly opaque with some precipitate upon visual inspection. No resonances appeared when the compound was diluted in buffer from 200 μM to 12 μM (Fig. 6.9A) and no resonances were

seen in the NMR T2-CPMG Assay (Fig. 6.9B). These observations are consistent with a lack of lone molecules or small aggregates and suggests that the compound is either partially insoluble or that it forms large aggregates. To our surprise, no significant increases in resonance intensities were noted upon addition of detergents in the NMR Detergent Assay (Fig. 6.9C) (The peak appearing at 8.3 ppm is one of an impurity). Given these observations, it could not be confirmed whether the lack of resonances is due to the compound being partially insoluble or large, hard aggregates were being formed in the solution. We thus proceeded to further orthogonal methods to confirm the solution behaviors.

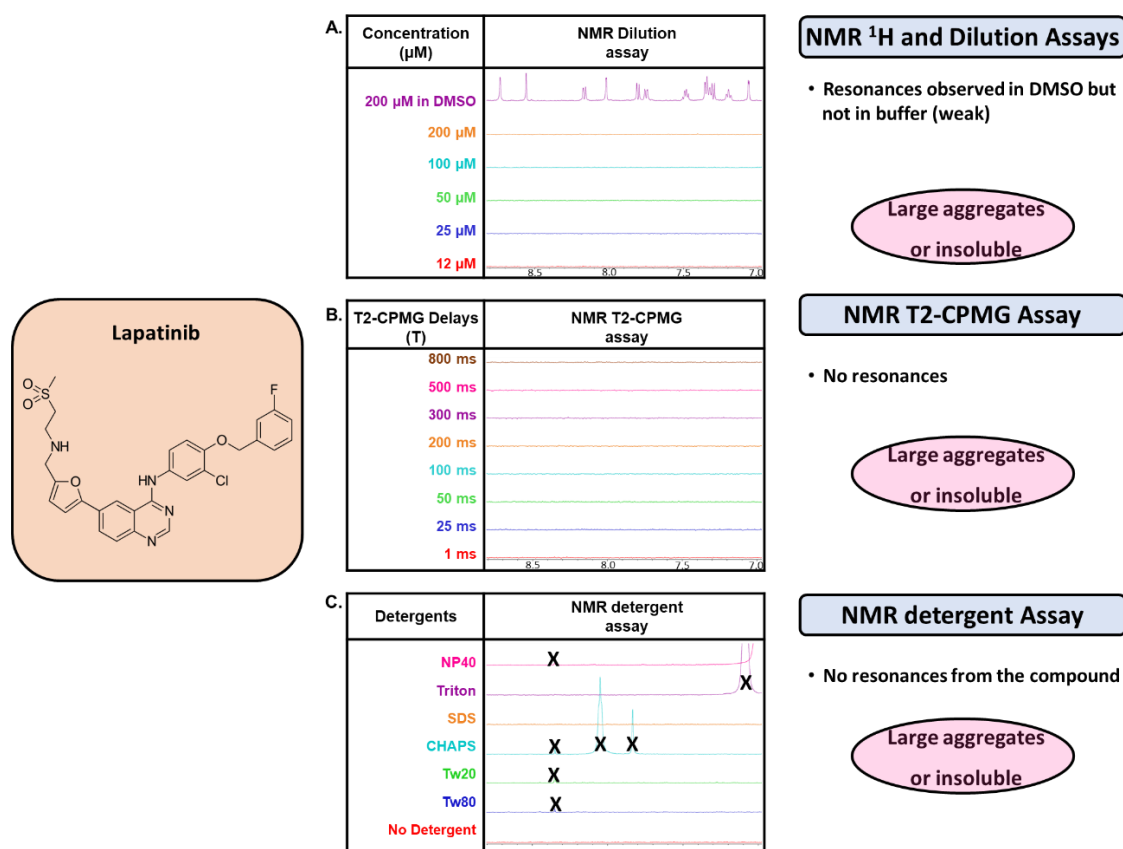


Fig. 6.9 | Probing the solution behavior of lapatinib.

a–c, Shown are NMR data from the NMR ¹H and dilution assays (a), the T2-CPMG assay (b) and the NMR detergent assay (c). The chemical structure is shown on the left. The 'X's in c denote resonances that arise from the detergent or impurities and not from the compound.

Large aggregates were seen by CLSM (Fig. 6.10A) and TEM (Fig. 6.10B) and further confirmed using DLS (Fig. 6.10C). It is however intriguing that addition of Tween 80 lead to a loss of detection of lapatinib aggregates by DLS (Fig. 6.10C), suggesting breaking of the entity, but no signal was observed by NMR in the presence of detergent. Due to the use of a shared high-throughput sample handler (SampleJet) on the NMR, sample acquisition can sometimes only be done several hours after sample submission. Therefore, it is possible that lapatinib aggregates precipitate out of solution over time. Visual precipitate was observable upon

sample preparation and storage in a refrigerated NMR SampleJet such as was used here could also have accelerated sample precipitation.

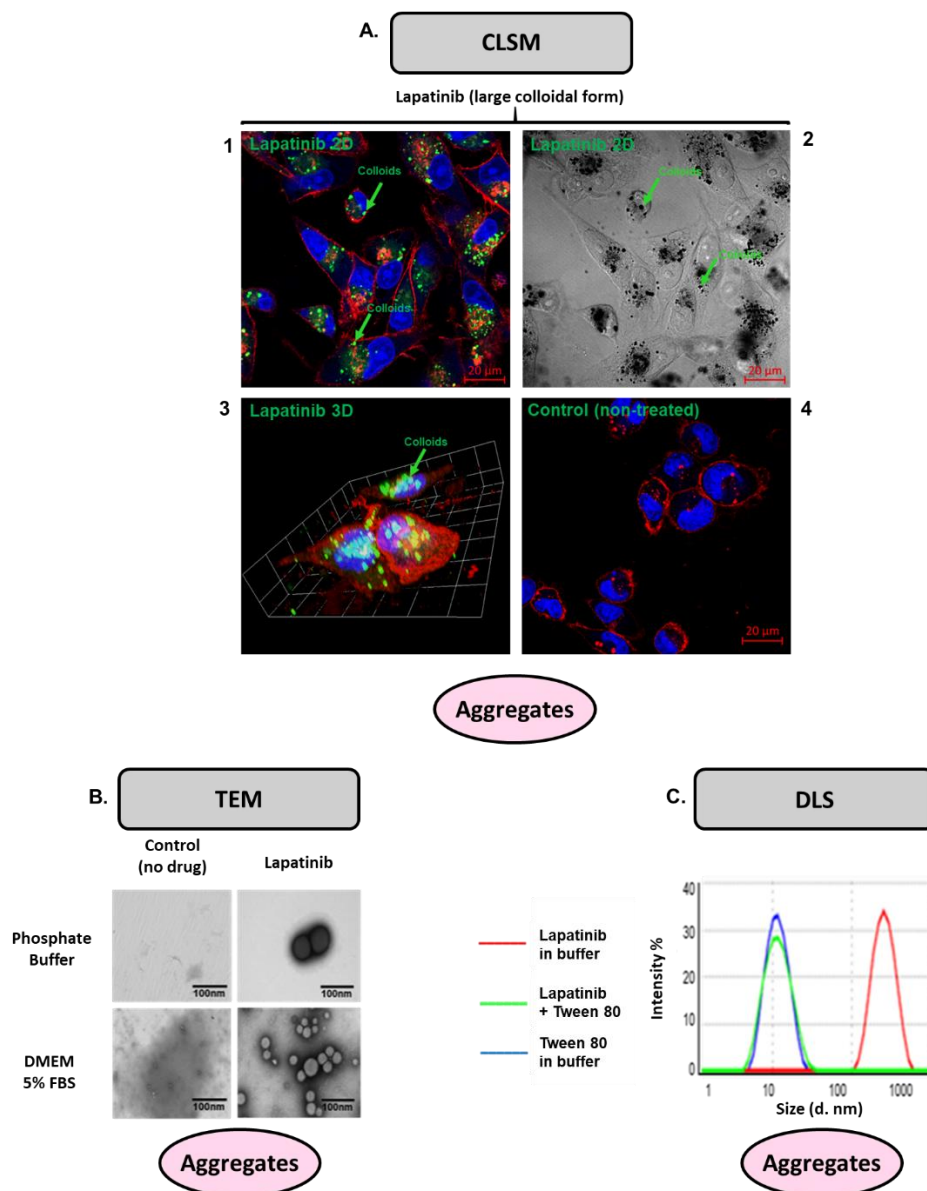


Fig. 6.10 | Probing the solution behavior of lapatinib by using orthogonal techniques.

a–c, Shown are data from the orthogonal methods CLSM (100 μM) (a), TEM (50 μM) (b) and DLS (200 μM) (c). a, CLSM images of lapatinib in Raw 264.7 cells. The aggregates are in green (fluorescence of compound), the membrane of the cells in red (WGA 555 staining) and the nucleus in blue (DRAQ-5 staining). The three primary images show the aggregates in cells in 2D (with fluorescence (1) and without fluorescence (2)) and 3D (3). The last picture (4), shows the cells without compound (control). The 3D picture (3) is a zoom on one cell. b, TEM images of lapatinib in phosphate buffer and DMEM with 5% (vol/vol) FBS and its controls. c, Lapatinib at 200 μM in sodium phosphate buffer in the presence and absence of 0.025% (vol/vol) Tween 80 for 24 h. The size of lapatinib aggregates can be different between TEM (b) and DLS (c), possibly because of dehydration of the sample during the preparation for the observation with the TEM or the differences in concentrations used. d.nm, diameter values in nanometers.

The examples above highlight that no one technique can detect all the types of aggregates that exist, thus a combination of strategies is necessary as proposed in this protocol. One of the examples demonstrates that no single methods can expose the full range of nano-entities that exist, highlighting the importance of using coordinated orthogonal strategies. We hypothesise that there are distinct attributes of aggregates that can be further identified and anticipate that further attributes such as these will have distinct properties that merit revealing and exploitation. We hope that the wide use of this protocol along with future improved versions will advance knowledge of the largely unexplored world of drug nano-entities. We suspect that there are many types of nano-entities that exist which have a variety of sizes and architectures, and that these will be correlated with properties that can potentially be exploited, for example, for drug delivery, anti-aggregates, cell penetrators, bioavailability enhancers, etc.

Data Availability

The NMR data that supports figures 6-9 and supplementary figures 1-5 are available in figshare (<https://doi.org/10.6084/m9.figshare.15019755.v1>).

6.6 REFERENCES

1. LaPlante, S. R. *et al.* Monitoring drug self-aggregation and potential for promiscuity in off-target in vitro pharmacology screens by a practical nmr strategy. *Journal of Medicinal Chemistry* **56**, 7073–7083 (2013).
2. Duan, D. *et al.* Internal structure and preferential protein binding of colloidal aggregates. *ACS Chemical Biology* **12**, 282–290 (2017).
3. Feng, B. Y. & Shoichet, B. K. A detergent-based assay for the detection of promiscuous inhibitors. *Nature Protocols* **1**, 550–553 (2006).
4. Feng, B. Y. *et al.* A high-throughput screen for aggregation-based inhibition in a large compound library. *Journal of Medicinal Chemistry* **50**, 2385–2390 (2007).
5. Owen, S. C., Doak, A. K., Wassam, P., Shoichet, M. S. & Shoichet, B. K. Colloidal Aggregation Affects the Efficacy of Anticancer Drugs in Cell Culture. (2012) doi:10.1021/cb300189b.
6. Dlim, M. M., Shahout, F. S., Khabir, M. K., Labonté, P. P. & Laplante, S. R. Revealing Drug Self-Associations into Nano-Entities. *ACS Omega* **4**, 8919–8925 (2019).
7. Ayotte, Y. *et al.* Exposing Small-Molecule Nanoentities by a Nuclear Magnetic Resonance Relaxation Assay. *Journal of Medicinal Chemistry* **62**, (2019).
8. LaPlante, S. R. *et al.* Compound aggregation in drug discovery: Implementing a practical NMR assay for medicinal chemists. *Journal of Medicinal Chemistry* **56**, 5142–5150 (2013).
9. Beaulieu, P. L. *et al.* Multi-parameter optimization of aza-follow-ups to BI 207524, a thumb pocket 1 HCV NS5B polymerase inhibitor. Part 2: Impact of lipophilicity on promiscuity and in vivo toxicity. *Bioorganic & Medicinal Chemistry Letters* **25**, 1140–1145 (2015).
10. Owen, S. C. *et al.* Colloidal drug formulations can explain ‘bell-shaped’ concentration-response curves. *ACS Chemical Biology* **9**, 777–784 (2014).
11. Beaulieu, P. L. *et al.* Multi-parameter optimization of aza-follow-ups to BI 207524, a thumb pocket 1 HCV NS5B polymerase inhibitor. Part 2: Impact of lipophilicity on promiscuity and in vivo toxicity. *Bioorganic and Medicinal Chemistry Letters* **25**, 1140–1145 (2015).
12. Tres, F., Posada, M. M., Hall, S. D., Mohutsky, M. A. & Taylor, L. S. The Effect of Promiscuous Aggregation on in Vitro Drug Metabolism Assays. *Pharmaceutical Research* **36**, 1–9 (2019).
13. Ganesh, A. N. *et al.* Colloidal Drug Aggregate Stability in High Serum Conditions and Pharmacokinetic Consequence. *ACS Chemical Biology* **14**, 751–757 (2019).

14. Frenkel, Y. V. *et al.* Concentration and pH dependent aggregation of hydrophobic drug molecules and relevance to oral bioavailability. *Journal of Medicinal Chemistry* **48**, 1974–1983 (2005).
15. Frenkel, Y. V., Gallicchio, E., Das, K., Levy, R. M. & Arnold, E. Molecular dynamics study of non-nucleoside reverse transcriptase inhibitor 4-[[4-[[4-[(E)-2-cyanoethenyl]-2,6-dimethylphenyl]amino]-2-pyrimidinyl]amino] benzonitrile (TMC278/rilpivirine) aggregates: Correlation between amphiphilic properties of the drug and oral bioavailability. *Journal of Medicinal Chemistry* **52**, 5896–5905 (2009).
16. Ganesh, A. N., Donders, E. N., Shoichet, B. K. & Shoichet, M. S. Colloidal Aggregation: From Screening nuisance to formulation nuance. *Nano Today* **19**, 188–200 (2018).
17. Hoo, C. M., Starostin, N., West, P. & Mecartney, M. L. A comparison of atomic force microscopy (AFM) and dynamic light scattering (DLS) methods to characterize nanoparticle size distributions. *Journal of Nanoparticle Research* **10**, 89–96 (2008).
18. Tomaszewska, E. *et al.* Detection limits of DLS and UV-Vis spectroscopy in characterization of polydisperse nanoparticles colloids. *Journal of Nanomaterials* **2013**, (2013). <https://doi.org/10.1155/2013/313081>
19. Akoka, S., Barantin, L. & Trierweiler, M. Concentration measurement by proton NMR using the ERETIC method. *Analytical Chemistry* **71**, 2554–2557 (1999).
20. Seidler, J., McGovern, S. L., Doman, T. N. & Shoichet, B. K. Identification and prediction of promiscuous aggregating inhibitors among known drugs. *Journal of Medicinal Chemistry* **46**, 4477–4486 (2003).
21. Doak, A. K., Wille, H., Prusiner, S. B. & Shoichet, B. K. Colloid formation by drugs in simulated intestinal fluid. *Journal of Medicinal Chemistry* **53**, 4259–4265 (2010).
22. Hassan, P. A., Rana, S. & Verma, G. Making sense of Brownian motion: Colloid characterization by dynamic light scattering. *Langmuir* **31**, 3–12 (2015).
23. Ganesh, A. N., McLaughlin, C. K., Duan, D., Shoichet, B. K. & Shoichet, M. S. A New Spin on Antibody-Drug Conjugates: Trastuzumab-Fulvestrant Colloidal Drug Aggregates Target HER2-Positive Cells. *ACS Applied Materials and Interfaces* **9**, 12195–12202 (2017).
24. Wiest, J. *et al.* Geometrical and Structural Dynamics of Imatinib within Biorelevant Colloids. *Molecular Pharmaceutics* **15**, 4470–4480 (2018).
25. Hong, Y., Lam, J. W. Y. & Tang, B. Z. Aggregation-induced emission. *Chemical Society Reviews* **40**, 5361–5388 (2011).

26. Hong, Y., Lam, J. W. Y. & Tang, B. Z. Aggregation-induced emission: Phenomenon, mechanism and applications. *Chemical Communications* 4332–4353 (2009) doi:10.1039/b904665h.
27. Kestens, V., Bozatzidis, V., De Temmerman, P. J., Ramaye, Y. & Roebben, G. Validation of a particle tracking analysis method for the size determination of nano- and microparticles. *Journal of Nanoparticle Research* **19**, (2017). <https://doi.org/10.1007/s11051-017-3966-8>
28. Bevan, C. D. & Lloyd, R. S. A high-throughput screening method for the determination of aqueous drug solubility using laser nephelometry in microtiter plates. *Analytical Chemistry* **72**, 1781–1787 (2000).
29. Vom, A. *et al.* Detection and Prevention of Aggregation-based False Positives in STD-NMR-based Fragment Screening. *Australian Journal of Chemistry* **66**, 1518 (2013).
30. Boulton, S. *et al.* Mechanisms of Specific versus Nonspecific Interactions of Aggregation-Prone Inhibitors and Attenuators. *Journal of Medicinal Chemistry* **62**, 5063–5079 (2019).
31. Yang, Z. Y. *et al.* Structural Analysis and Identification of Colloidal Aggregators in Drug Discovery. *Journal of Chemical Information and Modeling* **59**, 3714–3726 (2019).
32. Irwin, J. J. *et al.* An Aggregation Advisor for Ligand Discovery. *Journal of Medicinal Chemistry* **58**, 7076–7087 (2015).
33. Meiboom, S. & Gill, D. Modified spin-echo method for measuring nuclear relaxation times. *Review of Scientific Instruments* **29**, 688–691 (1958).
34. Ryan, A. J., Gray, N. M., Lowe, P. N. & Chung, C. W. Effect of detergent on ‘promiscuous’ inhibitors. *Journal of Medicinal Chemistry* **46**, 3448–3451 (2003).
35. Feng, B. Y., Shelat, A., Doman, T. N., Guy, R. K. & Shoichet, B. K. High-throughput assays for promiscuous inhibitors. *NATURE CHEMICAL BIOLOGY* **1**, (2005). <https://doi.org/10.1038/nchembio718>
36. Pellecchia, M., Sem, D. S. & Wüthrich, K. NMR in drug discovery. *Nature Reviews Drug Discovery* **1**, 211–219 (2002).
37. Hwang J., T. L. and S. Water suppression that works. *Journal of Magnetic Resonance Series A* vol. 112 275–279 (1995).

Acknowledgements

We thank the following agencies for helping fund this research - NSERC (Natural Sciences and Engineering Research Council of Canada), CQDM (Quebec Consortium for Drug Discovery), CFI (Canada Foundation for Innovation), Mitacs, INRS (Institut national de la recherche scientifique), Institut Pasteur, la région Auvergne-Rhône-Alpes, le ministère de l'enseignement supérieur et de la recherche (France) and NMX Research and Solutions Inc. We also thank our colleagues for their help, suggestions and encouragement – P. Bouchard, N. Girard, D. Bendahan, D. Girard, J. Tremblay and A. Nakamura.

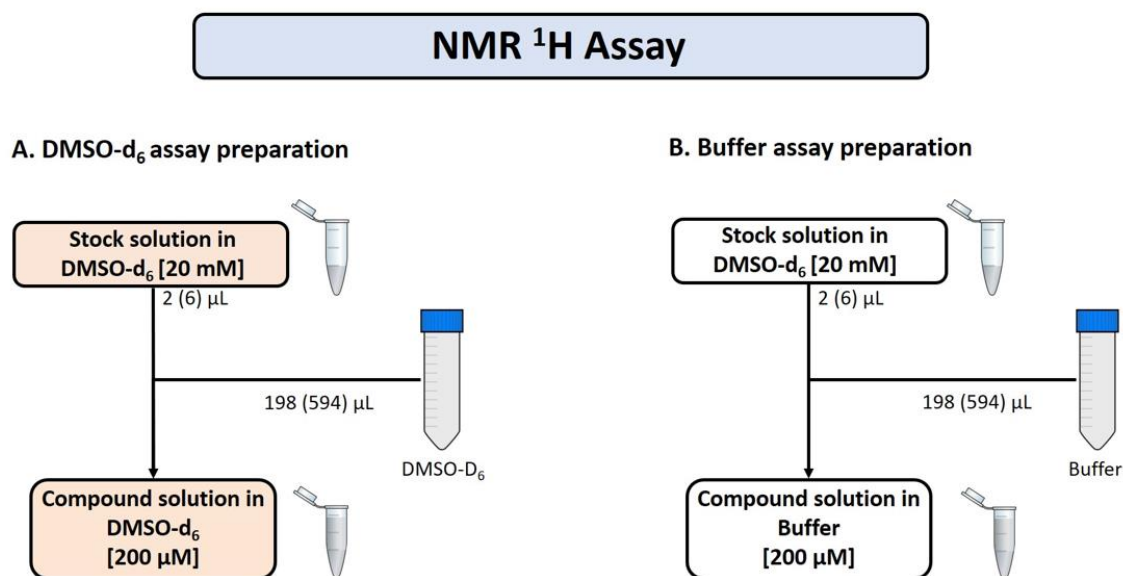
Supplementary information

Further data are available as Supplementary Information.

Data Availability Statement

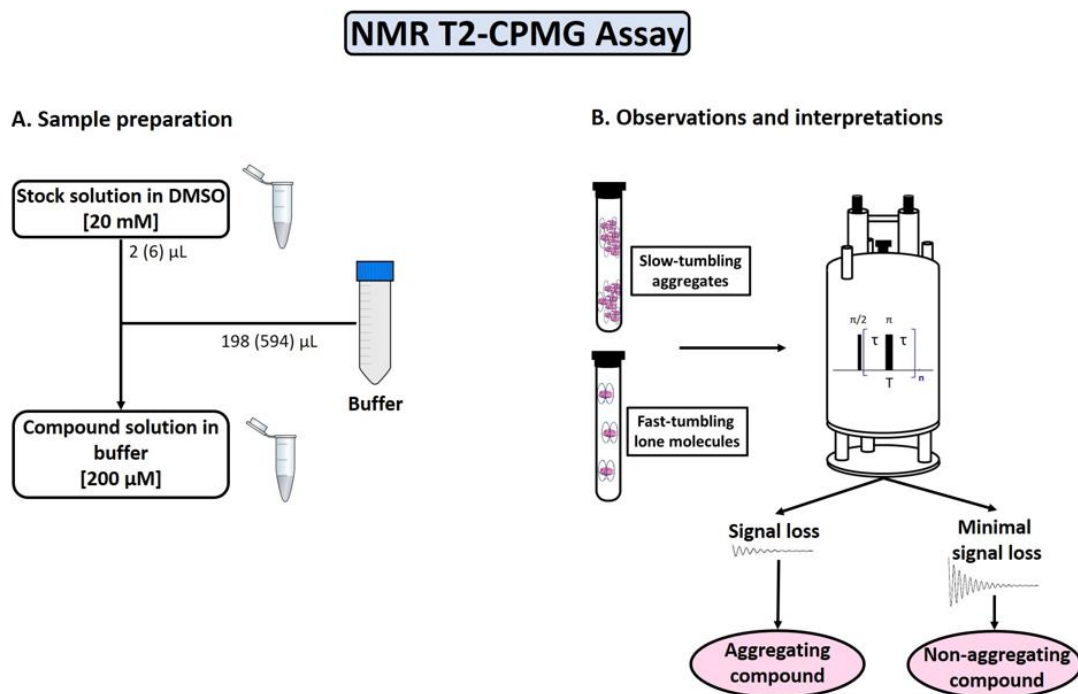
The NMR data that supports figures 6-9 and supplementary figures 1-5 are available in figshare (<https://doi.org/10.6084/m9.figshare.15019755.v1>).

6.7 EXTENDED DATA



Extended Data Fig. 1 | NMR ^1H assay.

a, Preparation for assay in DMSO- d_6 . b, Preparation for assay in buffer. Shown are volumes suggested for 3-mm NMR tubes, and volumes for 5-mm tubes are in parentheses.

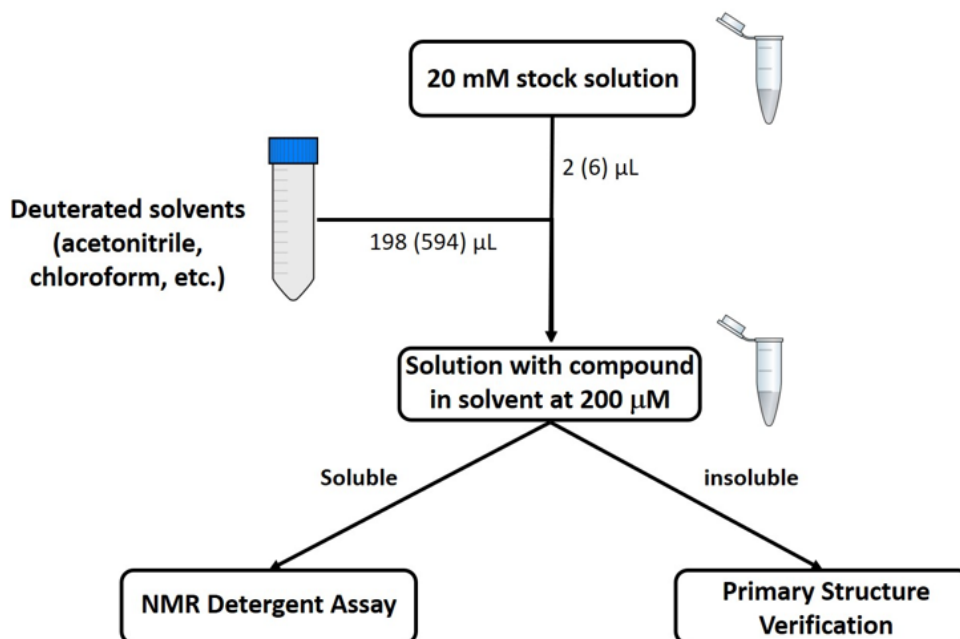


Extended Data Fig. 2 | NMR T2-CPMG assay

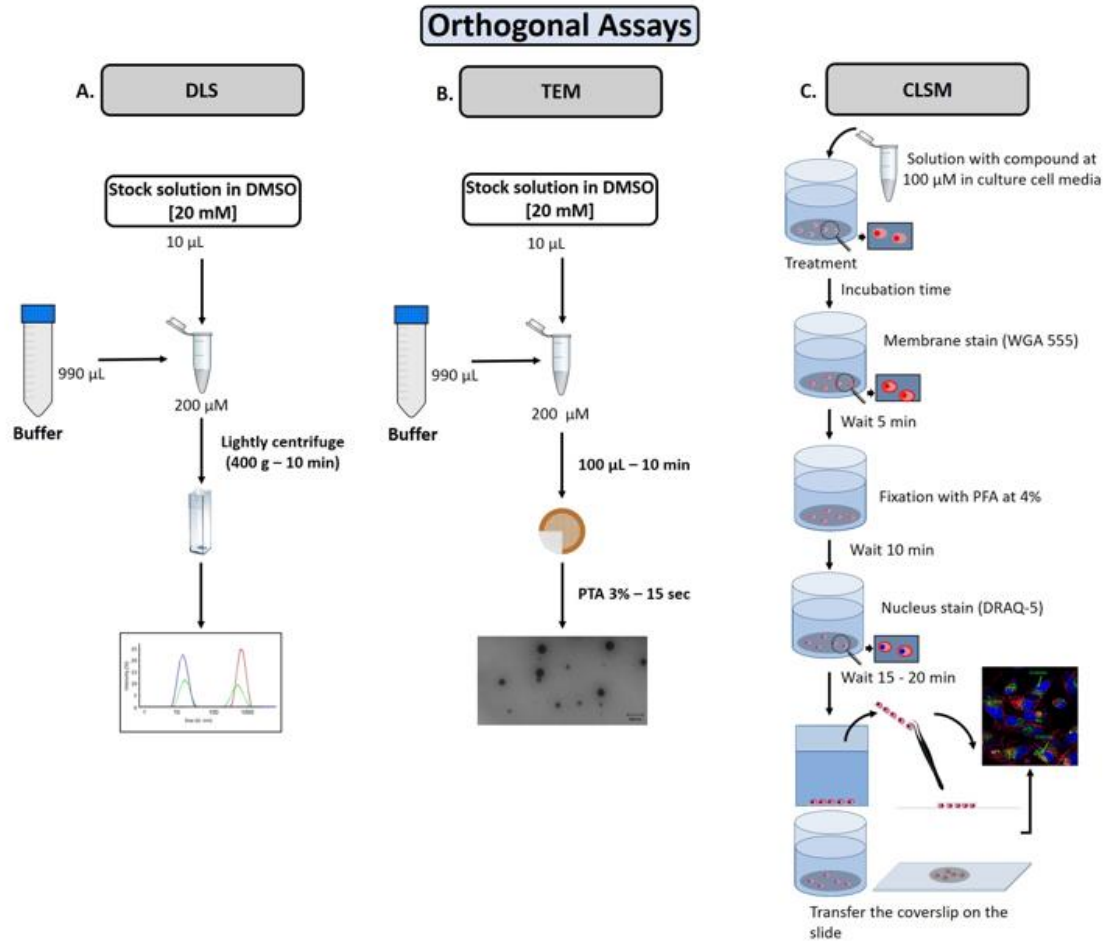
a, Preparation of the sample. b, Interpretation of the results.

Solvent Solubility Assay

Sample preparation and interpretations



Extended Data Fig. 3 | Solvent solubility assay. Preparation of the sample and interpretations.



Extended Data Fig. 4 | Orthogonal assays
a–c, Preparation of the samples for DLS (a), TEM (b) and CLSM (c)

6.8 SUPPLEMENTARY INFORMATION

Table of contents:

Supplementary Figure 1. Probing the solution behavior of etodolac

Supplementary Figure 2. Probing the solution behavior of riluzole

Supplementary Figure 3. Probing the solution behavior of imatinib

Supplementary Figure 4. Probing the solution behavior of lansoprazole

Supplementary Figure 5. Probing the solution behavior of pranlukast

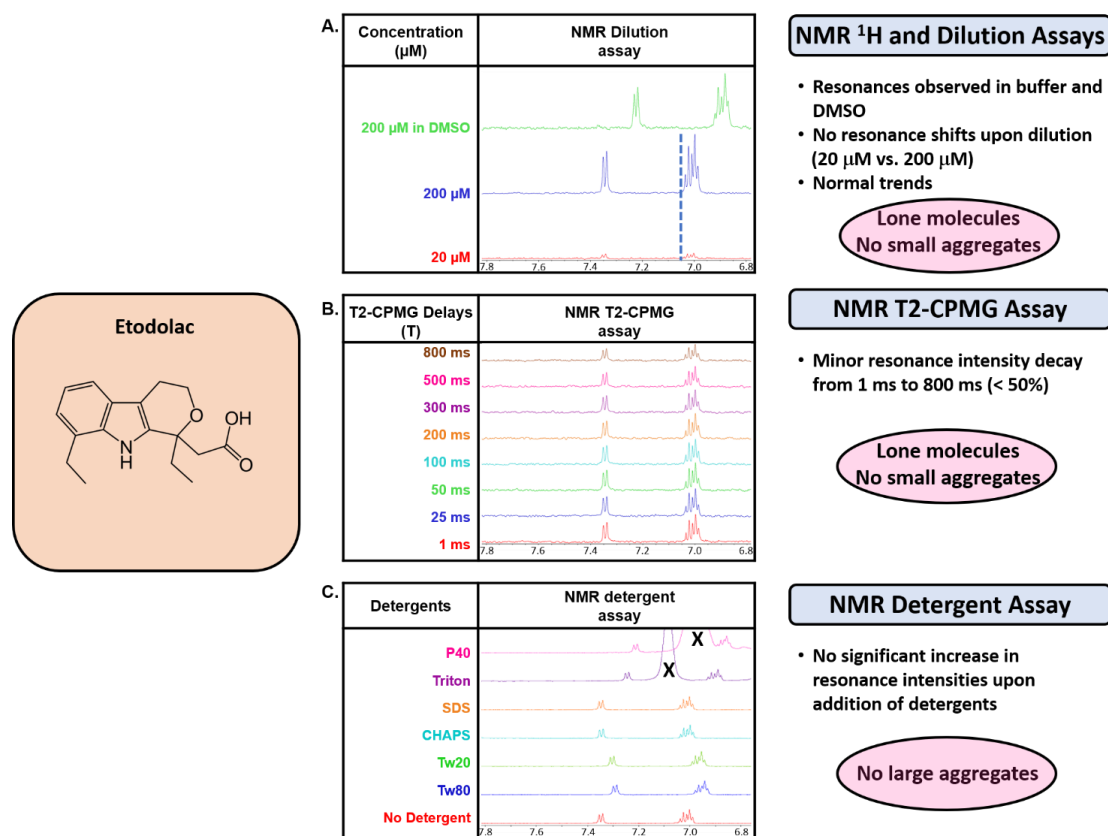
Supplementary Figure 6. Example of a possible DMSO aggregator

Supplementary Table 1. Detergents properties

Supplementary Table 2. Experimental guidelines for various sample set sizes

Supplementary Table 3. Compounds information

Probing the solution behavior of etodolac

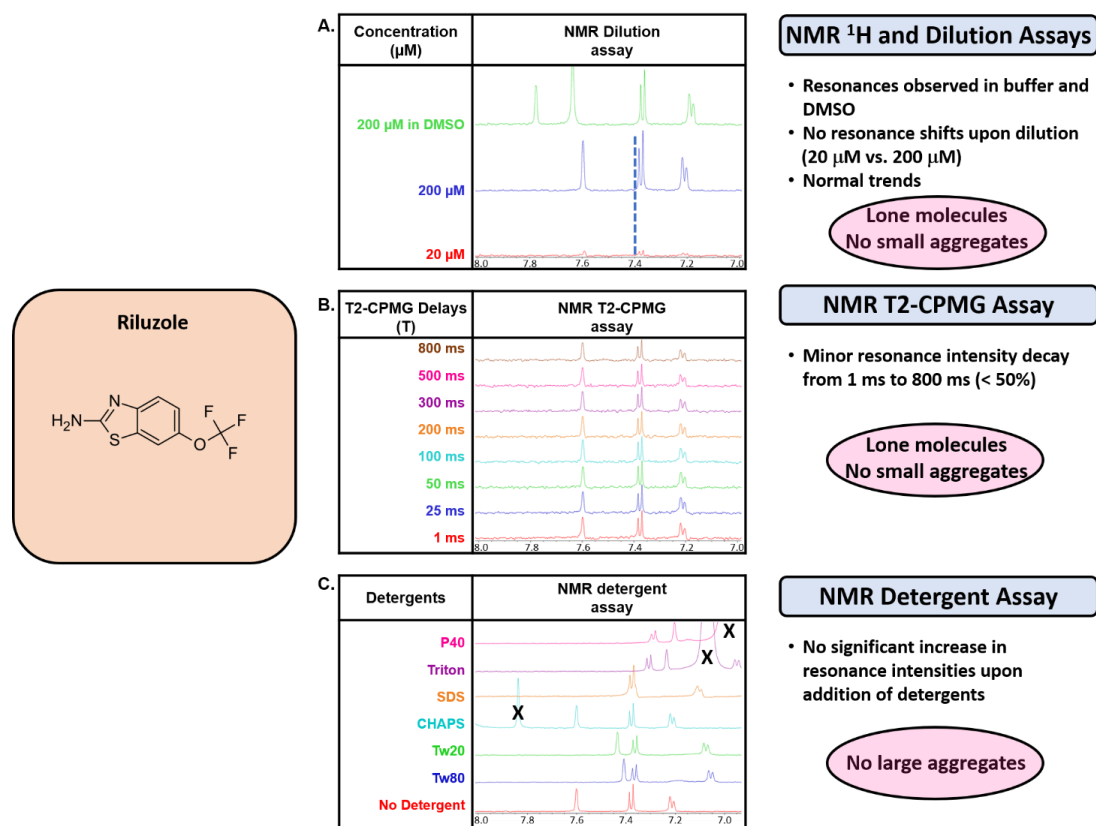


Supplementary Figure 1 | Probing the solution behavior of etodolac

Shown are NMR data from, (A) the NMR ¹H and Dilution Assays, (B) the T2-CPMG Assay, and (C) The NMR Detergent Assay. The chemical structure is shown on the left. “x” in (C) denote resonances that arise from the detergent and not from the compound.

The NMR ¹H Assay for etodolac in Supplementary Figure 1A resulted in observable resonances in both buffer and DMSO-d₆ at 200 μM nominal concentration. Also, the samples were clear with no precipitate upon visual inspection, confirming that etodolac was soluble in both solvents. Furthermore, upon dilution in buffer from 200 μM to 20 μM, normal trends were notable (i.e. Supplementary Figure 1A - decreases in signal intensity with no change in chemical shifts). These observations were consistent with a behavior of lone tumbling molecules with no self-association tendencies. These conclusions were corroborated by data from the NMR T2-CPMG Assay (Supplementary Figure 1B) where the resonance intensities were minimally affected upon comparison of the resonances of the spectra employing delay times of 1 ms versus 800 ms (minor resonance intensity decay < 50%). Additionally, no significant increases in resonance intensities were noted upon addition of detergents in the NMR Detergent Assay (Supplementary Figure 1C) reporting that no large aggregates exist. The same finding can be observed with riluzole (Supplementary Figure 2). None of these two drugs exhibit evidence of aggregation at these concentrations.

Probing the solution behavior of riluzole

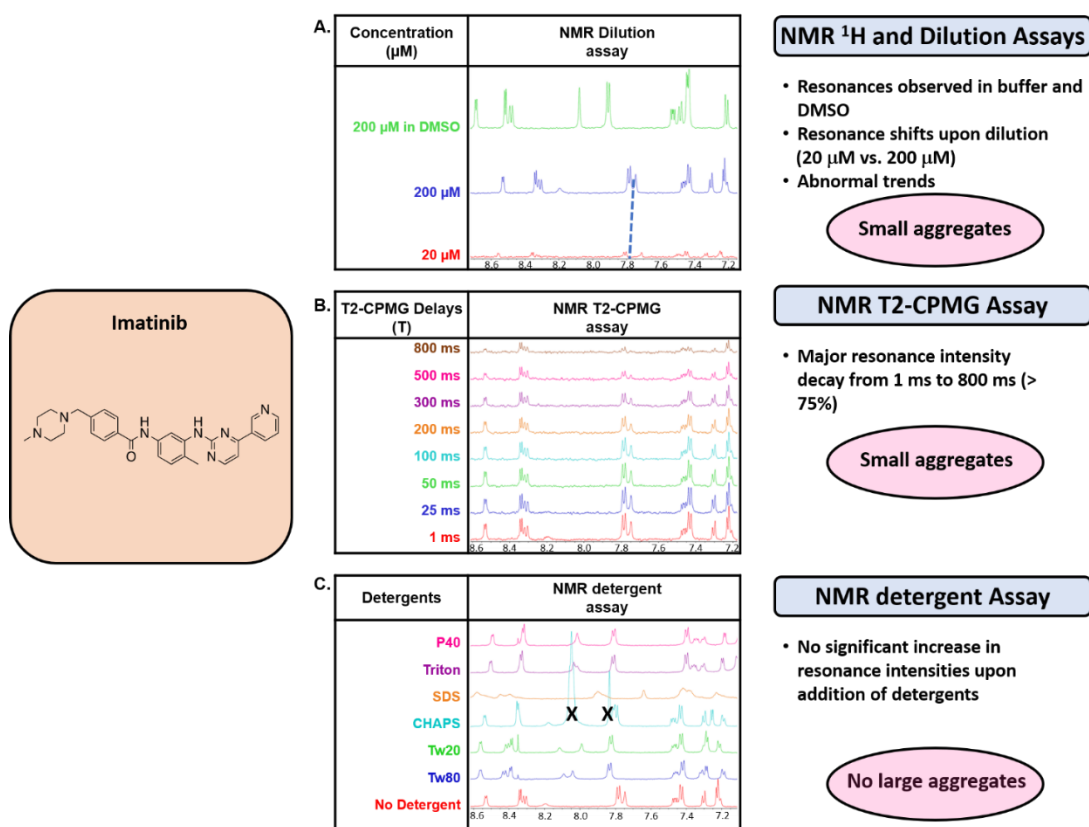


Supplementary Figure 2 | Probing the solution behavior of riluzole

Shown are NMR data from, (A) the NMR ¹H and Dilution Assays, (B) the T2-CPMG Assay, and (C) The NMR Detergent Assay. The chemical structure is shown on the left. “x” in (C) denote resonances that arise from the detergent and not from the compound.

Probing the solution behavior of imatinib

NMR resonances were observed for imatinib in the NMR ¹H Assay acquired in buffer and DMSO-d₆ at 200 μM nominal concentration (Supplementary Figure 3A). Again, the samples were clear with no precipitate upon visual inspection. Dilution in buffer from 200 μM to 20 μM results in observation of abnormal trends (i.e. Supplementary Figure 3A - decreases in intensity along with changes in chemical shifts). This would be consistent with a behavior of self-association into small aggregates. The NMR T2-CPMG Assay (Supplementary Figure 3B) supports these conclusions as resonance intensities were significantly reduced after 800 ms (intensity decay > 75%). Interestingly, no significant increases in resonance intensities were noted upon addition of detergents in the NMR Detergent Assay (Supplementary Figure 3C) reporting that no large aggregates exist. Thus, the data suggests that imatinib self-associates into small aggregates and not into large aggregates.

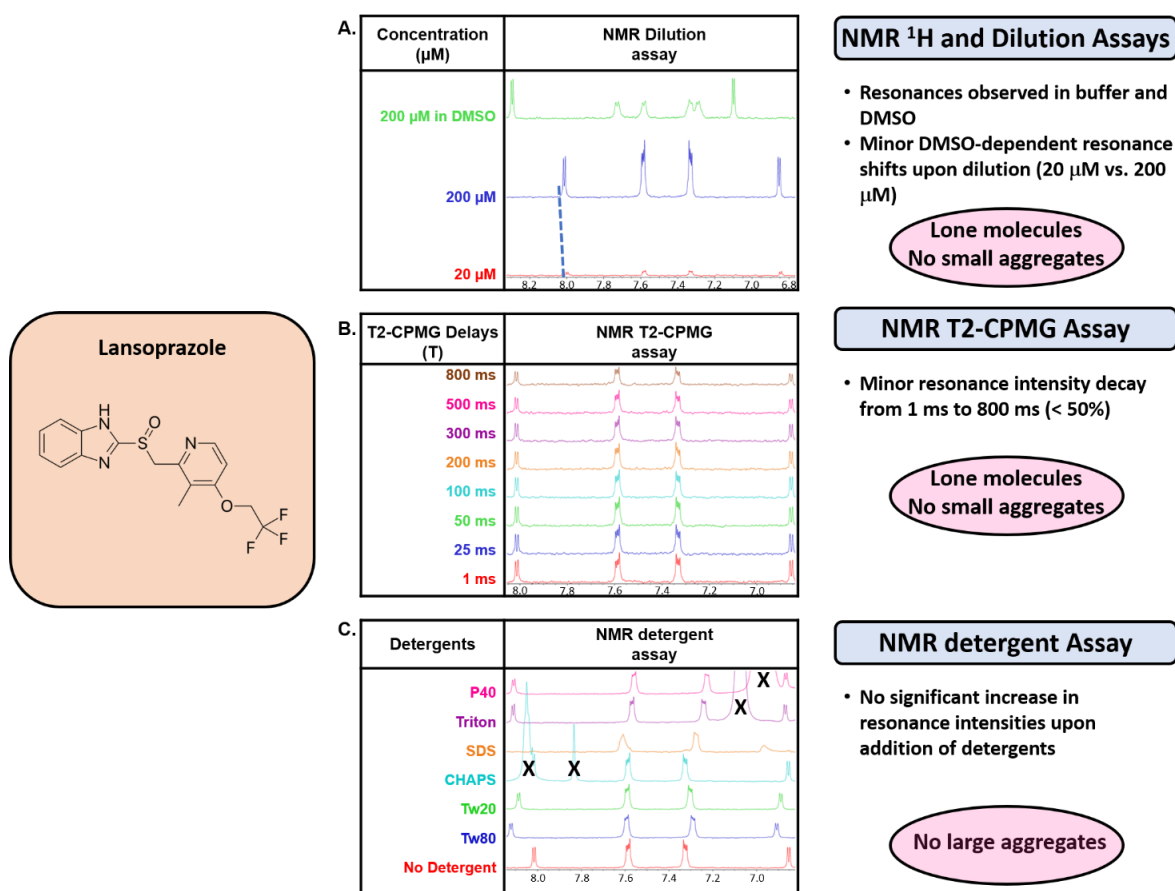


Supplementary Figure 3 | Probing the solution behavior of imatinib.

Shown are NMR data from, (A) the NMR ¹H and Dilution Assays, (B) the T2-CPMG Assay, and (C) The NMR Detergent Assay. The chemical structure is shown on the left. “x” in (C) denote resonances that arise from the detergent and not from the compound.

Probing the solution behavior of lansoprazole

Here is a particular example where caution must be taken upon interpretation of the data. T2-CPMG and detergent assays of lansoprazole do not suggest any aggregation phenomenon. However, upon looking at the dilution assay, small changes in chemical shifts can be observed for some resonances upon dilution from 200 to 20 μM. For the sake of simplicity and speed, the dilution assay involves diluting the samples while also diluting the amount of DMSO at the same time. Therefore, some cases as this one may arise where observed shift can be attributed to such variation in DMSO concentration. Retesting of lansoprazole dilutions with constant amount of DMSO results in no observable changes in chemical shifts (data not shown). The fact that only some lansoprazole resonances would shift upon dilution can be an indication that care must be taken with interpretation. It is likely that some hydrogens are more sensitive to the changes in chemical environment caused by this variation in DMSO. Although, it is conceivable that some aggregates could also preferentially induce changes in chemical shifts for specific resonances. This highlights the importance of looking at the data as a whole.

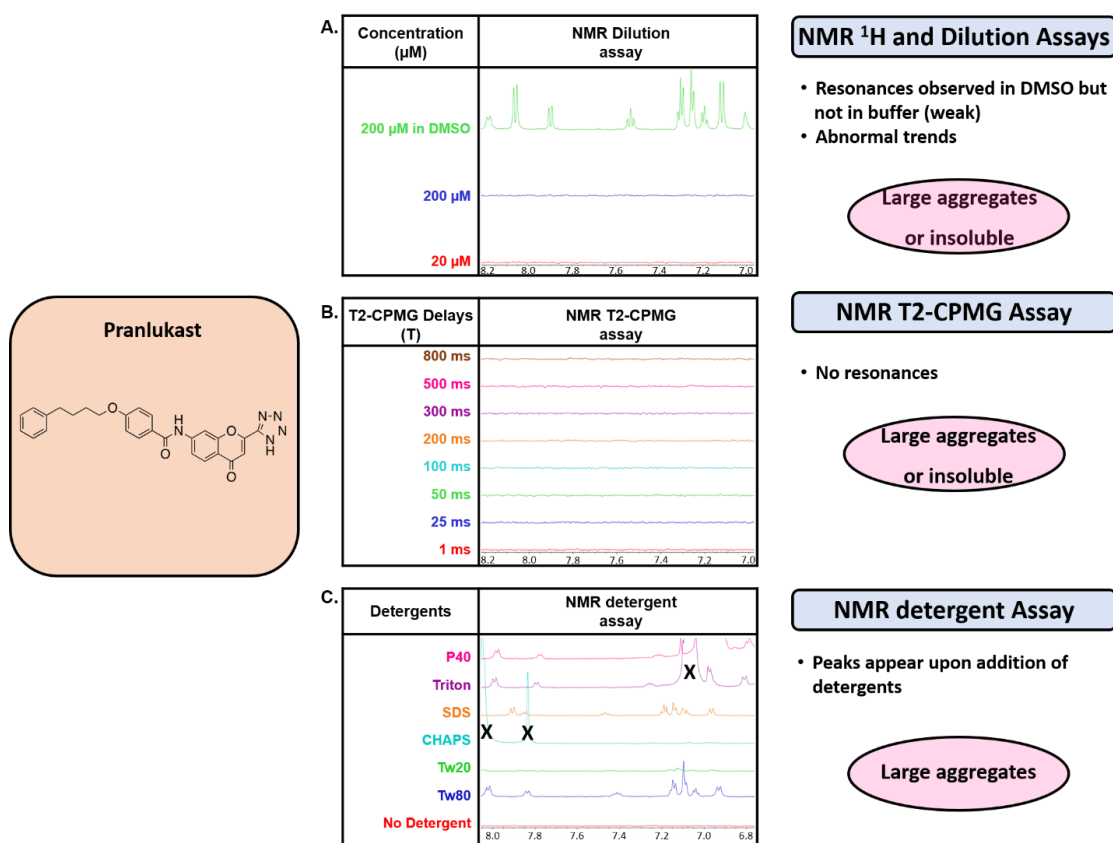


Supplementary Figure 4 | Probing the solution behavior of lansoprazole.

Shown are NMR data from, (A) the NMR ¹H and Dilution Assays, (B) the T2-CPMG Assay, and (C) The NMR Detergent Assay. The chemical structure is shown on the left. “x” in (C) denote resonances that arise from the detergent and not from the compound.

Probing the solution behavior of pranlukast

NMR resonance for pranlukast were observed in DMSO-d₆, but not in buffer at 200 μM nominal concentration in the NMR ¹H Assay (Supplementary Figure 5A). However, samples in buffer had cloudiness upon inspection but no precipitate, confirming that the compound was still in solution. Dilution in buffer from 200 μM to 20 μM did not result in appearance of signal but resulted in significant decrease in sample cloudiness without any observable precipitate. The NMR T2-CPMG Assay therefore did not provide any information due to the lack of resonances. The NMR Detergent Assay confirms the presence of large aggregates since the addition of several detergents results in appearance of resonances (Supplementary Figure 5C).

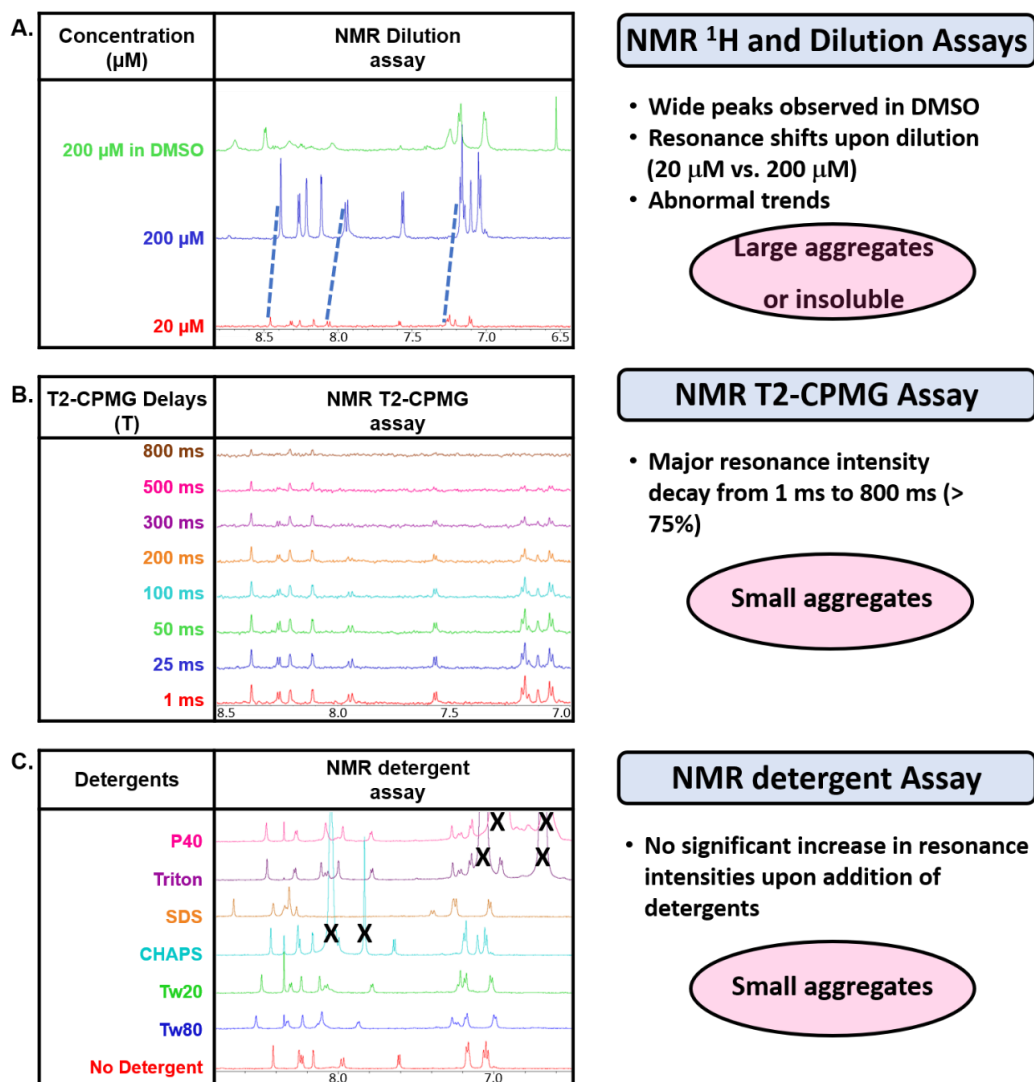


Supplementary Figure 5 | Probing the solution behavior of pranlukast.

Shown are NMR data from, (A) the NMR ¹H and Dilution Assays, (B) the T2-CPMG Assay, and (C) The NMR Detergent Assay. The chemical structure is shown on the left. “x” in (C) denote resonances that arise from the detergent and not from the compound.

Example of a possible DMSO aggregator

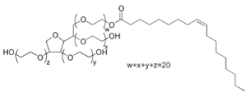
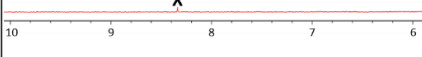
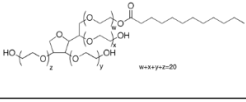
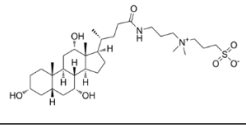
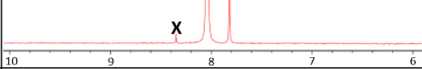
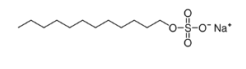
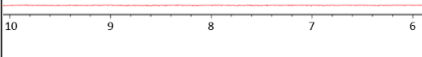
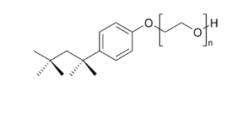
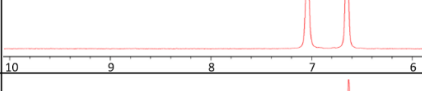
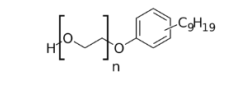
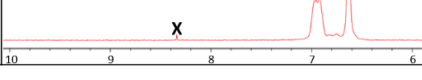
NMR resonances for an undisclosed compound were observed in both DMSO-d₆ and buffer. However, the NMR profile in DMSO would suggest that the compound is aggregating (broad peaks, low signal intensity) in this solvent (Supplementary Figure 6A). Although the NMR peaks appear much sharper in buffer, the dilution from 200 μM to 20 μM results in changes in chemical shifts for all the observed aromatic resonances. No precipitate or cloudiness could be visible in the samples. The NMR T2-CPMG Assay supports the dilution results as the signals exhibit a significant decay after 800 ms (Supplementary Figure 6B). Finally, no significant increase in resonance intensities could be observed in the NMR Detergent Assay (Supplementary Figure 6C). The overall data suggests the presence of small aggregates in buffer, with apparent aggregation of the molecule in DMSO as well.



Supplementary Figure 6| Example of a compound that possibly aggregates in both buffer and DMSO.

Shown are NMR data from, (A) the NMR ¹H and Dilution Assays, (B) the T2-CPMG Assay, and (C) The NMR Detergent Assay. The chemical structure is shown on the left. "x" in (C) denote resonances that arise from the detergent and not from the compound.

Detergents properties

Detergent	Chemical structure	Class	CMC	Spectrum (aromatic region)
Tween 80		Non-ionic	0.028 mM	
Tween 20		Non-ionic	0.042 mM	
CHAPS		Zwitterionic	8-10 mM	
SDS		Ionic	6-8 mM	
Triton X-100		Non-ionic	0.2 mM	
Nonidet P-40		Non-ionic	0.29 mM	

Supplementary Table 1 | Properties of detergents used in this report. “x” in NMR spectra denote resonances that arise from the impurities and not from detergents.

Experimental guidelines for various sample set sizes

Number of compounds	Time per compound	Methods
1 - 20	<ul style="list-style-type: none"> • Preparation time: 30-40 min • NMR time: For one sample <ul style="list-style-type: none"> • T2 CPMG : 5.5 min (4 scans) • ¹H NMR : 4 min (16 scans), 7 min (32 scans), 13.3 min (64 scans) and 26 min (128 scans) • Analysis time: 40-50 min 	<ul style="list-style-type: none"> • NMR dilution assay: All concentrations • NMR T2-CPMG assay: All delay times • NMR detergent assay: 3 detergents or more (e.g. Tween 80, NP40 and CHAPS) • Note: The number of scans should be same for all dilution experiments. However they can be 16, 32, 64, 128 or more (for dilution and detergent assays)
20 - 50	<ul style="list-style-type: none"> • Preparation time: 15-20 min • NMR time: For one sample <ul style="list-style-type: none"> • T2 CPMG : 5.5 min (4 scans) • ¹H NMR : 4 min (16 scans) or 7 min (32 scans) • Analysis time: 30 min 	<ul style="list-style-type: none"> • NMR dilution assay: Fast track method • NMR T2-CPMG assay: All delay times • NMR detergent assay: 1 or 2 detergents only (e.g. Tween 80 and NP40) • Number of scans (dilution and detergent assays): 16 or 32 • Note: The number of scans should be same for all dilution experiments. However they can be 16 or 32 (for dilution and detergent assays)
> 50	<ul style="list-style-type: none"> • Preparation time: 15-20 min • NMR time: For one sample <ul style="list-style-type: none"> • T2 CPMG : 5.5 min (4 scans) • ¹H NMR : 4 min (16 scans) • Analysis time: 25 min 	<ul style="list-style-type: none"> • NMR dilution assay: Fast track method • NMR T2-CPMG assay: 1 ms and 800 ms delays only • NMR detergent assay: 1 or 2 detergents only (e.g. Tween 80 and NP40) • Note: The number of scans should be same for all dilution experiments. 16 scans often result in satisfactory signal-to-noise (for dilution and detergent assays)

Supplementary Table 2 | Experimental guidelines according to various sample set sizes. Presented here are suggestions in order to mitigate increases in NMR acquisition time with larger sample sets.

Compounds information

Compounds	SMILES	Supplier	Catalog No.	CAS	Drug class	References in the manuscript
Valsartan	<chem>CCCCC(=O)N(CC1=CC=C(C=C1)C2=CC=CC=C2C3=NNN=N3)C(C(C)C)C(=O)O</chem>	BETAPHARMA	56-02004	137862-53-4	Antihypertensive	Figures 6
Etodolac	<chem>CCC1=C2C(=CC=C1)C3=C(N2)C(OCC3)(CC)CC(=O)O</chem>	SIGMA	E0516-50MG	41340-25-4	NSAID	Figure S1
Riluzole	<chem>C1=CC2=C(C=C1OC(F)(F)F)SC(=N2)N</chem>	SIGMA	R116-250MG	1744-22-5	Amyotrophic lateral sclerosis treatment	Figure S2
Methylene blue	<chem>CN(C)C1=CC2=C(C=C1)N=C3C=CC(=[N+](C)C)C=C3S2.[Cl-]</chem>	SIGMAALDRICH	M9140-25G	7220-79-3	Antidote for methemoglobinization poisoning	Figure 7
Imatinib	<chem>CC1=C(C=C(C=C1)NC(=O)C2=CC=C(C=C2)CN3CCN(CC3)C)NC4=NC=CC(=N4)C5=CN=CC=C5</chem>	BETAPHARMA	86-33437	152459-95-5	Chemotherapy	Figure S3
Lansoprazole	<chem>CC1=C(C=CN=C1CS(=O)C2=NC3=CC=C(C=C3N2)OCC(F)(F)F</chem>	SIGMA	L8533-250MG	103577-45-3	Proton pump inhibitor	Figure S4
Pranlukast	<chem>C1=CC=C(C=C1)CC(COC2=CC=C(C=C2)C(=O)NC3=CC=CC4=C3OC(=CC4=O)C5=NNN=N5</chem>	BETAPHARMA	56-05418	103177-37-3	Antiasthmatic agent (anti-inflammatory)	Figure S5

Candesartan Cilexetil	<chem>CCOC2=NC1=CC=C C(=C1[N]2CC3=CC= C(C=C3)C4=CC=CC =C4C5=N[N]N=N5)C(=O)OC(C)OC(=O)OC 6CCCCC6</chem>	BETAPHA RMA	14-31650	145040 -37-5	Antihypertensive	Figur e 8
Lapatinib	<chem>CS(=O)(=O)CCNCC1 =CC=C(O1)C2=CC3= C(C=C2)N=CN=C3N C4=CC(=C(C=C4)OC C5=CC(=CC=C5)F)Cl</chem>	Ontario Chemicals Inc	L1034	231277 -92-2	Chemotherapy	2, 10
Clofazimine	<chem>CC(C)N=C1C=C2C(= NC3=CC=CC=C3N2 C4=CC=C(C=C4)Cl) C=C1NC5=CC=C(C= C5)Cl</chem>	Sigma	C8895	2030- 63-9	Anti-leprosy	2
Sorafenib	<chem>CNC(=O)C1=NC=CC (=C1)OC2=CC=C(C= C2)NC(=O)NC3=CC(=C(C=C3)Cl)C(F)(F)F</chem>	SynChem	BAM66401	475207 -59-1	Chemotherapy	2
Curcumin	<chem>COC1=C(C=CC(=C1) C=CC(=O)CC(=O)C= CC2=CC(=C(C=C2)O)OC)O</chem>	Sigma	C1386	458-37- 7	NA	2

Supplementary Table 3 | Compounds information.

7 ARTICLE 4:

Drug Self-aggregation Into Nano-entities Can Induce Immune Responses

Fatma Shahout¹, Marion Vanharen¹, Abdelaziz Saafane¹, James Gillard, Denis Girard¹, Steven R, LaPlante^{*1,2}

¹ Université du Québec, INRS-Centre Armand-Frappier Santé Biotechnologie, 531 Boulevard des Prairies, Laval, Québec, H7V 1B7, CANADA

² NMX Research and Solutions, Inc., 500 Boulevard Cartier Ouest, Laval, Québec, H7V 5B7, CANADA

Target Journal: Journal of the American Chemical Society (JACS)

Contribution of the author:

I, Prof. Steven LaPlante, confirm that Fatma Shahout is the primary author of this publication.

All experiments including nuclear magnetic resonance, dynamics light scattering, electron microscopy (including sample preparation in buffer and media and data acquisition), confocal microscopy and ultra-thin section microscopy (including cell seeding, compound preparation and treatments), and ELISA assay were done by **F.S.** All figures generated, analyzed and interpreted by **F.S.** The manuscript was written by **F.S.**

7.1 Abstract

The free-state solution behaviors of small-molecules profoundly affect their respective properties. Recently, correlations are becoming evident between the existence of self-assemblies into drug nano-entities and unintended side-effects. This report describes our pilot study involving a selection of drugs and dyes to explore if there may be a correlation between the existence of drug nano-entities and immune responses. We first implement practical strategies for detecting the drug self-assemblies using a combination of NMR, DLS, TEM and confocal microscopy. We then used ELISA assays to monitor the modulation of immune responses on two cellular models, murine macrophage and human neutrophils, upon exposure to the drugs and dyes. The results suggest that exposure to some aggregates correlated with an increase in IL-8 and TNF- α in these model systems. Given this pilot study, further correlations merit pursuing on a larger scale given the importance and potential impact of drug-induced immune-related side-effects.

7.2 Introduction

A central challenge in drug discovery is to design small-molecule medicaments that bind with high affinity and specificity to pockets of the target proteins of interest, and understandably, they must also be safe for human consumption^{1,2}. However, unexpected side-effects are often prevalent and can result in a wide range of phenotypic effects – some desirable and others not. There are some well documented cases of desirable phenotypic effects that have been exploited³, while other cases have been disruptive or even disastrous⁴. Unfortunately, the identification of the exact sources of such side-effects can, in general, be complex and would require significant investments. Thus, the required investigations are often considered too onerous to pursue, so the sources of many side-effects typically go uncharacterized and remain elusive.

In this study, we wished to explore if a peculiar free-state drug behavior could be implicated in side-effects related to immune responses. We wondered if the natural trend for drugs to self-aggregate into larger nano-entities could illicit an immune response – for example, perhaps the sizes of the nano-entities are within an acceptable size range that they may be recognized by antibodies and thus induce a defensive response. It is well understood that a large study would be required to fully address this question. However, we opted to launch a pilot approach with four drugs that have already been FDA-approved and are currently on the market, along with five dyes. Central to this approach was the necessity to first develop practical strategies for experimentally detecting the existence of nano-entities.

The nano-entities formed by drugs remain poorly characterized, so a brief description is warranted here about the peculiar and amazing free-state behaviors that drugs can adopt in solution. It has been widely assumed that when a drug is placed into aqueous solution, it naturally tends to solubilize into solution or form a solid precipitate. Relatively recent studies are now shedding light onto a natural phenomenon where drugs, in fact, adopt what can be described as a three-state equilibrium. This equilibrium involves, (1) soluble lone molecules that tumble fast, (2) soluble medium- to large-sized self-assemblies of nano-entities that tumble slowly, and (3) solid precipitates. Moreover, it is becoming evident that many small-molecule drugs can surprisingly adopt a wide range of intermediate sizes of nano-entities^{5,6}. But to date, little is known about the size and types of these nano-entities given that they remain largely uncharacterized. This is due to our limited awareness in the pharmaceutical industry, and detection techniques are only recently being developed to detect the full range of nano-entity sizes that can exist. Also, the situation can be complicated by the fact that each compound adopts its own fingerprint three-state equilibrium that changes depending on the environment and solution conditions. In practice, these issues have resulted in multiple real “gaps” that have

hindered the pharmaceutical industry from pursuing and revealing the presence of compound aggregation that can impact the whole drug discovery pathway ⁵.

To date, no single scientific technique can fully reveal the existence of compound self-associates nor directly expose their full range of sizes and types. Thus, one must carefully weigh the advantages and limitations of each experimental technique. To help with this, we recently published a practical workflow that involves nuclear magnetic resonance (NMR) spectroscopy and dynamic light scattering (DLS). The NMR technique can be used to monitor small- to medium-sized nano-entities, and can indirectly reveal larger aggregates by the addition of detergents that break up the “soft” aggregates into smaller detectable nano-entities⁶. However, some colloidal aggregates are impervious to dissociation by detergents – we classify these as “hard” aggregates. To complement the detection of the large colloids, DLS and transmission electron microscopy (TEM) have proven valuable, and confocal laser scanning microscopy (CLSM) have been shown to expose drug aggregates within cells⁷. Despite the limitations of each technique, a practical strategy is described herein.

Only once the detection methods are implemented, can one begin to establish the correlation of nano-entities with their properties. Interestingly, reports have already shown some correlations that have serious impacts on drug discovery efforts. For example, they have been unexpectedly implicated in giving rise to false positives in high throughput screening assays (HTS)⁸, and false negative results in cells-based assays^{9, 10}. Also, studies have revealed that drug self-aggregates, can somehow predispose them to undesirable physicochemical properties, such as non-specific protein adsorption, likelihood of toxicity^{5, 7, 11, 12} and promiscuous undesirable off-target inhibition (*in vitro*)^{5, 13}. Interestingly, nano-entities have also been correlated with desirable attributes such as improved drug bioavailability¹⁴, use as drug delivery systems and potential drug carriers¹⁵. However, the investigation of other correlations must await the development of robust detection strategies and the support and interest from project managers in the pharmaceutical industry.

Here, we launched a pilot study to explore the possible correlation and involvement of drug nano-entities with unintended immune responses. Our interest was based on unexplained observations that some drugs and dyes have been associated with unintended immune-mediated hypersensitivity reactions^{16, 17}, such as rashes, allergies, anaphylaxis events and other dermatologic side-effect¹⁸⁻²⁰. Also, interesting correlations with toxicity have been noted^{5, 6}. To explore a potential correlation with immune responses we used a selection of drug-like molecules including anticancer drugs and synthetic dyes as model systems. We carefully detect their nano-entity characteristics, and evaluate their potential influence on immune responses using murine macrophage cell line and human neutrophils.

7.3 Results and Discussion

7.3.1 Morphological and Physicochemical Characterization of Colloidal and Non-colloidal Aggregates.

Here, we implemented strategies to explore the free-state behavior of four compounds (Figure 7.1 a) in cell-culture medium and biochemical buffers that enabled us to explore their unique three-phase equilibria. The compounds consisted of three anticancer drugs (Lapatinib, Erlotinib and Gefitinib) and one non-amyotrophic lateral sclerosis drug (ALS) (Riluzole). We first employed TEM technique to monitor compound aggregation of the four compounds as shown in Figure 7.1 a. Our interest in exploring TEM strategy as a tool to detect the free state equilibrium of the compounds arose from observations made by our previous studies and other several reports^{7,9}. We often noted by TEM that while some small-molecules can form large colloidal aggregate sizes, others can exhibit single lone tumbling molecule behaviors when placed in aqueous media. Thus, aggregates either large, medium or small can be detected by TEM.

We began our study by incubating the drugs in the cell culture medium RPMI-1640 at 50 μ M in the presence of 10 % FBS at 37 °C. Interestingly, a visual perusal of the images clearly revealed the presence of small to large nanometer-sized aggregates. Some are spherical globs such as those found for Lapatinib and Erlotinib while others are crystal-like form such as Gefitinib. On the other side of the image, no nano-meter-sized aggregates are noted for the well-known aggregator Riluzole, which clearly confirms that this drug behaves as a single/lone tumbling molecule. Similar experiments in cell culture medium, in the presence of only 5% FBS, were also reported in our previous study in which we found that the two chemotherapeutic drugs Lapatinib and Gefitinib formed aggregate like colloids at 37 °C. Consistent with those observations, the aggregate types and shapes were very similar to those in this current study (Lapatinib forms spherical colloids while Gefitinib forms crystal-like colloids⁷). Moreover, others found that the behavior of Lapatinib in potassium phosphate buffer with or without 10% of FBS was consistent with the formation of aggregation globs⁹. It must be kept in mind that our samples were prepared according to the manufacturing protocol required for TEM observation in which the compound must be soaked with a spherical copper grid coated with carbon. This has allowed larger slow-tumbling molecule species on the double-digit nanometer scale to be visible by TEM, while single lone molecules that tumble freely in the solution would be invisible by TEM (see Figure 7.1b).

We next investigated the aggregation properties of the above four drugs in aqueous buffer using the NMR method as introduced in our previous work⁷. NMR spectroscopy is a practical technique that can monitor compounds' solution behaviors and their multi-phase equilibrium.

Fast-tumbling single lone molecules and slow tumbling small-medium nano-entities can be directly exposed. However, larger colloidal aggregates can only be detected by a simple trick via the disruption of NMR resonances. Here, we implemented the ^1H NMR detergent based-assay as a simple method that can easily expose features of the unique three-phase equilibrium of our compounds in buffer. Our interest in exploring this NMR detergent assay to monitor compound aggregations arose from our recent observations across several reports^{5, 6, 21}. They often noted that while many compounds exhibited expected/no change in resonance intensities upon exposure to detergents, others exhibited significant increases/unusual features in resonance intensities upon the addition of detergents, which can report the existence of large (hard or soft aggregates) that could be disturbed by the detergents.

According to these observations, we began our study to explore the existence of aggregates of the four compounds by using three different detergents including Tween 80, Triton 100X and CHAPS. As expected, a sharp NMR spectra was noted for Riluzole at 200 μM and the addition of the detergents had no effects on the NMR resonances. In other words, no increases in resonance intensities nor peak shifts were observed upon the addition of detergents, confirming that no aggregates exist. Thus, Riluzole behaves as fast-tumbling lone molecule. These observations were consistent with the data from the NMR T2-CPMG assay where are no loss of resonance intensities upon increasing to 800 ms (> 80% intensities maintained) (see Figure. S1d, Supporting information).

On the other hand, NMR resonances were also observed in the spectra acquired for Gefitinib in buffer at 200 μM (Figure 7.1c), and also in NMR T2-CPMG assay, where are a minimal loss of resonance intensities was noted upon comparison of the peaks using (e.g 1 ms versus 800 ms) (see Figure S 1c. Supporting information). However, it should be mentioned that the drug sample in buffer was a little opaque with precipitate that was obvious by the naked eye. Interestingly, significant increase in resonance intensities were observed upon the addition of Triton 100x, but not Tween 80 or CHAPS, reporting that Gefitinib can exist as aggregates in aqueous solutions.

Interestingly, unusual trends of the solution behavior was also noted for Erlotinib (Figure 7.1 c). Unlike Gefitinib, no NMR resonances were observed in buffer at 200 μM . It should be also kept in mind that some precipitate was present upon visual inspection. Interestingly, significant increase in resonance intensities were also noted upon the addition of Triton 100x, but no changes to the NMR spectra was observed upon the addition of Tween 80 or CHAPS, reporting that Erlotinib can exist as hard aggregates in aqueous solutions. The last NMR study involved an evaluation of the solution behavior of Lapatinib. The NMR ^1H assay in Figure 1c, shows that no resonance acquired in buffer at 200 μM and also in T2-CPMG (Figure S 1a. Supporting information). Also, the drug sample in buffer was opaque with solid precipitates that

were obvious upon visual inspections. Unlike Gefitinib and Erlotinib, no increase in resonance intensities upon the addition of all the three detergents. Given these observations, yet to be confirmed if the lack of resonances is due to compound insolubility in buffer or to the existence of large and hard aggregates. Therefore, other orthogonal methods must be considered to confirm the free state solution behavior of the drugs.

As a complementary detection method, we then applied DLS to confirm the existence of drug self-association. Although it is a low throughput screening assay, DLS can quantitatively measure the size of compound aggregates by measuring the scattering intensities of the particles suspended within a solution. We began our study by evaluating the particle size of aggregates at four different concentrations 12.5 μ M, 25 μ M, 50 μ M, and 100 μ M. We acquired the DLS data using phosphate buffered HPLC water as shown in (Figure 7.1d). After samples subjected to mild centrifugation, data clearly showed the existence of aggregate sizes in the nanometer range. On the other hand, data showed no readout of the particle size for the known non-aggregator Riluzole which might prove the potential complementarity of all techniques TEM, NMR and DLS. Although the exact environmental conditions and parameters that dictate the three phase equilibrium have yet to be understood, it is mostly obvious that environmental conditions can have a serious impact on the aggregate size, type and other properties. For instance, when using different aqueous medias (biochemical or biological), changes in aggregate features can be clearly observed.

We also evaluated the particle size for all dyes included in this study under the same conditions. To our surprise, we were only able to detect the size of Acid 18 and Acid 49. However, we were unable to detect the presence of nanometer sized aggregates for the known aggregator Methylene blue and the two known non-aggregators Tartarazine and Nephtol Yellow (Figure S2, Supporting information). This latter observation by DLS unequivocally explains our limitations to probing the solution behavior of colloidal aggregates and to fully reveal their aggregate size, types and all respective properties. As said, that no one method can reveal the full range of nano-entities, a combination of different strategies as proposed above is necessary. Also, another orthogonal method including cellular-based assays such as CLSM must be considered to monitor the tendency of compounds to self-associate which described below.

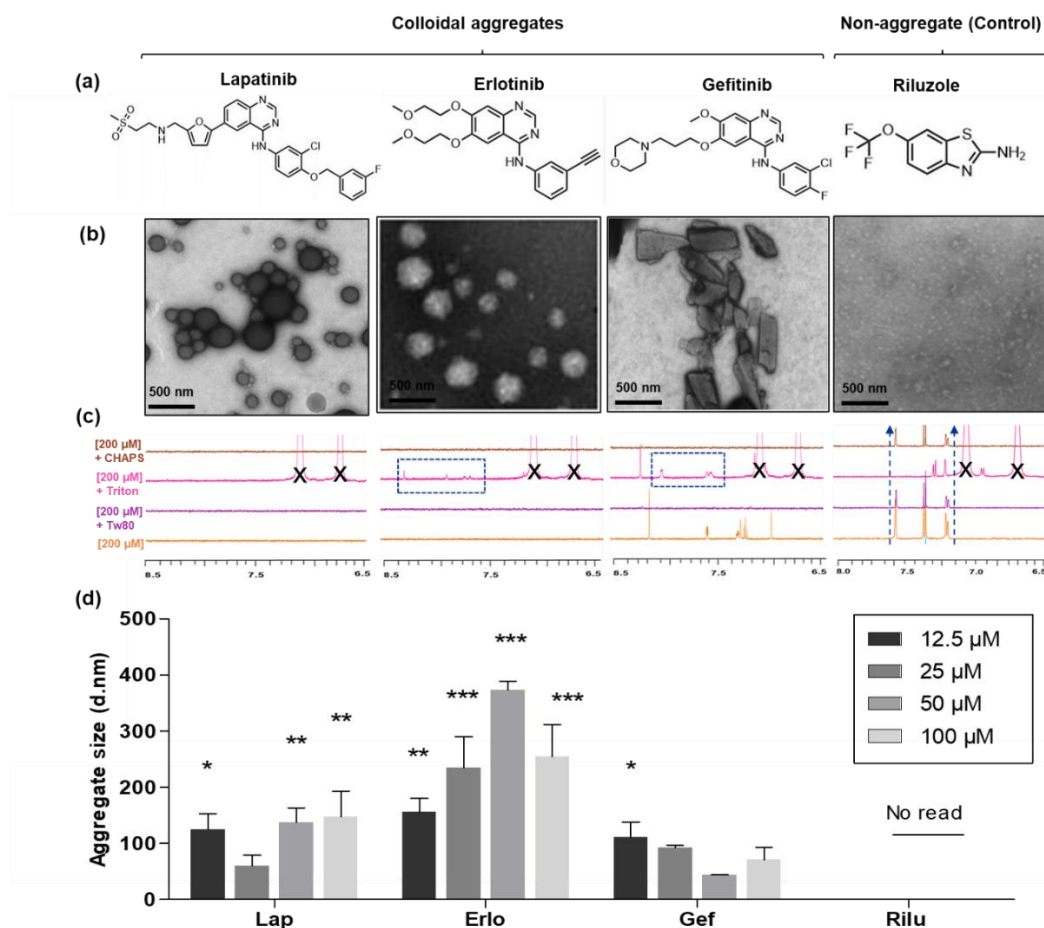


Figure 7.1. Shown are the characterization of aggregates and non-aggregates.

(a) Shows the structure of drug models used in the study. (b) TEM images of three aggregator drugs (Lapatinib, Erlotinib and Gefitinib) respectively, and a known non-aggregator, amyotrophic lateral sclerosis drug sample (Riluzole). (c) 1D 1H NMR data at 200uM in the presence and absence of detergents. (d) DLS data shows the particle size in (d.nm) of all drug aggregates and the non-aggregate, which shows no read by DLS together with the control (buffer) (considered as zero value) (see also supporting information). Data presented as (mean \pm SEM). * $p < 0.05$ vs Ctrl, ** $p < 0.001$ vs Ctrl, *** $p < 0.0001$ vs Ctrl.

7.3.2 Cellular Uptake and Internalization of Aggregates. The combination of techniques is necessary to fully detect compound self-aggregation along with their three-state solution behaviors. CLSM can be a convincing method to reveal and characterize nano-entities at the cellular level as shown in our previous report⁷. CLSM was also used here to assess the cellular uptake of compounds and their aggregates by murine macrophages. However, one must consider that to render compound aggregates visible by CLSM, they must be fluorescent to generate sufficient signals within the cells.

We began this study by the exposure of murine macrophages RAW 264.7 cells to 50 μ M of Lapatinib, Erlotinib and Gefitinib which prepared at 37 $^{\circ}$ C for up to >72h prior to treatments. Cellular uptake and internalization of drug aggregates were then visualized by

CLSM. Note that the complete cell image can be visualized by using markers such as membrane stain, the red dye (Alexa Fluor WGA555) and nucleus stain, the blue dye (DRAQ 5). After 24h of exposure, acquired CLSM views showed that drugs, in particular Lapatinib, was indeed uptaken by the cells as shown by its natural green fluorescent that typically displayed a punctuated pattern in the cytoplasm (Figure 7.2 a and e).

Other drugs including Erlotinib and Gefitinib were also studied by CLSM and distinct views were obtained (see Figure 7.2 (b, f) and (c, g)). Although Lapatinib was well-distributed as stronger green fluorescence within the cytoplasm of macrophage cells, less green signals arising from the Erlotinib and Gefitinib in the cytoplasm and appear as more diffusing signals within the cells. In order to verify that colloidal aggregates were indeed existing intracellularly, cells were washed three times with phosphate-buffered saline (PBS) to remove any existing extracellular aggregates. Given the differences in the cellular uptake between control non-treated macrophages and cells treated with the three aggregator compounds, aggregates had indeed entered the macrophage cells and may have properties that will be studied herein.

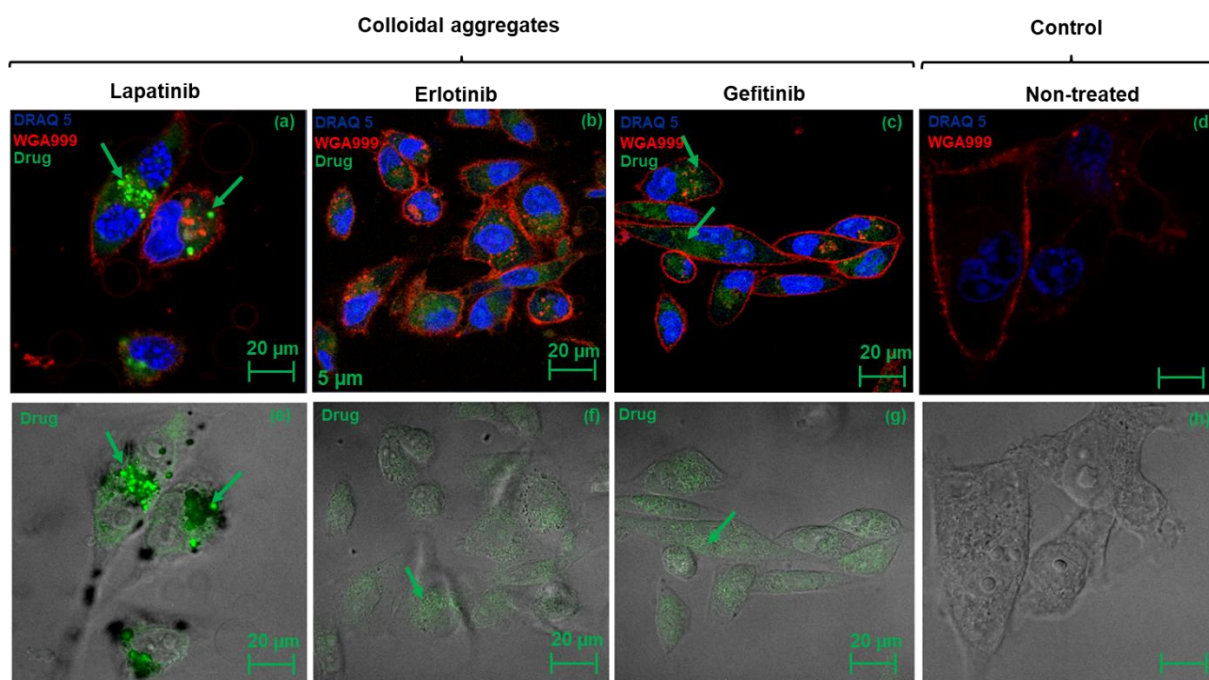


Figure 7.2. Cellular uptake of drug aggregates.

Drugs including (Lapatinib, Erlotinib, and Gefitinib) were added to the macrophage cell line RAW 264 at 50 μM . The presence of colloidal aggregates inside the cells was evaluated by confocal laser scanning microscopy, as described in “Materials and methods”. Of note, (a) Lapatinib aggregates were more observable (as green fluorescence spots localized in the cytoplasm) compare to the two other drugs (b,c) (Erlotinib and Gefitinib) that appear diffused in the cytoplasm with less fluorescence signals. (d) The non-treated macrophage cells were used here as control and shows no fluorescence signals raising from the cells. The lower raw (e, f, g, and h) is the bright images of the upper raw.

For studying the cellular uptake of aggregates by human neutrophils, our study employed ultrathin section electron microscopy (USEM) as a higher resolution method to evaluate the

ingestion of aggregates by human neutrophils *in vitro*. Interestingly, as shown in Figure 7.3, the images obtained by USEM illustrate that aggregation of Lapatinib, Erlotinib, Gefitinib and Methylene blue are indeed penetrated through the cell membrane and entered the neutrophils. The aggregate assemblies appeared as distinct dark inclusions localized within the cell organelles, and seemed to resemble the shape and distribution to the compound self-assemblies monitored by TEM as seen in Figure 7.1b. Of note, the well-known aggregator (Riluzole) was not observable within the neutrophils compared to aggregated compounds, this is probably due to its single lone molecule properties as corroborated by the other strategies described above and by a previous report ⁶. The neutrophil uptake of Acid 49, the well-known aggregator dye, was also studied by USEM (Figure S3, Supporting information). However, the outcome was not clearly addressed. Other complementary methods must be implemented to evaluate the cellular uptake of Acid 49 aggregates by human neutrophils.

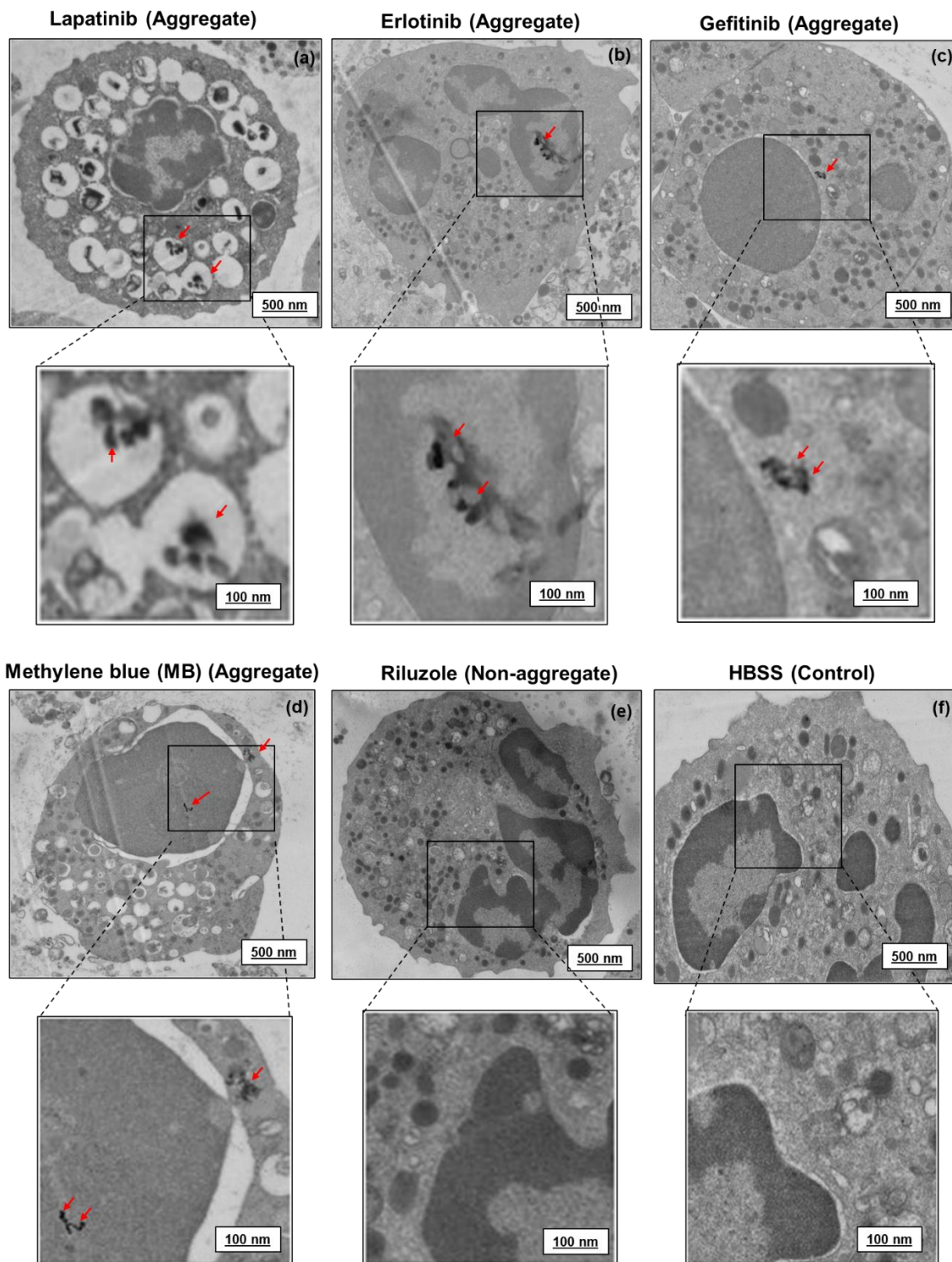


Figure 7.3. Cellular uptake of drug and dye aggregates by human neutrophils.

The penetration of aggregates and their presence inside the cells was monitored by Ultrathin-section-transmission electron microscopy. Neutrophils at (10×10^6 cells/ml cells/ ml) were incubated for 24 h with $50 \mu\text{M}$ of Lapatinib aggregates (a) Erlotinib aggregates (b) Gefitinib aggregates (c) or MB aggregates (d). Cells were also incubated with the non-aggregator (Riluzole) (e) and HBSS (f), which were used as controls. Samples were then prepared for TEM analysis.

7.3.3 Mapping the Effect of Drugs and Dyes Aggregation on Murine Macrophage RAW 264.7 and Human Neutrophils. Perhaps once the detection methods are implemented, can one begin to correlate nano-entities to their consequential properties. Recently, reports have already shown some associated properties that have serious effects on drug discovery efforts such as false positives in HTS assays, off-target promiscuity *in vitro*^{5, 30} and toxicity¹². Nano-entities have also been associated with desirable features such as drug delivery systems and potential drug carriers¹⁵. However, other respective properties such as the possible correlation of nano-entities with immune responses is largely undetected.

Our interest arose from unexplained observations made across several reports that some drugs and dyes have been associated with immune-mediated hypersensitivity reactions^{16, 17}. Such these events may eventually result to the development of drug-induced rash, allergy and other adverse related-events. Recently, there have been several studies that reported such reactions, including immune-related adverse events associated with many effective molecular-targeting small molecules³¹. For example, it was reported that several approved epidermal growth factor receptor tyrosine kinase inhibitors (EGFR TKIs), which are successful and effective key chemotherapeutics for the treatments for non-small cell lung cancer were among the small molecules that were studied for their adverse events. These reactions include skin rashes^{33, 34, 35, 36, 46}, acneiform eruption, pruritus, xerosis³⁷, interstitial lung disease (ILD)³ and other dermatologic effects³⁹, which were reported as effectively managed and tolerated by all patients^{32, 37}. The related mechanisms of these reactions are far from being elucidated. Some believe that they may be related to many different factors, for example, to the mechanism of action or to other environmental and genetic attributes of the host.

Perhaps the lack of knowledge on different immunological mechanisms and associated properties of compounds, might be the main factors that hinder the development of validated predictive screening tools meant to assess the immune response mediated by compounds. Several well-defined cell lines and even fresh immune cells isolated from the blood of healthy donors are currently promising models for this purpose, but validation is still required by implementing other candidates.

To begin exploring the potential correlation of nano-entities with immune responses, a selection of drug-like molecules including anticancer drugs and synthetic dyes as model systems were used. We carefully evaluated their potential influence on immune responses using murine macrophage cell line and human neutrophils.

After determining the internalization of aggregates by murine macrophage and neutrophils detailed above, colloidal aggregation may certainly have properties. We evaluated the immune response to nano-entities by studying the activation of the immune cells and the

production of several cytokine profiles *in vitro*. We used an ELISA assay as a screening tool to identify the release of some cytokines by macrophage RAW 264.7 and neutrophil models as shown in Figure 7.4 and Figure 7.5. The two cellular models were used because they are well-known for their roles in inflammation and host defense. Moreover, the cytokines such as tumor necrosis factor α (TNF- α) was used because it is a primary proinflammatory cytokine that is produced by macrophage cells during some conditions such as infections or injuries by external stimuli. Macrophage can also lead to the secretion of IL-6 upon acute inflammation. We also employed interleukin-8 (IL-8), which is an important cytokine that can modulate the innate immune response. It was involved in proinflammatory actions upon secretion and neutrophil cells is a major source of this cytokine.

It must be kept in mind that all small-molecule aggregates used in this study prepared in cell culture medium RPMI-1640, which were left to spontaneously self-associate in this media for up to 72h at 37 °C prior to treatments. For macrophage RAW 264.7 cells, after 24h of incubation, there was a production in the basal level of tumor necrosis factor α (TNF- α) increased after incubation of the well-known aggregator Gefitinib with macrophages only at higher doses 50 μ M and 100 μ M (Figure 7.4).

Similar to macrophage cell, the basal production of interleukin -8 (IL-8) also increased by neutrophils following the 24h of incubation with Gefitinib (Figure 7.5). Interestingly, Gefitinib has been carefully studied for its self-aggregation attributes and clearly showed slow-tumbling nano-entities by NMR, DLS⁶, T2-CPMG, TEM⁷ and cell culture-based assay as reported in our previous study⁷. Despite these reports, no studies correlate immune like-events to the slow-tumbling aggregates and thus this property remains poorly characterized. As shown in the outcomes provided in Figures 7.3 and Figure 7.4, it could be possible that the slight upregulation of both biomarkers TNF- α and IL-8 following the treatment of Gefitinib at 100 μ M is aggregation dependent.

Certainly, such effects should require massive validation, and implement other screening techniques. Recent reports had investigated that Gefitinib can lead to inflammation-based side effects, and their finding was supported by the evidence that Gefitinib provokes immune responses by upregulating interleukin-1 β (IL-1 β) and activating inflammasomes in macrophage THP-1 cells⁴¹, which may eventually provide insights into the potential of Gefitinib to trigger side effects or at least has a key role in e.g interstitial pneumonitis⁴⁰⁻⁴³. However, the mechanisms involved remained unknown. Other studies showed that Gefitinib can trigger side effects related interstitial pneumonitis⁴⁰⁻⁴³, which is related to lung tissue inflammation caused by some small molecules or other infectious agents. Other studies showed that produced level

of cytokine signals such as TNF α and interleukins IL-18, IL-1 β can be exhibited in the lung of some patients with pneumonitis conditions^{44, 45}.

Other drugs such as Erlotinib, which formed very large aggregate globs (as observed by TEM and DLS), also tested and showed a slight significance in the production of the basal TNF- α at 50 μ M following macrophage exposure (Figure 7.4) and IL-8 release when incubated with neutrophils at 12 μ M (Figure 7.5). It was interesting to us that the non-aggregator Riluzole did not upregulate the cytokine level in both cell models. Those observations might suggest that the drug Riluzole behaved *in vitro* immune models as a fast-tumbling small molecule, whereas the two molecules Erlotinib and Gefitinib behaved as a slow-tumbling aggregate.

To our surprise, Lapatinib as a well-defined aggregator as reported by our previous report⁷ and by others⁹ did not show any increase in the level of both cytokines (see Figure 7.4 and 7.5). Thus, it is evident yet surprising that the three aggregators (Lapatinib, Erlotinib and Gefitinib) have very distinct solution behaviors, sizes and even aggregate types. Thus, mediating the immune system and related effects should be variable, and each compound should have its unique fingerprints and properties that reflect its influence on the *in vitro* immune system and related events. Perhaps, this would further need to be corroborated by other studies and verifications (e.g. western blot observation as a complementary method to complete the picture and verify signalling transduction pathways). Finally, other cytokine biomarkers were also quantified following exposure to RAW 264.7 or neutrophils such as interleukin-6 (IL-6), but IL-6 cytokine level was not produced upon treatments of all drug aggregates (Lapatinib, Erlotinib and Gefitinib) and the non-aggregate (Riluzole). The results were non-significant at all concentrations (Fig. S4 and S5, Supporting information).

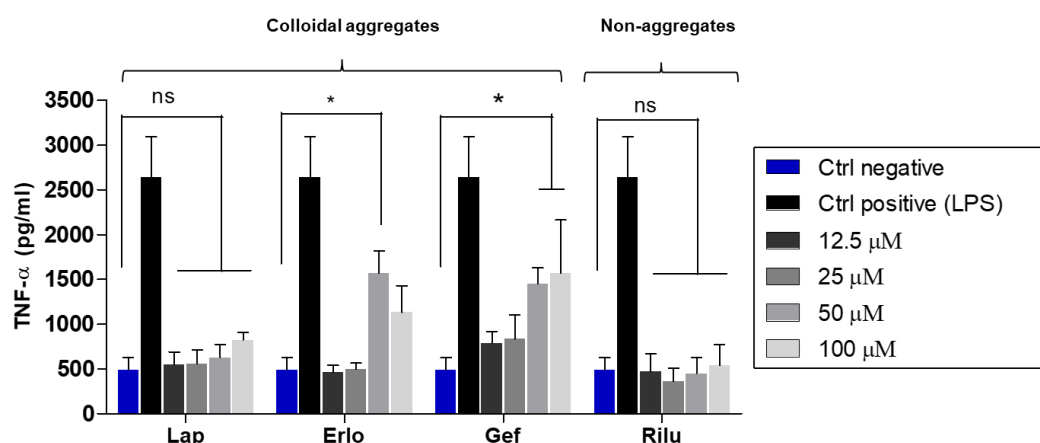


Figure 7.4. Effects of compound aggregation on the production of cytokine (TNF- α) using the mouse macrophage cells (RAW264).

Cells were incubated in the presence of drug aggregates and non-aggregate, LPS (Ctrl positive) or in the absence of compounds (Ctrl negative) for 24 h and the supernatants were harvested and used for the detection of the indicated TNF- α by ELISA as described in "Materials and methods". Data presented as (mean \pm SEM). * p <0.05 vs Ctrl.

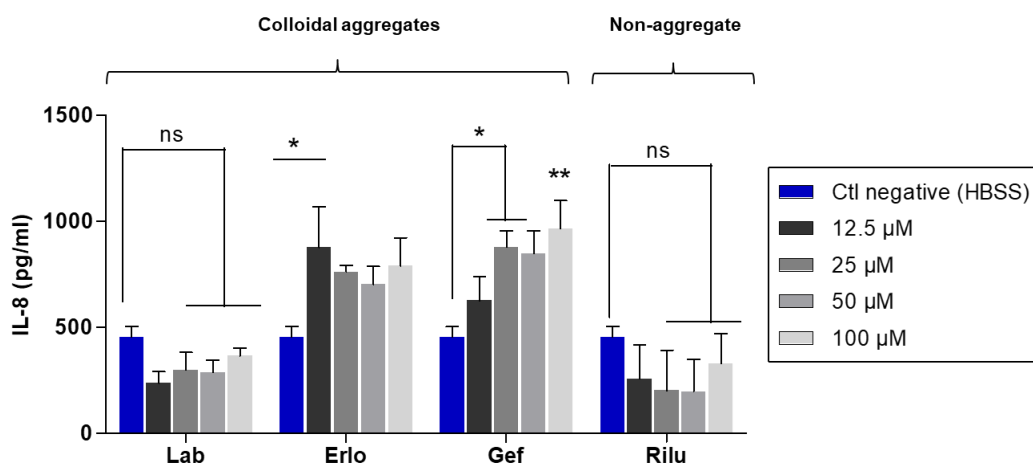


Figure 7.5. Effect of compound aggregation on the production of cytokines (IL-8) using human neutrophils.

Freshly isolated human neutrophil cells were incubated in the presence of buffer HBSS (Ctrl negative), drug aggregates and non-aggregate for 24 h and the supernatants were harvested from 3 healthy donors and used for the detection of the indicated interleukin IL-8 by ELISA as described in “Materials and methods”. Data presented as (mean \pm SEM). * $p < 0.05$ vs Ctrl, ** $p < 0.001$ vs Ctrl.

The study was then subsequently extended to additional small-molecule aggregator and non-aggregators such as FDA approved dyes. Those dyes have been extensively studied for their solution behaviors and tendency to self-aggregate using 1D NMR assay as shown in our previous report²¹. Some dyes can self-associate into a wide-range of nano-entities and adopt aggregates of distinct sizes, whereas others can exist as single-molecules and tumble more freely in solution.

We began establishing the correlation of dyes nano-entities with immune responses. Our interest was based on unexplained observations that several synthetic dyes have been associated with several adverse-like events and hypersensitivity reactions, that is rarely can be fatal¹⁶. To date, no studies correlated dye aggregates to severe allergic and hypersensitivity reactions that are more likely to be immune response-like events related. Regarding these assumptions, we set out here our study by evaluating the production of several cytokines released from human neutrophils after 24h of dyes exposure by using ELISA assay as described previously. We quantified the basal production of IL-8, and outcomes are provided in Figure 7.6. Interestingly, the two well-known dye aggregators Methylene blue (MB) and Acid 49 have significantly increased the level of IL-8 compare to the buffer HBSS-treated neutrophils. Although aggregates can exist as revealed in our previous report²¹, Acid 18 did not show observable upregulation of the IL-8 level. Some points are worth mentioning here. All dyes included in this study are structurally different and are not from the same series. It is reported that each of which can have such distinct solution behaviors²¹. One notable and

contentious assumption is that the properties of compound aggregation may play a critical role in mediating the immune response, and again as mentioned earlier this might depend on the aggregate size, type, membrane permeability, serum binding and to name a few.

To determine if the elevated IL-8 level by Methylene blue and Acid 49 and related immune response is aggregation dependent, we tested two well identified non-aggregator dyes Nephthol Yellow and Taratarzine as negative controls, and distinct findings were observed. Interestingly, there were no production of the IL-8 level following 24h of exposure compare to the two aggregators Methylene blue (MB) and Acid 49. Not only IL-8 level was measured following incubation with dyes, but other biomarker such as IL-6 was also quantified. No production was observed by neutrophils. Only, a slight induction of IL-6 level was observable when neutrophils treated with the aggregator Acid18 for 24h, but the result was not significant (see Figure S6, Supporting information).

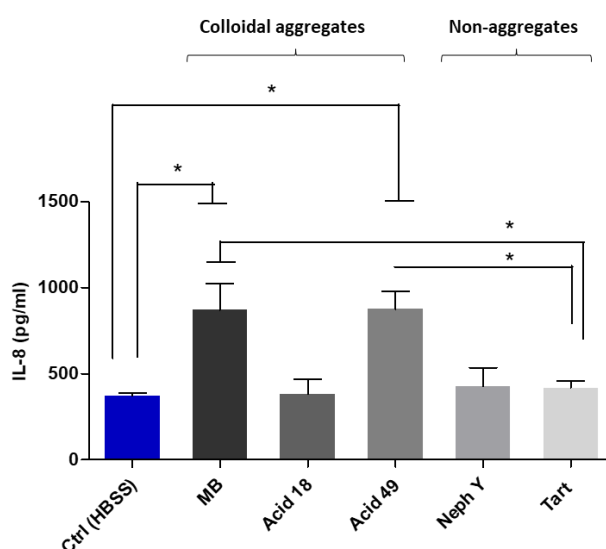


Figure 7.6. Effect of dye aggregation on the production of cytokines (IL-8) using human neutrophil cells.

Freshly isolated human neutrophils were incubated in the presence of buffer HBSS (Ctrl negative), dye aggregates and non-aggregate for 24 h and the supernatants were harvested from 3 healthy donors and used for the detection of the indicated interleukin IL-8 by ELISA as described in “Materials and methods”. Data presented as (mean \pm SEM). * $p < 0.05$ vs Ctrl.

7.4 Experimental Section

Drugs and Reagents. Anticancer drugs and dyes were obtained from commercial vendors. Their CAS numbers are as following: Lapatinib (388082-78-8) from Larid Road; Gefitinib (184475-35-2); Erlotinib (183321-74-6) from Sigma; Napthol Yellow (846-70-8), Methylene blue (61-73-4), Tartrazine (1934-21-0), Alexa fluor WGA555 and Prolong Diamond Anti-fade with DAPI were purchased from Thermo Fisher Scientific. Preparation of 20 mM compound stock solutions are described in previous reports(LaPlante *et al.*, 2013a; LaPlante *et al.*, 2013b;

Murugesan *et al.*, 2018). Appropriate amounts of stocks were then added to buffer or cell culture media to attain the desired concentrations, followed by a waiting period of up to 72h at 37 °C prior to subsequent treatments.

Transmission Electron Micrograph (TEM). Morphological characterizations of compound aggregators and non-aggregators were analyzed in cell culture medium (RPMI-1640) by transmission electron microscopy (Hitachi H-7100). The photographs were processed with the digital camera AMT version 600.147.

Nuclear Magnetic Resonance (NMR). Compounds were weighed according to the NMR dilution protocol as previously published (LaPlante *et al.*, 2013a; LaPlante *et al.*, 2013b; Murugesan *et al.*, 2018). Deuterated DMSO was then added to prepare 20mM drug stock solutions. Appropriate amounts of DMSO stock solutions were added to buffer solutions containing 50mM sodium phosphate pH 7.4 in 100% D₂O. The samples were then centrifuged and supernatants were collected for acquiring ¹H NMR spectra.

Dynamic Light Scattering (DLS). Aggregate size distributions were evaluated using dynamic light scattering, Zetasizer Nano ZS (Malvern) model ZEN3600 (Westborough, MA) as previously published (Durocher & Girard, 2016; Durocher *et al.*, 2017; Noël *et al.*, 2016). Samples were prepared in and measurements taken using polystyrol/polystyrene 10 × 10 × 45 mm cuvettes. Measurements were made for samples containing compounds at 12.5 μM, 25 μM, 50 μM and 100 μM in phosphate buffer (HPLC water), RPMI-1640 or in RPMI-1640 +10% human serum.

Cell Culture (Murine Macrophage RAW 264.7). RAW 264.7 was obtained from American Type Culture Collection (ATCC TIB-71, Manassas, VA, USA). Cells were cultured in Dulbecco's modified Eagle's medium (DMEM), supplemented with 10% FBS, 1% penicillin/streptomycin in a humidified atmosphere of 5% CO₂ at 37 °C. Once they reach 80-90% of confluency, cells were then cultured in 24 well plates at (1 × 10⁴ cells) overnight. The media were then removed and replaced with various concentrations of each compound. All aggregate and non-aggregate samples were left sitting for up to 72h at 37 °C prior to treatments. Cells were also exposed to lipopolysaccharide (LPS) (1 μg/mL) used as a positive control in the absence of drug conditions. Cultures were incubated overnight under stimulated/non-stimulated conditions for 24h and supernatants were then harvested and stored at (-20) for ELISA analysis.

Confocal Laser Scanning Microscopy (CLSM). RAW 264.7 cells were grown on glass coverslips in 24 well plates and cultured overnight in DMEM (5% FBS, 1% penicillin/streptomycin) at 37 °C in 5% CO₂. Cell culture media was then removed and washed twice with 1X PBS. Cells were incubated with 50 μM of drugs for 24 h, washed twice with 1X

PBS and fixed with 4% paraformaldehyde for 10 minutes. Further, cells were stained with nucleus stain DRAQ-5 for 20 mins, and coverslips were then mounted on a prolong diamond antifade and imaged by a Zeiss CLSM-780 confocal microscopy (ZEISS, Jena, Germany) on an Olympus FV1000 at 60X magnification.

ELISA Assay (Murine Macrophage RAW 264.7). The amount of interleukin 6 (IL-6) and tumor necrosis factor (TNF- α) were determined by commercially available ELISA kits (BioLegend, USA) that contained all the reagents for the assay according to the manufacturer's instructions. Absorbances were then read at 450 nm using a TECAN spectrophotometer.

Neutrophil Isolation. From blood of healthy volunteers, fresh human neutrophils cells were isolated by dextran sedimentation. Then centrifuged by Ficoll-Hypaque (Pharmacia Biotech, Inc., Quebec, Canada) as described previously (Babin *et al.*, 2013; Poirier *et al.*, 2014; Simard *et al.*, 2011). Blood was obtained from individuals according to institutionally approved procedures. Cell viability of neutrophils was evaluated by trypan blue $\geq 97\%$. The purity of cells was checked and was about ($\geq 98\%$), which was verified by cytology from cytocentrifuged preparations stained by Hema-3 stain (Biochemical sciences Inc., Swedesboro, NJ).

Ultrathin-section transmission electron microscopy (USEM). Human neutrophils (10×10^6 cells/ml) were isolated as previously published (Noël *et al.*, 2016), and incubated with drug and dye aggregates at 50 μM for 24h, fixed with glutaraldehyde (2.5%) and analyzed by transmission electron microscope Hitachi (H-7100).

ELISA Assay (Neutrophils). Freshly isolated human neutrophils were seeded at (1×10^6 cells/ml) in 96-well plates and incubated at 37 °C 5% CO₂ for 24h in the presence of HBSS, drug/dye aggregates and non-aggregates at the desired concentrations. Again, all aggregates and non-aggregates were left sitting for up to 72h at 37 °C prior to treatments. Cells were then collected, centrifuged and supernatants were harvested and stored at -20 °C. The IL-8 and IL-6 levels were quantified by commercially available ELISA kit (BioLegend, USA).

7.5 CONCLUSIONS

This study began with evaluating the self-association of small-molecule like-drugs into nano-entities by employing several techniques including TEM, NMR and DLS. The characterization was also assessed by CLSM to determine the cellular uptake of aggregation. As expected, some strengths and weaknesses of a set of techniques have been found, that nonetheless enabled us to detect and monitor features of aggregates at the atomic level together with morphological, physical and cellular level scales. It was observed that compounds can adopt a variety of aggregate sizes and types, which may depend on the unique fingerprints of the compound itself or environmental conditions.

Interestingly, it was found that nano-entities of several compounds can indeed enter the macrophage and neutrophils, therefore they may have properties. We then evaluated whether or not there is a correlation between these compound self-associates and an immune response. As we compare datasets to control-non-aggregator small molecules, we noted by the two cellular models and an ELISA assay that nano-entities can have respective impact on modulating and inducing immune response. Perhaps, this could be related to aggregate size and type dependent. However, the exact mechanism remains unknown. It is still unclear whether nano-entities can enter the immune cells as the monomer form and then self-associate or they enter as aggregate forms. Perhaps both exist, and the respective mechanism again remains speculative.

To better address these two questions above, further experimental studies are warranted involving the lack of having such a good monomeric form to be used as a control. Unfortunately, separating the two phases, single-monomeric and the aggregate form do not exist, which impeded such experiments. If possible, it must be done by high-speed centrifugation, but the outcomes are not guaranteed. This report will allow lead discovery and scientific community to reveal this fascinating aggregation phenomena and to better correlate their silent properties. For instance, it has been already well documented that nano-entities can result to promiscuity, false-positives in screens, toxicity, to name a few. We understand that a definitive investigation to completely address this immune response property could be quite large. We wished with our pilot study to provide a better understanding of nano-entities and their correlation with immune response, and perhaps to develop practical strategies for experimentally revealing the existence of nano-entities for drug discovery efforts.

ASSOCIATED CONTENT

Supporting information

Further data are available as Supplementary Information.

AUTHOR INFORMATION

Corresponding author

*E-mail: steven.laplante@inrs.ca. Phone: +1-514-914-8501

ACKNOWLEDGMENTS

The authors acknowledge the technical support team Jessy. Tremblay for (confocal microscopy CLSM), and the technician Arnaldo Nakamura for (electron microscopy TEM). This work was supported by NMX Research and Solutions Inc., NSERC, CQDM and PROTE

7.6 REFERENCES

1. Price, D. A.; Blagg, J.; Jones, L.; Greene, N.; Wager, T. Physicochemical drug properties associated with in vivo toxicological outcomes: a review. *Expert Opin Drug Metab Toxicol* **2009**, *5*, 921-31.
2. Cronin, M. T. *Predicting chemical toxicity and fate*. CRC press: 2004.
3. Moreira, S. G., Jr.; Brannigan, R. E.; Spitz, A.; Orejuela, F. J.; Lipshultz, L. I.; Kim, E. D. Side-effect profile of sildenafil citrate (Viagra) in clinical practice. *Urology* **2000**, *56*, 474-6.
4. Dimopoulos, M. A.; Eleutherakis-Papaiakovou, V. Adverse effects of thalidomide administration in patients with neoplastic diseases. *Am J Med* **2004**, *117*, 508-15.
5. LaPlante, S. R.; Aubry, N.; Bolger, G.; Bonneau, P.; Carson, R.; Coulombe, R.; Sturino, C.; Beaulieu, P. L. Monitoring drug self-aggregation and potential for promiscuity in off-target in vitro pharmacology screens by a practical NMR strategy. *J Med Chem* **2013**, *56*, 7073-83.
6. LaPlante, S. R.; Carson, R.; Gillard, J.; Aubry, N.; Coulombe, R.; Bordeleau, S.; Bonneau, P.; Little, M.; O'Meara, J.; Beaulieu, P. L. Compound Aggregation in Drug Discovery: Implementing a Practical NMR Assay for Medicinal Chemists. *Journal of Medicinal Chemistry* **2013**, *56*, 5142-5150.
7. Dlim, M. M.; Shahout, F. S.; Khabir, M. K.; Labonté, P. P.; LaPlante, S. R. Revealing Drug Self-Associations into Nano-Entities. *ACS Omega* **2019**, *4*, 8919-8925.
8. Seidler, J.; McGovern, S. L.; Doman, T. N.; Shoichet, B. K. Identification and prediction of promiscuous aggregating inhibitors among known drugs. *J Med Chem* **2003**, *46*, 4477-86.
9. Owen, S. C.; Doak, A. K.; Wassam, P.; Shoichet, M. S.; Shoichet, B. K. Colloidal aggregation affects the efficacy of anticancer drugs in cell culture. *ACS chemical biology* **2012**, *7*, 1429-1435.
10. Schreier, S.; Malheiros, S. V.; de Paula, E. Surface active drugs: self-association and interaction with membranes and surfactants. Physicochemical and biological aspects. *Biochim Biophys Acta* **2000**, *1508*, 210-34.
11. Beaulieu, P.; Bolger, G.; Deon, D.; Duplessis, M.; Fazal, G.; Gagnon, A.; Garneau, M.; LaPlante, S.; Stammers, T.; Kukolj, G.; Duan, J. Multi-parameter optimization of aza-follow-ups to BI 207524, a thumb pocket 1 HCV NS5B polymerase inhibitor. Part 2: Impact of lipophilicity on promiscuity and in vivo toxicity. *Bioorganic & medicinal chemistry letters* **2015**, *25*.
12. Leeson, P. D.; Springthorpe, B. The influence of drug-like concepts on decision-making in medicinal chemistry. *Nat Rev Drug Discov* **2007**, *6*, 881-90.
13. McGovern, S. L.; Helfand, B. T.; Feng, B.; Shoichet, B. K. A Specific Mechanism of Nonspecific Inhibition. *Journal of Medicinal Chemistry* **2003**, *46*, 4265-4272.

14. Frenkel, Y. V.; Clark, A. D., Jr.; Das, K.; Wang, Y. H.; Lewi, P. J.; Janssen, P. A.; Arnold, E. Concentration and pH dependent aggregation of hydrophobic drug molecules and relevance to oral bioavailability. *J Med Chem* **2005**, 48, 1974-83.
15. Ganesh, A. N.; McLaughlin, C. K.; Duan, D.; Shoichet, B. K.; Shoichet, M. S. A New Spin on Antibody-Drug Conjugates: Trastuzumab-Fulvestrant Colloidal Drug Aggregates Target HER2-Positive Cells. *ACS Appl Mater Interfaces* **2017**, 9, 12195-12202.
16. Schönmann, C.; Brockow, K. Adverse reactions during procedures: Hypersensitivity to contrast agents and dyes. *Ann Allergy Asthma Immunol* **2020**, 124, 156-164.
17. Nierkens, S.; Aalbers, M.; Bleumink, R.; Boon, L.; Pieters, R. Drug-induced type 1 and type 2 immune responses are characterized by distinct profiles of cell kinetics, cytokine production, and expression of co-stimulatory molecules in the popliteal lymph node assay. *J Immunotoxicol* **2005**, 2, 141-50.
18. Robert, C.; Soria, J. C.; Spatz, A.; Le Cesne, A.; Malka, D.; Pautier, P.; Wechsler, J.; Lhomme, C.; Escudier, B.; Boige, V.; Armand, J. P.; Le Chevalier, T. Cutaneous side-effects of kinase inhibitors and blocking antibodies. *Lancet Oncol* **2005**, 6, 491-500.
19. Agero, A. L.; Dusza, S. W.; Benvenuto-Andrade, C.; Busam, K. J.; Myskowski, P.; Halpern, A. C. Dermatologic side effects associated with the epidermal growth factor receptor inhibitors. *J Am Acad Dermatol* **2006**, 55, 657-70.
20. Hu, J. C.; Sadeghi, P.; Pinter-Brown, L. C.; Yashar, S.; Chiu, M. W. Cutaneous side effects of epidermal growth factor receptor inhibitors: clinical presentation, pathogenesis, and management. *J Am Acad Dermatol* **2007**, 56, 317-26.
21. Murugesan, J. R.; Shahout, F.; Dlim, M.; Langella, M. M.; Cuadra-Foy, E.; Forgione, P.; LaPlante, S. R. Revealing dye and dye-drug aggregation into nano-entities using NMR. *Dyes and Pigments* **2018**, 153, 300-306.
22. Durocher, I.; Noël, C.; Lavastre, V.; Girard, D. Evaluation of the in vitro and in vivo proinflammatory activities of gold (+) and gold (-) nanoparticles. *Inflamm Res* **2017**, 66, 981-992.
23. Noël, C.; Simard, J. C.; Girard, D. Gold nanoparticles induce apoptosis, endoplasmic reticulum stress events and cleavage of cytoskeletal proteins in human neutrophils. *Toxicol In Vitro* **2016**, 31, 12-22.
24. Durocher, I.; Girard, D. In vivo proinflammatory activity of generations 0-3 (G0-G3) polyamidoamine (PAMAM) nanoparticles. *Inflamm Res* **2016**, 65, 745-55.
25. Poirier, M.; Simard, J. C.; Antoine, F.; Girard, D. Interaction between silver nanoparticles of 20 nm (AgNP20) and human neutrophils: induction of apoptosis and inhibition of de novo protein synthesis by AgNP20 aggregates. *J Appl Toxicol* **2014**, 34, 404-12.

26. Simard, J. C.; Simon, M. M.; Tessier, P. A.; Girard, D. Damage-associated molecular pattern S100A9 increases bactericidal activity of human neutrophils by enhancing phagocytosis. *J Immunol* **2011**, 186, 3622-31.
27. Babin, K.; Antoine, F.; Goncalves, D. M.; Girard, D. TiO₂, CeO₂ and ZnO nanoparticles and modulation of the degranulation process in human neutrophils. *Toxicol Lett* **2013**, 221, 57-63.
28. Savoie, A.; Lavastre, V.; Pelletier, M.; Hajto, T.; Hostanska, K.; Girard, D. Activation of human neutrophils by the plant lectin *Viscum album* agglutinin-I: modulation of de novo protein synthesis and evidence that caspases are involved in induction of apoptosis. *J Leukoc Biol* **2000**, 68, 845-53.
29. Goncalves, D. M.; Girard, D. Zinc oxide nanoparticles delay human neutrophil apoptosis by a de novo protein synthesis-dependent and reactive oxygen species-independent mechanism. *Toxicol In Vitro* **2014**, 28, 926-31.
30. McGovern, S. L.; Caselli, E.; Grigorieff, N.; Shoichet, B. K. A common mechanism underlying promiscuous inhibitors from virtual and high-throughput screening. *J Med Chem* **2002**, 45, 1712-22.
31. Li, X.; Kamenecka, T. M.; Cameron, M. D. Bioactivation of the epidermal growth factor receptor inhibitor gefitinib: implications for pulmonary and hepatic toxicities. *Chem Res Toxicol* **2009**, 22, 1736-42.
32. Herbst, R. S.; LoRusso, P. M.; Purdom, M.; Ward, D. Dermatologic side effects associated with gefitinib therapy: clinical experience and management. *Clin Lung Cancer* **2003**, 4, 366-9.
33. Nardone, B.; Nicholson, K.; Newman, M.; Guitart, J.; Gerami, P.; Talarico, N.; Yang, X. J.; Rademaker, A.; West, D. P.; Lacouture, M. E. Histopathologic and immunohistochemical characterization of rash to human epidermal growth factor receptor 1 (HER1) and HER1/2 inhibitors in cancer patients. *Clin Cancer Res* **2010**, 16, 4452-60.
34. Belum, V. R.; Fontanilla Patel, H.; Lacouture, M. E.; Rodeck, U. Skin toxicity of targeted cancer agents: mechanisms and intervention. *Future Oncol* **2013**, 9, 1161-70.
35. Sugiura, Y.; Nemoto, E.; Kawai, O.; Ohkubo, Y.; Fusegawa, H.; Kaseda, S. Skin rash by gefitinib is a sign of favorable outcomes for patients of advanced lung adenocarcinoma in Japanese patients. *Springerplus* **2013**, 2, 1-5.
36. Dudek, A. Z.; Lesniewski-Kmak, K.; Koopmeiners, J.; Keshtgarpour, M. Skin rash and bronchoalveolar histology correlates with clinical benefit in patients treated with gefitinib as a therapy for previously treated advanced or metastatic non-small cell lung cancer. *Lung cancer* **2006**, 51, 89-96.

37. Chen, K.-L.; Lin, C.-C.; Cho, Y.-T.; Yang, C.-W.; Sheen, Y.-S.; Tsai, H.-E.; Chu, C.-Y. Comparison of Skin Toxic Effects Associated With Gefitinib, Erlotinib, or Afatinib Treatment for Non–Small Cell Lung Cancer. *JAMA Dermatology* **2016**, *152*, 340-342.
38. Togashi, Y.; Masago, K.; Hamatani, Y.; Sakamori, Y.; Nagai, H.; Kim, Y. H.; Mishima, M. Successful erlotinib rechallenge for leptomeningeal metastases of lung adenocarcinoma after erlotinib-induced interstitial lung disease: a case report and review of the literature. *Lung Cancer* **2012**, *77*, 464-468.
39. Segal, S.; Van Cutsem, E. Clinical signs, pathophysiology and management of skin toxicity during therapy with epidermal growth factor receptor inhibitors. *Annals of oncology* **2005**, *16*, 1425-1433.
40. Miyake, K.; Tani, K.; Kakiuchi, S.; Suzuka, C.; Toyoda, Y.; Kishi, J.; Tezuka, T.; Yuasa, S.; Hanibuchi, M.; Aono, Y.; Nishioka, Y.; Sone, S. Epidermal growth factor receptor-tyrosine kinase inhibitor (gefitinib) augments pneumonitis, but attenuates lung fibrosis in response to radiation injury in rats. *J Med Invest* **2012**, *59*, 174-85.
41. Noguchi, T.; Sekiguchi, Y.; Kudoh, Y.; Naganuma, R.; Kagi, T.; Nishidate, A.; Maeda, K.; Ishii, C.; Toyama, T.; Hirata, Y.; Hwang, G. W.; Matsuzawa, A. Gefitinib initiates sterile inflammation by promoting IL-1 β and HMGB1 release via two distinct mechanisms. *Cell Death Dis* **2021**, *12*, 49.
42. Maemondo, M.; Inoue, A.; Kobayashi, K.; Sugawara, S.; Oizumi, S.; Isobe, H.; Gemma, A.; Harada, M.; Yoshizawa, H.; Kinoshita, I.; Fujita, Y.; Okinaga, S.; Hirano, H.; Yoshimori, K.; Harada, T.; Ogura, T.; Ando, M.; Miyazawa, H.; Tanaka, T.; Saijo, Y.; Hagiwara, K.; Morita, S.; Nukiwa, T. Gefitinib or chemotherapy for non-small-cell lung cancer with mutated EGFR. *N Engl J Med* **2010**, *362*, 2380-8.
43. Inoue, A.; Saijo, Y.; Maemondo, M.; Gomi, K.; Tokue, Y.; Kimura, Y.; Ebina, M.; Kikuchi, T.; Moriya, T.; Nukiwa, T. Severe acute interstitial pneumonia and gefitinib. *Lancet* **2003**, *361*, 137-9.
44. Zhang, Y.; Lee, T. C.; Guillemin, B.; Yu, M. C.; Rom, W. N. Enhanced IL-1 beta and tumor necrosis factor-alpha release and messenger RNA expression in macrophages from idiopathic pulmonary fibrosis or after asbestos exposure. *J Immunol* **1993**, *150*, 4188-96.
45. Ishii, H.; Mukae, H.; Kadota, J.; Fujii, T.; Abe, K.; Ashitani, J.; Kohno, S. Increased levels of interleukin-18 in bronchoalveolar lavage fluid of patients with idiopathic nonspecific interstitial pneumonia. *Respiration* **2005**, *72*, 39-45.
46. Friedman, M. D.; Lacouture, M.; Dang, C. Dermatologic Adverse Events Associated With Use of Adjuvant Lapatinib in Combination With Paclitaxel and Trastuzumab for HER2-Positive Breast Cancer: A Case Series Analysis. *Clin Breast Cancer* **2016**, *16*, e69-74.

47. Ayotte, Y.; Marando, V. M.; Vaillancourt, L.; Bouchard, P.; Heffron, G.; Coote, P. W.; Larda, S. T.; LaPlante, S. R. Exposing Small-Molecule Nanoentities by a Nuclear Magnetic Resonance Relaxation Assay. *Journal of Medicinal Chemistry* **2019**, 62, 7885-7896.

7.7 SUPPLEMENTARY INFORMATION

S1. Probing the Solution Behavior of Colloidal Aggregates Using T2-CPMG

Characterization of aggregates and non-aggregates were also carried out by practical NMR methods. Of course, most compounds behave differently in organic solvents as compared to aqueous solutions, and therefore, the three-phase equilibrium remained largely unexplored. Here, we used NMR aggregation assay based on spin-spin T2-CPMG relaxation assay to determine the presence of nano-entities and aggregates in aqueous buffer (Fig 1S). The NMR spectra acquired in phosphate buffer at 200 μ M nominal concentration. As illustrated, there were notable slow tumbling rate and no resonance for the two compounds Lapatinib and Erlotinib. These observations were consistent with a behavior of self-association into small larger/hard aggregates. On the other hand, more sharper NMR resonance are noted for gefitinib in aqueous media as compared to Lapatinib and Erlotinib. However, by taking the difference in peak area between the spectra with 1 ms and 800 ms, there are relatively observable signal decay of intensity for the aromatic resonances of the drug. Such these observations are indicative of the presence of nano-entities. Both Lapatinib and Gefitinib are two well-known aggregators as previously reported. Interestingly, in the example of Riluzole, each molecule is distal to one another, tumbles so freely and no signal decay of intensity was noticed with increasing spin-echo delay times. The T2-CPMG spectra of the drug in aqueous buffer exhibits long T2-CPMG relaxation times indicating the existence of non-aggregate like form.

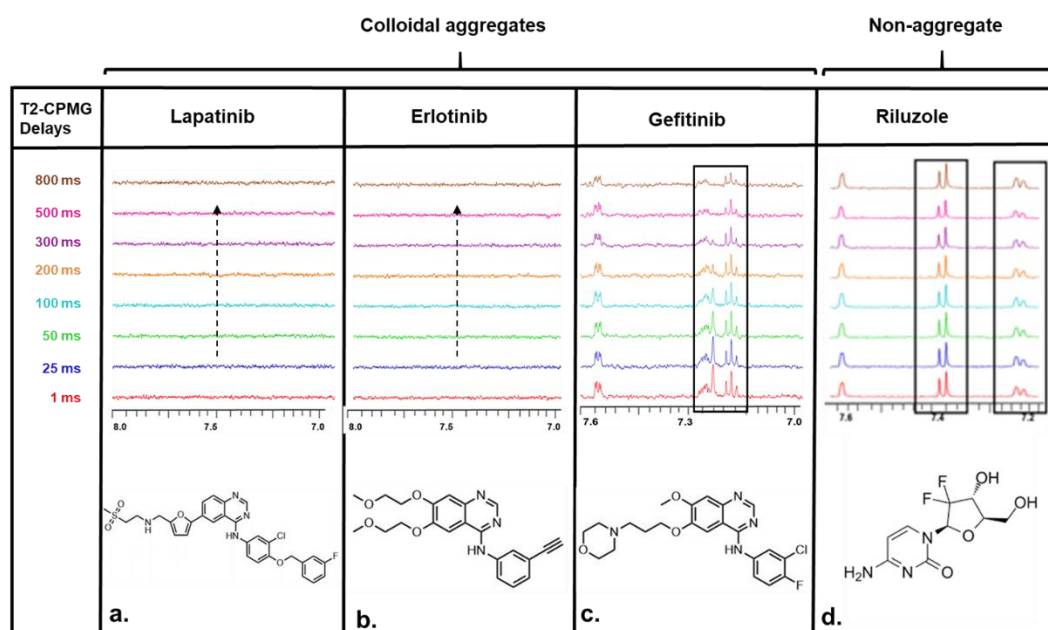


Figure S1: Shown are T2-CPMG Assay of three anticancer drugs (Lapatinib, Erlotinib and Gefitinib) (a, b, c), and an amyotrophic lateral sclerosis (Riluzole) (d) in phosphate buffer.

S2. Probing the solution behavior of colloidal dye-aggregates in buffered-HPLC using DLS

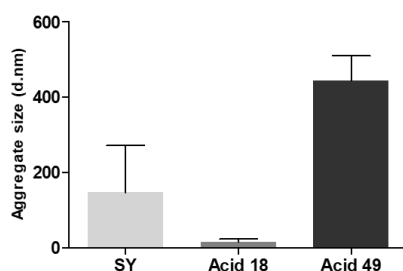


Figure S2. Particle size for colloidal dye aggregates by DLS

S3. Cellular Uptake of Acid49 Dye by Human Neutrophils

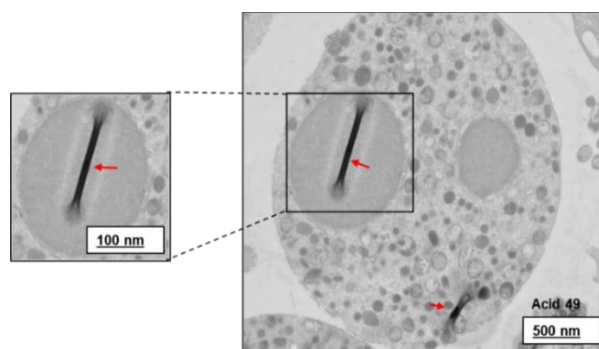


Figure S3. Cellular uptake of Acid49 aggregates by human neutrophils.

S4. Effects of Compound Aggregation on the Production of Other Cytokines (IL-6) Using Murine Macrophage RAW 264.7

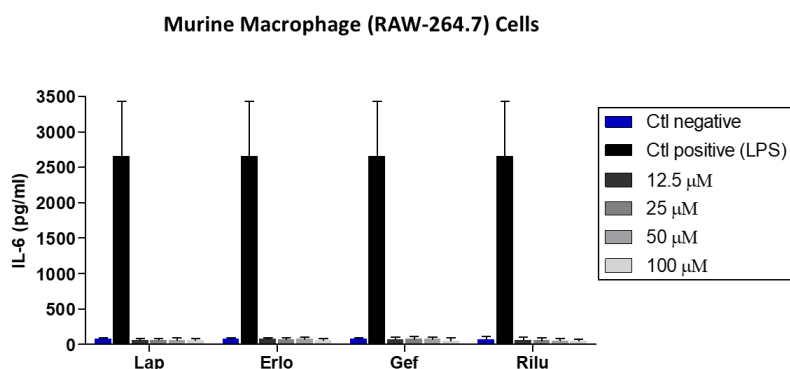


Figure S4. Effects of compound aggregation on the production of IL-6 using Macrophage RAW 264.7.

Cells were incubated in the presence of drug aggregates and non-aggregate or LPS (Ctrl positive) and (non-treated negative control) for 24 h and the supernatants were harvested and used for the detection of the indicated cytokines by ELISA assay as described in “Materials and methods”.

S5. Effects of Compound Aggregation on the Production of Other Cytokines (IL-6) Using Neutrophils

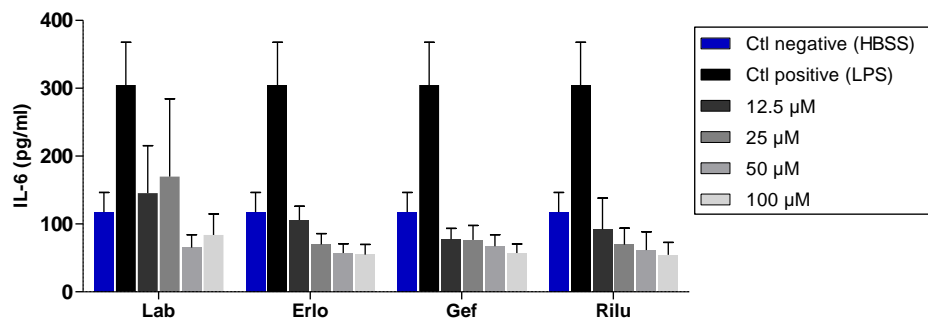


Figure S5. Effects of compound aggregation on the production of IL-6 using neutrophil cells.

Cells were incubated with drug aggregates and non-aggregate or LPS (Ctrl positive) and HBSS (negative control) for 24 h and the supernatants were harvested and used for the detection of the indicated cytokines by ELISA assay as described in “Materials and methods”.

S6. Effects of Dye Aggregation on the Production of Other Cytokines (IL-6) Using Neutrophils

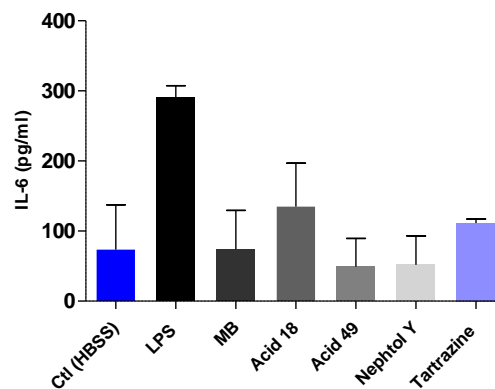


Figure S6. Effects of dye aggregation on the production of IL-6 using human neutrophils.

Cells were incubated in the presence of dye aggregates and non-aggregate or LPS (Ctrl positive) and HBSS (Ctrl negative) for 24 h and the supernatants were harvested and used for the detection of the indicated cytokines by ELISA assay as described in “Materials and methods”

8 GENERAL DISCUSSION

Compound aggregation ‘nano-entities’ has been correlated with properties that can have a significant impact on drug discovery efforts. Aggregation can be implicated in 85–95% false positive hits in HTS and false negative in cell penetration assays (Feng *et al.*, 2007; McGovern *et al.*, 2002a; Owen *et al.*, 2012a; Seidler *et al.*, 2003; Shoichet, 2006). In addition, recent studies have found that nano-entities, can somehow predispose them to some undesirable attributes and side effects, such as *in vivo* toxicity (Kola & Landis, 2004; Kramer *et al.*, 2007; Krejsa *et al.*, 2003), promiscuity, etc (Azzaoui *et al.*, 2007; LaPlante *et al.*, 2013a). Despite these reports, the correlated properties of nano-entities remained largely unexplored. This is due to the fact that each compound has its own/unique fingerprints and equilibrium which are highly dependent on various conditions such as temperature, solutions, pH, etc (Frenkel *et al.*, 2005; Ma *et al.*, 2016; Rao *et al.*, 2010). Also, the situation can be complicated by the limited detection techniques that can help to explore the existence of nano-entities and reveal their full range of sizes and types. These issues unfortunately have caused serious “gaps” in the pharmaceutical industry, which can have significant impact on all drug discovery and development stages. To date, still there is no single method that can fully characterize aggregation and detect their full range of physical features including sizes and types, given that this peculiar phenomenon remained poorly understood (LaPlante *et al.*, 2013a). In this regard, this thesis focused on characterizing these fascinating nano-entities and fully reveal their attributes at the biophysical and cellular levels. Owing to the multiple properties that nano-entities can be correlated with, this thesis hypothesized that nano-entities could be implicated in side-effects related to immune responses.

Characterizing and revealing compound aggregation

All compounds can adopt a multi-phase solution behavior. When a compound place in aqueous solution, it can exist as three phase equilibria between soluble lone molecule, intermediate soluble self-associated nano-entities or solid amorphous precipitates. Initially, we investigated compound tri-phasic solution behaviors, with an emphasis on the intermediate phase “nano-entities”. Whereas the precipitate phase can be easily detected by the naked eye, the single lone molecule and the aggregate phases cannot be apparent. This is due to the limitation of detection methods that can fully expose the solution three-phase equilibria. DLS, for example, is a practical method that can only detect homogeneous and large aggregates, but smaller nano-entities would not be visible.

As discussed in the literature review, the full range of physical features of nano-entities including size and type remained poorly understood. In this regard, the objective focused on better characterizing these nano-entities using new sets of compounds ‘dyes’ and better

analyze their aggregate size using NMR. We began our investigations with dyes since they are highly prevalent in our society and extensively consumed. Interestingly, we found that some dyes can exist as soluble-lone molecules, while others can aggregate into a variety of aggregate sizes. For dyes that are not aggregating, normal NMR trends are expected. For example, dye molecules should tumble so freely in the solution and not affected by increasing the concentrations. Other features that are also expected with non-aggregating molecules include sharp resonances, no spectral shift left or right and no changes in the resonance number. On the other hand, for aggregating dye molecules, unusual NMR trends are expected. This includes broad resonances, chemical resonance shift upon increasing the concentration and changes in the resonance number. Keep in mind that the resonance intensities are expected for both non-aggregating and aggregating molecules which is the result of dilutions.

Since aggregate-property relationships can exist, in this thesis we also explored the potential correlations of aggregation tendencies of dyes with structure nano-entity relationship (SNR). Interestingly, we found that some dyes including (Sunset yellow, Allura red and Orange II) which are highly related in their chemical structure, can all expose unusual NMR trends and all form different sizes of nano-entities. Given that SNR property can indeed exist. Of course, further studies are needed to elucidate SNR trends with new sets of structurally similar compounds.

Since dyes are used in a variety of applications in our society, we wondered whether there have been direct interactions of aggregating dyes with medical drugs as a property of nano-entities. Unfortunately, only a few reports addressed drug-dye interactions, and as a result a detailed important information is lacking. In my thesis, we addressed this potential property using NMR tool. We added Quetiapine drug, that is widely used to treat schizophrenia to Congo red nano-entities. The NMR spectra of Quetiapine showed sharp and normal trends of non-aggregating molecule, whereas Congo red spectra showed unusual trends of aggregation. Surprisingly, when both compounds are mixed, the Quetiapine exhibited very broad resonance. Therefore, it is apparent that there should be interactions between Quetiapine and Congo red entities. In other words, we found that aggregates could have direct impacts on the behavior of other molecules, and this could further highlight the use of NMR as a practical tool for studying direct drug-drug or dye-drug interactions. Taken together, the employed NMR dilution assay can be a feasible strategy to monitor the solution behaviors of dyes and to further understand their unfavorable properties such as off-target promiscuity and toxicity or their favorable properties such as drug encapsulation, carriers and delivery systems.

Again, one of the main issues that hindered drug discovery and pharmaceutical industry from properly characterizing nano-entities is insufficient detection techniques. To date, no single strategy can fully expose all the physical features of compounds including sizes, shapes

and types that can exist. For example, our introduced NMR technique can reveal the existence of nano-entities that drugs can adopt and reveal their small to large sizes, but it can not detect their morphological features and types. In this regard, we employed TEM to expose the presence of self-assemblies in different aqueous conditions such as phosphate buffer, cell culture medium with and without FBS. We found that all drugs can form colloidal aggregates in the three conditions. However, there was a variety of aggregate sizes ranging from small to large. For example, we found that clofazimine can form smaller nano-entities compare to Fulvestrant, Sorafenib, and Lapatinib that formed larger globs in buffer. Interestingly, solid-like forms are noted for Gefitinib. Dramatic changes in the aggregates are observed when drugs are dissolved in cell culture medium with and without FBS. This can demonstrate that compound aggregation is highly dependent on its environmental conditions.

We then decided to confirm the presence of aggregates and determine the impact of detergents on large nano-entities that can exist. For samples that are suspected to form large self-assemblies, detergent strategy is now widely accepted in biochemical assays and can somehow be used to identify false-positive hits in HTS assays. Thus, we used TEM to expose the breakup of drug aggregates by the addition of detergents. For this purpose, we used Tween 80 at (0.025% v/v) that showed no toxicity as reported by other studies (Owen *et al.*, 2012a). Surprisingly, the addition of Tween 80 seriously disrupted drug aggregates (Lapatinib and Clofazimine). Interestingly, 1 HNMR experiment in which we added Tween 80 to aggregates, was consistent with TEM changes which resulted to the break up of aggregates into smaller nan-entities. However, although TEM clearly showed disruption of Sorafenib large aggregates upon the addition of Tween 80, the 1H NMR experiment did not prove that. This could demonstrate the existence of some aggregate types that cannot be detected by NMR and TEM. Again, this could also demonstrate that each compound assumes its own attributes of self-associations which is also dependent on many other conditions.

Due to the assumptions that compound aggregates can not diffuse through cell membrane nor exist in plasma, we set out here a protocol using confocal microscopy to evaluate if aggregation can exist within the cells (second objective). Indeed, this can be used as a tool to study compound aggregation at the cellular level. Initially, we focused on studying two drugs (Lapatinib and Clofazimine) and one dye (Light Green SF Yellowish) that can fluoresce at distinct range of wavelengths which can be detected by confocal microscopy. We found that all three compounds can exist within the cells and localized within the cytoplasm for Lapatinib and Light Green SF Yellowish. However, we observed strong fluorescence signals related to Clofazimine arising from both cytoplasm and nucleus. To better characterize the existence of aggregation within the cells, we employed a higher resolution USEM as a complementary method. We found that distinct dark self-assemblies of Lapatinib, Clofazimine

and Light green SF yellowish were clearly observable within the cytoplasm of HeLa cells compare to non-treated control. Interestingly, the size and distribution of these self-assemblies appeared to be consistent with the aggregation observed by TEM in buffer and media. These results suggests that compound aggregation can exist within cells. However, additional investigations are needed to elucidate if aggregation cross cell membrane through one of entry mechanisms or they accumulate after cell entry.

Based on these findings, in our third objective, we launched a protocol that will enable scientists to expose and monitor the self-aggregation of their libraries of compounds. Initially, the protocol begins with screening compounds by simple ¹H NMR assay, and then based on the results, dilution assay by NMR, T2-CPMG and NMR detergent assay are subsequently used to better monitor the solution behavior and differentiate between single-lone molecules, soluble small nano-entities and also large micelle-like colloids. Further, we used the three orthogonal methods (DLS, TEM and CLSM) to expose any larger aggregates and to confirm the presence of them. This suggests that our protocol to detect compound self-aggregation can allow the scientific community to evaluate their small-molecule libraries within days.

8.2. Aggregation induce immune response

Once the detection techniques are implemented, studies begin to correlate nano-entities with their respective properties. To date, the pharmaceutical industry initiatives have established that correlated properties of aggregation can have a significant impact on drug discovery and development stages. As mentioned above, nano-entities can have undesirable properties such as toxicity (Kola & Landis, 2004) and promiscuity (LaPlante *et al.*, 2013a; McGovern *et al.*, 2002a). They can also be correlated with desirable properties such as improved bioavailability (Frenkel *et al.*, 2005; Volovik Frenkel *et al.*, 2009), drug encapsulation and delivery systems. However, other correlated properties of nano-entities such as the effect on immune response might exist but they are waiting for the development of robust evaluation strategies and support from the pharmaceutical industry.

In the fourth objective, we proceeded to reveal whether the unusual free-state behavior of drugs can be implicated in side-effects related to immune responses. We wondered if the natural tendencies for several compounds to self-associate into small-to-large nano-entities can trigger an immune response. Perhaps the size range of aggregates that might be recognized by antibodies should be within an acceptable range and thus stimulate a defensive response. It is well-understood that an extensive and large study would be needed to fully address this question. However, we opted to launch a pilot study to explore the possible correlations of nano-entities with immune response if exist. Our hypothesis was based on unexplained observations that some small molecules such as drugs and dyes have been

widely associated with immune mediated-hypersensitivity reactions (Nierkens *et al.*, 2005; Schönmann & Brockow, 2020). These reactions include dermatologic side-effects such as redness, rashes, allergies, anaphylaxis events and many others (Agero *et al.*, 2006; Hu *et al.*, 2007; Robert *et al.*, 2005). Others have also noted correlations with toxicity (LaPlante *et al.*, 2013a; LaPlante *et al.*, 2013b).

Initially, we investigated the correlation of these peculiar nano-entities with immune response. We used a selection of well-known aggregator and non-aggregator of drugs and dyes as model systems such as anticancer drugs and synthetic dyes. We carefully characterized their self-aggregation attributes and determined their ingestion by macrophage and neutrophil cells. We then evaluated the immune response to nano-entities by studying the activation of the immune cells and the production of several cytokine profiles *in vitro*. Our results showed that drugs and dyes that naturally tend to aggregate such as Gefitinib, Erlotinib, Methylene blue and Acid 49 can somehow induce an immune response at some concentrations. This effect was comparable to non-aggregators Riluzole, Tartarazine and Nephthol yellow that showed no production of cytokine levels either TNF- α or IL-8. To our surprise, no increase in the level of both cytokines was observed by the well-known aggregator Lapatinib in either macrophage or neutrophils cells. Thus, it is evident yet surprising that the three aggregators (Lapatinib, Erlotinib and Gefitinib) have very distinct solution behaviors, sizes and even aggregate types. Thus, mediating the immune system and related effects should be variable, and each compound and its multi-phase equilibria should have its unique fingerprints and properties that reflect its influence on the *in vitro* immune system and related events. Similar to drugs, an increase in IL-8 level as a biomarker of immune response was observed by the two aggregator dyes (Methylene blue and Acid 49) but no induction was seen after incubation with the aggregator (Acid 18). Again, this can indicate that compound aggregation is highly dependent on the unique properties of the compound itself and its surrounding environment. Perhaps, this would further need to be corroborated by other extensive studies and verifications—for example, western blot observation.

In chapters 2 and 4, we used small-molecules candidates that are most prone to aggregate such anticancer drugs. The chemotherapeutic drugs are usually tested as antiproliferative agents at concentrations above their CACs as reported by (Owen *et al.*, 2012a). Most of chemotherapeutic drugs are administered intramuscularly (IM) or intravenously (IV). The antiproliferative effects of these anticancers in relevant cell lines according to their mechanism of action has been reported. For example, MDA-MB-23 cells was treated with Lapatinib aggregates at a concentration of (100 μ M) and the inhibition of cancer growth was essentially eliminated (Owen *et al.*, 2012a). Using our cells, we

characterized and better understood the associated properties of nano-entities in physiological conditions.

9 CONCLUSIONS

Compounds can naturally adopt into an amazing multi-state equilibrium when placed in aqueous solution. The principle states of this equilibrium can be classified as, (1) soluble-lone tumbling molecules, (2) soluble self-assembled nano-entities, and (3) solid amorphous precipitates. In this thesis, the fascinating world of nano-entities was explored. Our investigations indeed found that drugs can adopt some amazing and unique free-state behaviors when placed in solution. These studies were carried out by specialized techniques including NMR, TEM, DLS and CLSM. Expectedly, we found some strengths and weaknesses of the techniques we used, that nonetheless enabled us to detect aggregation at the atomic and micrometer scales.

This dissertation introduced the NMR dilution assay to monitor compound aggregation in the solution using dyes as model systems. Our studies indeed found that dyes can adopt a variety of aggregate sizes and types ranging from small to large aggregates when placed in buffer solution. The utility of this tool is to correlate nano-entities with their potential associated properties. Some of these properties are well-known such as off-target promiscuity and even toxicity. This thesis also explored the existence of SAR trends when interestingly found that some highly related structure dyes can expose similar unusual NMR trends. However, further SAR studies need to be elucidated with new sets of structurally similar compounds. In addition, NMR tool led to the finding that nano-entities can have direct impacts on the behavior of other drugs and there is indeed a direct interaction between dye nano-entities and some FDA medical drugs. This has been eventually correlated as properties of nano-entities.

Further, we observed these fascinating nano-entities using specialized techniques such as TEM. Our studies by TEM suggested that compounds can adopt a variety of aggregate sizes, types and shapes, which may depend on the unique fingerprints of the compound itself or on the solution and environmental conditions. Further, CLSM was used as a tool to monitor nano-entities at the cellular level. Interestingly, our experiments showed that nano-entities can enter and accumulate within cells. Of course, this depends on the aggregate itself and type of cells. The entry of nano-entities was further studied by a higher resolution method such as thin-section electron microscopy, which confirmed that nano-entities can exist within the cells and have properties. However, the mechanism by which aggregates enter cells remains elusive.

Indeed, drug solution behaviors can significantly affect their silent properties. Therefore, based on our finding to detect nano-entities, this thesis established a protocol that will enable researchers and scientific community to properly evaluate the multiphase equilibrium of

libraries of compounds, with an emphasis on the fascinating intermediate nano-entity phase. Indeed, the full range of nano-entities that compounds can adopt when placed in aqueous solution has been well explored in this thesis. Examples and workflows on how to detect the three phases of solution behavior and the fascinating nano-entities phase have been well described.

This thesis established a platform of techniques, which will help the scientific community in a greater understanding of nano-entities and their associated properties. For instance, nano-entities have already been correlated with off-target promiscuity, false positives and toxicity. Other silent properties of nano-entities such as immune response has been demonstrated *in vitro* by our results using murine macrophage and human neutrophil models. Our hypothesis suggests that there might be an association between the existence of nano-entities and immune response. Given the increase in the two biomarkers IL-8 and TNF- α , our pilot study suggested that some drug or dye nano-entities can be correlated with immune response. Interestingly, this increase has not been observed by non-aggregator drugs and dyes. Also, some medium to large nano-entities of drugs and dyes have not shown to elevate the level of IL-8 and TNF- α , given that inducing an immune response might be aggregation dependant. Indeed, further investigations to fully study these correlations need to be pursued on a larger scale with robust strategies, given the importance and potential influence of small molecule-induced immune-related side-effects.

In conclusion, our finding has significantly increased our understanding of nano-entities and their associated properties. In addition, this research introduced potential tools that will help the scientific community, experts and even non-experts, to explore the peculiar solution behavior of many compounds and monitor the nano-entities. The two proposed immune cell models can be potential models to study other biomarkers to advance our understanding of the correlation of nano-entities with immune response-related side effects.

10 PERSPECTIVES

In our research, we have shown that drugs can self-assemble in a variety of particle sizes when placed in aqueous solution. The practical techniques presented in this work can provide considerable information on compound nano-entities. They can be used as higher-throughput screening assays, given that the analysis requires only a single sample per compound or drug. For example, in our lab, we have used simple NMR and T2 CPMG methods as high-throughput to analyze thousands of compounds, including fragments and drugs under different solution conditions. It is anticipated that NMR aggregation assays will help drug discovery initiatives to reveal wide range of nano-entities.

Of course, no single technique can fully expose all the features of nano-entities including size, type, shape and distribution. In this regard, we employed other strategies including TEM, DLS and CLSM to fully characterize nano-entities at different scales and under different solution conditions. Indeed, advantages and disadvantages must exist. However, employing other techniques such as nano-particle tracking analyzer (NTA) might provide a more complete picture of nano-entities and their existence in aqueous solutions. The nano-site tracking analyzer is a higher resolution strategy that can provide information of size distribution and concentration. Moreover, a visual picture of nano-entities and validation can be produced with high quality.

With regards to the presence of aggregates within the cells, future experiments are important to address their mechanism of entry. In addition, it has still not been clarified whether aggregates enter live cells as a monomer and then accumulate or enter as aggregate form. Further studies are required to resolve these questions. With respect to the properties of nano-entities, our study looked into their impact on the immune response and their correlations with side-effects, but there is still much to be learned about this property. Also, it is still not clear whether the size and/or the type of nano-entities play the key role in inducing the immune response. So, in future experiments, use of more well-known aggregators could be useful to determine the correlation of nano-entities and immune response with respect to their sizes/types. In addition, future experiments using different *in vitro* and *in vivo* models and more potential biomarkers are also required to confirm such this effect. Of course, this will provide a more detailed and complete overview of the existence of nano-entities and their impact on the immune system *in vivo*. A murine air pouch is a potential model to study whether or not our aggregates can possess proinflammatory response by themselves (Durocher & Girard, 2016). This study indeed will need a potential non-aggregate control from the same family of drug aggregates.

Indeed, a clear understanding of nano-entities could finally help promote the safety of compounds with minimizing undesirable properties. They may also serve as drug carriers and delivery systems. This later property can be another amazing future area of nano-entities to address the issue of drug loading and improve bioavailability, selectivity and effectiveness of a drug.

11 BIBLIOGRAPHY

- Adler-Abramovich L, Vaks L, Carny O, Trudler D, Magno A, Caflich A, Frenkel D & Gazit E (2012) Phenylalanine assembly into toxic fibrils suggests amyloid etiology in phenylketonuria. *Nat Chem Biol* 8(8):701-706.
- Agero AL, Dusza SW, Benvenuto-Andrade C, Busam KJ, Myskowski P & Halpern AC (2006) Dermatologic side effects associated with the epidermal growth factor receptor inhibitors. *J Am Acad Dermatol* 55(4):657-670.
- Allen SJ, Dower CM, Liu AX & Lumb KJ (2020) Detection of Small-Molecule Aggregation with High-Throughput Microplate Biophysical Methods. *Current protocols in chemical biology* 12(1):e78.
- Ayotte Y, Marando VM, Vaillancourt L, Bouchard P, Heffron G, Coote PW, Larda ST & LaPlante SR (2019) Exposing Small-Molecule Nanoentities by a Nuclear Magnetic Resonance Relaxation Assay. *J Med Chem* 62(17):7885-7896.
- Azzaoui K, Hamon J, Faller B, Whitebread S, Jacoby E, Bender A, Jenkins JL & Urban L (2007) Modeling promiscuity based on in vitro safety pharmacology profiling data. *ChemMedChem* 2(6):874-880.
- Babin K, Antoine F, Goncalves DM & Girard D (2013) TiO₂, CeO₂ and ZnO nanoparticles and modulation of the degranulation process in human neutrophils. *Toxicol Lett* 221(1):57-63.
- Bender A, Scheiber J, Glick M, Davies JW, Azzaoui K, Hamon J, Urban L, Whitebread S & Jenkins JL (2007) Analysis of pharmacology data and the prediction of adverse drug reactions and off-target effects from chemical structure. *ChemMedChem* 2(6):861-873.
- Bleicher KH, Böhm H-J, Müller K & Alanine AI (2003) Hit and lead generation: beyond high-throughput screening. *Nature reviews Drug discovery* 2(5):369-378.
- Chan LL, Lidstone EA, Finch KE, Heeres JT, Hergenrother PJ & Cunningham BT (2009) A Method for Identifying Small-Molecule Aggregators Using Photonic Crystal Biosensor Microplates. *JALA Charlottesv Va* 14(6):348-359.
- Coan KE, Maltby DA, Burlingame AL & Shoichet BK (2009) Promiscuous aggregate-based inhibitors promote enzyme unfolding. *Journal of medicinal chemistry* 52(7):2067-2075.
- Coan KE & Shoichet BK (2008) Stoichiometry and physical chemistry of promiscuous aggregate-based inhibitors. *Journal of the American Chemical Society* 130(29):9606-9612.
- Cronin MT (2004) *Predicting chemical toxicity and fate*. CRC press,
- D'Addio SM & Prud'homme RK (2011) Controlling drug nanoparticle formation by rapid precipitation. *Adv Drug Deliv Rev* 63(6):417-426.
- DeWitte RS (2006) Avoiding physicochemical artefacts in early ADME-Tox experiments. *Drug discovery today* 11(17-18):855-859.
- Doak AK, Wille H, Prusiner SB & Shoichet BK (2010) Colloid formation by drugs in simulated intestinal fluid. *Journal of medicinal chemistry* 53(10):4259-4265.
- Duan D, Doak AK, Nedyalkova L & Shoichet BK (2015) Colloidal aggregation and the in vitro activity of traditional Chinese medicines. *ACS Chem Biol* 10(4):978-988.
- Durocher I & Girard D (2016) In vivo proinflammatory activity of generations 0-3 (G0-G3) polyamidoamine (PAMAM) nanoparticles. *Inflamm Res* 65(9):745-755.
- Durocher I, Noël C, Lavastre V & Girard D (2017) Evaluation of the in vitro and in vivo proinflammatory activities of gold (+) and gold (-) nanoparticles. *Inflamm Res* 66(11):981-992.
- Feng BY, Shelat A, Doman TN, Guy RK & Shoichet BK (2005) High-throughput assays for promiscuous inhibitors. *Nat Chem Biol* 1(3):146-148.
- Feng BY & Shoichet BK (2006a) A detergent-based assay for the detection of promiscuous inhibitors. *Nature protocols* 1(2):550-553.
- Feng BY & Shoichet BK (2006b) A detergent-based assay for the detection of promiscuous inhibitors. *Nat Protoc* 1(2):550-553.

- Feng BY, Simeonov A, Jadhav A, Babaoglu K, Inglese J, Shoichet BK & Austin CP (2007) A high-throughput screen for aggregation-based inhibition in a large compound library. *J Med Chem* 50(10):2385-2390.
- Feng J, Zeng Y, Ma C, Cai X, Zhang Q, Tong M, Yu B & Xu P (2006) The surfactant tween 80 enhances biodesulfurization. *Appl Environ Microbiol* 72(11):7390-7393.
- Frenkel YV, Clark AD, Jr., Das K, Wang YH, Lewi PJ, Janssen PA & Arnold E (2005) Concentration and pH dependent aggregation of hydrophobic drug molecules and relevance to oral bioavailability. *J Med Chem* 48(6):1974-1983.
- Ganesh AN, Donders EN, Shoichet BK & Shoichet MS (2018) Colloidal aggregation: from screening nuisance to formulation nuance. *Nano Today* 19:188-200.
- Ganesh AN, Logie J, McLaughlin CK, Barthel BL, Koch TH, Shoichet BK & Shoichet MS (2017a) Leveraging Colloidal Aggregation for Drug-Rich Nanoparticle Formulations. *Mol Pharm* 14(6):1852-1860.
- Ganesh AN, McLaughlin CK, Duan D, Shoichet BK & Shoichet MS (2017b) A New Spin on Antibody-Drug Conjugates: Trastuzumab-Fulvestrant Colloidal Drug Aggregates Target HER2-Positive Cells. *ACS Appl Mater Interfaces* 9(14):12195-12202.
- Gaudin A, Yemisci M, Eroglu H, Lepetre-Mouelhi S, Turkoglu OF, Dönmez-Demir B, Caban S, Sargon MF, Garcia-Argote S, Pieters G, Loreau O, Rousseau B, Tagit O, Hildebrandt N, Le Dantec Y, Mougin J, Valetti S, Chacun H, Nicolas V, Desmaële D, Andrieux K, Capan Y, Dalkara T & Couvreur P (2014) Squalenoyl adenosine nanoparticles provide neuroprotection after stroke and spinal cord injury. *Nat Nanotechnol* 9(12):1054-1062.
- Giannetti AM, Koch BD & Browner MF (2008) Surface plasmon resonance based assay for the detection and characterization of promiscuous inhibitors. *Journal of medicinal chemistry* 51(3):574-580.
- Hu JC, Sadeghi P, Pinter-Brown LC, Yashar S & Chiu MW (2007) Cutaneous side effects of epidermal growth factor receptor inhibitors: clinical presentation, pathogenesis, and management. *J Am Acad Dermatol* 56(2):317-326.
- Hughes JD, Blagg J, Price DA, Bailey S, DeCrescenzo GA, Devraj RV, Ellsworth E, Fobian YM, Gibbs ME & Gilles RW (2008) Physicochemical drug properties associated with in vivo toxicological outcomes. *Bioorganic & medicinal chemistry letters* 18(17):4872-4875.
- Ilevbare GA & Taylor LS (2013) Liquid-liquid phase separation in highly supersaturated aqueous solutions of poorly water-soluble drugs: implications for solubility enhancing formulations. *Crystal growth & design* 13(4):1497-1509.
- J Edwards P & Sturino C (2011) Managing the liabilities arising from structural alerts: a safe philosophy for medicinal chemists. *Current medicinal chemistry* 18(20):3116-3135.
- Jackson MJ, Toth SJ, Kestur US, Huang J, Qian F, Hussain MA, Simpson GJ & Taylor LS (2014) Impact of polymers on the precipitation behavior of highly supersaturated aqueous danazol solutions. *Mol Pharm* 11(9):3027-3038.
- Kalgutkar AS, Fate G, Didiuk MT & Bauman J (2008) Toxicophores, reactive metabolites and drug safety: when is it a cause for concern? *Expert review of clinical pharmacology* 1(4):515-531.
- Kim S, Shi Y, Kim JY, Park K & Cheng JX (2010) Overcoming the barriers in micellar drug delivery: loading efficiency, in vivo stability, and micelle-cell interaction. *Expert Opin Drug Deliv* 7(1):49-62.
- Kola I & Landis J (2004) Can the pharmaceutical industry reduce attrition rates? *Nat Rev Drug Discov* 3(8):711-715.
- Kramer JA, Sagartz JE & Morris DL (2007) The application of discovery toxicology and pathology towards the design of safer pharmaceutical lead candidates. *Nat Rev Drug Discov* 6(8):636-649.
- Krejsa CM, Horvath D, Rogalski SL, Penzotti JE, Mao B, Barbosa F & Migeon JC (2003) Predicting ADME properties and side effects: the BioPrint approach. *Curr Opin Drug Discov Devel* 6(4):470-480.

- LaPlante SR, Aubry N, Bolger G, Bonneau P, Carson R, Coulombe R, Sturino C & Beaulieu PL (2013a) Monitoring drug self-aggregation and potential for promiscuity in off-target in vitro pharmacology screens by a practical NMR strategy. *J Med Chem* 56(17):7073-7083.
- LaPlante SR, Carson R, Gillard J, Aubry N, Coulombe R, Bordeleau S, Bonneau P, Little M, O'Meara J & Beaulieu PL (2013b) Compound Aggregation in Drug Discovery: Implementing a Practical NMR Assay for Medicinal Chemists. *Journal of Medicinal Chemistry* 56(12):5142-5150.
- Li N, Gilpin CJ & Taylor LS (2017) Understanding the Impact of Water on the Miscibility and Microstructure of Amorphous Solid Dispersions: An AFM-LCR and TEM-EDX Study. *Mol Pharm* 14(5):1691-1705.
- Ma W, Cheetham AG & Cui H (2016) Building Nanostructures with Drugs. *Nano Today* 11(1):13-30.
- McGovern SL, Caselli E, Grigorieff N & Shoichet BK (2002a) A common mechanism underlying promiscuous inhibitors from virtual and high-throughput screening. *Journal of medicinal chemistry* 45(8):1712-1722.
- McGovern SL, Caselli E, Grigorieff N & Shoichet BK (2002b) A common mechanism underlying promiscuous inhibitors from virtual and high-throughput screening. *J Med Chem* 45(8):1712-1722.
- McGovern SL, Helfand BT, Feng B & Shoichet BK (2003) A Specific Mechanism of Nonspecific Inhibition. *Journal of Medicinal Chemistry* 46(20):4265-4272.
- McGovern SL & Shoichet BK (2003) Kinase inhibitors: not just for kinases anymore. *Journal of medicinal chemistry* 46(8):1478-1483.
- Meiboom S & Gill D (1958) Modified spin-echo method for measuring nuclear relaxation times. *Review of scientific instruments* 29(8):688-691.
- Murugesan JR, Shahout F, Dlim M, Langella MM, Cuadra-Foy E, Forgione P & LaPlante SR (2018) Revealing dye and dye-drug aggregation into nano-entities using NMR. *Dyes and Pigments* 153:300-306.
- Nierkens S, Aalbers M, Bleumink R, Boon L & Pieters R (2005) Drug-induced type 1 and type 2 immune responses are characterized by distinct profiles of cell kinetics, cytokine production, and expression of co-stimulatory molecules in the popliteal lymph node assay. *J Immunotoxicol* 2(3):141-150.
- Noël C, Simard JC & Girard D (2016) Gold nanoparticles induce apoptosis, endoplasmic reticulum stress events and cleavage of cytoskeletal proteins in human neutrophils. *Toxicol In Vitro* 31:12-22.
- Owen SC, Doak AK, Wassam P, Shoichet MS & Shoichet BK (2012a) Colloidal aggregation affects the efficacy of anticancer drugs in cell culture. *ACS chemical biology* 7(8):1429-1435.
- Owen SC, Doak AK, Wassam P, Shoichet MS & Shoichet BK (2012b) Colloidal aggregation affects the efficacy of anticancer drugs in cell culture. *ACS Chem Biol* 7(8):1429-1435.
- Palmer III AG (2014) Chemical exchange in biomacromolecules: past, present, and future. *Journal of magnetic resonance* 241:3-17.
- Park K (2013) Facing the truth about nanotechnology in drug delivery. *ACS Nano* 7(9):7442-7447.
- Poirier M, Simard JC, Antoine F & Girard D (2014) Interaction between silver nanoparticles of 20 nm (AgNP20) and human neutrophils: induction of apoptosis and inhibition of de novo protein synthesis by AgNP20 aggregates. *J Appl Toxicol* 34(4):404-412.
- Price DA, Blagg J, Jones L, Greene N & Wager T (2009) Physicochemical drug properties associated with in vivo toxicological outcomes: a review. *Expert Opin Drug Metab Toxicol* 5(8):921-931.
- Rao H, Li Z, Li X, Ma X, Ung C, Li H, Liu X & Chen Y (2010) Identification of small molecule aggregators from large compound libraries by support vector machines. *J Comput Chem* 31(4):752-763.
- Robert C, Soria JC, Spatz A, Le Cesne A, Malka D, Pautier P, Wechsler J, Lhomme C, Escudier B, Boige V, Armand JP & Le Chevalier T (2005) Cutaneous side-effects of kinase inhibitors and blocking antibodies. *Lancet Oncol* 6(7):491-500.
- Schönmann C & Brockow K (2020) Adverse reactions during procedures: Hypersensitivity to contrast agents and dyes. *Ann Allergy Asthma Immunol* 124(2):156-164.

- Seidler J, McGovern SL, Doman TN & Shoichet BK (2003) Identification and prediction of promiscuous aggregating inhibitors among known drugs. *J Med Chem* 46(21):4477-4486.
- Shoichet BK (2006) Interpreting steep dose-response curves in early inhibitor discovery. *Journal of medicinal chemistry* 49(25):7274-7277.
- Simard JC, Simon MM, Tessier PA & Girard D (2011) Damage-associated molecular pattern S100A9 increases bactericidal activity of human neutrophils by enhancing phagocytosis. *J Immunol* 186(6):3622-3631.
- Volovik Frenkel Y, Gallicchio E, Das K, Levy RM & Arnold E (2009) Molecular dynamics study of non-nucleoside reverse transcriptase inhibitor 4-[[4-[[4-[(E)-2-cyanoethenyl]-2, 6-dimethylphenyl] amino]-2-pyrimidinyl] amino] benzonitrile (TMC278/rilpivirine) aggregates: correlation between amphiphilic properties of the drug and oral bioavailability. *Journal of medicinal chemistry* 52(19):5896-5905.
- Wang J & Matayoshi E (2012) Solubility at the molecular level: development of a critical aggregation concentration (CAC) assay for estimating compound monomer solubility. *Pharmaceutical research* 29(7):1745-1754.